ADVANCES AND TRENDS IN MICROBIAL PRODUCTION OF BIOPOLYMERS AND THEIR BUILDING BLOCKS

EDITED BY: Xinjun Feng, Xinglin Jiang and Guang Zhao

PUBLISHED IN: Frontiers in Bioengineering and Biotechnology

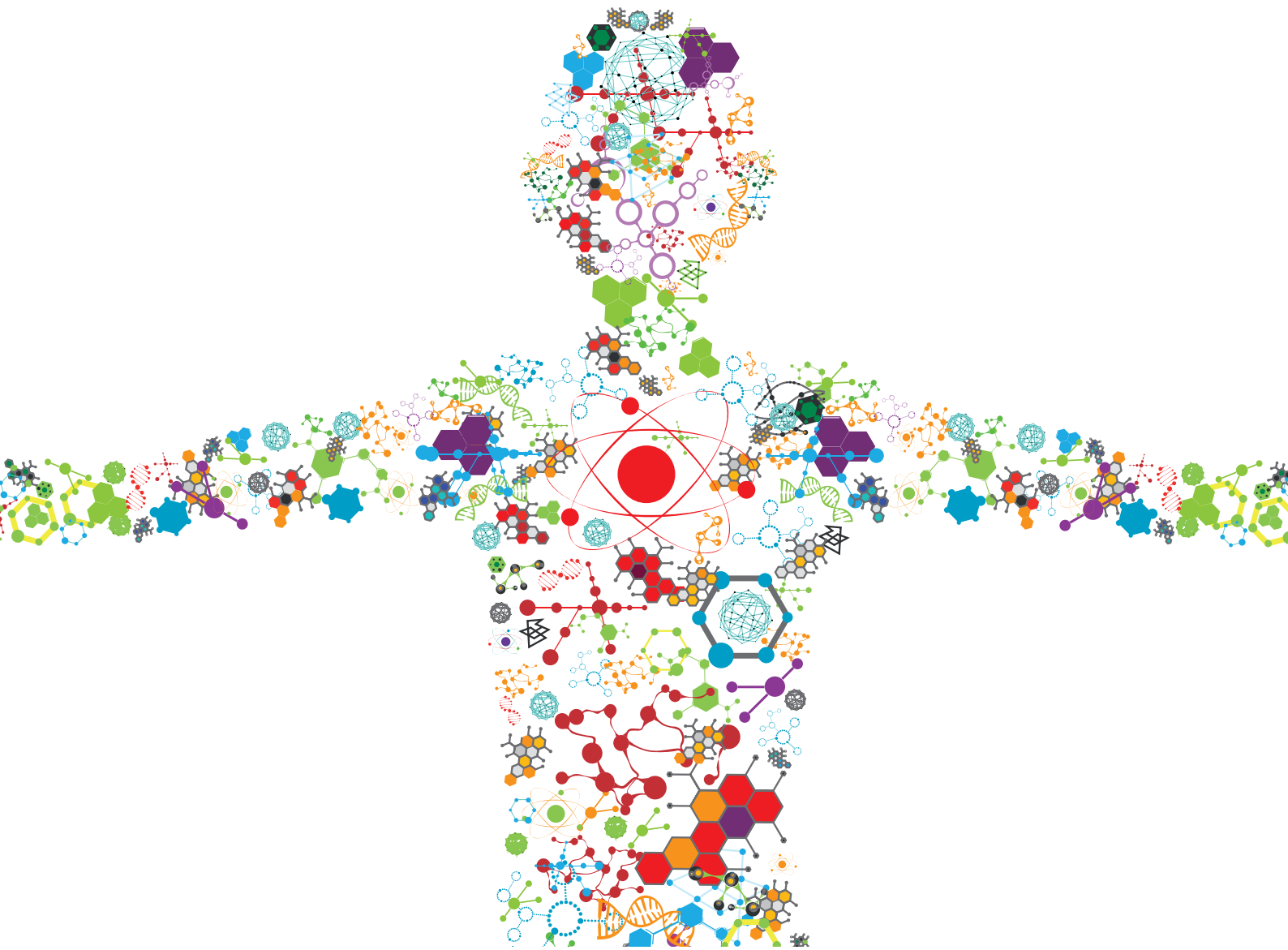

frontiers Research Topics

frontiers

ISSN 1664-8714
ISBN 978-2-83250-457-4
DOI 10.3389/978-2-83250-457-4

About Frontiers

Frontiers is more than just an open-access publisher of scholarly articles: it is a pioneering approach to the world of academia, radically improving the way scholarly research is managed. The grand vision of Frontiers is a world where all people have an equal opportunity to seek, share and generate knowledge. Frontiers provides immediate and permanent online open access to all its publications, but this alone is not enough to realize our grand goals.

Frontiers Journal Series

The Frontiers Journal Series is a multi-tier and interdisciplinary set of open-access, online journals, promising a paradigm shift from the current review, selection and dissemination processes in academic publishing. All Frontiers journals are driven by researchers for researchers; therefore, they constitute a service to the scholarly community. At the same time, the Frontiers Journal Series operates on a revolutionary invention, the tiered publishing system, initially addressing specific communities of scholars, and gradually climbing up to broader public understanding, thus serving the interests of the lay society, too.

Dedication to Quality

Each Frontiers article is a landmark of the highest quality, thanks to genuinely collaborative interactions between authors and review editors, who include some of the world's best academicians. Research must be certified by peers before entering a stream of knowledge that may eventually reach the public - and shape society; therefore, Frontiers only applies the most rigorous and unbiased reviews.
Frontiers revolutionizes research publishing by freely delivering the most outstanding research, evaluated with no bias from both the academic and social point of view. By applying the most advanced information technologies, Frontiers is catapulting scholarly publishing into a new generation.

What are Frontiers Research Topics?

Frontiers Research Topics are very popular trademarks of the Frontiers Journals Series: they are collections of at least ten articles, all centered on a particular subject. With their unique mix of varied contributions from Original Research to Review Articles, Frontiers Research Topics unify the most influential researchers, the latest key findings and historical advances in a hot research area! Find out more on how to host your own Frontiers Research Topic or contribute to one as an author by contacting the Frontiers Editorial Office: frontiersin.org/about/contact

ADVANCES AND TRENDS IN MICROBIAL PRODUCTION OF BIOPOLYMERS AND THEIR BUILDING BLOCKS

Topic Editors:
Xinjun Feng, Qingdao Institute of Bioenergy and Bioprocess Technology, Chinese Academy of Sciences (CAS), China
Xinglin Jiang, Technical University of Denmark, Denmark
Guang Zhao, Shandong University, China

Citation: Feng, X., Jiang, X., Zhao, G., eds. (2022). Advances and Trends in Microbial Production of Biopolymers and Their Building Blocks. Lausanne: Frontiers Media SA. doi: 10.3389/978-2-83250-457-4

Table of Contents

frontiers | Frontiers in Bioengineering and Biotechnology

TYPE Editorial
PUBLISHED 27 September 2022
DOI 10.3389/fbioe.2022.1025797

OPEN ACCESS

EDITED AND REVIEWED BY
Georg M. Guebitz,
University of Natural Resources and Life Sciences, Austria

*CORRESPONDENCE
Xinjun Feng,
fengxj@qibebt.ac.cn

SPECIALTY SECTION
This article was submitted to Industrial Biotechnology, a section of the journal Frontiers in Bioengineering and Biotechnology

RECEIVED 23 August 2022
ACCEPTED 09 September 2022
PUBLISHED 27 September 2022

CITATION
Feng X, Jiang X and Zhao G (2022), Editorial: Advances and trends in microbial production of biopolymers and their building blocks.
Front. Bioeng. Biotechnol. 10:1025797.
doi: 10.3389/fbioe.2022.1025797

Editorial: Advances and trends in microbial production of biopolymers and their building blocks

Xinjun Feng[1]*, Xinglin Jiang[2] and Guang Zhao[3]

[1]CAS Key Laboratory of Biobased Materials, Qingdao Institute of Bioenergy and Bioprocess Technology, Chinese Academy of Sciences, Qingdao, China, [2]The Novo Nordisk Foundation Center for Biosustainability, Technical University of Denmark, Kongens Lyngby, Denmark, [3]State Key Laboratory of Microbial Technology, Shandong University, Jinan, China

KEYWORDS

biopolymer, polyhydroxyalkanoates, polysaccharide, poly (lactic acid), succinic acid, 3-hydroxypropionic acid, microbial technology, carbon emission

Editorial on the Research Topic
Advances and trends in microbial production of biopolymers and their building blocks

Petroleum-based polymers have played an important role in human daily life, but they also cause serious environmental pollution due to their low biodegradability. In contrast, biopolymers have attracted unprecedented attentions with advantage of life cycle carbon emission reduction under the global achievement of “carbon peak” and “carbon neutrality”. However, some shortcomings of biopolymes remain and restrict their popular application, such as high cost, low productivity, and poor material properties.

This special issue consists of six original papers, one brief research report, two specialized review papers and one mini review article covering workhorse strains, cheap raw materials utilization, enzyme screening, monomer biosynthesis and bio-process optimization, which showcase current progress on biopolymers and aim to provide possible solutions to the existing problems.

Polyhydroxyalkanoates (PHAs) are one of the most popular biopolymers that exhibit similar mechanical properties to petrochemical-derived polymers with the added benefit of biodegradability and biocompatibility (Rekhi et al., 2022). To date, over 150 types of PHAs have been produced in the form of homopolymers, random and block copolymers, thus supporting a wide range of applications. Gao et al., systematically reviewed the recent advances in microbial synthesis of PHAs, including chassis engineering, substrate utilization, PHA synthase modification, and scale-up biomanufacturing, which will be of special interest to the researchers in the field of PHA biosynthesis.

The microbial hosts are crucial to desired biopolymer production. More than 70 genera of microbes have been identified and/or engineered for PHAs production

(Alcântara et al., 2020), such as *Ralstonia eutropha*, *Pseudomonas*, *Escherichia coli*, etc. The choice of microbiological strains directly impacts the chemical composition, structure and properties of the final polymers, as well as the substrate used. In recent years, some bacteria with particular characteristics have been proved to be economical and effective hosts. *Halomonas bluephagenesis*, a halophilic bacteria, can accumulate poly-3-hydroxybutyrate (PHB) up to more than 80% of the cell dry weight in an open unsterile process (Tan et al., 2011). *Rhodopseudomonas palustris*, a photosynthetic bacteria, has the ability to convert various carbon sources, especially CO_2, into valuable chemicals and biopolymers. A review by Li et al. provided a comprehensive overview of the advantages, the challenges and possible solutions of *R. palustris* as a powerful microbial cell factory, specifically discussed its applications in production of PHAs, polysaccharides and isoprenoids monomers.

PHA synthases polymerize various hydroxyacyl-CoAs into different PHA polymers. However, PHA synthases prefer 3-hydroxyacyl-CoAs rather than 2-hydroxyacyl-CoAs, which makes it very difficult to synthesize polylactic acid (PLA) directly in microbial cells. To screen robust PHA synthase for PLA homopolymer biosynthesis, Shi et al. evaluated the class I PHA synthase from *Chromobacterium* sp. USM2 in engineered *E. coli* using glucose as carbon source, and demonstrated that it is feasible to catalyze the polymerization of lactyl-CoA with better performance in PLA production than that of the evolved class II PHA synthase $PhaC1_{Ps6\text{-}19}$. This work proved that class I PHA synthase has catalytic ability to 2-hydroxyacyl-CoAs.

As the cost of the substrate can account for up to 50% of the overall production cost (Urtuvia et al., 2014), various renewable and inexpensive carbon sources including lignocellulosic biomass hydrolysates, sugarcane molasses, crude glycerol, have been evaluated for PHAs production. Szacherska et al. explores to use short- and medium-chain fatty acids (SMCFAs) as raw materials for PHA production in three individual *Pseudomonas* strains. This study demonstrated that high PHA productivity can be obtained in *Pseudomonas* sp. Gl06 cultivation under nitrogen limitation conditions with cheap SMCFA-rich stream from a cheese production line, and the extracted polymers possess better properties with lower melting point and degradation temperature.

Moreover, many bio-monomers can be utilized for polyesters production directly through chemical polymerization. Succinic acid is one of building blocks of the commercial polyester poly (butylene succinate) (PBS) with wide temperature window for thermoplastic processing. Liu et al. summarized different succinic acid biosynthetic pathways, concentrating on the key enzymes and metabolic engineering approaches, and future perspectives were also proposed. 3-Hydroxypropionic acid (3-HP) is a versatile platform compound which can be polymerized into polymers. Liu et al. engineered a 3HP biosynthetic pathway from glucose with glycerol as intermediate in *Klebsiella pneumoniae*, and improved 3-HP production by CRISPR interference. 2-fluoro-3-hydroxypropionic acid was firstly biosynthesized by Liu et al., which is expected to obtain fluorine-containing materials such as poly (2-fluoro-3-hydroxypropionic acid) with better properties. Liu et al. investigated the biosynthesis of lactate in *E. coli* and proved that lysine acetylation of lactate dehydrogenase can regulate lactate synthesis effectively. In another study, Zhang et al. improved the bioconversion of phenylpyruvate to L-phenyllactate, whose homopolymer exhibits high-ultraviolet-absorbing properties, by introducing a NADH-dependent L-lactate dehydrogenase mutant into *Pichia pastoris* coupling with a NADH regeneration system.

As an important natural biopolymer, polysaccharides have been widely used in the food, pharmacy, cosmetics, and chemical industries, and microbial polysaccharides in particular offer many advantages compared to plant-derived polysaccharides (Chaabouni et al., 2014). Xu et al., presented the systematic optimization of fermentation process of exopolysaccharide using *Candida glabrata* mutant, resulting in significantly improved production of exopolysaccharide that shows great industrial application potential.

Finally, we sincerely thank all the submitting authors for considering to share their updated research outcomes and opinions in this special issue, the reviewers for their time and constructive comments to improve the manuscripts, also the editors Dr. Xiao-Jun Ji and Dr. Ka Yu Cheng for their kind support. We hope that readers find these articles in this special issue interesting and useful for their own research.

Author contributions

XF and GZ conceived the manuscript; XF wrote the manuscript; XF, XJ, and GZ reviewed and edited the manuscript.

Funding

XF is supported by the Youth Innovation Promotion Association of Chinese Academy of Sciences (2020214), National Natural Science Foundation of China (31800081), and Natural Science Foundation of Shandong Province (ZR2019QB015). GZ is supported by the National Natural Science Foundation of China (32170085, 31961133014).

Conflict of interest

The authors declare that the research was conducted in the absence of any commercial or financial relationships that could be construed as a potential conflict of interest.

Publisher's note

References

Alcântara, J. M. G., Distante, F., Storti, G., Moscatelli, D., Morbidelli, M., and Sponchioni, M. (2020). Current trends in the production of biodegradable bioplastics: The case of polyhydroxyalkanoates. *Biotechnol. Adv.* 42, 107582. doi:10.1016/j.biotechadv.2020.107582

Chaabouni, E., Gassara, F., and Brar, S. K. (2014). "Biopolymers synthesis and application," in *Biotransformation of waste biomass into high value biochemicals*. Editors S. K. Brar, G. S. Dhillon, and C. R. Soccol (New York: Springer Press), 415–443.

Rekhi, P., Goswami, M., Ramakrishna, S., and Debnath, M. (2022). Polyhydroxyalkanoates biopolymers toward decarbonizing economy and sustainable future. *Crit. Rev. Biotechnol.* 42 (5), 668–692. doi:10.1080/07388551.2021.1960265

Tan, D., Xue, Y. S., Aibaidula, G., and Chen, G. Q. (2011). Unsterile and continuous production of polyhydroxybutyrate by Halomonas TD01. *Bioresour. Technol.* 102, 8130–8136. doi:10.1016/j.biortech.2011.05.068

Urtuvia, V., Villegas, P., González, M., and Seeger, M. (2014). Bacterial production of the biodegradable plastics polyhydroxyalkanoates. *Int. J. Biol. Macromol.* 70, 208–213. doi:10.1016/j.ijbiomac.2014.06.001

frontiers in Bioengineering and Biotechnology

ORIGINAL RESEARCH
published: 18 February 2022
doi: 10.3389/fbioe.2022.846489

Enantioselective Biosynthesis of L-Phenyllactic Acid From Phenylpyruvic Acid *In Vitro* by L-Lactate Dehydrogenase Coupling With Glucose Dehydrogenase

Dong Zhang[1], *Ting Zhang*[2], *Yuqing Lei*[1], *Wenqian Lin*[1], *Xingyi Chen*[3] *and Minchen Wu*[3]*

[1]Key Laboratory of Carbohydrate Chemistry and Biotechnology, Ministry of Education, School of Biotechnology, Jiangnan University, Wuxi, China, [2]Haiyan Food and Drug Inspection and Testing Center, Haiyan, China, [3]Wuxi School of Medicine, Jiangnan University, Wuxi, China

As a valuable versatile building block, L-phenyllactic acid (L-PLA) has numerous applications in the fields of agriculture, pharmaceuticals, and biodegradable plastics. However, both normally chemically synthesized and naturally occurring PLA are racemic, and the production titer of L-PLA is not satisfactory. To improve L-PLA production and reduce the high cost of NADH, an *in vitro* coenzyme regeneration system of NADH was achieved using the glucose dehydrogenase variant *Ls*GDH^{D255C} and introduced into the L-PLA production process. Here an NADH-dependent L-lactate dehydrogenase-encoding variant gene (L-*Lcldh*1$^{Q88A/I229A}$) was expressed in *Pichia pastoris* GS115. The specific activity of L-*Lc*LDH1$^{Q88A/I229A}$ (Pp) was as high as 447.6 U/mg at the optimum temperature and pH of 40°C and 5.0, which was 38.26-fold higher than that of wild-type L-*Lc*LDH1 (Pp). The catalytic efficiency (k_{cat}/K_m) of L-*Lc*LDH1$^{Q88A/I229A}$ (Pp) was 94.3 mM^{-1} s^{-1}, which was 67.4- and 25.5-fold higher than that of L-*Lc*LDH1(Pp) and L-*Lc*LDH1$^{Q88A/I229A}$ (Ec) expressed in *Escherichia coli*, respectively. Optimum reactions of L-PLA production by dual-enzyme catalysis were at 40°C and pH 5.0 with 10.0 U/ml L-*Lc*LDH1$^{Q88A/I229A}$ (Pp) and 4.0 U/ml *Ls*GDH^{D255C}. Using 0.1 mM NAD^+, 400 mM (65.66 g/L) phenylpyruvic acid was completely hydrolyzed by fed-batch process within 6 h, affording L-PLA with 90.0% yield and over 99.9% ee_p. This work would be a promising technical strategy for the preparation of L-PLA at an industrial scale.

Keywords: L-PLA, coenzyme regeneration system, L-lactate dehydrogenase, fed-batch, asymmetric reduction

OPEN ACCESS

Edited by:
Xinjun Feng,
Qingdao Institute of Bioenergy and Bioprocess Technology (CAS), China

Reviewed by:
Yanning Zheng,
Institute of Microbiology (CAS), China
Huibin Zou,
Qingdao University of Science and Technology, China

***Correspondence:**
Minchen Wu
biowmc@126.com

Specialty section:
This article was submitted to Industrial Biotechnology, a section of the journal Frontiers in Bioengineering and Biotechnology

Received: *31 December 2021*
Accepted: *18 January 2022*
Published: *18 February 2022*

Citation:
Zhang D, Zhang T, Lei Y, Lin W, Chen X and Wu M (2022) Enantioselective Biosynthesis of L-Phenyllactic Acid From Phenylpyruvic Acid In Vitro by L-Lactate Dehydrogenase Coupling With Glucose Dehydrogenase. Front. Bioeng. Biotechnol. 10:846489. doi: 10.3389/fbioe.2022.846489

INTRODUCTION

Phenyllactic acid (PLA), a natural organic acid with high value added, is considered a promising preservative widely used in food and feed due to its broad antimicrobial activity (Ning et al., 2017). The optically pure PLA is also a high-value-added chiral compound with potential applications in the pharmaceutical and biomaterial areas—for example, L-PLA was applied to synthesize non-amino acid statine, protease inhibitors, and anti-HIV reagents (Kano et al., 1988; Urban and Moore, 1992; Fujita et al., 2013), while D-PLA was also applied as a building block in biopolyester polyhydroxyalkanoate and a hypoglycemic agent englitazone (Xu et al., 2016; Yang et al., 2018).

Additionally, L-PLA is a promising building block for bio-based materials, as L-PLA can be polymerized into the biopolymer poly(L-phenyllactic acid)s. Unlike poly(L-lactic acid)s, poly(L-phenyllactic acid)s exhibit high-ultraviolet-absorbing properties due to the bulky aromatic side chain at the C-3 group of L-lactic acid, which has been applied in plastics, pharmaceutics, and agrochemistry in terms of its superior chemical–physical and antimicrobial properties (Chifiriuc et al., 2007; Zheng et al., 2015). Due to its potential application for the synthesis of aromatic polymers, L-PLA production has aroused great interest recently.

With the increasing environmental awareness, biocatalysis using enzymes or whole cells has attracted much attention, given its properties such as high enantioselectivity (ee_p >99%), 100% theoretical yield, no or little byproducts, and being an environment-friendly process (Hou et al., 2019). To date, various biotechnological methods have been developed for L-PLA production, mainly including microbial fermentation and enzymatic/whole-cell cascade biocatalysis (Zheng et al., 2013). In general, L-PLA is mainly produced by L-lactate dehydrogenases (LDHs), owing to the above-mentioned advantages. However, few L-LDHs exhibited a high catalytic activity, catalytic efficiency (k_{cat}/K_m), and yield, especially towards the bulkier substrates such as phenylpyruvic acid (PPA), which made them unable to be utilized effectively—for instance, the activities of L-*Lp*LDH from *Lactobacillus plantarum* and L-*Bs*LDH from *Geobacillus stearothermophilus* were 28.11 and 7.39 U/mg wet cell, respectively (Aslan et al., 2016; Zhu et al., 2017). In addition, by fed-batch conversion, the highest PLA production reached 21.43 g/L after 13.5 h, and the final conversion ratio of PPA was 82.38% (Wang et al., 2016). LDHs using NADH or NADPH as its co-substrate catalyze the reduction and oxidation reaction between pyruvate and lactic acid (Al-Jassabi, 2002). L-LDHs are NADH dependent, which do not have enough reduction activity if the cofactor is oxidized. However, the high cost of NADH has made it uneconomical to add pure NADH for PLA production and thus limited its application in industries (Li et al., 2019). Interestingly, glucose dehydrogenases (GDHs) can catalyze the conversion of oxygen and glucose to gluconic acid and hydrogen peroxide, while NAD^+ is reduced to NADH, which could be used as a versatile biocatalyst for NADH regeneration. Therefore, an NADH/NAD^+ regeneration system could be introduced into the recycle to increase the availability of NADH and improve the yield of L-PLA (Zhang et al., 2009). To break through these bottlenecks, one of the effective strategies was to excavate novel LDHs having a high activity and/or construct an efficient coenzyme NADH regeneration system.

Previously, two single site-directed mutagenesis of L-*Lcldh*1, L-*Lcldh*1^{Q88A}, and L-*Lcldh*1^{I229A} were constructed by whole-plasmid PCR as designed theoretically and expressed in *Escherichia coli* BL21 (DE3) (Li et al., 2018). Based on homology modeling and molecular dynamics (MD) simulation, it was found that both Q88 and I229 in L-*Lc*LDH1 are located at the entrance of the substrate-binding pocket. Then, the two specific residues in L-LDH1, Gln^{88} and Ile^{229}, were subjected to a combinatorial double-directed mutagenesis to superimpose the superior catalytic properties of L-*Lcldh*1^{Q88A} and L-*Lcldh*1^{I229A} (Li, 2018). The catalytic performance analysis indicated that L-LDH1$^{Q88A/I229A}$ (Ec) obtained remarkably improved specific activities towards PPA. Similar to the majority of known wild-type L-LDHs, L-LDH1$^{Q88A/I229A}$ (Ec) displayed a lower specific activity (195.5 U/g wet cell) and catalytic efficiency (k_{cat}/K_m = 3.7 mM^{-1} s^{-1}) towards PPA, which could catalyze 10 mM PPA to L-PLA with 99% ee_p and 77% yield within 140 min. In this work, in order to improve the yield of L-PLA and avoid the formation of byproducts, L-LDH1$^{Q88A/I229A}$ was expressed in *Pichia pastoris* GS115 successfully. Then, according to the previous findings about GDHs widely used for NADH regeneration in bioconversion process, *Ls*GDH^{D250C}, *Bs*GDH$^{E170K/Q250L}$, and SyGDH were expressed in *E. coli* BL21 (DE3), respectively. After screening, the asymmetric reduction of PPA was conducted by L-*Lc*LDH1$^{Q88A/I229A}$ (Pp) coupling with *Ls*GDH^{D250C} (**Figure 1**). Finally, L-PLA was efficiently prepared by fed-batch process.

MATERIALS AND METHODS

Materials

The strains, plasmids, and genes used in this work are summarized in **Table 1**. *E. coli* BL21 (DE3), *P. pastoris* GS115, pET-28a(+), and pPIC9K were used for the construction of recombinant plasmids and the expression of GDHs and L-*Lc*LDH1$^{Q88A/I229A}$. The recombinant plasmids pET-22b-L-*Lcldh1*^{Q88A}, pET-22b-L-*Lcldh1*^{I229A}, pET-22b-L-*Lcldh1*$^{Q88A/I229A}$, and pET-28a-Sy*gdh* were constructed and stored in our lab. The recombinant plasmids pET-28a-*Lsgdh*^{D252C} and pET-28a-*Bsghd*$^{E170K/Q250L}$ were synthesized by GENEWIZ. IPTG, PPA, NAD^+, and L/D-PLA were purchased from Sigma-Aldrich (St. Louis, MO, United States). All the other chemical reagents used were of analytical grade and commercially available (Wuxi, China).

Expression of L-LDH1$^{Q88A/I229A}$ in *P. pastoris* GS115

L-*Lcldh*1$^{Q88A/I229A}$ was excised from recombinant plasmid pET-22b-L-*Lcldh*1$^{Q88A/I229A}$ by digestion with *Eco*R I and *Not* I and inserted into pPIC9K digested with the same enzymes, followed by transforming it into *E. coli* JM109. The resulting recombinant expression plasmid was then linearized with *Sal*I and transformed into *P. pastoris* GS115 by electroporation using a Gene Pulser apparatus (Bio-Rad, Hercules, CA, United States) according to the manufacturer's instruction. All *P. pastoris* transformants were primarily screened based on their ability to grow on a MD plate and subsequently inoculated on a geneticin G418-containing YPD plate at concentration of 4.0 mg/ml for the screening of multiple copies. In total, 50 of the G418-resistant *P. pastoris* transformants were isolated and determined by colony PCR using vector-specific primers. Then, 20 *P. pastoris* transformants were selected for the flask expression test. After screening, the best transformant was induced by adding 1.0% (v/v) methanol at 24-h intervals for

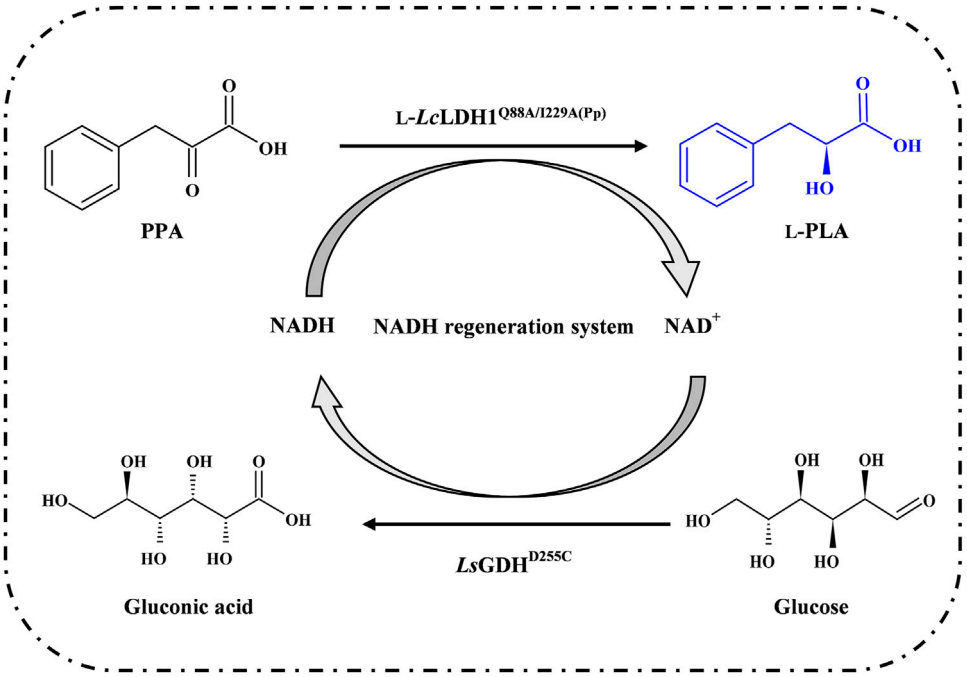

FIGURE. 1 | Schematic view of L-phenyllactic acid production from phenylpyruvic acid with NADH regeneration system.

TABLE 1 | Strains, plasmids, and genes used in this work.

Strains, plasmids, and genes	Resource	References
E. coli BL21 (DE3)	Novagen, Madison, WI	NI
P. pastoris GS115	Novagen, Madison, WI	NI
pET-28a(+)	Novagen, Madison, WI	NI
pPIC9K	Novagen, Madison, WI	NI
L-*Lcldh1*^{Q88A}	*Lactobacillus casei* B1192	Li et al. (2018)
L-*Lcldh1*^{I229A}	*Lactobacillus casei* B1192	Li et al. (2018)
L-*Lcldh1*$^{Q88A/I229A}$	*Lactobacillus casei* B1192	Li (2018)
Sygdh	*Thermoplasma acidophilum*	Yu et al. (2015)
Lsgdh^{D252C}	*Lysinibacillus sphaericus* G10	Ding et al. (2013)
Bsghd$^{E170K/Q250L}$	*Bacillus subtilis* strain 168	Vazquez-Figueroa et al. (2007)

NI, no information.

72 h. Then, a total of 200 ml of cultured supernatant was harvested for further study. Comparatively, GS115/L-*Lcldh*1 was used as a positive control, while GS115 transformed with pPIC9K, named GS115/pPIC9K, was used as a negative control.

Screening of GDHs

The genes *Lsgdh*^{D255C} and *Bsghd*$^{E170K/Q250L}$ were synthesized by GENEWIZ (Suzhou, China) and ligated into pET-28a(+) plasmid, followed by transforming them into *E. coli* BL21 (DE3), respectively. Then, the transformants were selected on Luria–Bertani (LB) agar medium with 100 μg/ml kanamycin, and the positive clones screened and confirmed by DNA sequencing were named *E. coli*/*Lsgdh*^{D252C} and *E. coli*/*Bsghd*$^{E170K/Q250L}$, respectively. *E. coli*/*Sygdh* was constructed and stored in our lab.

Preparation of Recombinant Proteins

The expressed recombinant L-*Lc*LDH1$^{Q88A/I229A}$ (Pp) or L-*Lc*LDH1 (Pp) with a 6× His tag at its C-terminus was purified by affinity column chromatography. Briefly, the fermentation supernatant was centrifuged (5,000 × *g*, 10 min, 4°C) and collected. Then, the obtained supernatant (200 ml) was filtered through a 0.22-μm filter, adjusted to pH 7.8, and loaded onto a nickel-nitrilotriacetic acid column (Tiandz, Beijing, China) pre-equilibrated with binding buffer (20 mM Tris-HCl, 500 mM NaCl, and 20 mM imidazole, pH 7.8), followed by elution at a rate of 0.4 ml/min with elution buffer that was the same as the binding buffer except for 200 mM imidazole. Aliquots of 1.0 ml eluent only containing the target protein, L-*Lc*LDH1$^{Q88A/I229A}$ (Pp) or L-*Lc*LDH1 (Pp), were pooled, dialyzed against 50 mM Na_2HPO_4–NaH_2PO_4 buffer (pH 7.0), and concentrated by

ultrafiltration using a 10-kDa cutoff membrane (Millipore, Billerica, MA, United States). The target protein was assessed by SDS-PAGE, and the protein concentration was determined by the Bradford method using bovine serum albumin as the standard.

A different method of preparing GDHs was used. Firstly, *E. coli* transformant cells were cultured in LB medium supplemented with 100 μg/ml kanamycin at 37°C and 220 rpm until OD_{600} reached 0.6–0.8. After having been induced by 0.05 mM IPTG at 25°C for 10 h, *E. coli* cells were harvested by centrifugation at 4°C, resuspended in 50 mM Na_2HPO_4–NaH_2PO_4 buffer (pH 7.0), and disrupted by sonication in ice-water bath. Then, the obtained supernatant was used as cell-free extracts for crude enzyme activity assay. In order to reduce the influence of miscellaneous protein in the crude enzyme solution of the three selected GDHs, the crude enzyme solutions were treated in a hot water bath at 50°C for 1 h, and then their relative activities were measured, respectively.

Enzyme Activity Assay

The activities of LDHs and GDHs were assayed by measuring respectively as described previously (Zhu et al., 2017; Li et al., 2018), with a slight modification. L-LDH activity on PPA was assayed by the reaction mixture containing 50 mM sodium acetate–acetate buffer (pH 5.0), 2 mM NADH, and 10 mM PPA. One activity unit (U) of LDH activity was defined as the amount of enzyme catalyzing the reduction of 1 μmol PPA per minute under the given assay conditions (40°C, 5 min). GDH activity was measured by the reaction mixture containing 50 mM sodium acetate–acetate buffer (pH 5.0), 2 mM NAD+, and 40 mM glucose. One activity unit (U) of GDH was defined as the amount of enzyme that produced 1 μmol NADH per minute under the given assay conditions (40°C, 5 min).

Determination of NAD^+ and *Ls*GDH^{D255C} on L-PLA production

The recombinant *E. coli*/*Lsgdh*^{D252C} cells were induced, harvested, and disrupted by sonication; then, the obtained supernatant was incubated for 1 h at 50°C. To determine the effect of the addition of NAD^+ on L-PLA production, a bioconversion reaction was performed in the final volume of 5 ml of 50 mM sodium acetate–acetate buffer system (pH 5.0) containing 100 mM PPA, 120 mM glucose, 10.0 U/ml L-*Lc*LDH1$^{Q88A/I229A}$ (Pp), 5.0 U/ml *Ls*GDH^{D250C}, and NAD^+ at elevated concentrations ranging from 0.025 to 0.50 mM, respectively, at 40°C and 200 rpm for 1 h. Furthermore, using L-PLA production as the criteria, bioconversion reactions, in the final volume of 5 ml of 50 mM sodium acetate–acetate buffer system (pH 5.0) containing 100 mM PPA, 120 mM glucose, 10.0 U/ml L-*Lc*LDH1$^{Q88A/I229A}$ (Pp), 0.1 mM NAD^+, and *Ls*GDH^{D250C} at the concentration range of 1.0–6.0 U/ml, were conducted, respectively, at 40°C and 200 rpm for 1 h. After completion of the reactions, the samples were treated in boiling water bath at 100°C for 10 min and centrifuged at 12,000 rpm for 5 min. The concentrations of PPA and L-PLA in the resulting supernatants were quantitatively analyzed by high-performance liquid chromatography (HPLC).

Bioconversion of PPA to L-PLA by Coupling L-*Lc*LDH1$^{Q88A/I229A}$ (Pp) With *Ls*GDH^{D250C}

The bioconversion was initiated in 50 mM sodium acetate–acetate buffer (pH 5.0) containing 100 mM PPA, 120 mM glucose, 0.1 mM NAD^+, 10.0 U/ml L-*Lc*LDH1$^{Q88A/I229A}$ (Pp), and 4.0 U/ml *Ls*GDH^{D250C} at 40°C. Furthermore, a higher substrate concentration (200 mM PPA) was used to verify substrate inhibition. Then, fed-batch bioconversion was performed in a 250-ml beaker containing 100 ml of the reaction mixture. The initial reaction mixtures containing 100 mM PPA, 120 mM glucose, 0.1 mM NAD^+, 10.0 U/ml L-*Lc*LDH1$^{Q88A/I229A}$ (Pp), and 4.0 U/ml *Ls*GDH^{D250C} were incubated at 40°C and 200 rpm. PPA powder (4.93 g) and glucose powder (6.48 g) were both averagely supplemented at 0.5, 1, and 2 h, respectively. During the bioconversion process, aliquots of 500-μl samples were drawn out periodically and then analyzed by HPLC.

Analytical Methods

PPA and PLA were assayed by inversed-HPLC using a Waters e2695 apparatus (Waters, Milford, MA, United States) equipped with a Prontosil C18 AQ chromatographic column. The mobile phase of methanol/H_2O (4:6, v/v) with 0.05% acetocaustin (v/v) was used at a flow rate of 0.8 ml/min and monitored using a 2489 UV–Vis detector at 210 nm. The yield of L-PLA (c_m) was calculated using the equation: $c_m = (c_p / c_s) \times 100\%$, in which c_p was the concentration of PLA (mM), and c_s was the concentration of PPA (mM).

Different from that of inversed-HPLC, positive-phase HPLC equipped with an OD-H chiral column (Daicel, Tokyo, Japan; 4.6 mm × 250 mm, 5 μm) was used to analyze the optical purity of L-PLA under the same assay conditions as described above, except for the mobile-phase n-hexane/isopropanol (98:2, v/v) with 0.05% acetocaustin (v/v). The enantiomeric excess product (ee_p) of L-PLA was calculated by using the equation: $ee_p = [(A_L - A_D) / (A_L + A_D)] \times 100\%$, where A_L and A_D are the concentrations of L-PLA and D-PLA, respectively. The space time yield (STY) and the average turnover frequency (aTOF) were calculated by using the equations: $STY\ (g/L/h) = C_p / t$, $aTOF\ (g/g/h) = C_p / (t \times C_e)$, in which C_p was the concentration of L-PLA (g/L), t was the reaction time, and C_e was L-*Lc*LDH1$^{Q88A/I229A}$ (Pp) protein concentration (g/L).

RESULTS AND DISCUSSION

Enzyme Assay of L-*Lc*LDH1$^{Q88A/I229A}$ (Pp) Expressed in *P. pastoris* GS115

To improve the L-phenyllactic acid (L-PLA) production efficiency and reduce costs, we attempted the expression of *L-LcLDH1*$^{Q88A/I229A}$ in *P. pastoris* GS115. The fermentation supernatant and the purified L-*Lc*LDH1$^{Q88A/I229A}$ (Pp) displayed one single protein band with an apparent molecular weight of approximately 36.8 kDa on SDS-PAGE gels (**Figure 2**, lanes 2 and 3), equal to the theoretical one (36.75 kDa) of L-

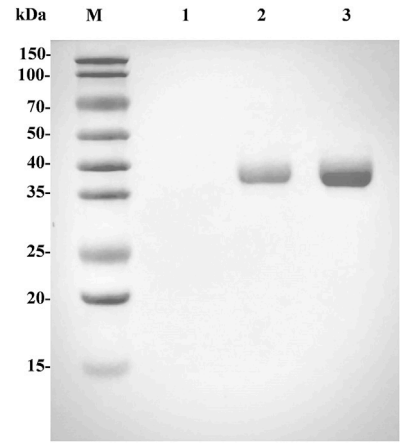

FIGURE. 2 | SDS-PAGE analysis of the expressed and purified L-*Lc*LDH1$^{Q88A/I229A}$ (Pp). Lane M, standard protein molecular mass markers; lane 1, the cultured supernatant of GS115/pPIC9K; lane 2, the cultured supernatant of GS115/L-*lcldh1*$^{Q88A/I229A}$; lane 3, the purified L-*Lc*LDH1$^{Q88A/I229A}$ (Pp).

*Lc*LDH1$^{Q88A/I229A}$, which indicated that the L-*Lc*LDH1$^{Q88A/I229A}$ (Pp) was expressed successfully in *P. pastoris* GS115. The specific activity of L-*Lc*LDH1$^{Q88A/I229A}$ (Pp) was as high as 447.6 U/mg towards PPA at the optimum temperature and pH of 40°C and 5.0, which was obviously higher than the other L-LDHs reported by Zhu (28.11 U/g) (Zhu et al., 2017), Jia (71.06 U/g) (Jia et al., 2010), Aslan (51.3 U/g) (Aslan et al., 2016), and Zheng (72.6 U/g) (Zheng et al., 2011). Many studies regarding engineering of target enzymes have been reported, while almost all research demonstrated the feasibility of improving the L-LDH activity towards PPA by site-directed mutagenesis. As a key enzyme in L-PLA production, most of the L-LDHs reported were expressed in *E. coli*, which exhibited low catalytic efficiency (k_{cat}/K_m), production efficiency, and yield and produced many more byproducts. Here L-*Lc*LDH1$^{Q88A/I229A}$ (Pp) expressed in *P. pastoris* GS115 was different from all the previously reported LDHs, which had a higher enzyme activity and catalytic efficiency. Moreover, one of the advantages of the *P. pastoris* expression system was that the purities of the expressed recombinant proteins were very high, which could greatly simplify the purification processes. *P. pastoris* enables some post-translational modifications of a recombinant protein, such as

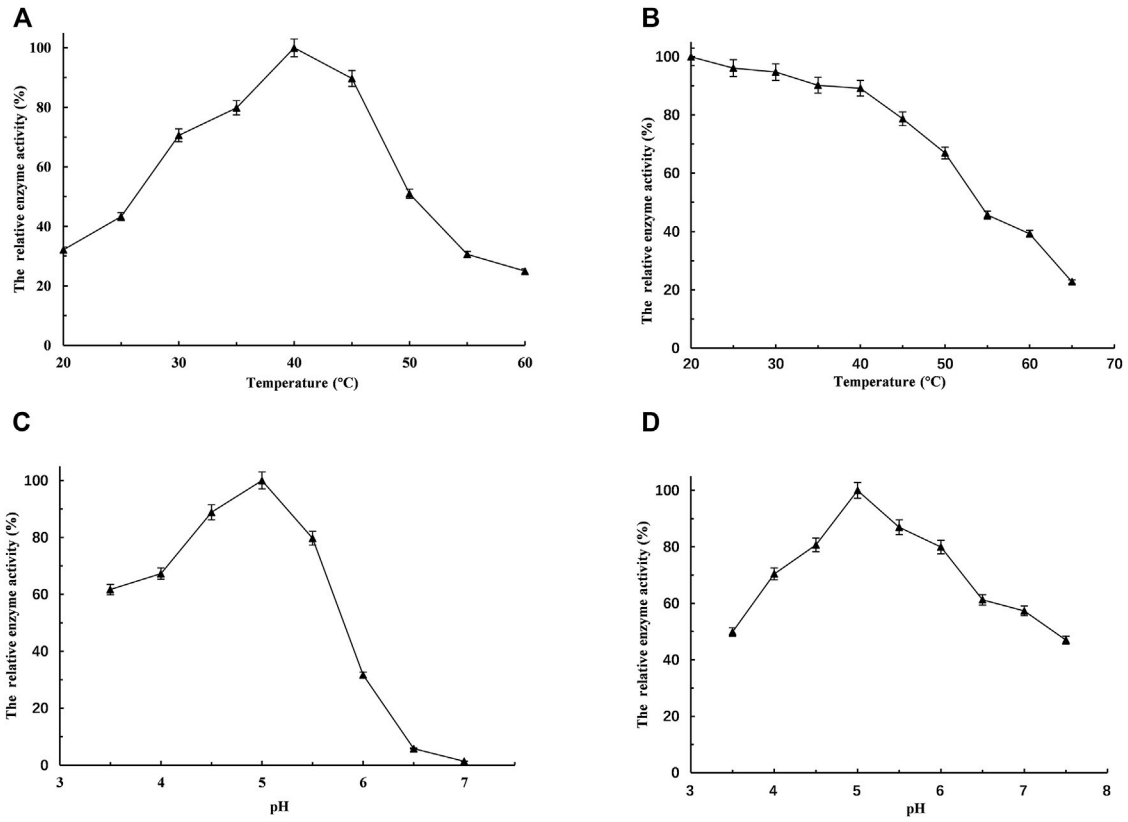

FIGURE. 3 | Optimization of bioconversion conditions of the recombinant L-*Lc*LDH1$^{Q88A/I229A}$ (Pp). **(A)** The temperature optima were measured under the standard assay conditions, but temperatures ranged from 20 to 60°C. **(B)** To estimate the temperature stability, the recombinant L-*Lc*LDH1$^{Q88A/I229A}$ (Pp) was incubated for 2 h from 20 to 65°C, respectively. **(C)** The pH optima were measured under the above-mentioned assay conditions, except for pH ranging from 3.5 to 7.0. **(D)** To estimate the pH stability, the recombinant L-*Lc*LDH1$^{Q88A/I229A}$ (Pp) was incubated for 1 h in a different pH buffer at 4°C, and then the relative activity was determined at the optimal temperature of 40°C and optimal pH of 5.0. Means and standard deviations of triplicate experiments are shown.

TABLE 2 | The kinetic parameters of the recombinant enzymes.

Recombinant enzymes	K_m (mM)	V_{max} (U/mg)	k_{cat} (s^{-1})	k_{cat}/K_m ($mM^{-1}·s^{-1}$)
L-*Lc*LDH1$^{Q88A/I229A}$ (Pp)	4.08 ± 0.12	627.0 ± 17	385 ± 12	94.3
L-*Lc*LDH1 (Pp)	9.52 ± 0.26	22.5 ± 0.58	13.8 ± 0.28	1.4
L-*Lc*LDH1$^{Q88A/I229A}$ (Ec)	3.84 ± 0.11	24.0 ± 0.45	14.7 ± 0.14	3.7

*L-*Lc*LDH1$^{Q88A/I229A}$ (Pp), double-site mutant enzyme of L-*Lc*LDH1 expressed in* P. pastoris*; L-*Lc*LDH1 (Pp), the wild-type enzyme expressed in* P. pastoris*; L-*Lc*LDH1$^{Q88A/I229A}$ (Ec), double-site mutant enzyme of L-*Lc*LDH1 expressed in* E. coli.

glycosylation, whereas there is no N-glycosylation site in this work. The difference of L-*Lc*LDH1$^{Q88A/I229A}$ expressed in the two expression systems will be further investigated in the following work.

To determine the influence of temperature on the activity of L-*Lc*LDH1$^{Q88A/I229A}$ (Pp), the temperature–activity profiles were assessed from 20 to 60°C with PPA as the substrate (**Figure 3A**). To evaluate the temperature stabilities, the residual activities were measured after incubation at various temperatures for 2.0 h (**Figure 3B**). The optimum temperature was at 40°C (**Figure 3A**), and L-*Lc*LDH1$^{Q88A/I229A}$ (Pp) was stable at temperatures below 45°C (**Figure 3B**). Within the range of the thermal tolerance of L-*Lc*LDH1$^{Q88A/I229A}$ (Pp), the high temperature increased the solubility and dissolution rate of PPA, contributing to the effective conversion of PPA into L-PLA at a high concentration and with a high yield. Because pH would considerably affect the enzyme activity and stability in application, the influence of pH on L-*Lc*LDH1$^{Q88A/I229A}$ (Pp) was also assessed. Its optimal pH was at 5.0 (**Figure 3C**), and it was stable at 4.5–5.0 (**Figure 3D**). Then, the half-life value was measured at its optimal temperature and pH (40°C, 5.0). During the process, aliquots of 50-μl enzyme samples were drawn out, and their relative enzyme activities were determined. The half-life value calculated was 6.1 h, which was longer than that of L-*Lc*LDH1$^{Q88A/I229A}$ (Ec) (4.4 h) (data not shown). Next, taking economic efficiency and catalytic activity into consideration, L-*Lc*LDH1$^{Q88A/I229A}$ (Pp) expressed in *P. pastoris* exhibited better superiority than L-*Lc*LDH1$^{Q88A/I229A}$ (Ec) expressed in *E. coli*.

The kinetic parameters of the recombinant enzymes were determined using PPA as substrate (**Table 2**). The K_m of L-*Lc*LDH1$^{Q88A/I229A}$ (Pp) towards PPA was 4.08 mM, which was 57.1% lower than that of wild-type enzyme L-*Lc*LDH1. Moreover, the k_{cat}/K_m of L-*Lc*LDH1$^{Q88A/I229A}$ (Pp) (94.3 mM^{-1} s^{-1}) was significantly increased, which was 67.4 times higher than that of L-*Lc*LDH1 (Pp) (1.4 mM^{-1} s^{-1}). This study also found that the V_{max} (627.0 U/mg) and the catalytic efficiency k_{cat}/K_m of L-*Lc*LDH1$^{Q88A/I229A}$ (Pp) were 26.1 times and 25.5 times higher, respectively, than those of L-*Lc*LDH1$^{Q88A/I229A}$ (Ec) (24.0 U/mg and 3.7 mM^{-1} s^{-1}) expressed in *E. coli*. Therefore, for bioconversion of PPA to L-PLA, an appropriate L-LDH with a high PPA specificity and specific activity is required. The L-*Lc*LDH1$^{Q88A/I229A}$ (Pp) in this study is a relatively good candidate.

Screening of Coenzymes Based on the Preference for NAD$^+$

After *E. coli* cells sonication, the GDH activities were measured at 50°C, respectively. Then, after incubation for 1 h at 50°C, their relative activities were measured. The *Ls*GDH^{D255C} showed the highest specific activity (11.1 ± 0.21 U/mg) and still retained 97.3% of its initial activity after incubation for 1 h at 50°C without any protective agent (**Table 3**). Because L-*Lc*LDH1$^{Q88A/I229A}$ (Pp) is acidophilic and sensitive to pH, the pH of the reaction mixture should be consistent with L-*Lc*LDH1$^{Q88A/I229A}$ (Pp). Before coupling with L-*Lc*LDH1$^{Q88A/I229A}$ (Pp), it was necessary to determine the stability of the three GDHs under optimal catalytic conditions (40°C, pH 5.0). Under the conditions of 40°C and pH 5.0, the relative enzyme activities of GDHs are shown in **Figure 4**. The relative enzyme activity of GDHs was significantly decreased with increasing reaction time, while that of SyGDH and *Ls*GDH^{D255C} was decreased at a slower reaction rate. Subsequently, the half-life values of GDHs were measured at 40°C and pH 5.0. The results showed that the half-life value of

TABLE 3 | Analysis of the activities of the three glucose dehydrogenases before and after heat treatment.

Item	SyGDH	*Bs*GDH$^{E170K/Q252L}$	*Ls*GDH^{D255C}
Before (U/mg)	0.865 ± 0.025	4.99 ± 0.17	11.1 ± 0.21
After (U/mg)	0.806 ± 0.022	4.72 ± 0.11	10.8 ± 0.29
Relative activity (%)	93.2 ± 0.88	94.6 ± 0.65	97.3 ± 1.38

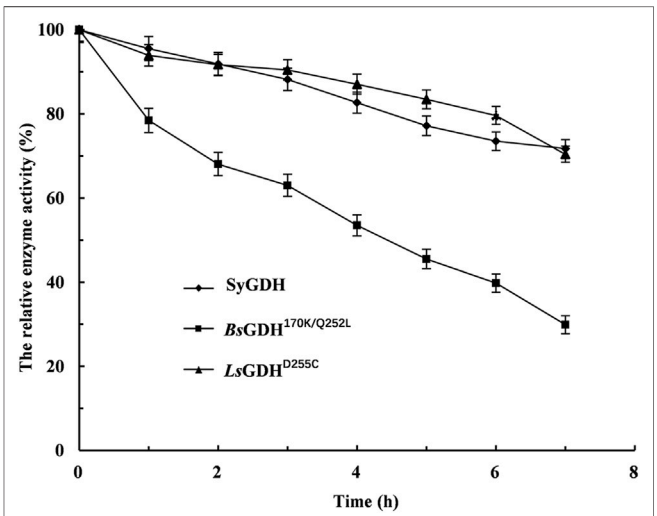

FIGURE. 4 | Effect of the time of heat treatment on the stability of glucose dehydrogenases under the optimal catalytic conditions of 40°C and pH 5.0. ◆, the cell lysate of induced *E. coli*/Sy*gdh*; ■, the cell lysate of induced *E. coli*/*Bsgdh*$^{170k/Q252L}$; ▲, the cell lysate of induced *E. coli*/*Lsgdh*^{D255C}. Means and standard deviations of triplicate experiments are shown.

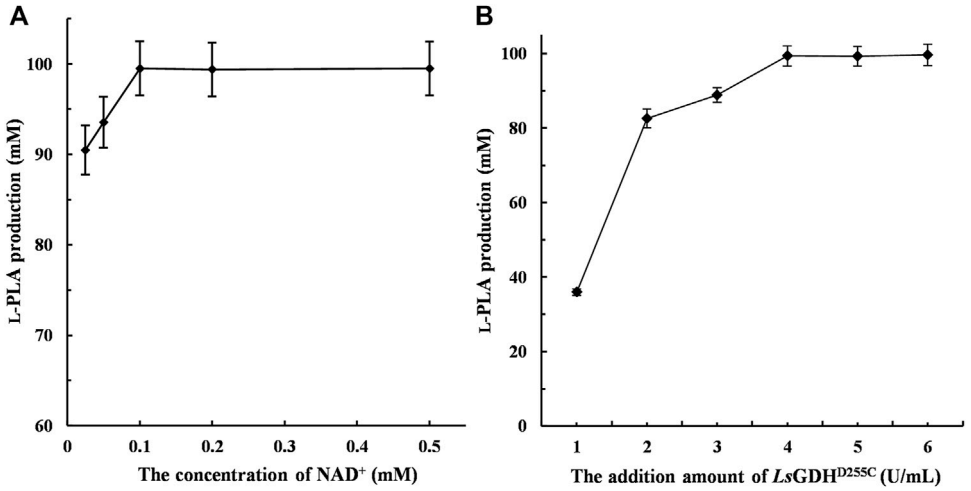

FIGURE. 5 | Effect of the concentration of NAD^+ and *Ls*GDH^{D255C} on L-phenyllactic acid (L-PLA) production. **(A)** Effect of the concentration of NAD^+ on L-PLA production. **(B)** Effect of the *Ls*GDH^{D255C} amount on L-PLA production. The bioconversion was conducted in 50 mM sodium acetate–acetate buffer (pH 5.0) containing 100 mM PPA and 120 mM glucose at 40°C for 1 h. Means and standard deviations of triplicate experiments are shown.

Bs$GDH^{170k/Q252L}$ was 4.5 h, which was the lowest of the three GDHs and shorter than that of L-*Lc*$LDH1^{Q88A/I229A}$ (Pp) (6.1 h). The half-life value of *Ls*GDH^{D255C} was 18.5 h, longer than that of SyGDH (13.8 h). Combined with the latest research results of our team on SyGDH, the K_m and catalytic efficiency (k_{cat}/K_m) of SyGDH towards $NADP^+$ were 0.67 mM and 104.0 $mM^{-1}s^{-1}$, respectively, while they were 157.9 mM and 0.64 $mM^{-1}s^{-1}$ towards NAD^+, suggesting that it preferred $NADP^+$ as a coenzyme rather than NAD^+ (Hu et al., 2020). Based on the above-mentioned study, *Ls*GDH^{D255C} with its good affinity for NAD^+, high thermal stability, and acid resistance was the best choice as a coenzyme for coupling with L-*Lc*$LDH1^{Q88A/I229A}$ (Pp) to be introduced into the coenzyme regeneration system.

Optimization of Bioconversion Conditions

The large-scale production of L-PLA from PPA requires large amounts of NADH and therefore has limited applications in the industry. In this study, NADH/NAD^+ can be transformed reversibly by coupling L-*Lc*$LDH1^{Q88A/I229A}$ (Pp) with *Ls*GDH^{D225C}, thereby maintaining the intracellular redox balance. The initial activity of the reaction mixture was an important factor that affected L-PLA production. To investigate the effect of NAD^+ on L-PLA production, the concentrations of NAD^+ from 0.025 to 0.5 mM were determined as shown in **Figure 5A**. High L-PLA production was achieved in a broad range of NAD^+ from 0.025 to 0.5 mM, while the highest L-PLA production could be obtained at a low concentration of 0.1 mM.

Compared with a single-enzyme [L-$LDH1^{Q88A/I229A}$ (Pp)] reaction, no or little byproducts were generated in this coenzyme regeneration system (**Supplementary Figure S1**). Moreover, *Ls*GDH^{D225C} can be utilized to regenerate NADH because of its low-cost substrate (glucose). Therefore, the effect of adding an amount of *Ls*GDH^{D225C} on L-PLA production was determined, and it was shown that L-PLA production was significantly improved with increasing enzyme amounts of *Ls*GDH^{D225C} up to 6.0 U/ml and that the highest L-PLA production (> 99.9 mM) with over 99% yield could be obtained at a low concentration of 4.0 U/ml (**Figure 5B**).

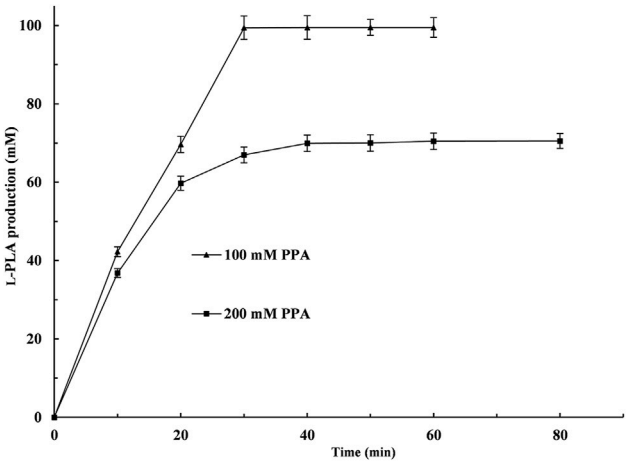

FIGURE. 6 | Time course of L-phenyllactic acid production from phenylpyruvic acid (PPA) by coupling L-*Lc*$LDH1^{Q88A/I229A}$ (Pp) with *Ls*GDH^{D225C} *in vitro*. ▲, PPA concentration of 100 mM; ■, PPA concentration of 200 mM. The bioconversion was conducted in 50 mM sodium acetate–acetate buffer (pH 5.0) containing 100 or 200 mM PPA and 120 mM glucose at 40°C within 80 min. Means and standard deviations of triplicate experiments are shown.

Under the above-mentioned optimal conditions, 100 and 200 mM PPA were used to investigate the potential for the production of L-PLA, respectively. As shown in **Figure 6**, 100 mM PPA could be almost completely hydrolyzed (99.4% yield) at 50°C within 30 min. When the PPA concentration was up to 200 mM and the reaction time was prolonged to 80 min, the yield of L-PLA was only 35.0%. Moreover, 200 mM PPA showed obvious inhibitory effects on *Ls*GDH^{D255} or/and L-$LDH1^{Q88A/I229A}$ (Pp) in the

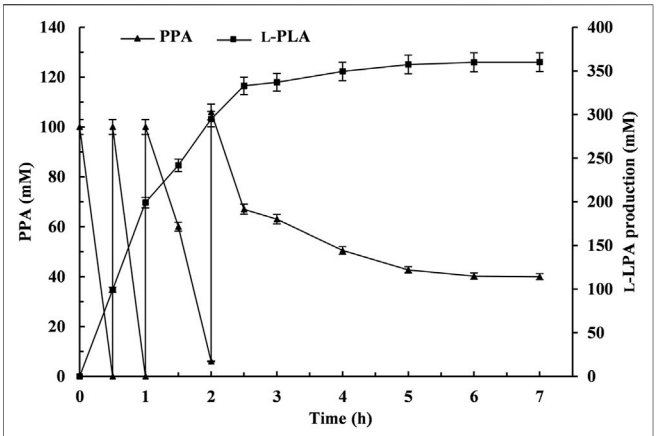

FIGURE. 7 | Time course of the fed-batch production of L-phenyllactic acid (L-PLA) by coupling L-*Lc*LDH1$^{Q88A/I229A}$ (Pp) with *Ls*GDH ^{D225C} *in vitro*. ▲, phenylpyruvic acid concentration; ■, L-PLA production. Means and standard deviations of triplicate experiments are shown.

biotransformation process. Similarly, substrate inhibition is a universal problem in an enzymatic reaction (Li et al., 2008; Lin et al., 2008; Reed et al., 2010), which can be alleviated by intermittent feeding with PPA to produce a high amount of L-PLA.

Large-Scale Production by an Enzyme Coupling System by Fed-Batch Biotransformation

The fed-batch bioconversion was carried out with 100 ml 50 mM sodium acetate–acetate buffer system (pH 5.0) containing initial PPA and glucose concentrations of 100 and 120 mM under the abovementioned optimal conditions. L-PLA was rapidly accumulated with the decrease of PPA during the first 0.5 h, and then PPA powder (4.92 g) and glucose powder (6.48 g) feedings were performed at 0.5, 1, and 2 h, respectively. Subsequently, it went on until 7 h without further additions. As shown in **Figure 7**, the reaction can be divided into two stages: rapid reaction stage (0–2.5 h) and slow reaction stage (2.5–6 h). With the feeding of the substrates PPA and glucose during the fed-batch conversion process, the L-PLA concentration was continuously increasing at a relatively high rate before the third feeding. After incubation for 6 h, 400 mM PPA was almost completely hydrolyzed, affording L-PLA with 99.9% ee_p, 90% yield (359.8 mM), and a high STY of 10 g/L/h and aTOF of 269.3 g/g/h. Additionally, the number of coenzyme cycles was 3,598, which was 3.6 times than that of 100 mM PPA (995).

Several biosynthesis methods, mostly by means of whole cells, have been reported for L-PLA production. However, highly stereoselective and efficient biosynthesis of L-PLA was rare—for example, a NADH regeneration system developed in *Lactobacillus plantarum* by expressing the *fdh* gene coding for formate dehydrogenase from *Candida boidinii* was used to convert PPA to L-PLA, but only 85.24 mM L-PLA with a low yield of 71.03% and STY of 0.9 g/L/h was produced (Li et al., 2019). Recently, 103.8 mM L-PLA (ee_p > 99.7%) was produced by using whole cells (OD_{600} = 25) of recombinant *E. coli*/Duet-*ldh*L-*gdh* co-expressing L-lactate dehydrogenase from *L. plantarum* and GDH from *Bacillus megaterium*, but the general conversion ratio of 55.8% was still unsatisfactory (Zhu et al., 2017). In our study, 359.8 mM L-PLA with 99.9% ee_p was achieved from 400 mM PPA, at an excellent conversion ratio of 90%, which were 3.47 and 1.61 times higher than that of *E. coli* reported by Zhu, respectively (Zhu et al., 2017). The above-mentioned results indicated that the cofactor-dependent biotransformation system was imperative for high productivity and conversion ratio. Moreover, the optically pure L-PLA and high conversion ratio of PPA could be reached by a fed-batch bioconversion mode in an enzyme coupling system *in vitro*.

CONCLUSION

In conclusion, a NADH regeneration system was introduced into L-PLA production. Firstly, L-LDH1$^{Q88A/I229A}$ (Pp) was expressed in *P. pastoris* GS115 successfully. Additionally, a glucose dehydrogenase variant *Ls*GDH^{D255C} with good affinity for NAD^+ was screened and successfully introduced into the coenzyme NADH regeneration system. This NADH regeneration system obviously increased the space–time yield and total turnover number of coenzyme NAD^+. Benefiting from coenzyme regeneration, the accumulation of intermediate Phe dramatically decreased, and L-PLA production dramatically increased in fed-batch bioconversion. The coenzyme NADH regeneration system can be considered a promising strategy for increasing the yield of highly optically pure L-PLA at high productivity and high stereoselectivity.

DATA AVAILABILITY STATEMENT

The original contributions presented in the study are included in the article/**Supplementary Material**, further inquiries can be directed to the corresponding author.

AUTHOR CONTRIBUTIONS

MW: Conceptualization, Methodology, Review and Editing. DZ: Project administration, Data curation and Original draft preparation. TZ, YL, WL, and XC: Formal analysis, Resources and Article modification.

FUNDING

This work was financially supported by China Postdoctoral Science Foundation (No. 2018M630522) and the Natural Science Foundation of Jiangsu Province for Youth of China (No. BK20180622).

SUPPLEMENTARY MATERIAL

The Supplementary Material for this article can be found online at: https://www.frontiersin.org/articles/10.3389/fbioe.2022.846489/full#supplementary-material

REFERENCES

Al-Jassabi, S. (2002). Purification and Kinetic Properties of Skeletal Muscle Lactate Dehydrogenase from the Lizard *agama Stellio*. *Biochemistry* 67, 786–789. doi:10.1023/A:1016300808378

Aslan, A. S., Birmingham, W. R., Karagüler, N. G., Turner, N. J., and Binay, B. (2016). Semi-Rational Design of Geobacillus Stearothermophilus L-Lactate Dehydrogenase to Access Various Chiral α-Hydroxy Acids. *Appl. Biochem. Biotechnol.* 179, 474–484. doi:10.1007/s12010-016-2007-x

Chifiriuc, M. C., Veronica, L., Dracea, O., Ditu, L.-M., Smarandache, D., Bucur, M., et al. (2007). Drastic Attenuation of *pseudomonas Aeruginosa* Pathogenicity in a Holoxenic Mouse Experimental Model Induced by Subinhibitory Concentrations of Phenyllactic Acid (PLA). *Ijms* 8, 583–592. doi:10.3390/i8070583

Ding, H., GaoLiu, F., Liu, D., Li, Z., Xu, X., Wu, M., et al. (2013). Significant Improvement of thermal Stability of Glucose 1-dehydrogenase by Introducing Disulfide Bonds at the Tetramer Interface. *Enzyme Microb. Technology* 53, 365–372. doi:10.1016/j.enzmictec.2013.08.001

Fujita, T., Nguyen, H. D., Ito, T., Zhou, S., Osada, L., Tateyama, S., et al. (2013). Microbial Monomers Custom-Synthesized to Build True Bio-Derived Aromatic Polymers. *Appl. Microbiol. Biotechnol.* 97, 8887–8894. doi:10.1007/s00253-013-5078-4

Hou, Y., Gao, B., Cui, J., Tan, Z., Qiao, C., and Jia, S. (2019). Combination of Multi-Enzyme Expression fine-tuning and Co-substrates Addition Improves Phenyllactic Acid Production with an *Escherichia coli* Whole-Cell Biocatalyst. *Bioresour. Technology* 287, 121423. doi:10.1016/j.biortech.2019.121423

Hu, D., Wen, Z., Li, C., Hu, B., Zhang, T., Li, J., et al. (2020). Characterization of a Robust Glucose 1-dehydrogenase, SyGDH, and its Application in NADPH Regeneration for the Asymmetric Reduction of Haloketone by a Carbonyl Reductase in Organic Solvent/buffer System. *Process Biochem.* 89, 55–62. doi:10.1016/j.procbio.2019.09.037

Jia, J., Mu, W., Zhang, T., and Jiang, B. (2010). Bioconversion of Phenylpyruvate to Phenyllactate: Gene Cloning, Expression, and Enzymatic Characterization of D- and L1-Lactate Dehydrogenases from *Lactobacillus Plantarum* SK002. *Appl. Biochem. Biotechnol.* 162, 242–251. doi:10.1007/s12010-009-8767-9

Kano, S., Yuasa, Y., Yokomatsu, T., and Shibuya, S. (1988). Highly Stereocontrolled Synthesis of the Four Individual Stereoisomers of Statine. *J. Org. Chem.* 53, 3865–3868. doi:10.1021/jo00251a042

Li, J.-F., Li, X.-Q., Liu, Y., Yuan, F.-J., Zhang, T., Wu, M.-C., et al. (2018). Directed Modification of L - Lc LDH1, an L -lactate Dehydrogenase from Lactobacillus Casei , to Improve its Specific Activity and Catalytic Efficiency towards Phenylpyruvic Acid. *J. Biotechnol.* 281, 193–198. doi:10.1016/j.jbiotec.2018.05.011

Li, M., Meng, X., Sun, Z., Zhu, C., and Ji, H. (2019). Effects of NADH Availability on 3-phenyllactic Acid Production by *Lactobacillus Plantarum* Expressing Formate Dehydrogenase. *Curr. Microbiol.* 76, 706–712. doi:10.1007/s00284-019-01681-0

Li, X. (2018). *Expression, Directed Modification of* Lactobacillus Casei *L-Lactate Dehydrogenase and its Application. (D)*. Wuxi: Jiangnan University. CNKI: CDMD:2.1018.252016.

Li, X., Jiang, B., Pan, B., Mu, W., and Zhang, T. (2008). Purification and Partial Characterization of Lactobacillus Species SK007 Lactate Dehydrogenase (LDH) Catalyzing Phenylpyruvic Acid (PPA) Conversion into Phenyllactic Acid (PLA). *J. Agric. Food Chem.* 56, 2392–2399. doi:10.1021/jf0731503

Lin, S. K. C., Du, C., Koutinas, A., Wang, R., and Webb, C. (2008). Substrate and Product Inhibition Kinetics in Succinic Acid Production by Actinobacillus Succinogenes. *Biochem. Eng. J.* 41, 128–135. doi:10.1016/j.bej.2008.03.013

Ning, Y., Yan, A., Yang, K., Wang, Z., Li, X., and Jia, Y. (2017). Antibacterial Activity of Phenyllactic Acid against *listeria Monocytogenes* and *Escherichia coli* by Dual Mechanisms. *Food Chem.* 228, 533–540. doi:10.1016/j.foodchem.2017.01.112

Reed, M. C., Lieb, A., and Nijhout, H. F. (2010). The Biological Significance of Substrate Inhibition: a Mechanism with Diverse Functions. *BioEssays* 32, 422–429. doi:10.1002/bies.200900167

Urban, F. J., and Moore, B. S. (1992). Synthesis of Optically Active 2-benzyldihydrobenzopyrans for the Hypoglycemic Agent Englitazone. *J. Heterocycl Chem.* 29, 431–438. doi:10.1002/jhet.5570290223

Vázquez-Figueroa, E., Chaparro-Riggers, J., and Bommarius, A. S. (2007). Development of a Thermostable Glucose Dehydrogenase by a Structure-Guided Consensus Concept. *Chembiochem* 8, 2295–2301. doi:10.1002/cbic.200700500

Wang, M., Zhu, L., Xu, X., Wang, L., Yin, R., and Yu, B. (2016). Efficient Production of Enantiomerically Pure D-Phenyllactate from Phenylpyruvate by Structure-Guided Design of an Engineered D-Lactate Dehydrogenase. *Appl. Microbiol. Biotechnol.* 100, 7471–7478. doi:10.1007/s00253-016-7456-1

Xu, G.-C., Zhang, L.-L., and Ni, Y. (2016). Enzymatic Preparation of D-Phenyllactic Acid at High Space-Time Yield with a Novel Phenylpyruvate Reductase Identified from *Lactobacillus* Sp. CGMCC 9967. *J. Biotechnol.* 222, 29–37. doi:10.1016/j.jbiotec.2015.12.011

Yang, J. E., Park, S. J., Kim, W. J., Kim, H. J., Kim, B. J., Lee, H., et al. (2018). One-step Fermentative Production of Aromatic Polyesters from Glucose by Metabolically Engineered *Escherichia coli* Strains. *Nat. Commun.* 9, 79. doi:10.1038/s41467-017-02498-w

Yu, T., Li, J.-F., Zhu, L.-J., Hu, D., Deng, C., Cai, Y.-T., et al. (2015). Reduction of *M*-Chlorophenacyl Chloride Coupled with Regeneration of NADPH by Recombinant *Escherichia coli* Cells Co-expressing Both Carbonyl Reductase and Glucose 1-dehydrogenase. *Ann. Microbiol.* 66, 343–350. doi:10.1007/s13213-015-1114-1

Zhang, Y., Huang, Z., Du, C., Li, Y., and Cao, Z. a. (2009). Introduction of an NADH Regeneration System into *Klebsiella Oxytoca* Leads to an Enhanced Oxidative and Reductive Metabolism of Glycerol. *Metab. Eng.* 11, 101–106. doi:10.1016/j.ymben.2008.11.001

Zheng, Z., Ma, C., Gao, C., Li, F., Qin, J., Zhang, H., et al. (2011). Efficient Conversion of Phenylpyruvic Acid to Phenyllactic Acid by Using Whole Cells of *Bacillus Coagulans* SDM. *Plos One* 6, e19030. doi:10.1371/journal.pone.0019030

Zheng, Z., Sheng, B., Gao, C., Zhang, H., Qin, T., Ma, C., et al. (2013). Highly Stereoselective Biosynthesis of (R)-α-hydroxy Carboxylic Acids through Rationally Re-designed Mutation of D-Lactate Dehydrogenase. *Sci. Rep.* 3, 3401. doi:10.1038/srep03401

Zheng, Z., Zhao, M., Zang, Y., Zhou, Y., and Ouyang, J. (2015). Production of Optically Pure L-Phenyllactic Acid by Using Engineered *Escherichia coli* Coexpressing L-Lactate Dehydrogenase and Formate Dehydrogenase. *J. Biotechnol.* 207, 47–51. doi:10.1016/j.jbiotec.2015.05.015

Zhu, Y., Wang, Y., Xu, J., Chen, J., Wang, L., and Qi, B. (2017). Enantioselective Biosynthesis of L-Phenyllactic Acid by Whole Cells of Recombinant *Escherichia coli*. *Molecules* 22, 1966. doi:10.3390/molecules22111966

Conflict of Interest: The authors declare that the research was conducted in the absence of any commercial or financial relationships that could be construed as a potential conflict of interest.

frontiers in Bioengineering and Biotechnology

REVIEW
published: 08 March 2022
doi: 10.3389/fbioe.2022.843887

Biosynthetic Pathway and Metabolic Engineering of Succinic Acid

Xiutao Liu[1], Guang Zhao[2], Shengjie Sun[1], Chuanle Fan[3,4], Xinjun Feng[3] and Peng Xiong[1]**

[1]School of Life Sciences and Medicine, Shandong University of Technology, Zibo, China, [2]State Key Lab of Microbial Technology, Shandong University, Qingdao, China, [3]CAS Key Laboratory of Biobased Materials, Qingdao Institute of Bioenergy and Bioprocess Technology, Chinese Academy of Sciences, Qingdao, China, [4]School of Chemical Engineering, University of Chinese Academy of Sciences, Beijing, China

Succinic acid, a dicarboxylic acid produced as an intermediate of the tricarboxylic acid (TCA) cycle, is one of the most important platform chemicals for the production of various high value-added derivatives. As traditional chemical synthesis processes suffer from nonrenewable resources and environment pollution, succinic acid biosynthesis has drawn increasing attention as a viable, more environmentally friendly alternative. To date, several metabolic engineering approaches have been utilized for constructing and optimizing succinic acid cell factories. In this review, different succinic acid biosynthesis pathways are summarized, with a focus on the key enzymes and metabolic engineering approaches, which mainly include redirecting carbon flux, balancing NADH/NAD^+ ratios, and optimizing CO_2 supplementation. Finally, future perspectives on the microbial production of succinic acid are discussed.

Keywords: succinic acid, biosynthesis pathways, metabolic engineering, CO2 fixation, NADH/NAD + ratio

OPEN ACCESS

Edited by:
Xiao-Jun Ji,
Nanjing Tech University, China

Reviewed by:
Jiangfeng Ma,
Nanjing Tech University, China
Katja Bettenbrock,
Max Planck Society, Germany

****Correspondence:***
Xinjun Feng
fengxj@qibebt.ac.cn
Peng Xiong
xiongp@sdut.edu.cn

Specialty section:
This article was submitted to Bioprocess Engineering, a section of the journal Frontiers in Bioengineering and Biotechnology

Received: *27 December 2021*
Accepted: *16 February 2022*
Published: *08 March 2022*

Citation:
Liu X, Zhao G, Sun S, Fan C, Feng X and Xiong P (2022) Biosynthetic Pathway and Metabolic Engineering of Succinic Acid. Front. Bioeng. Biotechnol. 10:843887. doi: 10.3389/fbioe.2022.843887

1 INTRODUCTION

Succinic acid is a C4-dicarboxylic acid produced as a key intermediate of the tricarboxylic acid (TCA) cycle. As a widely investigated high-value chemical, it has numerous applications in the fields of agriculture, green solvents, pharmaceuticals, and biodegradable plastics. It can also be chemically converted into a variety of important industrial chemicals such as 1,4-butanediol, butadiene, and tetrahydrofuran. Succinic acid has been identified as one of the 12 value-added bio-based platform chemicals by the United States Department of Energy (DOE) (Werpy et al., 2004). The market potential of succinic acid and its direct derivatives is estimated to be as high as 245,000 tons per year, while the market size of succinic acid-based polymers is expected to be 25 million tons per year (Bozell and Petersen, 2010). In traditional chemical synthesis methods, maleic anhydride from petrochemical feedstocks serves as the key substrate for succinic acid, and Ni or Pd-based catalysts have been employed for the hydrogenation of maleic anhydride to succinic acid (Zhang et al., 2020). Although the conversion rate is high, many problems still exist, such as the complex operations required for synthesis, the high-energy consumption, and the harsh reaction conditions (Louasté and Eloutassi, 2020; Zhang et al., 2020). Therefore, much attention has focused on succinic acid biosynthesis, and to date, some efficient succinic acid bio-producers have been successfully applied for industrial purposes (Willke and Vorlop, 2004; Kequan et al., 2008). Compared with chemical processing, the raw materials of biosynthesis are more widely availableand lower in cost. Crude glycerol (Gao et al., 2016), food processing waste (Li et al., 2019), corn fiber (Chen et al., 2011), cassava root (Thuy et al., 2017), lignocellulose hydrolyzate (Zhang et al., 2020), maltose syrup, and other renewable biomass resources are potential sources of the raw materials for these reactions. Significantly, CO_2 fixation and utilization processes are an integral part of succinic acid biosynthesis

TABLE 1 | Comparison of different succinic acid biosynthetic pathways.

Pathways	rTCA (PPC)	rTCA (PCK)	rTCA (PYC)	rTCA (MAE)	oTCA pathway	GAC pathway	3HP pathway
Precursors	PEP CO_2	PEP CO_2	PEP CO_2	PEP CO_2	Acetyl-CoA OAA	Acetyl-CoA OAA	Acetyl-CoA CO_2
Reaction steps	4	4	5	4	5	3	6
ATP/SA (mol/mol)	0	+1	0	+1	+1	0	–2
NADH/SA (mol/mol)	–2	–2	–2	–2	+2	0	–3
CO_2/SA (mol/mol)	–1	–1	–1	–1	+2	0	–2
CO_2-fixing enzymes	PPC	PCK	PYC	MAE	NE	NE	ACC, PCC

SA: succinic acid.
NE: non-existent.
Abbreviationr: TCA, the reductive branch of the TCA, cycle; oTCA, the oxidative branch pathway of the TCA, cycle; GAC, the glyoxylate shunt pathway.
(–) means to consume (+) means to produce.

TABLE 2 | Production capacity of succinic acid by main natural microbes.

Strains	Substrate	Fermentation type	Titer (g/L)	Productivity (g/h/L)	Yield (g/g)	References
A. succinogenes FZ53	Glucose	Anaerobic batch	105.8	1.36	0.82	Pateraki et al. (2016)
A. succinogenes 130 Z	Cheese whey	Anaerobic batch	21.5	0.44	0.57	Wan et al. (2008)
A. succinogenes 130 Z	Glucose	Anaerobic batch	67.2	0.80	N/A	Guettler et al. (1996)
A. succinogenes 130 Z	Xylose	Anaerobic batch	38.4	0.94	0.70	Michael et al. (2015)
A. succinogenes CGMCC1593	Glucose	Anaerobic batch	60.2	1.30	0.75	Wang et al. (2011)
A. succinogenes CGMCC1593	Cane molasses	Anaerobic batch	50.6	0.84	0.80	Liu et al. (2008)
A. succinogenes NJ113	Glucose	Anaerobic batch	35.4	N/A	0.73	Chen et al. (2018)
A. succinogenes CGMCC1593	Straw hydrolysate	Anaerobic batch	45.5	0.19	0.81	Zheng et al. (2009)
A. succinogenes CGMCC2650	Cotton stalk	Anaerobic batch	15.8	0.62	1.23	Li et al. (2010)
A.succiniciproducens ATCC53488	Glucose	Anaerobicbatch	1.5	0.75	N/A	Meynial-Salles et al. (2010)
M. succiniciproducens MBEL55 E	Whey	Anaerobic batch	13.4	1.18	0.71	Lee et al. (2003)
M. succiniciproducens MBEL55 E	Glucose	Anaerobic batch	14	1.87	0.7	Lee et al. (2002)
M. succiniciproducens MBEL55 E	Wood hydrolysate	Anaerobic batch	11.73	1.17	0.56	Kim et al. (2004)
B. succiniciproducens DD1	Glucose	Anaerobic batch	20	0.68	0.49	Becker et al. (2013)
E. coli	Glucose	Anaerobic batch	1.18	0.13	0.12	Gokarn et al. (1998)
C. glutamicum R	Glucose	Micro-aerobic, fed-batch with membrane for cell recycling	23.0	3.63	0.19	Okino et al. (2005)

in almost all pathways (**Table 1**). Theoretically speaking, the biological production of 1 kg of succinic acid can fix at least 0.37 kg CO_2, which presents an environmental benefit to the use of succinic acid biosynthesis upstream of the production of other chemicals (Wang et al., 2011).

Many anaerobic and facultative anaerobic microbes produce succinic acid as their fermentation end product. These succinic acid-producing strains can be divided into two categories, namely, the natural succinic acid producers (**Table 2**) and the metabolic engineering succinic acid producers (**Table 3**). The natural succinic acid producers mainly include *Actinobacillus succinogenes* (Thuy et al., 2017), *Anaerobiospirillum succiniciproducens* (Meynial-Salles et al., 2010), *Mannheimia succiniciproducens* (Lee et al., 2003), *Basfia succiniciproducens* (Choi et al., 2015) and *Escherichia coli* (Thakker et al., 2011). Among these strains, *A. succinogenes* and *A. succiniciproducens* were the first identified natural overproducers of succinic acid (Bretz and Kabasci, 2012). *A. succinogenes*, originally isolated from bovine rumen, is a Gram-negative, capnophilic, facultative anaerobic bacterium, and has been used as a succinic acid-producing chassis since 1981 by the Michigan Biotechnology Institute (MBI). *A. succinogenes* has a better tolerance of high concentrations of succinic acid than other strains (Wan et al., 2008) and can utilize extensive carbon sources, including glucose, xylose, glycerol, cellobiose, cheese whey (Wan et al., 2008), cane molasses (Liu et al., 2008), straw hydrolysate (Zheng et al., 2009), and crop stalk wastes. However, *A. succinogenes* also has some drawbacks as a succinic acid production platform, such as numerous auxotrophies and lack of useful genetic tools (Ahn et al., 2016). *A. succiniciproducens* is a Gram-negative and strictly

TABLE 3 | Production capacity of succinic acid by metabolic engineering strains in selected papers.

Strains	Genotype	Substrate	Fermentation type	Titer (g/L)	Productivity (g/h/L)	Yield (g/g)	References
E. coli W1485	*ΔpflAB::Cm, ΔldhA::Kan, ΔptsG,* expression of *E. coli cra* gene with mutation at R57K, A58G, G59Q, R60Q, S75H, T76Y, D148I, R149I	Glucose	Two-stage fed-batch	79.8	1.00	0.78	Zhu et al. (2016)
E. coli W1485	*ΔackA-pta, ΔiclR, ΔpoxB, ΔmgsA, ΔsdhA::kan*^{R}, expression of *C.glutamicum* ATCC13032 *pyc* gene	Glucose	Aerobic fed-batch	36.1	0.69	0.37	Yang et al. (2014)
E. coli DY329	*ΔackA, Δpta, ΔldhA, ΔpstG*, expression of *E. coli mdh* gene	Glucose	Two-stage fed-batch	32.3	0.40	-	Zhu et al. (2014)
E. coli SD121	Expression of *ppc*; deletion of *pflB*, *ldhA* and *pts*G	Glucose	Dual-phase fed- batch	116.2	1.55	1.13	Wang et al. (2011)
E. coli AFP111	Deletion of *pflB, ldhA* and *ptsG*	Glucose	Dual-phase fed- batch	101.2	1.89	1.07	Jiang et al. (2010)
E. coli MG1655	*ΔadhE, ΔldhA,* expression of *Lactococcus lactis pyc* gene	Glucose	Anaerobic fed-batch	15.6	0.65	0.85	Sánchez et al. (2005)
E. coli HL27659k (pKK313)	*ΔsdhAB, ΔackA-pta, ΔpoxB, ΔiclR, ΔptsG,* expression of *Sorghum vulgare pepc* gene	Glucose	Aerobic fed-batch	58.3	0.99	0.61	Lin et al. (2005d)
E. coli NZN111	Expression of *Ascaris suummaeA*gene	Glucose	Anaerobic shake flask	7.07	-	-	Stols et al. (1997)
E. coli JCL1208	lacks the *lac* operon but contains a chromosomally inserted*lacI*^{q}gene, expression of *E. coli ppc*under *tac* promoter	Glucose	Anaerobic batch	10.7	0.59	0.30	Millard et al. (1996)
E. coli K-12	*Δppc,* expression of *A. succinogenes pckA* gene	Glucose	Anaerobic batch	20.2	-	-	Millard et al. (1996)
M. succiniciproducens MBEL55 E	*ΔldhA::Km*^{r}*, ΔpflB::Cm*^{r}*, Δpta-ackA::Sp*^{r}	Glucose	Anaerobic fed-batch	52.4	1.80	1.16	Lee et al. (2006)
M. succiniciproducens PALK	*ΔldhA::Km*^{r}*, Δpta-ackA::Sp*^{r}*,* expression of *C. glutamicummdh*gene	Glucose	Two-stage fed-batch	134.3	21.3	0.81	Ahn et al. (2020)
M. succiniciproducens PALFK	Deletion of *ldhA, fruA* and *pta-ackA*	Sucrose and glycerol	Anaerobic fed-batch	78.4	6.02	1.07	Lee et al. (2016)
M. succiniciproducens LPK7	Expression of *fdh;* deletion of *ldhA, pflB* and *pta-ackA*	Sucrose and formic acid	Anaerobic fed-batch	76.1	4.08	-	Ahn et al. (2017)
*S. cerevisiae*strain PMCFfg	*MATa ura3-52, Δhis3, Δfum1, Δgpd1, Δpdc1, Δpdc5, Δpdc6* (YIP-PYC2MDH3R, pRS313CF)	Glucose At PH 3.8	Aerobic batch	13.0	0.11	-	Yan et al. (2014)
*S.cerevisiae*CEN. PK 2-1C	*Δsdh2,* expression of *Rhizopus oryzaepyc* gene	Glucose	Anaerobic shake flask	0.8	0.01	-	Chen et al. (2019)
Y. lipolytica Y-3314	Expression of *pck, scs2;* deletion of *ach*	Glycerol	Aerobic fed-batch	110.7	0.80	0.53	Cui et al. (2017)
Y. lipolytica PGC01003	Deletion of *sdh5*	Glycerol	Aerobic fed-batch	198.2	-	-	Li et al. (2017)
Y. lipolytica Y-3314	Deletion of *sdh1*, *sdh2* and *suc2*	Glycerol	Aerobic fed-batch	45.4	0.28	0.36	Yuzbashev et al. (2010)
*C. glutamicum*ATCC 13032	*Δldh, Δpta-ackA, ΔactA, ΔpoxB, pyc*^{P458}*, Δpck*_P_{tuf}*::Ms.pckG,* P_{tuf}*::ppc, ΔptsG*,expression of *C. glutamicum NCgl0275* gene	Glucose	Two-stage fed-batch	152.2	0.95	1.1	Chung et al. (2017)
C. glutamicum	Expression of *pyc;* deletion of *ldhA*	Glucose	Micro-aerobic fed- batch with membrane for cell recycling	146.0	3.17	0.92	Okino et al. (2008)
C. glutamicum BOL	Expression of *pyc, fdh* and *gapA;* deletion of *cat, pqo, ldhA* and *pta-ackA*	Glucose	Dual phase fed- batch	133.8	2.53	1.09	Litsanov et al. (2012)

anaerobic bacterium (Wang et al., 2011) that produces succinic acid and acetate as its major end products, while producing lactate and ethanol as minor products, depending on culture conditions (Lee et al., 1999). Compared with *A. succinogenes*, *A. succiniciproducens* shows only weak salt tolerance (Bretz and Kabasci, 2012), which partly hinders the wide application of this strain. *M. succiniciproducens*, also isolated from bovine rumen, is a facultatively anaerobic, mesophilic, non-motile, non-spore-forming, Gram-negative bacterium, and can utilize a wide variety of carbon sources, similar to *A. succinogenes* (Lee et al., 2002). This bacterium has an excellent CO_2-fixing pathway and can produce succinic acid as a major end product through simple anaerobic fermentation. Nevertheless, this species also has some disadvantages, such as its pH sensitivity and auxotrophy for several amino acids and vitamins (Ahn et al., 2016). *B. succiniciproducens*, a new member of the family

Pasteurellaceae, was isolated from the rumen of a German cow in 2008, and shows high similarity to *M. succiniciproducens* (Ahn et al., 2016). In the 2,363 open reading frames (ORFs) of *B. succiniciproducens* DD1 and the 2,380 ORFs of *M. succiniciproducens* MBEL55 E, 2006 ORFs were found to be homologous (Kuhnert et al., 2010). This bacterium can export succinic acid as an end product and has been used as a succinic acid-producing chassis by the Succinity Company (a joint venture of BASF and Purac). Wild-type *E. coli* can also produce minor amounts of succinic acid under anaerobic conditions, whereas under aerobic conditions succinic acid is formed only as an intermediate of the TCA cycle unless the glyoxylate bypass is operating (Thakker et al., 2012). **Table 2** shows a summary of bio-based succinic acid production by different wild-type strains with various fermentation substrates reported in selected papers. Among this list, *A. succinogenes*, *B. succiniciproducens*, and *M. succiniciproducens* are the most promising wild-type bacterial strains which have relatively high yield and productivity, but they still cannot satisfy industrial production requirements. Most wild-type strains show a tendency to degenerate (Lin et al., 2005b), pH sensitivity and auxotrophy, and they require a rich, complex medium for efficient growth. Thus, further optimization and improvement is needed before natural succinic acid producers can be used for industrial purposes.

Metabolic engineering strategies, however, is a promising way of generating succinic acid-producing strains, using not only natural succinic acid producers, but also unnatural producers, such as *Corynebacterium glutamicum, Yarrowia lipolytica, Saccharomyces cerevisiae, and Pichia kudriavzevii* (**Table 3**). Taking *C. glutamicum* as an example, the highest concentration of 152.2 g/L of succinic acid with a yield and productivity of 1.1 g/g glucose and 1.11 g/L/h, respectively, were achieved by the engineered strain S071 (*Δldh*, *Δpta-ackA*, *ΔactA*, *ΔpoxB*, *pyc*^{P458}, *Δpck*_P_{tuf}:*Ms.pckG*, P_{tuf}:*ppc*, *ΔptsG*)/pGEX4-NCgl0275 under anaerobic conditions. Compared with the initial strain, this engineered strain showed more than 30-fold increase in succinic acid production. (Chung et al., 2017). In the case of *Y. lipolytica*, the highest succinic acid concentration of 110.7 g/L was achieved, by the engineered strain *Y. lipolytica* PGC202 (*ΔSdh5*, *ΔAch1*, with *pck* from *S. cerevisiae* overexpression and *SCS2* from *Y. lipolytica* overexpression) in fed-batch cultivation using glycerol without pH control. Compared with the initial strain, this engineered strain showed 4.3-fold increase and has the highest fermentative succinic acid titer achieved in yeast at low pH condition (Cui et al., 2017). For *E. coli*, metabolic engineering strategies could be used to improve its succinic acid biosynthesis ability. Wu et al. constructed an engineered strain *E. coli* K12 (*Δpfl, ΔldhA, ΔptsG*)/pMD19T-*gadBC*. This strain could produce 32.01 g/L succinic acid at pH 5.6, which was 2.6-fold higher than the initial strain (Wu et al., 2017). These metabolic engineering producers have shown high production efficiency, demonstrating the great potential of the production of industrially competitive bio-based succinic acid.

In this review, several different typical succinic acid biosynthetic pathways reported in recent years are summarized, and the main metabolic engineering strategies to improve the production efficiency are presented in detail. Additionally, the main challenges as well as the future perspectives for succinic acid biosynthesis are discussed.

2 BIOSYNTHETIC PATHWAY OF SUCCINIC ACID

To date, seven natural or artificial succinic acid biosynthesis pathways have been reported in the literature (**Figure 1**), including the reductive branch of the TCA cycle coupled to PEP carboxylase (PPC) pathway, the reductive branch of the TCA cycle coupled to PEP carboxykinase (PCK) pathway, the reductive branch of the TCA cycle coupled to pyruvate carboxylase (PYC) pathway, the reductive branch of the TCA cycle coupled to malic enzyme (MAE) pathway, the glyoxylate shunt pathway, the oxidative branch pathway of the TCA cycle, and the 3-hydroxypropionate cycle for the production of succinic acid. Each biosynthesis pathway has its own characteristics that determine the scope of their unique application (**Table 1**). The reductive branch pathways of the TCA cycle are the main succinic acid-producing approaches under anaerobic conditions (Zhu and Tang, 2017), while the other pathways can be effective under aerobic conditions. In the next subsections, these different pathways and their specific features are discussed.

2.1 Anaerobic Succinic Acid-Producing Pathways

The reductive branch of the TCA cycle coupled to PEP carboxylase (PPC) for succinic acid formation (rTCA (PPC) pathway), which exists in almost all microbes, is one of the most commonly used processes in bio-based succinic acid production. In this pathway, PEP carboxylase (PPC) converts PEP and CO_2 into oxaloacetate, which is then converted into malate catalyzed by malate dehydrogenase (MDH). Then, malate is transformed into fumarate by fumarate hydratase (FumABC). Finally, fumarate and NADH are turned into succinic acid catalyzed by fumarate reductase (FrdABCD). Through this pathway, succinic acid is synthesized from PEP and CO_2 at a stoichiometric ratio of 1:1. Among the components in this process, PPC (EC 4.1.1.31) plays a critical role in CO_2 fixation. Taking *E. coli* as an example, PPC is produced during growth on glycolytic substrates (Keseler et al., 2011). PPC catalyzes the carboxylation of PEP with bicarbonate to form oxaloacetate and inorganic phosphate using Mg^{2+} as a cofactor (Millard et al., 1996; Kai et al., 1999). The main function of PPC is to replenish the oxaloacetate consumed by biosynthetic reactions, and under anaerobic fermentation conditions, it can direct a portion of PEP to succinic acid (Millard et al., 1996). Studies have shown that under a CO_2 atmosphere, *E. coli Δppc* strains grow slower and more poorly than wild-type strains in glucose-based medium (40% reduction in biomass and more than 70% reduction in succinic acid production) (Millard et al., 1996; Ahn et al., 2020). PPC also exhibits high catalytic velocity (the enzymatic activity is 250 μmol/min/mg) and high substrate affinity (the K_m value for HCO_3^- is 0.1 mM and the K_m value

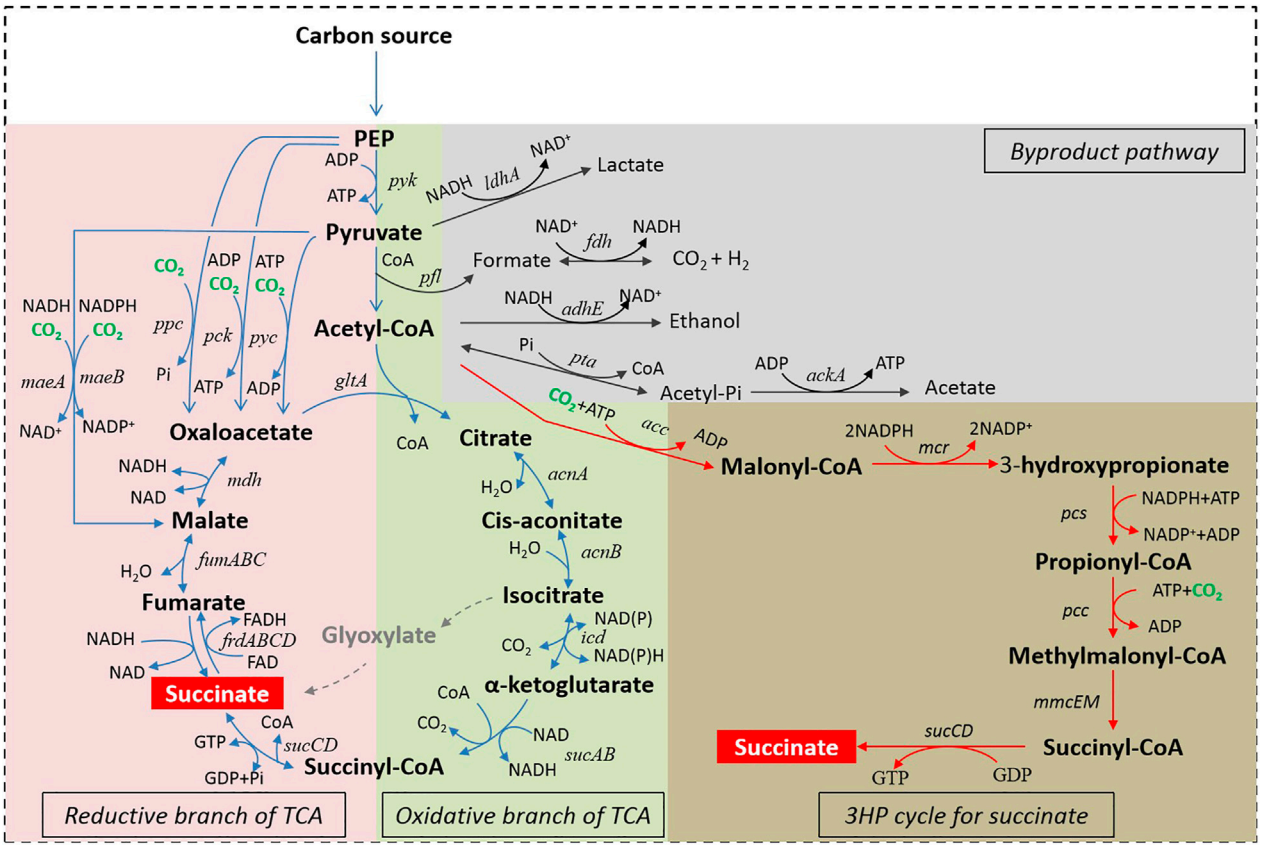

FIGURE 1 | Succinic acid production biosynthetic pathways. Abbreviations: PEP, Phosphoenolpyruvic acid; *ldhA*, lactic dehydrogenase; *pfl*, pyruvate formate lyase; *fdh*, formate dehydrogenase; *adhE*, alcohol dehydrogenase; *pta*, phosphotransacetylase; *ackA*, acetate kinase; *gltA*, citrate synthetase; *acnAB*, aconitase; *icd*, isocitrate dehydrogenase; *sucABCD*, succinyl-CoA synthetase; *frdABCD*, succinate dehydrogenase; *fumABC*, fumarate hydratase; *mdh*, malate dehydrogenase; *ppc*, PEP carboxylase; *pck,* PEP carboxykinase; *pyc*, pyruvate carboxylase; *pyk*, pyruvate kinase; *maeAB*, malic enzyme; *acc*, acetyl-CoA carboxylase; *mcr*, malonyl-CoA reductase; *pcc*, propionyl-CoA carboxylase; *pcs*, propionyl-CoA synthase; *mmcEM*, methylmalonyl-CoA epimerase and mutase.

for PEP is 0.19 mM), which is conducive to succinic acid biosynthesis (Millard et al., 1996; Kai et al., 1999; Tan et al., 2013). Millard et al. evaluated the effect of PPC on the amount of succinic acid produced in *E. coli* under control of the *tac* promoter. The engineered strain that overexpressed PPC showed a 3.5-fold increase in the concentration of succinic acid, from 3.0 g/L in a control culture to 10.7 g/L, and the yield showed a 3.75-fold increase, from 0.12 mol/mol glucose to 0.45 mol/mol glucose (**Table 3**) (Millard et al., 1996). There seemed to be a positive correlation between PPC activity and succinic acid production, but excessive PPC activity was detrimental to cell growth and succinic acid formation (Tan et al., 2013). Tan et al. found higher PPC activity along with higher succinic acid production, when the PPC activity was equal to or less than 0.47 U/mg protein (Tan et al., 2013). The reason may have been that the overexpression of PPC caused a shortage of PEP. PEP is also essential for the PEP-PTS (phosphoenolpyruvate-phosphotransferase) system, which has both a transport function and an extensive regulatory function. And the shortage of PEP will lead to a compromise in glucose uptake and cell growth (Gokarn et al., 2000). Therefore, the regulation of PPC expression was significant when using the PPC dependent biosynthesis pathway for succinic acid production.

The reductive branch of the TCA cycle coupled to PEP carboxykinase (PCK) for succinic acid formation (rTCA (PCK) pathway), is another representative succinic acid biosynthesis route that mainly exists in bacteria and fungi, especially in some natural succinic acid producers (Werf et al., 1997; Lee et al., 2006). This process is almost the same as the PPC-dependent pathway, except for the key CO_2-fixation enzyme. In this pathway, the key CO_2-fixation enzyme is PCK (EC 4.1.1.31) which can catalyze the carboxylation of PEP with bicarbonate and ADP to form oxaloacetate and ATP. Compared with PPC, the PCK catalytic process is accompanied by the production of energy, and as such it is more suitable for cell growth and succinic acid production (Zhu and Tang, 2017). However, the overexpression of PCK in *E. coli* at low CO_2 concentrations in fact has no effect on succinic acid biosynthesis. PCK can be valuable for succinic acid production but only in the presence of high HCO_3^- concentrations (Millard et al., 1996; Kwon et al., 2006). There are two possible explanations for this result: 1) PCK has low HCO_3^- affinity (the K_m value for HCO_3^- is 13 mM, 130 times larger than that of PPC, the *K*m value for PEP is 0.07 mM and the

*K*m value for ADP is 0.05 mM); 2) PCK has low catalytic velocity (the enzymatic activity is 28 μmol/min/mg, which is just 11.2% of the PPC activity) (Krebs and Bridger, 1980; Zhang et al., 2009a; Tan et al., 2013). Previous studies have demonstrated that when 20 g/L $NaHCO_3$ was added to a culture, the succinic acid titer in recombinant *E. coli* overexpressing PCK was 2.2-fold higher than a wild-type strain, from 6.4 g/L in a control culture to 14.2 g/L (Kwon et al., 2006). Kim et al. found that in wild-type *E. coli* K12 cells, PCK overexpression had no effect on succinic acid fermentation, but the overexpression of PCK in an engineered *E. coli* K12 *Δppc* strain was 6.5-fold higher than *E. coli* K12 *Δppc*, and rose from 3.1 g/L to 20.2 g/L (**Table 3**) (Millard et al., 1996). In addition, the PCK activity was closely related to succinic acid biosynthesis. Tan et al. reported that the succinic acid titer and yield were positively correlated with the PCK activity. A 16-fold increase in PCK activity resulted in a 57-fold increase in succinic acid titer (from 4 to 226 mM) in *E. coli* Suc-T108 (Tan et al., 2013). In some natural succinic acid producers, such as *A. succiniciproducens* (Millard et al., 1996), *M. succiniciproducens* (Hong et al., 2004; Lee et al., 2006), and *A. succinogenes* (Millard et al., 1996; Werf et al., 1997), PCK is mainly employed in CO_2 fixation and cell growth instead of PPC. Taking *M. succiniciproducens* as an example, genes encoding PPC, PCK, or MAE were separately disrupted, and fermentation results showed that strains with PPC or MAE deletion did not show much effect on succinic acid productivity or cell growth, while the strain with PCK inactivation showed severe growth retardation and a remarkable decrease in succinic acid productivity (Lee et al., 2006). This result was significant because although PCK has a high K_m value for HCO_3^-, it still plays a major role in succinic acid biosynthesis in *M. succiniciproducens*. Compared with *M. succiniciproducens*, the indispensable feature of PCK was not observed in wild-type *E. coli*. It might have been due to the differences in the internal concentration of HCO_3^- in these two organisms (Millard et al., 1996). These results also suggests that the optimization of a CO_2 delivery system and the amelioration of the intracellular inorganic carbon concentration may be a good choice for improving the PCK depended succinic acid biosynthesis route (Xiao et al., 2017). Except for PCK, MDH was reported to be another rate-limiting enzyme for succinic acid production (Hong et al., 2004; Ahn et al., 2020). In *M. succiniciproducens*, MDH reduces oxaloacetate to malate using NADH as a cofactor, but it shows low specific activity and strong uncompetitive inhibition towards oxaloacetate (Ahn et al., 2020). *In silico* simulation suggested that MDH is instrumental in succinic acid production (Ahn et al., 2020). Jung et al. reported biochemical and structural analyses of various MDH variants and discovered a key amino acid residue (Gly-11) required for high kinetic efficiency in MDH. After screening, a valuable MDH mutant (MDH-G11Q) was obtained, which had high enzyme activity (2.9-fold increase in activity) and less substrate inhibition (6.4-fold increase in k_i) compared with a wild type MDH. Furthermore, the application of this MDH-G11Q mutant in engineering bacteria led to a 1.4-fold increase in succinic acid production, indicating the significance of enzyme optimization in strain development (Choi et al., 2016; Ahn et al., 2020).

The reductive branch of the TCA cycle coupled to pyruvate carboxylase (PYC) for succinic acid formation (rTCA (PYC) pathway), is widespread in fungi, plants, as well as some bacteria (Modak and Kelly, 1995), but it is absent in Enterobacteriaceae (Gokarn et al., 2000). In this pathway, PEP is first converted into pyruvate by pyruvate kinase (PYK). Then PYC (EC 6.4.1.1) catalyzes the ATP-dependent carboxylation of pyruvate to produce oxaloacetate. Oxaloacetate is further converted into succinic acid through MDH, FumABC and FrdABCD. As the key CO_2-fixation step, the reaction catalyzed by PYC also plays an anaplerotic role in the provision of oxaloacetate for maintaining the dynamic balance of the TCA cycle. In *R. etli*, the anaplerotic role of PYC has been shown to be essential for its normal growth (Jitrapakdee et al., 2008), and thus PYC can be considered to be one of the most significant regulatory enzymes in this pathway (Modak and Kelly, 1995). In most PYC catalytic reactions, acetyl-CoA acts as a positive allosteric activator (Jitrapakdee et al., 2008; Tong, 2013), except for PYC from *L. lactis*, which is regulated by the bacterial second messenger c-di-AMP (Choi et al., 2017). The PYC depended route is a promising tool for succinic acid biosynthesis. Yan et al. reconstructed this pathway in *S. cerevisiae*, and found that the engineered strain showed a 19.3-fold increase in succinic acid production in shaken flasks, rising from 0.32 g/L to 6.17 g/L (Yan et al., 2014). Chen et al. reported that the overexpression of PYC from *R. oryzae* in a *S. cerevisiaeΔsdh2* strain resulted in a 1.2-fold increase in the concentration of succinic acid, from 0.709 g/L to 0.841 g/L (**Table 3**) (Chen et al., 2019). In addition, the functions of PYC, PPC and MAE on the carboxylation processes for high succinic acid productivity in *E. coli* were analyzed *in silico*. According to analysis results, carboxylation reactions catalyzed by PYC were the most suitable ones for obtain high productivity in *E. coli*. Furthermore, based on these analysis results, PYC from *C. glutamicum* ATCC13032 was overexpressed in *E. coli* ZJG13 and the final succinic acid production was 36.1 g/L, with a specific productivity and yield of 2.75 mmol g CDW^{-1} h^{-1} and 0.72 mol mol^{-1} glucose, respectively (**Table 3**) (Yang et al., 2014). Sánchez et al. overexpressed the *L. lactis pyc* gene in *E. coli* MG1655 (*ΔadhE, ΔldhA*) and found that a 25-fold increasein succinic acid production, from 0.6 g/L to 15.6 g/L, as well as a 6-fold increase in the yield, from 0.13 g/g glucose to 0.78 g/g glucose (**Table 3**) (Sánchez et al., 2005).

The reductive branch of the TCA cycle coupled to malic enzyme (MAE) for succinic acid formation (rTCA (MAE) pathway), is shorter than the PYC dependent pathway. In the MAE dependent pathway, pyruvate and CO_2 are directly converted into malate by malic enzyme, and malate is further converted into succinic acid through FumABC and FrdABCD. There are two forms of malic enzymes: MaeA (EC 1.1.1.38) and MaeB (EC 1.1.1.40), which can use NADH and NADPH as electron donors, respectively. Stols et al. overexpressed MAE from *A. suum* in *E. coli* NZN111 to produce succinic acid, resulting in a 2.9-fold increase, from 2.45 g/L to 7.07 g/L (**Table 3**) (Stols et al., 1997). Kwon et al. cloned MaeA and MaeB, derived from *E. coli* W3110, and overexpressed them in *E. coli* W3110 under anaerobic conditions. They found that the enzyme activities of overexpressed MaeA and MaeB were 2.34

and 1.69 μmol $min^{-1}mg_{protein}{}^{-1}$, whereas their activities were only 0.82 and 0.01 μmol $min^{-1}mg_{protein}{}^{-1}$ in the wild-type W3110 strain, respectively (Kwon et al., 2007). Furthermore, the succinic acid yields were measured in different strains. MaeB overexpression resulted in a 2.4-fold increase in succinic acid production, to 15.43 mmol/L, compared with 6.41 mmol/L in wild-type *E. coli* W3110. However, MaeA overexpression resulted in just 6.69 mmol/L succinic acid, which was similar to a wild-type strain under the same anaerobic fermentation conditions (Kwon et al., 2007). In this study, there was a negative correlation between succinic acid production and the activities of MaeA and MaeB. The main reason for this result might have been related to the differences in the intracellular co-substrate availability of MaeA and MaeB. The intracellular concentration of NADPH was 146 μmol/L, which was 9.12-fold higher than the 16 μmol/L of NADH intracellular concentration (Bochner and Ames, 1982; Kwon et al., 2007). Correspondingly, NADPH-dependent MaeB showed an advantage over the NADH-dependent MaeA, which would encourage CO_2 fixation by MaeB over by MaeA in wild-type *E. coli* (Kwon et al., 2007). In addition, the reaction catalyzed by MAE is reversible and this enzyme prefers to form pyruvate, which is unfavorable for succinic acid formation (Hong and Lee, 2002). The K_m values of MAE for malate and pyruvate in *E. coli* are 0.4 and 16 mM, respectively. Similarly, the K_m values of MAE in *C. glutamicum*are 3.8 mM for malate and 13.8 mM for pyruvate, respectively (Stols and Donnelly, 1997; Gourdon et al., 2000). This indicates that sufficiently high intracellular pyruvate concentrations may have a significant influence to overcome the unfavorable equilibrium of MAE catalytic processes. However, the wild-type strain is unable to accumulate a sufficiently high pyruvate concentration to allow MAE to be effective for producing excessive malate (Stols et al., 1997). Therefore, the enhancement of the PYK catalytic process, which can convert PEP and ADP into pyruvate and ATP, maybe a good choice for intracellular pyruvate enrichment. In some natural succinic acid producers, this reaction is also closely related to normal metabolic activity. Taking *M. succiniciproducens* as an example, Lee found that PYK operates by providing the pyruvate and ATP required for cell growth, as its pyruvate concentration increases with cell growth and remains constant after cell growth has stopped (Lee et al., 2006).

2.2 Aerobic Succinic Acid-Producing Pathways

Although high productivities and yields of succinic acid can be achieved through anaerobic biosynthesis pathways, some drawbacks still exist with using these pathways, such as their slow carbon throughput, limitation of NADH availability (2 mol of NADH are required for 1 mol succinic acid formation) and poor cell growth (Yang et al., 2014). One solution is to produce succinic acid under aerobic conditions, which can generate higher biomass and extensive energy with O_2 as the electron acceptor (Lin et al., 2005a; 2005b; Yang et al., 2014). The oxidative branch pathway of the TCA cycle (oTCA pathway) is one of the candidate aerobic biosynthesis routes for succinic acid production. In this pathway, acetyl-CoA and oxaloacetate are converted into succinic acid through citrate synthetase (GltA), aconitase (AcnAB), isocitrate dehydrogenase (ICD), and Succinyl-CoA synthetase (SucABCD), accompanied by the synthesis of NADH at a stoichiometric ratio of 2:1. Although succinic acid can be generated by oTCA under aerobic conditions, most of it will be further converted in the TCA cycle or to biomass and cannot be excreted from the cells. Thus, the metabolic engineering studies are necessary to improve its yield. Taking *E. coli* as an example, succinic acid is a minor fermentation product under anaerobic conditions. Under aerobic conditions, however, succinic acid is only an intermediate of the TCA cycle and cannot be detected in the extracellular medium (Clark, 1989; Lin et al., 2005b). Correspondingly, acetate is the main byproduct under the same aerobic conditions (Lin et al., 2005b). In order to produce succinic acid as a major product aerobically, Lin et al. created a mutant *E. coli* HL27659k (pKK313) strain that overexpressed of *S. vulgare pepc* and had five enzymes inactivated: *ΔsdhAB, Δ(ackA-pta), ΔpoxB, ΔiclR, andΔptsG.* This mutant strain could use both the oxidative branch pathway of the TCA cycle and the glyoxylate shunt pathway to produce succinic acid under aerobic conditions, and its maximum theoretical succinic acid yield could reach 1.0 mol/mol glucose consumed (Lin et al., 2005c). Fed-batch fermentation results showed that this strain could produce 58.3 g/L of succinic acid under complete aerobic conditions with a yield of 0.94 mol/mol glucose consumed (**Table 3**) (Lin et al., 2005b; 2005d). Arikawa et al. constructed a *Saccharomyces cerevisiae* mutant with fumarate reductase (FRDS) and succinate dehydrogenase (SDH1) inactivated. However, under aerobic conditions, this mutant strain could synthesize succinic acid through the oxidative branch pathway of the TCA cycle and the succinic acid yield showed a 2.7-fold increase compared with the parental strain (Arikawa et al., 1998). *S. cerevisiae* exhibits a high tolerance to low pH values, which makes it superior for succinic acid production (Qiang et al., 2010). These results were significant and Lin et al. inferred the potential of the oTCA pathway for aerobic succinic acid biosynthesis (Lin et al., 2005b).

The glyoxylate shunt pathway (GAC pathway) is another aerobic succinic acid biosynthesis route. In this process, 2 mol of acetyl-CoA and 1 mol of oxalacetate are converted into 1 mol of malate and 1 mol of succinic acid by citrate synthetase (GltA), aconitase (AcnAB) and isocitrate lyase (AceAB). Compared with the oxidative branch pathway of the TCA cycle, this process bypasses the two oxidative steps where CO_2 is released, and thus it is considered to be an atom-economic aerobic pathway (Lin et al., 2004). Additionally, malate is produced as the main byproduct in the glyoxylate shunt pathway. Malate can be catalyzed by malate dehydrogenase (MDH) to generate NADH and regeneration of oxaloacetate. Under anaerobic conditions, 1 mol of malate can also be further transformed into 1 mol of succinic acid by FumABC and FrdABCD by consuming 1 mol of NADH. Compared with the traditional rTCA pathway (formation of 1 mol of succinic acid requires 2 mol of NADH), the glyoxylate shunt pathway does not contain NADH consumption process. Therefore, its application will be

beneficial for solving the limitation of NADH availability during succinic acid biosynthesis (Sánchez et al., 2005). Vemuri et al. found that in the absence of an additional electron acceptor under dual-phase conditions (an aerobic growth phase followed by an anaerobic production phase), the maximum theoretical succinic acid yield was up to 1.714 mol/mol glucose, when 28.6% of the carbon flows to the glyoxylate shunt pathway and 71.4% of the carbon flows to the reductive branch pathway of the TCA cycle. It is worth noting that the maximal yield of succinic acid cannot be achieved without an active glyoxylate shunt pathway (Vemuri et al., 2002). It should be noticed that C2 substrates like acetate or fatty acids are very prominent activators for the glyoxylate shunt pathway under aerobic conditions (Gui et al., 1996). The *aceBAK* operon, which encodes enzymes of the glyoxylate cycle, is controlled by IclR. Under aerobic conditions, acetate can induce *aceBAK* and reduce the repressor activity of IclR, resulting in activation of the glyoxylate cycle (Gui et al., 1996; Sánchez et al., 2005). Meanwhile, studies have also revealed that the disruption of *iclR* could dramatically induce the expression of the *aceBAK* operon even when growing on glucose (Gui et al., 1996; Lin et al., 2004; Hendrik et al., 2011). Thus, the inactivation of *iclR* is significant for activating the glyoxylate shunt pathway for succinic acid production (Sánchez et al., 2005). Lin et al. constructed an engineered *E. coli* HL27615k strain with mutations in the TCA cycle (*ΔiclR, Δicd,* and *ΔsdhAB*) and acetate pathways (*ΔpoxB,* and *ΔackA-pta*) for maximal aerobic succinic acid production through the glyoxylate shunt pathway. The results of aerobic batch fermentation showed that the succinic acid production reached 43 mM with a yield of 0.7, which was close to the maximum theoretical yield of 1 mol/mol glucose (Lin et al., 2004). Except for the absence of the *iclR* mutation, Zhu et al. demonstrated that the glyoxylate shunt pathway could also be activated by deleting other relevant genes in *E. coli* under anaerobic conditions. The key genes included *ackA* (a gene encoding an acetate kinase) and *pta* (a gene encoding a phosphotransacetylase). Metabolic flux analysis reflected that the carbon flow shunted to the glyoxylate pathway from oxalacetate in wild-type *E. coli* DY329 was 0 and 31% in the mutant YJ003 (*ΔackA, Δpta, ΔldhA,* and *ΔpstG*). In addition, the succinic acid production also showed a 6-fold increase, from 25.13 mM in DY329 to 150.78 mM in YJ003, implying the importance of the activation of the glyoxylate shunt pathway (Zhu et al., 2014).

The 3-hydroxypropionate cycle is one of the natural aerobic CO_2-fixation pathways, and mainly exists in photosynthetic green nonsulfur bacteria (Herter et al., 2001). This cycle is complex, containing 16 enzymatic reaction steps that are catalyzed by 13 enzymes (Gong et al., 2016). Liu et al. introduced part of this cycle into recombinant *E. coli* for succinic acid production (3HP pathway) (Liu et al., 2020). In this process, acetyl-CoA is carboxylated by acetyl-CoA carboxylase (ACC) to generate malony-CoA. Malony-CoA is converted into propionyl-CoA by malonyl-CoA reductase (MCR) and propionyl-CoA synthase (PCS). Then propionyl-CoA is carboxylated by propionyl-CoA carboxylase (PCC) to generate (*S*)-methylmalonyl-CoA. Next, methylmalonyl-CoA epimerase (MmcE) and methylmalonyl-CoA mutase (MmcM) convert (*S*)-methylmalonyl-CoA into its isomer succinyl-CoA. Finally, succinyl-CoA is deesterificated by succinyl-CoA synthetase (SucCD) to generate succinic acid (Menendez et al., 1999; Liu et al., 2020). The conversion of 1 mol of acetyl-CoA into 1 mol of succinic acid via the 3-hydroxypropionate cycle can fix 2 mol of CO_2, which was confirmed by isotope labeling experiments with $NaH^{13}CO_3$ (Liu et al., 2020). Compared with succinic acid production based on carboxylation of PEP or pyruvate, this route showed a higher CO_2 fixation efficiency. Among these pathway, ACC (EC 6.4.1.2) and PCC (EC 6.4.1.3) are the key CO_2-fixing and rate-limiting enzymes. Both ACC and PCC belong to a subgroup of biotin-dependent short-chain acyl-CoA carboxylases that contain biotin carboxyl carrier protein domain (BCCP), biotin carboxylase domain (BC), and carboxyltransferase domain (CT), and utilize a covalently bound biotin as a cofactor (Wongkittichote et al., 2017; Liu and Jiang, 2021). The CT domain determines the specificity of the substrate, and these proteins can even work with other BCCP and BC domains from different enzymes (Lombard and Moreira, 2012; Tong, 2013). To obtain PCC with high enzymatic activity, Liu et al. tested different CT subunits of the PCC homologs from diverse bacterial species and developed a direct evolution strategy to further optimize this protein. A highly active PCC mutant ($PccB_{BS}$-N220I/I391T) was obtained, which showed a 94-fold increase in overall catalytic efficiency indicated by k_{cat}/K_m compared with a wild-type PCC. In addition, the application of this PCC mutant resulted in a 1.5-fold increase in succinic acid production compared to the engineered strain with wild-type PCC, which indicated the significance of this rate-limiting enzyme engineering strategy for microbial production (Liu et al., 2020). ACC acts as another CO_2-fixing enzyme and ACC is essential for most living organism's growth (Baba et al., 2006). The intracellular concentration of its carboxylation product (malonyl-CoA) is tightly regulated to be very low, leading to limited production of ACC-derived compounds (Zha et al., 2009; Liu et al., 2010). It has been reported that ACC is negatively regulated by AMP-activated serine/threonine protein kinase (Snf1) in *S. cerevisiae* when glucose is depleted. Moreover, the phosphorylation triggered by Snf1 at one or more serine residues results in the deactivation of ACC (Woods et al., 1994; Scott et al., 2002). Jin et al. identified a critical amino acid (Ser-1157) responsible for deactivation via phosphorylation and mutated it to an alanine. The *in vitro* activity results showed that this ACC mutant (ACC-S1157A) resulted in 9-fold higher specific activity relative to wild-type ACC (Choi and Silva, 2014). Shi et al. demonstrated that introduction of this S659A mutation in ACC-S1157A could also lead to an enhanced enzyme activity with 1.72-fold increase (Shi et al., 2014). Further utilization of these modified acetyl-CoA carboxylase will be beneficial for product biosynthesis built from malonyl-CoA, such as succinic acid (Choi and Silva, 2014). Except for ACC and PCC, malonyl-CoA reductase (MCR), a characteristic enzyme of the 3-hydroxypropionate cycle, is regarded as another rate-limiting enzyme (Fixation et al., 2002). MCR catalyzes a two-step NADPH-dependent reduction of malonyl-CoA to 3-hydroxypropionate, and malonate semialdehyde has been suggested to be the likely free

intermediate (Fixation et al., 2002; Liu et al., 2013). Liu et al. demonstrated that MCR, a natural fusion protein of two short-chain dehydrogenase/reductases, has higher enzyme activity when dissected into two functionally individual fragments, including an MCR-C fragment (amino acids 550–1,219) and MCR-N fragment (amino acids 1–549) (Liu et al., 2013). Further studies indicated that the initial reduction of malonyl-CoA to malonate semialdehyde catalyzed by MCR-C was the rate-limiting step of MCR (Liu et al., 2013; Liu et al., 2016). Liu et al. developed a direct evolution strategy to further optimize MCR-C. A triple MCR-C mutant (N940V/K1106W/S1114R) was obtained, which showed a 5.54-fold increase in enzyme activity. Combined with fine tuning of the MCR-N expression levels and culture condition optimization, the 3-hydroxypropionate yield showed a 270-fold increase, which could relieve the pressure of being the rate-limiting step in succinic acid biosynthesis (Liu et al., 2016). Although some progress has been achieved in this succinic acid pathway, some problems are still worthy of attention. The main challenge is that significant amounts of ATP and reducing power (3ATP and 3NADPH) are consumed from one molecule acetyl-CoA to one molecule succinic acid. Using fatty acids as carbon sources or feeding electricity to bacteria to produce intracellular energy may be optional promising approaches (Chen et al., 2018; Liu et al., 2019).

3 METABOLIC ENGINEERING FOR ENHANCING SUCCINIC ACID BIOSYNTHESIS

Up to now, the bio-based succinic acid synthetic process has become increasingly mature. There are several strategies to enhance succinic acid biosynthesis, which mainly include redirecting carbon flux, balancing the redox ratio ($NADH/NAD^+$) and optimizing CO_2 supplementation. And the different strategies will be discussed in more details in the later chapters.

3.1 Redirecting Carbon Flux

Whether under anaerobic or aerobic conditions, succinic acid is not the main product of many microbes. In general, microbes preferentially accumulate substances such as acetate, lactate, and ethanol etc. These by-product pathways compete with the succinic acid pathway for ATP or reducing power. Therefore, it is necessary to redirect the carbon flux from these competitive pathways into succinic acid production (Li et al., 2020). The redirection methods often used mainly include blocking these competitive pathways and regulating succinic acid biosynthesis pathways.

3.1.1 Blocking Competitive Pathways

As the main competing by-products, acetate, lactate, and ethanol are the targets of metabolic regulation, and deletion of the genes related to their production is usually performed. Specifically, single deletion of *ldhA* (encoding lactate dehydrogenase), which can convert pyruvate and NADH into lactate and NAD^+ in *E. coli*, led to a 1.6-fold increase in succinic acid yield under anaerobic conditions, from 0.13 to 0.21 mol/mol glucose. Meanwhile, the lactate concentration of this *ΔldhA* mutant was 92% lower than a wild-type strain, dropping from 214 to 17 mM (Zhang et al., 2009b). Single deletion of *adhE* (encoding alcohol dehydrogenase), which converts acetyl-CoA and NADH into ethanol and NAD^+, resulted in a 1.125-fold increase in succinic acid yield. Correspondingly, the ethanol concentration of this *ΔadhE* mutant was 0, compared with 133 mM in a wild-type strain (Zhang et al., 2009b). Zhang et al. constructed an *E. coli ΔldhAΔadhE* double mutant strain, which showed a 1.77-fold increase in succinic acid yield, and lactate and ethanol were not detected in its fermentation broth (Zhang et al., 2009b). There are two major acetate-producing pathways in *E. coli*, respectively through the enzyme pyruvate oxidase (encoded by *poxB*) and acetate kinase/phosphotransacetylase (encoded by *ackA-pta*). Pyruvate oxidase catalyzes the decarboxylation of pyruvate to acetate and CO_2, and is more active in the stationary stage of cell growth (Mey et al., 2007; Dittrich, 2010). Ahmed et al. demonstrated that PoxB was useful for overall metabolism functioning and single deletion of *poxB* led to a decrease of 24% in biomass. Thus, they suggested that employing *poxB* served as a method to decrease acetate production (Abdel-Hamid et al., 2001). The *ackA-pta* pathway, which is more active in the exponential phases of cell growth, involves two consecutive reactions. PTA converts acetyl-CoA and Pi into acetyl phosphate and CoA. AckA then converts acetyl phosphate and ADP into acetate and ATP (Zhu et al., 2014). It was demonstrated that *pta* mutants grow more slowly than wild-type strains. The specific rate of growth of *E. coli* MG1655 Δ*pta* was 9.3% lower than the parent strain under aerobic conditions and 37.2% lower under anaerobic conditions (Schütze et al., 2020). This may have been due to pyruvate accumulation, acetyl-P accumulation or a redox imbalance in *pta* mutants (Wolfe, 2005). Wolfe reported that *pta* mutants or *ackA-pta* mutants did not accumulate extracellular acetate, and *ackA* mutants could accumulate small amounts of acetate (Wolfe, 2005). Compared to a particular mutation, the combination of mutations was proved more useful for enhancing succinic acid production in many cases. Zhang et al. constructed a *ΔldhAΔadhEΔackA* triple mutant, which showed a 3.2-fold increase in succinic acid concentration and a 5.4-fold increase in yield (Zhang et al., 2009b). Lu et al. constructed a *E. coli* JH208 (*ΔldhA*, *ΔpflB*, *ΔadhE, ΔpoxB, ΔackA, ΔcscR*) mutant strain, and found that this mutant could produce 48.46 g/L succinic acid in 46 h with the productivity of 1.01 g/L/h and the yield of 0.83 g/g sucrose. Compared with the initial strain, the production efficiency of succinic acid has been improved 72% (Lu et al., 2015). Olajuyin et al. constructed an *E. coli* K-12 (*ΔldhA*, *ΔpflB*, *ΔpoxB, Δpta-ackA*) mutant for succinic acid production, the concentration and molar yield of succinic acid were respectively 22.40 ± 0.12 g/L and 1.13 ± 0.02 mol/mol total sugar after 72 h dual phase fermentation, and the final concentration of succinic acid was 6.2-fold higher than the wild-type strain (Olajuyin et al., 2016). These results indicated the necessity of blocking competitive pathways for improving succinic acid yield.

3.1.2 Regulating Succinic Acid Pathways

Direct overexpression of important enzymes (mentioned in **Section 2**) is the most frequently used method for enhancing the production of the succinic acid pathways. However, biosynthetic processes are usually regulated by multiple genes, and positive expected results are difficult to obtain by simple genetic engineering. In recent years, investigation of the global regulation of gene expression has been shown to be effective for solving the limitations of classical metabolic engineering approaches (Chong et al., 2014; Zhu and Tang, 2017). Some global regulators are good targets for improving the succinic acid biosynthesis process, such as ArcA, Crp, Cya and Cra. Among them, the Arc (anoxic respiration control) system composed of ArcA and ArcB regulates gene expression in response to redox conditions (Liu and Wulf, 2004; Sun et al., 2020). As reported, ArcA, when phosphorylated, represses the expressions of the genes involved in the TCA cycle and the glyoxylate shunt genes (Shimizu, 2013). Knocking out of ArcA did not affect the growth rate and the glucose uptake rate, but increased the TCA cycle activity by over 60% under aerobic conditions. It is significant for the oTCA pathway and the glyoxylate shunt pathway (Perrenoud and Sauer, 2005). Crp (cyclic AMP receptor protein) is the catabolite repressor that is activated by adenylate cyclase (Cya)-synthesized cAMP (Zhang et al., 2014). Crp/cAMP is a positive transcriptional regulator for *mdh, ptsG, pckA, sdhABCD, acnAB, gltA* (Perrenoud and Sauer, 2005; Wilfredo et al., 2021). Research showed that knocking out of Crp or Cya would decrease the growth rate, the glucose consumption rate and reduce the metabolic flux from PEP to oxaloacetate (Perrenoud and Sauer, 2005). Catabolite repressor/activator (Cra), also known as FruR, is an important global transcription factor, and it plays a key role in balancing the levels of the genes involved in carbon metabolism in *E. coli* (Akira, 2000; Ishihama, 2010; Shimada et al., 2011). Cra can activate genes related to the tricarboxylic acid cycle, the glyoxylate shunt pathway (Cozzone and El-Mansi, 2005; Dayanidhi et al., 2008; Shimada et al., 2011), and negatively affects genes related with the ED and glycolytic pathways (Ramseier, 1996; Sarkar et al., 2008; Ramseier et al., 2010). In a study from Zhu et al., Cra was first engineered for achieving high product concentration through error-prone PCR. After screening and mutation site integration, a high succinic acid producing mutant strain (Cra-R57K/A58G/G59Q/R60Q/S75H/T76Y/D148I/R149I), was obtained. This strain (*E. coli* W1485 (*ΔpflAB, ΔldhA, ΔptsG*)/pTrc-mutant *cra*) produced succinic acid to a concentration of 79.8 g/L, which was 22.8% higher than a control strain (*E. coli* W1485 (*ΔpflAB, ΔldhA, ΔptsG*)/pTrc) (Zhu et al., 2016). Further studies demonstrated that the significant increase of succinic acid in a Cra mutant may be caused by the activation of PEP carboxylation, reductive branches of the TCA cycle and the glyoxylate pathway (Zhu et al., 2016). Meanwhile, Li et al. first reported a positive correlation between succinic acid production and the affinity of Cra for its effector fructose-1,6-bisphosphate (FBP) in *E. coli* (Wei et al., 2016). To heighten this affinity, a semi-rational strategy based on computer-assisted virtual saturation mutagenesis was designed, and a Cra mutant (D101R/D148R/G274R) was obtained. Compared with wild-type Cra (the K_d of Cra-FBP was 1,360 ± 6.2 nM), the triple mutant Cra showed a high affinity with its effector fructose-1,6-bisphosphate (FBP) (the K_d of Cra-FBP was 154.2 ± 4.3 nM). Further experimental results indicated that this enhanced affinity increased the activation of succinic acid biosynthetic pathways, especially *pck* and *aceB*, and led to a succinic acid concentration of 92.7 g/L in engineered strain (*E. coli* W1485 (*ΔpflAB, ΔldhA, ΔptsG*)/pTrc99A-*cra* D101R/D148R/G274R), which was 34% higher than a control strain (*E. coli* W1485 (*ΔpflAB, ΔldhA, ΔptsG*)/pTrc99A) (Wei et al., 2016). The advantage of using global transcription factors is that they can regulate the expression of multiple pathway-related genes (Wu et al., 2007; Wei et al., 2016). In conclusion, these results demonstrate the great potentials of global transcription factors combined with the traditional metabolic engineering strategies in succinic acid production process, and this strategy can also be used as a reference for other valuable chemical biosynthetic pathways.

3.2 Balancing the Redox Ratio (NADH/NAD$^+$)

The intracellular redox ratio is closely related to metabolite profiles, membrane transport, microbial fitness and cellular functions (Berríos-Rivera et al., 2004; Singh et al., 2009). The redox ratio is mainly reflected by the intracellular NADH/NAD$^+$ ratio, which is influenced by several factors, such as the physiological state of a given strain, the oxidation state of carbon sources, and the expression levels of NADH/NAD$^+$-related enzymes (such as formate dehydrogenase, membrane-bound transhydrogenase, NAD$^+$ dehydrogenase, terminal oxidases and lactic dehydrogenase) (Lin et al., 2005a; Singh et al., 2009). In microbes, both NADH and NAD$^+$ are kept in balance. NADH is oxidized to NAD$^+$ through the oxidative phosphorylation process or fermentation reactions. NADH provides the reducing power for reductive product formation and NAD$^+$ serves as an electron acceptor during substrate degradation (Li et al., 2017). In addition, the appropriate NADH/NAD$^+$ ratio is a major prerequisite of many biosynthetic processes, and it is also crucial for succinic acid production (Zhang Y. et al., 2009; Li et al., 2017).

Taking *E. coli* as an example, lactate dehydrogenase (encoded by *ldhA*), which drives the formation of lactate, and pyruvate formate lyase (encoded by *pflB*), which drives the formation of formate and acetyl-CoA derivants (acetate, ethanol), were deleted to redirect the carbon flux towards succinic acid under anaerobic conditions (Singh et al., 2010). This mutant was termed *E. coli* NZN111, and it has been considered an excellent candidate as a succinic acid producer (Hui et al., 2009). However, *E. coli* NZN111 lost its ability to ferment glucose anaerobically and accumulates high levels of pyruvate and NADH intracellularly (Wu et al., 2007; Ma et al., 2013). It has been reported that *E. coli*

NZN111 growth was impaired mainly due to the anomalously high NADH/NAD^+ ratio *in vivo*, which was shown to be three times higher than a wild-type *E. coli* strain (Singh et al., 2009; Singh et al., 2010). To reduce this NADH/NAD^+ ratio, an effective genomic library-based screening approach was employed, and genes including *pfkB* (encoding phosphofructokinase II), *marA* (encoding DNA-binding transcriptional repressor), and *moaE* (encoding the subunit of molybdopterin synthase), were shown to be significant for balancing the redox ratio. Overexpression of these genes was beneficial for succinic acid production, especially *pfkB*, and led to a 7.8-fold increase in M9+10 g/L glucose medium under microaerobic conditions (that means controlled dosing of small amount of air or oxygen into reactor).

Conversely, deficiency in NADH has a negative impact on succinic acid biosynthesis as well. Except for the glyoxylate shunt pathway, conversion of phosphoenolpyruvate, pyruvate or acetyl-CoA to one molecule of succinic acid requires a minimum of two molecules of reducing equivalents (Lin et al., 2005c). However, only two molecules of NADH can be obtained from one molecule of glucose through the glycolytic pathway. Thus, the shortage of NADH limits the succinic acid production to a theoretical yield of 1 mol/mol glucose (Zhu et al., 2014). One solution is to use the glyoxylate shunt pathway (mentioned in **section 2**), which has a theoretical yield of 1.7 mol/mol glucose (Vemuri et al., 2002). Another solution is to provide more NADH. NAD^+-dependent formate dehydrogenase can convert one molecule of formate into one molecule of CO_2 and NADH. In this reaction, formate is one of the main by-products produced by succinic acid producers, while CO_2 and NADH are necessary for succinic acid synthesis. When using glucose as a carbon source, the expression of formate dehydrogenase can double the maximum yield of NADH, from 2 to 4 mol NADH/mol glucose consumed (Berríos-Rivera et al., 2004). In Grant et al., *fdh* (encoding NAD^+-dependent formate dehydrogenase) from *C. boidiniiwas* and *pycA* (encoding pyruvate carboxylase) from *L. lactis* were co-expressed in *E. coli* MG1655 (*ΔadhE, ΔldhA, ΔiclR, Δack-pta*) under the control of the same promoters (Thakker et al., 2011). Compared with the overexpression of *pyc* alone, this co-expression strain had better succinic acid production capacity. The succinic acid yield at 24 h showed a 1.9-fold increase, from 176 to 334 mM, and the succinic acid productivity showed a 2-fold increase, from 1 to 2 g/L/h. Meanwhile the byproduct formate concentration showed a significant decrease, from 17 mM to 0–3 mM. This indicated that higher NADH availability conditions significantly changed the final metabolite concentration pattern and promoted an increase in the contents of succinic acid. Additionally, providing carbon sources with different oxidation states is also an optional method. Sorbitol, for instance, has a higher NADH maximum theoretical yield (3 mol NADH/mol sorbitol) than glucose (Berríos-Rivera et al., 2004). It has been reported that using sorbitol can also generate higher yield and productivity of succinic acid (Chatterjee et al., 2001).

3.3 Optimizing CO_2 Supplementation

In succinic acid biosynthesis, HCO_3^- is the major carboxylation substrate. During fermentation processes, CO_2 that is dissolved in the liquid medium, first crosses the cell membrane through passive diffusion, and is then converted into HCO_3^- in the cytoplasm to participate in carboxylation (Lu et al., 2009). However, the low concentration of CO_2 in the growth medium is the critical limiting step in succinic acid production (Zhu et al., 2015). To date, several strategies have been attempted to improve succinic acid production by optimizing CO_2 supplementation and several satisfying results have been achieved.

3.3.1 Promoting the Intracellular Conversion of HCO_3^- and CO_2

Under anaerobic fermentation conditions, both CO_2 or HCO_3^- can serve as a carboxylation substrate for PEP carboxykinase (PCK), but PCK prefers to use CO_2, and its catalytic velocity with CO_2 was shown to be 7.6-fold higher than that with HCO_3^- (Cotelesage et al., 2007). Therefore, promoting the intracellular interconversion of HCO_3^- and CO_2 is a way to improve its catalytic efficiency. Carbonic anhydrase (CA), which is an important component of the carboxysome, efficiently converts HCO_3^- to CO_2 (Cotelesage et al., 2007). For improving the carboxylation velocity of PCK, Xiao et al. introduced the CA gene from *Synechococcus* sp. PCC7002 into *E. coli* Suc-T110 *Δppc*. Due to the increase of the local CO_2 concentration, the carboxylation rate of PCK showed a 1.6-fold increase from 2.46 to 3.92 μmol/min/mg protein. As a result of CA gene overexpression, the succinic acid titer at 36 h showed a 35% increase as well (Xiao et al., 2017). These results demonstrated that carbonic anhydrase was useful for improving succinic acid productivity.

3.3.2 Enhancing HCO_3^- Transmembrane Transport

As the major carboxylation substrate, HCO_3^- can also cross the cell membrane through passive diffusion, but the rate is very slow, limiting its direct utilization (Badger and Price, 2003). One feasible strategy to increase intracellular HCO_3^- concentration is to use bicarbonate transporters. Among these, SbtA and BicA have been shown to be more efficient (Price et al., 2004). BicA, which was identified from *Synechococcus* sp. PCC7002, is a Na^+-dependent transporter, and it has low transport affinity but a high flux rate (Price et al., 2004). SbtA-mediated transport, which was identified from *Synechocystis* PCC6803, is also Na^+-dependent. Meanwhile, it can be induced by low CO_2 levels and shows a relatively high affinity for HCO_3^- (Shibata et al., 2002; Zhu et al., 2015). To optimize succinic acid production, Xiao et al. overexpressed the *bicA* and *pck* genes in *E. coli*, and reported that the final cell density and succinic acid titers at 36 h were 29 and 22% higher than those of control strains, respectively (Xiao et al., 2017). Zhu et al. contrasted SbtA and BicA in *E. coli* AFP111, and demonstrated that overexpression of *sbtA* or/and *bicA* genes showed a positive effect on CO_2 absorption but a negative effect on succinic acid biosynthesis. Meanwhile, they found that the succinic acid concentration was improved only when bicarbonate transporters and carboxylase (PCK or PPC)

were co-expressed. Among these, co-overexpression of the *sbtA* and *pck* genes was superior, and led to a 15% increase in succinic production (Zhu et al., 2015). For further optimization, Yu et al. balanced HCO_3^- transport and fixation to maximize succinic acid titer. They demonstrated that the highest succinic acid production was obtained when the *sbtA*, *bicA*, and *ppc* genes were co-expressed under the control of the weak P4 promoter and the *pck* gene under the control of the strong P19 promoter. This led to a 1.4-fold increase in succinic acid production from 65 to 89.4 g/L, and a 1.3-fold increase in succinic acid yield from 0.98 to 1.27 mol/mol glucose (Yu et al., 2016). All of these results indicated the necessity of CO_2 supplementation in succinic acid biosynthesis.

4 CONCLUSION AND PERSPECTIVES

Succinic acid is an important four-carbon building-block chemical that can be used as the precursor of numerous products, including biodegradable plastics, feed additives, green solvents, and pharmaceutical products. As an alternative to environmentally unfriendly traditional method, biosynthesis is a promising means for succinic acid production and has become increasingly mature as well. This review summarized different succinic acid biosynthesis pathways, key enzymes, and the metabolic engineering approaches, particularly those developed for adjusting the carbon flux, balancing the redox ratio, and CO_2 supplementation for succinic acid production. It needs to be clear that one or more strategies have been applied jointly to obtain high performance strains in practical application. To date, some efficient succinic acid producers have been obtained and applied in industry, but several problems still exist, such as the low robustness of engineered bacteria or the high cost of downstream product recovery. Thus, increasing attention should be paid to the following prospects in future research.

Firstly, an economical fermentation process should be further explored. Most succinic acid producing strains prefer neutral pH conditions, but succinic acid formation acidifies the medium. To keep a neutral pH, a common method is the conversion of succinic acid into succinate by titration with bases during fermentation. However, generation of salts increases the difficulty and cost of post-processing for succinic acid production. Compared with feedstock costs and some other upstream costs, the downstream costs are also considerable, and represent about 30–40% of the total production costs (López-Garzón and Straathof, 2014). One solution is to develop low pH (below or close to the pK_a) fermentation strategies, which can minimize the consumption of bases, reduce the generation of salts and avoid re-conversion of succinate into succinic acid. However, the highest succinic acid concentration has so far been achieved at neutral pH, not at low pH. The main reason is the low tolerance to low pH of most succinic acid producers, such as *C. glutamicum*, *E. coli*, *M. succiniciproducens*, *B. succiniciproducens* and *A. succinogenes* (Ahn et al., 2016). Therefore, to reduce the overall production costs, development of a competitive acid-tolerant strain is critical for enabling bio-based production of succinic acid. Meanwhile, more attention should be paid to revealing acid-tolerant mechanisms, which are meaningful for the production of any carboxylic acid.

Furthermore, efficient biosynthesis process should be further explored. Making a detailed analyze and comparison of the seven succinic acid biosynthetic pathways is very important for understanding and designing greater efficiency biosynthesis pathway. And no matter which pathway is selected, the metabolic process for its production is a multigene pathway. Key enzyme overexpression is the traditional genetic engineering strategy used to overcome this, but the enzyme expression level in a multistep pathway is not simply "the more the better". Liu et al. demonstrated the importance of metabolic balancing in a multistep biosynthetic pathway (Liu et al., 2016). Meanwhile, plasmid-based multigene over-expression systems can also lead to genetic instability and high cellular burdens. Thus, a functional balance between enzymes and the improvement of host stability in succinic acid biosynthetic processes should be considered. Some strategies are valuable, such as chromosomal integration, promoters or RBS engineering, microbial host engineering, and dynamic control of the pathway of interest.

AUTHOR CONTRIBUTIONS

XF and XL developed the idea for the review. XL and XF wrote the manuscript. XF, GZ, SS, CF, and PX revised this manuscript. All authors read and approved the final manuscript.

FUNDING

This study was financially supported by the Natural Science Foundation of Shandong Province (ZR2021QB176 and ZR2019QB015), National Natural Science Foundation of China (31800081), State Key Laboratory of Microbial Technology Open Projects Fund (Project No. M2021-15), and start-up fund from Shandong University of Technology (to XL).

REFERENCES

Abdel-Hamid, A. M., Attwood, M. M., and Guest, J. R. (2001). Pyruvate Oxidase Contributes to the Aerobic Growth Efficiency of *Escherichia coli*. *Microbiology* 147, 1483–1498. doi:10.1099/00221287-147-6-1483

Ahn, J. H., Bang, J., Kim, W. J., and Lee, S. Y. (2017). Formic Acid as a Secondary Substrate for Succinic Acid Production by Metabolically engineeredMannheimia Succiniciproducens. *Biotechnol. Bioeng.* 114, 2837–2847. doi:10.1002/bit.26435

Ahn, J. H., Jang, Y.-S., and Lee, S. Y. (2016). Production of Succinic Acid by Metabolically Engineered Microorganisms. *Curr. Opin. Biotechnol.* 42, 54–66. doi:10.1016/j.copbio.2016.02.034

Ahn, J. H., Seo, H., Park, W., Seok, J., Lee, J. A., Kim, W. J., et al. (2020). Enhanced Succinic Acid Production by Mannheimia Employing Optimal Malate Dehydrogenase. *Nat. Commun.* 11, 1970–1982. doi:10.1038/s41467-020-15839-z

Akira, I. (2000). Functional Modulation of *Escherichia coli* RNA Polymerase. *Annu. Rev. Microbiol.* 54, 499–518. doi:10.1146/annurev.micro.54.1.499

Arikawa, Y., Kuroyanagi, T., Shimosaka, M., Muratsubaki, H., Enomoto, K., Kodaira, R., et al. (1998). Effect of Gene Disruptions of the TCA Cycle on Production of Succinic Acid in *Saccharomyces cerevisiae*. *J. Biosci. Bioeng.* 87, 28–36. doi:10.1016/S1389-1723(99)80004-8

Baba, T., Ara, T., Hasegawa, M., Takai, Y., Okumura, Y., Baba, M., et al. (2006). Construction of *Escherichia coli* K-12 In-Frame, Single-Gene Knockout Mutants: the Keio Collection. *Mol. Syst. Biol.* 2, 2006–0008. doi:10.1038/msb4100050

Badger, M. R., and Price, G. D. (2003). CO2 Concentrating Mechanisms in Cyanobacteria: Molecular Components, Their Diversity and Evolution. *J. Exp. Bot.* 54, 609–622. doi:10.1093/jxb/erg076

Becker, J., Reinefeld, J., Stellmacher, R., Schäfer, R., Lange, A., Meyer, H., et al. (2013). Systems-wide Analysis and Engineering of Metabolic Pathway Fluxes in Bio-Succinate Producing Basfia Succiniciproducens. *Biotechnol. Bioeng.* 110, 3013–3023. doi:10.1002/bit.24963

Berríos-Rivera, S. J., Sánchez, A. M., Bennett, G. N., and San, K. Y. (2004). Effect of Different Levels of NADH Availability on Metabolite Distribution in *Escherichia coli* Fermentation in Minimal and Complex media. *Appl. Microbiol. Biotechnol.* 65, 426–432. doi:10.1007/s00253-004-1609-3

Bochner, B. R., and Ames, B. N. (1982). Complete Analysis of Cellular Nucleotides by Two-Dimensional Thin Layer Chromatography. *J. Biol. Chem.* 257, 9759–9769. doi:10.1016/s0021-9258(18)34138-3

Bozell, J. J., and Petersen, G. R. (2010). Technology Development for the Production of Biobased Products from Biorefinery Carbohydrates-The US Department of Energy's "Top 10" Revisited. *Green. Chem.* 12, 539–554. doi:10.1039/B922014C

Bretz, K., and Kabasci, S. (2012). Feed-control Development for Succinic Acid Production with Anaerobiospirillum Succiniciproducens. *Biotechnol. Bioeng.* 109, 1187–1192. doi:10.1002/bit.24387

Chatterjee, R., Millard, C. S., Champion, K., Clark, D. P., and Donnelly, M. I. (2001). Mutation of the ptsG Gene Results in Increased Production of Succinate in Fermentation of Glucose by *Escherichia coli*. *Appl. Environ. Microbiol.* 67, 148–154. doi:10.1128/AEM.67.1.148-154.2001

Chen, K.-Q., Li, J., Ma, J.-F., Jiang, M., Wei, P., Liu, Z.-M., et al. (2011). Succinic Acid Production by Actinobacillus Succinogenes Using Hydrolysates of Spent Yeast Cells and Corn Fiber. *Bioresour. Technol.* 102, 1704–1708. doi:10.1016/j.biortech.2010.08.011

Chen, X., Cao, Y., Li, F., Tian, Y., and Song, H. (2018). Enzyme-Assisted Microbial Electrosynthesis of Poly(3-Hydroxybutyrate) via CO2 Bioreduction by Engineered Ralstonia Eutropha. *ACS Catal.* 8, 4429–4437. doi:10.1021/acscatal.8b00226

Chen, Y., Cheng, H., Ningna, L. I., Ke, S. U., Jiayu, L. I., Xia, H., et al. (2019). Effects of Pyruvate Carboxylase on Succinic Acid Accumulation in *Saccharomyces cerevisiae*. *Food Ferment. Industries* 45, 38–44. doi:10.13995/j.cnki.11-1802/ts.018736

Choi, J. W., and Da Silva, N. A. (2014). Improving Polyketide and Fatty Acid Synthesis by Engineering of the Yeast Acetyl-CoA Carboxylase. *J. Biotechnol.* 187, 56–59. doi:10.1016/j.jbiotec.2014.07.430

Choi, P. H., Vu, T. M. N., Pham, H. T., Woodward, J. J., Turner, M. S., and Tong, L. (2017). Structural and Functional Studies of Pyruvate Carboxylase Regulation by Cyclic Di-AMP in Lactic Acid Bacteria. *Proc. Natl. Acad. Sci. U S A.* 114, E7226–E7235. doi:10.1073/pnas.1704756114

Choi, S., Song, C. W., Shin, J. H., and Lee, S. Y. (2015). Biorefineries for the Production of Top Building Block Chemicals and Their Derivatives. *Metab. Eng.* 28, 223–239. doi:10.1016/j.ymben.2014.12.007

Choi, S., Song, H., Lim, S. W., Kim, T. Y., Ahn, J. H., Lee, J. W., et al. (2016). Highly Selective Production of Succinic Acid by Metabolically engineeredMannheimia Succiniciproducensand its Efficient Purification. *Biotechnol. Bioeng.* 113, 2168–2177. doi:10.1002/bit.25988

Chong, H., Geng, H., Zhang, H., Song, H., Huang, L., and Jiang, R. (2014). EnhancingE. Coliisobutanol Tolerance through Engineering its Global Transcription Factor cAMP Receptor Protein (CRP). *Biotechnol. Bioeng.* 111, 700–708. doi:10.1002/bit.25134

Chung, S.-C., Park, J.-S., Yun, J., and Park, J. H. (2017). Improvement of Succinate Production by Release of End-Product Inhibition in Corynebacterium Glutamicum. *Metab. Eng.* 40, 157–164. doi:10.1016/j.ymben.2017.02.004

Clark, D. P. (1989). The Fermentation Pathways ofEscherichia Coli. *FEMS Microbiol. Lett.* 63, 223–234. doi:10.1111/j.1574-6968.1989.tb03398.x

Cotelesage, J. J. H., Puttick, J., Goldie, H., Rajabi, B., Novakovski, B., and Delbaere, L. T. J. (2007). How Does an Enzyme Recognize CO2? *Int. J. Biochem. Cel Biol.* 39, 1204–1210. doi:10.1016/j.biocel.2007.03.015

Cozzone, A. J., and El-Mansi, M. (2005). Control of Isocitrate Dehydrogenase Catalytic Activity by Protein Phosphorylation in *Escherichia coli*. *J. Mol. Microbiol. Biotechnol.* 9, 132–146. doi:10.1159/000089642

Cui, Z., Gao, C., Li, J., Hou, J., Lin, C. S. K., and Qi, Q. (2017). Engineering of Unconventional Yeast Yarrowia Lipolytica for Efficient Succinic Acid Production from Glycerol at Low pH. *Metab. Eng.* 42, 126–133. doi:10.1016/j.ymben.2017.06.007

Dayanidhi, S., Siddiquee, K. A., Araúzo-Bravo, M. J., Oba, T., and Shimizu, K. (2008). Effect of Cra Gene Knockout Together with Edd and iclR Genes Knockout on the Metabolism in *Escherichia coli*. *Arch. Microbiol.* 190, 559–571. doi:10.1007/s00203-008-0406-2

De Mey, M., De Maeseneire, S., Soetaert, W., and Vandamme, E. (2007). Minimizing Acetate Formation in *E. coli* Fermentations. *J. Ind. Microbiol. Biotechnol.* 34, 689–700. doi:10.1007/s10295-007-0244-2

Dittrich, C. R., Vadali, R. V., Bennett, G. N., and San, K. Y. (2010). Redistribution of Metabolic Fluxes in the Central Aerobic Metabolic Pathway of *E. coli* Mutant Strains with Deletion of the ackA-Pta and poxB Pathways for the Synthesis of Isoamyl Acetate. *Biotechnol. Prog.* 21, 627–631. doi:10.1021/bp049730r

Fixation, A. C., Hügler, M., Menendez, C., Schägger, H., and Fuchs, G. (2002). Malonyl-coenzyme A Reductase from Chloroflexus Aurantiacus, a Key Enzyme of the 3-hydroxypropionate Cycle for Autotrophic CO(2) Fixation. *J. Bacteriol.* 184, 2404–2410. doi:10.1128/JB.184.9.2404–2410.2002

Gao, C., Yang, X., Wang, H., Rivero, C. P., Li, C., Cui, Z., et al. (2016). Robust Succinic Acid Production from Crude Glycerol Using Engineered Yarrowia Lipolytica. *Biotechnol. Biofuels* 9, 179–190. doi:10.1186/s13068-016-0597-8

Gokarn, R. R., Eiteman, M. A., and Altman, E. (1998). Expression of Pyruvate Carboxylase Enhances Succinate Production in *Escherichia coli* without Affecting Glucose Uptake. *Biotechnol. Lett.* 20, 795–798. doi:10.1023/B:BILE.0000015925.52287.1f

Gokarn, R. R., Eiteman, M. A., and Altman, E. (2000). Metabolic Analysis of *Escherichia coli* in the Presence and Absence of the Carboxylating Enzymes Phosphoenolpyruvate Carboxylase and Pyruvate Carboxylase. *Appl. Environ. Microbiol.* 66, 1844–1850. doi:10.1128/AEM.66.5.1844-1850.2000

Gong, F., Cai, Z., and Li, Y. (2016). Synthetic Biology for CO2 Fixation. *Sci. China Life Sci.* 59, 1106–1114. doi:10.1007/s11427-016-0304-2

Gourdon, P., Baucher, M.-F., Lindley, N. D., and Guyonvarch, A. (2000). Cloning of the Malic Enzyme Gene from Corynebacterium Glutamicum and Role of the Enzyme in Lactate Metabolism. *Appl. Environ. Microbiol.* 66, 2981–2987. doi:10.1128/aem.66.7.2981-2987.2000

Guettler, M. V., Jain, M. K., and Rumler, D. (1996). Method for Making Succinic Acid, Bacterial Variants for Use in the Process, and Methods for Obtaining Variants. *United States Patent*. Available at http://www.google.com/patents/US5723322.

Gui, L., Sunnarborg, A., Pan, B., and Laporte, D. C. (1996). Autoregulation of iclR, the Gene Encoding the Repressor of the Glyoxylate Bypass Operon. *J. Bacteriol.* 178, 321–324. doi:10.1128/jb.178.1.321-324.1996

Hendrik, W., Joeri, B., Helena, M., Jo, M., Marjan, D. M., Maria, R., et al. (2011). Effect of iclR and arcA Knockouts on Biomass Formation and Metabolic Fluxes in *Escherichia coli* K12 and its Implications on Understanding the Metabolism of *Escherichia coli* BL21 (DE3). *Bmc Microbiol.* 11, 1–17. doi:10.1186/1471-2180-11-70

Herter, S., Farfsing, J., Gad'On, N., Rieder, C., Eisenreich, W., Bacher, A., et al. (2001). Autotrophic CO 2 Fixation by Chloroflexus Aurantiacus : Study of Glyoxylate Formation and Assimilation via the 3-Hydroxypropionate Cycle. *J. Bacteriol.* 183, 4305–4316. doi:10.1128/jb.183.14.4305-4316.2001

Hong, S. H., and Lee, S. Y. (2002). Importance of Redox Balance on the Production of Succinic Acid by Metabolically Engineered *Escherichia coli*. *Appl. Microbiol. Biotechnol.* 58, 286–290. doi:10.1007/s00253-001-0899-y

Hong, S. H., Kim, J. S., Lee, S. Y., In, Y. H., Choi, S. S., Rih, J.-K., et al. (2004). The Genome Sequence of the Capnophilic Rumen Bacterium Mannheimia Succiniciproducens. *Nat. Biotechnol.* 22, 1275–1281. doi:10.1038/nbt1010

Hui, W., Zhimin, L., Li, Z., and Qin, Y. (2009). Enhanced Anaerobic Succinic Acid Production by *Escherichia coli* NZN111 Aerobically Grown on Gluconeogenic Carbon Sources. *Enzyme Microb. Technol.* 44, 165–169. doi:10.1016/j.jbiotec.2008.07.964

Ishihama, A. (2010). Prokaryotic Genome Regulation: Multifactor Promoters, Multitarget Regulators and Hierarchic Networks. *FEMS Microbiol. Rev.* 34, 628–645. doi:10.1111/j.1574-6976.2010.00227.x

Jiang, M., Liu, S.-w., Ma, J.-f., Chen, K.-q., Yu, L., Yue, F.-f., et al. (2010). Effect of Growth Phase Feeding Strategies on Succinate Production by Metabolically Engineered *Escherichia coli*. *Appl. Environ. Microbiol.* 76, 1298–1300. doi:10.1128/AEM.02190-09

Jitrapakdee, S., St Maurice, M., Rayment, I., Cleland, W. W., Wallace, J. C., and Attwood, P. V. (2008). Structure, Mechanism and Regulation of Pyruvate Carboxylase. *Biochem. J.* 413, 369–387. doi:10.1042/bj20080709

Kai, Y., Matsumura, H., Inoue, T., Terada, K., Nagara, Y., Yoshinaga, T., et al. (1999). Three-dimensional Structure of Phosphoenolpyruvate Carboxylase: a Proposed Mechanism for Allosteric Inhibition. *Proc. Natl. Acad. Sci.* 96, 823–828. doi:10.1073/pnas.96.3.823

Kequan, C., Min, J., Ping, W., Jiaming, Y., and Hao, W. (2008). Succinic Acid Production from Acid Hydrolysate of Corn Fiber by Actinobacillus Succinogenes. *Appl. Biochem. Biotechnol.* 160, 477–485. doi:10.1016/j.biortech.2007.03.044

Keseler, I. M., Collado-Vides, J., Santos-Zavaleta, A., Peralta-Gil, M., Gama-Castro, S., Muñiz-Rascado, L., et al. (2011). EcoCyc: a Comprehensive Database of *Escherichia coli* Biology. *Nucleic Acids Res.* 39, D583–D590. doi:10.1093/nar/gkq1143

Kim, D. Y., Yim, S. C., Lee, P. C., Lee, W. G., Lee, S. Y., and Chang, H. N. (2004). Batch and Continuous Fermentation of Succinic Acid from wood Hydrolysate by Mannheimia Succiniciproducens MBEL55E. *Enzyme Microb. Technol.* 35, 648–653. doi:10.1016/j.enzmictec.2004.08.018

Krebs, A., and Bridger, W. A. (1980). The Kinetic Properties of Phosphoenolpyruvate Carboxykinase of *Escherichia coli*. *Can. J. Biochem.* 58, 309–318. doi:10.1139/o80-041

Kuhnert, P., Scholten, E., Haefner, S., Mayor, D., and Frey, J. (2010). Basfia Succiniciproducens Gen. nov., Sp. nov., a New Member of the Family Pasteurellaceae Isolated from Bovine Rumen. *Int. J. Syst. Evol. Microbiol.* 60, 44–50. doi:10.1099/ijs.0.011809-0

Kwon, Y.-D., Kwon, O.-H., Lee, H.-S., and Kim, P. (2007). The Effect of NADP-dependent Malic Enzyme Expression and Anaerobic C4 Metabolism in *Escherichia coli* Compared with Other Anaplerotic Enzymes. *J. Appl. Microbiol.* 103, 2340–2345. doi:10.1111/j.1365-2672.2007.03485.x

Kwon, Y. D., Lee, S. Y., and Kim, P. (2006). Influence of Gluconeogenic Phosphoenolpyruvate Carboxykinase (PCK) Expression on Succinic Acid Fermentation in *Escherichia coli* under High Bicarbonate Condition. *J. Microbiol. Biotechnol.* 16, 1448–1452. doi:10.1007/s10295-006-0128-x

Lee, J. W., Yi, J., Kim, T. Y., Choi, S., Ahn, J. H., Song, H., et al. (2016). Homo-succinic Acid Production by Metabolically Engineered Mannheimia Succiniciproducens. *Metab. Eng.* 38, 409–417. doi:10.1016/j.ymben.2016.10.004

Lee, P. C., Lee, S. Y., Hong, S. H., and Chang, H. N. (2003). Batch and Continuous Cultures of Mannheimia Succiniciproducens MBEL55E for the Production of Succinic Acid from Whey and Corn Steep Liquor. *Bioproc. Biosyst. Eng.* 26, 63–67. doi:10.1007/s00449-003-0341-1

Lee, P. C., Lee, W. G., Kwon, S., Lee, S. Y., and Chang, H. N. (1999). Succinic Acid Production by Anaerobiospirillum Succiniciproducens: Effects of the H2/CO2 Supply and Glucose Concentration. *Enzyme Microb. Technol.* 24, 549–554. doi:10.1016/S0141-0229(98)00156-2

Lee, S., Hong, H., Chang, P., Lee, S. Y., Hong, S. H., and Chang, H. N. (2002). Isolation and Characterization of a New Succinic Acid-Producing Bacterium, Mannheimia Succiniciproducens MBEL55E, from Bovine Rumen. *Appl. Microbiol. Biotechnol.* 58, 663–668. doi:10.1007/s00253-002-0935-6

Lee, S. J., Song, H., and Lee, S. Y. (2006). Genome-based Metabolic Engineering of Mannheimia Succiniciproducens for Succinic Acid Production. *Appl. Environ. Microbiol.* 72, 1939–1948. doi:10.1128/aem.72.3.1939-1948.2006

Li, C., Ong, K. L., Yang, X., and Lin, C. S. K. (2019). Bio-refinery of Waste Streams for green and Efficient Succinic Acid Production by Engineered Yarrowia Lipolytica without pH Control. *Chem. Eng. J.* 371, 804–812. doi:10.1016/j.cej.2019.04.092

Li, J., Li, Y., Cui, Z., Liang, Q., and Qi, Q. (2017). Enhancement of Succinate Yield by Manipulating NADH/NAD+ Ratio and ATP Generation. *Appl. Microbiol. Biotechnol.* 101, 3153–3161. doi:10.1007/s00253-017-8127-6

Li, M., Hou, F., Wu, T., Jiang, X., Li, F., Liu, H., et al. (2020). Recent Advances of Metabolic Engineering Strategies in Natural Isoprenoid Production Using Cell Factories. *Nat. Prod. Rep.* 37, 80–99. doi:10.1039/C9NP00016J

Li, Q., Yang, M., Wang, D., Li, W., Wu, Y., Zhang, Y., et al. (2010). Efficient Conversion of Crop Stalk Wastes into Succinic Acid Production by Actinobacillus Succinogenes. *Bioresour. Technol.* 101, 3292–3294. doi:10.1016/j.biortech.2009.12.064

Lin, H., Bennett, G. N., and San, K.-Y. (2005c). Effect of Carbon Sources Differing in Oxidation State and Transport Route on Succinate Production in Metabolically Engineered *Escherichia coli*. *J. Ind. Microbiol. Biotechnol.* 32, 87–93. doi:10.1007/s10295-005-0206-5

Lin, H., Bennett, G. N., and San, K.-Y. (2005d). Fed-batch Culture of a Metabolically engineeredEscherichia Coli Strain Designed for High-Level Succinate Production and Yield under Aerobic Conditions. *Biotechnol. Bioeng.* 90, 775–779. doi:10.1002/bit.20458

Lin, H., Bennett, G. N., and San, K.-Y. (2004). Genetic Reconstruction of the Aerobic central Metabolism inEscherichia Coli for the Absolute Aerobic Production of Succinate. *Biotechnol. Bioeng.* 89, 148–156. doi:10.1002/bit.20298

Lin, H., Bennett, G. N., and San, K.-Y. (2005a). Metabolic Engineering of Aerobic Succinate Production Systems in *Escherichia coli* to Improve Process Productivity and Achieve the Maximum Theoretical Succinate Yield. *Metab. Eng.* 7, 116–127. doi:10.1016/j.ymben.2004.10.003

Lin, H., San, K.-Y., and Bennett, G. N. (2005b). Effect of Sorghum Vulgare Phosphoenolpyruvate Carboxylase and Lactococcus Lactis Pyruvate Carboxylase Coexpression on Succinate Production in Mutant Strains of *Escherichia coli*. *Appl. Microbiol. Biotechnol.* 67, 515–523. doi:10.1007/s00253-004-1789-x

Litsanov, B., Brocker, M., and Bott, M. (2012). Toward Homosuccinate Fermentation: Metabolic Engineering of Corynebacterium Glutamicum for Anaerobic Production of Succinate from Glucose and Formate. *Appl. Environ. Microbiol.* 78, 3325–3337. doi:10.1128/AEM.07790-11

Liu, Y., and Jiang, H. (2011). Directed Evolution of Propionyl-CoA Carboxylase for Succinate Biosynthesis. *Trends Biotechnol.* 39, 330–331. doi:10.1016/j.tibtech.2021.02.006

Liu, B., Xiang, S., Zhao, G., Wang, B., Ma, Y., Liu, W., et al. (2019). Efficient Production of 3-hydroxypropionate from Fatty Acids Feedstock in *Escherichia coli*. *Metab. Eng.* 51, 121–130. doi:10.1016/j.ymben.2018.10.003

Liu, C., Wang, Q., Xian, M., Ding, Y., and Zhao, G. (2013). Dissection of Malonyl-Coenzyme A Reductase of Chloroflexus Aurantiacus Results in Enzyme Activity Improvement. *Plos One* 8, e75554–8. doi:10.1371/journal.pone.0075554

Liu, C., Ding, Y., Zhang, R., Liu, H., Xian, M., and Zhao, G. (2016). Functional Balance between Enzymes in Malonyl-CoA Pathway for 3-hydroxypropionate Biosynthesis. *Metab. Eng.* 34, 104–111. doi:10.1016/j.ymben.2016.01.001i

Liu, T., Vora, H., and Khosla, C. (2010). Quantitative Analysis and Engineering of Fatty Acid Biosynthesis in *E. coli*. *Metab. Eng.* 12, 378–386. doi:10.1016/j.ymben.2010.02.003

Liu, X., and De Wulf, P. (2004). Probing the ArcA-P Modulon of *Escherichia coli* by Whole Genome Transcriptional Analysis and Sequence Recognition Profiling. *J. Biol. Chem.* 279, 12588–12597. doi:10.1074/jbc.M313454200

Liu, X., Feng, X., Ding, Y., Gao, W., Xian, M., Wang, J., et al. (2020). Characterization and Directed Evolution of Propionyl-CoA Carboxylase and its Application in Succinate Biosynthetic Pathway with Two CO2 Fixation Reactions. *Metab. Eng.* 62, 42–50. doi:10.1016/j.ymben.2020.08.012

Liu, Y.-P., Zheng, P., Sun, Z.-H., Ni, Y., Dong, J.-J., and Zhu, L.-L. (2008). Economical Succinic Acid Production from Cane Molasses by Actinobacillus Succinogenes. *Bioresour. Technol.* 99, 1736–1742. doi:10.1016/j.biortech.2007.03.044

Lombard, J., and Moreira, D. (2012). Early Evolution of the Biotin-dependent Carboxylase Family. *BMC Evol. Biol.* 11, 232. doi:10.1186/1471-2148-11-232

López-Garzón, C., and Straathof, A. (2014). Recovery of Carboxylic Acids Produced by Fermentation. *Biotechnol. Adv.* 32, 873–904. doi:10.1016/j.biotechadv.2014.04.002

Lousté, B., and Eloutassi, N. (2020). Succinic Acid Production from Whey and Lactose by Actinobacillus Succinogenes 130Z in Batch Fermentation. *Biotechnol. Rep. (Amst)* 27, e00481–486. doi:10.1016/j.btre.2020.e00481

Lu, C. D., Xiong, Y. Y., Zhao, J. F., and Wang, J. H. (2015). Fermentation Production of Succinic Acid from Sucrose by Engineered Escherichia Coli JH208. *Amr* 1088, 503–506. doi:10.4028/www.scientific.net/AMR.1088.503

Lu, S., Eiteman, M. A., and Altman, E. (2009). Effect of CO2 on Succinate Production in Dual-phase *Escherichia coli* Fermentations. *J. Biotechnol.* 143, 213–223. doi:10.1016/j.jbiotec.2009.07.012

Ma, J., Gou, D., Liang, L., Liu, R., Chen, X., Zhang, C., et al. (2013). Enhancement of Succinate Production by Metabolically Engineered *Escherichia coli* with Co-expression of Nicotinic Acid Phosphoribosyltransferase and Pyruvate Carboxylase. *Appl. Microbiol. Biotechnol.* 97, 6739–6747. doi:10.1007/s00253-013-4910-1

Menendez, C., Bauer, Z., Huber, H., Nasser, G. o., Stetter, K.-O., Fuchs, G., et al. (1999). Presence of Acetyl Coenzyme A (Coa) Carboxylase and Propionyl-Coa Carboxylase in Autotrophic Crenarchaeota and Indication for Operation of a 3-Hydroxypropionate Cycle in Autotrophic Carbon Fixation. *J. Bacteriol.* 181, 1088–1098. doi:10.1128/JB.181.4.1088-1098.1999

Meynial-Salles, I., Dorotyn, S., and Soucaille, P. (2010). A New Process for the Continuous Production of Succinic Acid from Glucose at High Yield, Titer, and Productivity. *Biotechnol. Bioeng.* 99, 129–135. doi:10.1002/bit.21521

Michael, F. A. B., Ali, M., Davinia, S., Holly, S., Brenna, A. B., Nancy, D., et al. (2015). Continuous Succinic Acid Production by *Actinobacillus succinogenes* on Xylose-Enriched Hydrolysate. *Bioresour. Technol.* 8, 181–198. doi:10.1186/s13068-015-0363-3

Millard, C. S., Chao, Y. P., Liao, J. C., and Donnelly, M. I. (1996). Enhanced Production of Succinic Acid by Overexpression of Phosphoenolpyruvate Carboxylase in *Escherichia coli*. *Appl. Environ. Microbiol.* 62, 1808–1810. doi:10.1128/aem.62.5.1808-1810.1996

Modak, H. V., and Kelly, D. J. (1995). Acetyl-CoA-dependent Pyruvate Carboxylase from the Photosynthetic Bacterium Rhodobacter Capsulatus: Rapid and Efficient Purification Using Dye-Ligand Affinity Chromatography. *Microbiology* 141, 2619–2628. doi:10.1099/13500872-141-10-2619

Okino, S., Inui, M., and Yukawa, H. (2005). Production of Organic Acids by Corynebacterium Glutamicum under Oxygen Deprivation. *Appl. Microbiol. Biotechnol.* 68, 475–480. doi:10.1007/s00253-005-1900-y

Okino, S., Noburyu, R., Suda, M., Jojima, T., Inui, M., and Yukawa, H. (2008). An Efficient Succinic Acid Production Process in a Metabolically Engineered Corynebacterium Glutamicum Strain. *Appl. Microbiol. Biotechnol.* 81, 459–464. doi:10.1007/s00253-008-1668-y

Olajuyin, A. M., Yang, M., Liu, Y., Mu, T., Tian, J., Adaramoye, O. A., et al. (2016). Efficient Production of Succinic Acid from Palmaria Palmata Hydrolysate by Metabolically Engineered *Escherichia coli*. *Bioresour. Technol.* 214, 653–659. doi:10.1016/j.biortech.2016.04.117

Pateraki, C., Patsalou, M., Vlysidis, A., Kopsahelis, N., Webb, C., Koutinas, A. A., et al. (2016). Actinobacillus Succinogenes : Advances on Succinic Acid Production and Prospects for Development of Integrated Biorefineries. *Biochem. Eng. J.* 112, 285–303. doi:10.1016/j.bej.2016.04.005

Perrenoud, A., and Sauer, U. (2005). Impact of Global Transcriptional Regulation by ArcA, ArcB, Cra, Crp, Cya, Fnr, and Mlc on Glucose Catabolism in *Escherichia coli*. *J. Bacteriol.* 187, 3171–3179. doi:10.1128/JB.187.9.3171-3179.2005

Price, G. D., Woodger, F. J., Badger, M. R., Howitt, S. M., and Tucker, L. (2004). Identification of a SulP-type Bicarbonate Transporter in marine Cyanobacteria. *Proc. Natl. Acad. Sci.* 101, 18228–18233. doi:10.1073/pnas.0405211101

Qiang, l., Dan, W., Yong, W., and Wangliang, L. (2010). One Step Recovery of Succinic Acid from Fermentation Broths by Crystallization. *Separat. Purif. Technol.* 72, 294–300. doi:10.1016/j.seppur.2010.02.021

Ramseier, T. M., Bledig, S., Michotey, V., Feghali, R., and Saier, M. H. (2010). The Global Regulatory Protein FruR Modulates the Direction of Carbon Flow in *Escherichia coli*. *Mol. Microbiol.* 16, 1157–1169. doi:10.1111/j.1365-2958.1995.tb02339.x

Ramseier, T. M. (1996). Cra and the Control of Carbon Flux via Metabolic Pathways. *Res. Microbiol.* 147, 489–493. doi:10.1016/0923-2508(96)84003-4

Sánchez, A. M., Bennett, G. N., and San, K. Y. (2005). Efficient Succinic Acid Production from Glucose through Overexpression of Pyruvate Carboxylase in an *Escherichia coli* Alcohol Dehydrogenase and Lactate Dehydrogenase Mutant. *Biotechnol. Prog.* 21, 358–365. doi:10.1021/bp049676e

Sánchez, A. M., Bennett, G. N., and San, K.-Y. (2005). Novel Pathway Engineering Design of the Anaerobic central Metabolic Pathway in *Escherichia coli* to Increase Succinate Yield and Productivity. *Metab. Eng.* 7, 229–239. doi:10.1016/j.ymben.2005.03.001

Sarkar, D., Siddiquee, K. A. Z., Araúzo-Bravo, M. J., Oba, T., and Shimizu, K. (2008). Effect of Cra Gene Knockout Together with Edd and iclR Genes Knockout on the Metabolism in *Escherichia coli*. *Arch. Microbiol.* 190, 559–571. doi:10.1007/s00203-008-0406-2

Schütze, A., Benndorf, D., Püttker, S., Kohrs, F., and Bettenbrock, K. (2020). The Impact of ackA, Pta, and ackA-Pta Mutations on Growth, Gene Expression and Protein Acetylation in *Escherichia coli* K-12. *Front. Microbiol.* 11, 233. doi:10.3389/fmicb.2020.00233

Scott, J. W., Norman, D. G., Hawley, S. A., Kontogiannis, L., and Hardie, D. G. (2002). Protein Kinase Substrate Recognition Studied Using the Recombinant Catalytic Domain of AMP-Activated Protein Kinase and a Model Substrate. *J. Mol. Biol.* 317, 309–323. doi:10.1006/jmbi.2001.5316

Shi, S., Chen, Y., Siewers, V., and Nielsen, J. (2014). Improving Production of Malonyl Coenzyme A-Derived Metabolites by Abolishing Snf1-dependent Regulation of Acc1. *mBio* 5, e01130–14. doi:10.1128/mBio.01130-14

Shibata, M., Katoh, H., Sonoda, M., Ohkawa, H., Shimoyama, M., Fukuzawa, H., et al. (2002). Genes Essential to Sodium-dependent Bicarbonate Transport in Cyanobacteria: Function and Phylogenetic Analysis. *J. Biol. Chem.* 277, 18658–18664. doi:10.1074/jbc.M112468200

Shimada, T., Yamamoto, K., and Ishihama, A. (2011). Novel Members of the Cra Regulon Involved in Carbon Metabolism in *Escherichia coli*. *J. Bacteriol.* 193, 649–659. doi:10.1128/JB.01214-10

Shimizu, K. (2013). Metabolic Regulation of a Bacterial Cell System with Emphasis on *Escherichia coli* Metabolism. *ISRN Biochem.* 2013, 645983. doi:10.1155/2013/645983

Singh, A., Cher Soh, K., Hatzimanikatis, V., and Gill, R. T. (2010). Manipulating Redox and ATP Balancing for Improved Production of Succinate in *E. coli*. *Metab. Eng.* 13, 76–81. doi:10.1016/j.ymben.2010.10.006

Singh, A., Lynch, M. D., and Gill, R. T. (2009). Genes Restoring Redox Balance in Fermentation-Deficient *E. coli* NZN111. *Metab. Eng.* 11, 347–354. doi:10.1016/j.ymben.2009.07.002

Stols, L., and Donnelly, M. I. (1997). Production of Succinic Acid through Overexpression of NAD(+)-dependent Malic Enzyme in an *Escherichia coli* Mutant. *Appl. Environ. Microbiol.* 63, 2695–2701. doi:10.1128/aem.63.7.2695-2701.1997

Stols, L., Kulkarni, G., Harris, B. G., and Donnelly, M. I. (1997). Expression of *Ascaris suum* Malic Enzyme in a Mutant *Escherichia coli* Allows Production of Succinic Acid from Glucose. *Appl. Biochem. Biotechnol.* 63, 153–158. doi:10.1007/978-1-4612-2312-2_15

Sun, H., Song, Y., Chen, F., Zhou, C., and Feng, L. (2020). An ArcA-Modulated Small RNA in Pathogenic *Escherichia coli* K1. *Front. Microbiol.* 11, 1–13. doi:10.3389/fmicb.2020.574833

Tan, Z., Zhu, X., Chen, J., Li, Q., and Zhang, X. (2013). Activating Phosphoenolpyruvate Carboxylase and Phosphoenolpyruvate Carboxykinase in Combination for Improvement of Succinate Production. *Appl. Environ. Microbiol.* 79, 4838–4844. doi:10.1128/AEM.00826-13

Thakker, C., Martínez, I., San, K.-Y., and Bennett, G. N. (2012). Succinate Production in *Escherichia coli*. *Biotechnol. J.* 7 (2), 213–224. doi:10.1002/biot.201100061

Thakker, C., Zhu, J., San, K.-Y., and Bennett, G. (2011). Heterologous Pyc Gene Expression under Various Natural and Engineered Promoters in *Escherichia coli* for Improved Succinate Production. *J. Biotechnol.* 155, 236–243. doi:10.1016/j.jbiotec.2011.05.001

Thuy, N. T. H., Kongkaew, A., Flood, A., and Boontawan, A. (2017). Fermentation and Crystallization of Succinic Acid from Actinobacillus Succinogenes

ATCC55618 Using Fresh Cassava Root as the Main Substrate. *Bioresour. Technol.* 233, 342–352. doi:10.1016/j.biortech.2017.02.114

Tong, L. (2013). Structure and Function of Biotin-dependent Carboxylases. *Cell. Mol. Life Sci.* 70, 863–891. doi:10.1007/s00018-012-1096-0

Vemuri, G. N., Eiteman, M. A., and Altman, E. (2002). Effects of Growth Mode and Pyruvate Carboxylase on Succinic Acid Production by Metabolically Engineered Strains of *Escherichia coli*. *Appl. Environ. Microbiol.* 68, 1715–1727. doi:10.1128/AEM.68.4.1715-1727.2002

Wan, C., Li, Y., Shahbazi, A., and Xiu, S. (2008). Succinic Acid Production from Cheese Whey Using Actinobacillus Succinogenes 130 Z. *Appl. Biochem. Biotechnol.* 145, 111–119. doi:10.1007/s12010-007-8031-0

Wang, D., Li, Q., Song, Z., Zhou, W., Su, Z., and Xing, J. (2011). High Cell Density Fermentation via a Metabolically Engineered *Escherichia coli* for the Enhanced Production of Succinic Acid. *J. Chem. Technol. Biotechnol.* 86, 512–518. doi:10.1002/jctb.2543

Wei, L.-N., Zhu, L.-W., and Tang, Y.-J. (2016). Succinate Production Positively Correlates with the Affinity of the Global Transcription Factor Cra for its Effector FBP in *Escherichia coli*. *Biotechnol. Biofuels* 9, 264–279. doi:10.1186/s13068-016-0679-7

Werf, M. J. V. D., Guettler, M. V., Jain, M. K., and Zeikus, J. G. (1997). Environmental and Physiological Factors Affecting the Succinate Product Ratio during Carbohydrate Fermentation by Actinobacillus Sp. 130Z. *Arch. Microbiol.* 167, 332–342. doi:10.1007/s002030050452

Werpy, T., Petersen, G., Aden, A., Bozell, J. J., and Jones, S. (2004). Top Value Added Chemicals from Biomass. *Nato Adv. Sci. Institutes*. doi:10.1126/science.1146356

Wilfredo, E., James, K., Levani, Z., Alexandre, E., White, M. A., Gribenko, A. V., et al. (2021). Signal Transmission in *Escherichia coli* Cyclic AMP Receptor Protein for Survival in Extreme Acidic Conditions. *Biochemistry* 60, 2987–3006. doi:10.1021/acs.biochem.1c00388

Wolfe, A. J. (2005). The Acetate Switch. *Microbiol. Mol. Biol. Rev.* 69, 12–50. doi:10.1128/mmbr.69.1.12-50.2005

Wongkittichote, P., Ah Mew, N., and Chapman, K. A. (2017). Propionyl-CoA Carboxylase - A Review. *Mol. Genet. Metab.* 122, 145–152. doi:10.1016/j.ymgme.2017.10.002

Woods, A., Munday, M. R., Scott, J., Yang, X., Carlson, M., and Carling, D. (1994). Yeast SNF1 Is Functionally Related to Mammalian AMP-Activated Protein Kinase and Regulates Acetyl-CoA Carboxylase *In Vivo*. *J. Biol. Chem.* 269, 19509–19515. doi:10.1016/S0021-9258(17)32198-1

Wu, H., Li, Z.-m., Zhou, L., and Ye, Q. (2007). Improved Succinic Acid Production in the Anaerobic Culture of an *Escherichia coli* pflB ldhA Double Mutant as a Result of Enhanced Anaplerotic Activities in the Preceding Aerobic Culture. *Appl. Environ. Microbiol.* 73, 7837–7843. doi:10.1128/AEM.01546-07

Wu, M., Li, X., Guo, S., Lemma, W. D., Zhang, W., Ma, J., et al. (2017). Enhanced Succinic Acid Production under Acidic Conditions by Introduction of Glutamate Decarboxylase System in *E. coli* AFP111. *Bioproc. Biosyst Eng* 40, 549–557. doi:10.1007/s00449-016-1720-8

Xiao, M., Zhu, X., Bi, C., Ma, Y., and Zhang, X. (2017). Improving Succinate Productivity by Engineering a Cyanobacterial CO2 Concentrating System (CCM) in *Escherichia coli*. *Biotechnol. J.* 12, 1–7. doi:10.1002/biot.201700199

Yan, D., Wang, C., Zhou, J., Liu, Y., Yang, M., and Xing, J. (2014). Construction of Reductive Pathway in *Saccharomyces cerevisiae* for Effective Succinic Acid Fermentation at Low pH Value. *Bioresour. Technol.* 156, 232–239. doi:10.1016/j.biortech.2014.01.053

Yang, J., Wang, Z., Zhu, N., Wang, B., Chen, T., and Zhao, X. (2014). Metabolic Engineering of *Escherichia coli* and In Silico Comparing of Carboxylation Pathways for High Succinate Productivity under Aerobic Conditions. *Microbiol. Res.* 169, 432–440. doi:10.1016/j.micres.2013.09.002

Yu, J.-H., Zhu, L.-W., Xia, S.-T., Li, H.-M., Tang, Y.-L., Liang, X.-H., et al. (2016). Combinatorial Optimization of CO2transport and Fixation to Improve Succinate Production by Promoter Engineering. *Biotechnol. Bioeng.* 113, 1531–1541. doi:10.1002/bit.25927

Yuzbashev, T. V., Yuzbasheva, E. Y., Sobolevskaya, T. I., Laptev, I. A., Vybornaya, T. V., Larina, A. S., et al. (2010). Production of Succinic Acid at Low pH by a Recombinant Strain of the Aerobic Yeast Yarrowia Lipolytica. *Biotechnol. Bioeng.* 107, 673–682. doi:10.1002/bit.22859

Zha, W., Rubin-Pitel, S. B., Shao, Z., and Zhao, H. (2009). Improving Cellular Malonyl-CoA Level in *Escherichia coli* via Metabolic Engineering. *Metab. Eng.* 11, 192–198. doi:10.1016/j.ymben.2009.01.005

Zhang, X., Jantama, K., Moore, J. C., Jarboe, L. R., Shanmugam, K. T., and Ingram, L. O. (2009a). Metabolic Evolution of Energy-Conserving Pathways for Succinate Production in *Escherichia coli*. *Proc. Natl. Acad. Sci.* 106, 20180–20185. doi:10.1073/pnas.0905396106

Zhang, X., Jantama, K., Shanmugam, K. T., and Ingram, L. O. (2009b). Reengineering *Escherichia coli* for Succinate Production in Mineral Salts Medium. *Appl. Environ. Microbiol.* 75, 7807–7813. doi:10.1128/AEM.01758-09

Zhang, Y., Huang, Z., Du, C., Li, Y., and Cao, Z. a. (2009c). Introduction of an NADH Regeneration System into Klebsiella Oxytoca Leads to an Enhanced Oxidative and Reductive Metabolism of Glycerol. *Metab. Eng.* 11, 101–106. doi:10.1016/j.ymben.2008.11.001

Zhang, Y., Qiu, X., Chen, C., Yu, Z., and Hong, H. (2020). Recent Progress in Microbial Production of Succinic Acid. *CIESC J.* 71, 1964–1975. doi:10.11949/0438-1157.20191430

Zhang, Z., Aboulwafa, M., and Saier, M. H. (2014). Regulation of Crp Gene Expression by the Catabolite Repressor/Activator, Cra, in *Escherichia coli*. *J. Mol. Microbiol. Biotechnol.* 24, 135–141. doi:10.1159/000362722

Zheng, P., Dong, J.-J., Sun, Z.-H., Ni, Y., and Fang, L. (2009). Fermentative Production of Succinic Acid from Straw Hydrolysate by Actinobacillus Succinogenes. *Bioresour. Technol.* 100, 2425–2429. doi:10.1016/j.biortech.2008.11.043

Zhu, L.-W., and Tang, Y.-J. (2017). Current Advances of Succinate Biosynthesis in Metabolically Engineered *Escherichia coli*. *Biotechnol. Adv.* 35, 1040–1048. doi:10.1016/j.biotechadv.2017.09.007

Zhu, L.-W., Xia, S.-T., Wei, L.-N., Li, H.-M., Yuan, Z.-P., and Tang, Y.-J. (2016). Enhancing Succinic Acid Biosynthesis in *Escherichia coli* by Engineering its Global Transcription Factor, Catabolite Repressor/activator (Cra). *Sci. Rep.* 6, 36526–36537. doi:10.1038/srep36526

Zhu, L.-W., Zhang, L., Wei, L.-N., Li, H.-M., Yuan, Z.-P., Chen, T., et al. (2015). Collaborative Regulation of CO2 Transport and Fixation during Succinate Production in *Escherichia coli*. *Sci. Rep.* 5, 17321–17333. doi:10.1038/srep17321

Zhu, X., Tan, Z., Xu, H., Chen, J., Tang, J., and Zhang, X. (2014). Metabolic Evolution of Two Reducing Equivalent-Conserving Pathways for High-Yield Succinate Production in *Escherichia coli*. *Metab. Eng.* 24, 87–96. doi:10.1016/j.ymben.2014.05.003

Conflict of Interest: The authors declare that the research was conducted in the absence of any commercial or financial relationships that could be construed as a potential conflict of interest.

Publisher's Note: All claims expressed in this article are solely those of the authors and do not necessarily represent those of their affiliated organizations, or those of the publisher, the editors, and the reviewers. Any product that may be evaluated in this article, or claim that may be made by its manufacturer, is not guaranteed or endorsed by the publisher.

frontiers | Frontiers in Bioengineering and Biotechnology

REVIEW
published: 12 May 2022
doi: 10.3389/fbioe.2022.897003

Characteristics and Application of *Rhodopseudomonas palustris* as a Microbial Cell Factory

Meijie Li[1,2†], *Peng Ning*[1,2†], *Yi Sun*[3], *Jie Luo*[4]* and *Jianming Yang*[1,2]*

[1]Energy-Rich Compound Production by Photosynthetic Carbon Fixation Research Center, Shandong Key Lab of Applied Mycology, Qingdao Agricultural University, Qingdao, China, [2]College of Life Sciences, Qingdao Agricultural University, Qingdao, China, [3]Haiyang Comprehensive Administrative Law Enforcement Bureau (Agriculture), Haiyang, China, [4]Qingdao Garden Forestry Technology School, Qingdao, China

Rhodopseudomonas palustris, a purple nonsulfur bacterium, is a bacterium with the properties of extraordinary metabolic versatility, carbon source diversity and metabolite diversity. Due to its biodetoxification and biodegradation properties, *R. palustris* has been traditionally applied in wastewater treatment and bioremediation. *R. palustris* is rich in various metabolites, contributing to its application in agriculture, aquaculture and livestock breeding as additives. In recent years, *R. palustris* has been engineered as a microbial cell factory to produce valuable chemicals, especially photofermentation of hydrogen. The outstanding property of *R. palustris* as a microbial cell factory is its ability to use a diversity of carbon sources. *R. palustris* is capable of CO_2 fixation, contributing to photoautotrophic conversion of CO_2 into valuable chemicals. *R. palustris* can assimilate short-chain organic acids and crude glycerol from industrial and agricultural wastewater. Lignocellulosic biomass hydrolysates can also be degraded by *R. palustris*. Utilization of these feedstocks can reduce the industry cost and is beneficial for environment. Applications of *R. palustris* for biopolymers and their building blocks production, and biofuels production are discussed. Afterward, some novel applications in microbial fuel cells, microbial electrosynthesis and photocatalytic synthesis are summarized. The challenges of the application of *R. palustris* are analyzed, and possible solutions are suggested.

Keywords: *Rhodopseudomonas palustris*, biopolymer, biofuel, wastewater treatment, microbial cell factory, photoautotrophic

OPEN ACCESS

Edited by:
Ka Yu Cheng,
CSIRO Land and Water, Australia

Reviewed by:
Sanjay Kumar Singh Patel,
Konkuk University, South Korea
Jung Rae Kim,
Pusan National University, South Korea

***Correspondence:**
Jie Luo
qdluojie@126.com
Jianming Yang
yjming888@126.com

[†]These authors have contributed equally to this work and share first authorship

Specialty section:
This article was submitted to Industrial Biotechnology, a section of the journal Frontiers in Bioengineering and Biotechnology

Received: *15 March 2022*
Accepted: *27 April 2022*
Published: *12 May 2022*

Citation:
Li M, Ning P, Sun Y, Luo J and Yang J (2022) Characteristics and Application of Rhodopseudomonas palustris as a Microbial Cell Factory. Front. Bioeng. Biotechnol. 10:897003. doi: 10.3389/fbioe.2022.897003

1 INTRODUCTION

Rhodopseudomonas palustris belonging to purple nonsulfur bacterium (PNSB) is widely distributed in nature, mainly in anaerobic water environments with sufficient light, such as lakes, soils, swamps, and the sea (Guan et al., 2017). The PNSB constitute a group of versatile organisms in which most exhibit four modes of metabolism: photoautotrophic, photoheterotrophic, chemoheterotrophic and chemoautotrophic, switching from one mode to another depending on conditions available (**Figure 1**) (Larimer et al., 2003). This metabolic versatility allows *R. palustris* to use light, inorganic, and organic compounds as its carbon and energy sources under anaerobic or aerobic conditions (Madigan and Jung, 2009). Therefore, *R. palustris* is of interest for all sorts of industrial and environmental applications.

Traditionally, *R. palustris* is widely utilized in the areas of aquaculture industry and wastewater treatment. It is rich in biologically active chemicals, including proteins, vitamins, polysaccharides,

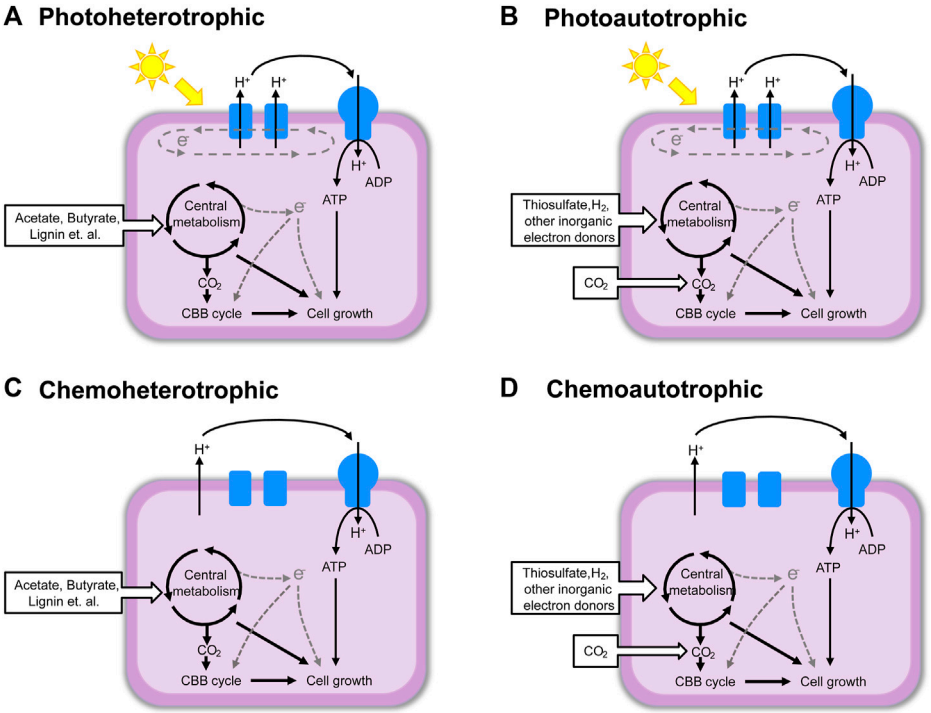

FIGURE 1 | The four types of metabolism of *R. palustris*. **(A)** Photoheterotrophic; **(B)** Photoautotrophic; **(C)** Chemoheterotrophic; **(D)** Chemoautotrophic. This figure was modified according to the figure in reference (Larimer et al., 2003).

pantothenic acid and folic acid, which contribute to its function as feed supplement. It can also increase the oxygen content of aquaculture water, stabilize the pH and purify the aquaculture water environment (Peirong and Wei, 2013). The addition of *R. palustris* to aquaculture water can improve the immunity of aquatic organisms and prevent diseases (Zhou et al., 2010). *R. palustris* has biodetoxification and biodegradation capacities toward components in livestock waste and industrial waste, such as lignin, nitride, chlorides and aromatic compounds (Harwood et al., 1998). Analysis of the complete genome sequence of *R. palustris* indicated a large inventory of genes encoding the four distinct ring cleavage pathways for degradation of the aromatic compounds, confirming its outstanding ability of biodegradation (Larimer et al., 2003).

In addition to the above applications, *R. palustris* has great potential to be applied in many other fields. As a microbial cell factory, *R. palustris* has been extensively researched for hydrogen production (McKinlay and Harwood, 2010b) *via* photo-fermentation or *via* complementation of photo-fermentation and dark-fermentation (Patel et al., 2012). Other biofuels production in *R. palustris*, such as methane (Fixen et al., 2016) and butanol (Doud et al., 2017), has also been reported. Production of valuable chemicals in *R. palustris*, such as poly-beta-hydroxybutyrate (PHB) (Wu et al., 2012), polysaccharide (Fritts et al., 2017) and isoprenoid (Xu et al., 2016), indicates the potential of *R. palustris* as a chassis organism for biopolymers and their building blocks production. Moreover, *R. palustris* can transfer electrons to solid electron acceptor such as electrode, enabling its application in microbial fuel cells (MFC) for electricity production (Lai et al., 2017). *R. palustris* also has the ability of electrons uptake from solid materials, leading to its application in the field of microbial electrosynthesis (MES) (Xing et al., 2008; Rengasamy et al., 2018). Similarly, *R. palustris* can absorb electrons from CdS nanoparticles attached to the cell surface, and a CdS-*R. palustris* hybrid system has been constructed for photocatalytic synthesis (Wang et al., 2019).

In this review, the advantages of *R. palustris* as a microbial cell factory were analyzed. Then, the applications of *R. palustris* in biopolymers and their building blocks production were discussed. Traditional application of *R. palustris* in the fields of wastewater treatment, bioremediation, agriculture, aquaculture and livestock breeding were summarized. Application in other fields, including biofuel production, microbial fuel cells, microbial electrosynthesis and photocatalytic synthesis, were also summarized. Finally, the challenges of applications of *R. palustris* are analyzed, and possible solutions are suggested.

2 ADVANTAGES OF *R. PALUSTRIS* AS A MICROBIAL CELL FACTORY

2.1 Utilization of Diverse Carbon Sources, Including CO_2

R. palustris can utilize various carbon sources for growth, including small molecule organic acids, alcohols, inorganic and aromatic compounds, which are the main components in industrial waste

TABLE 1 | Carbon sources utilized by *R. palustris*.

Category	Carbon source	References
Short-chain organic acid	Acetic acid, butyric acid, fumaric acid, succinic acid, cyclohexane carboxylic acid, lactic acid, malic acid.	Rey et al. (2007), Adessi et al. (2016), Fixen et al. (2016), Lazaro et al. (2017)
Alcohol compounds	Ethanol, crude glycerol, butanol.	Pott et al. (2014), Liu et al. (2015), Fixen et al. (2016)
Inorganic compounds	Bicarbonate (thiosulfate as electrons donor)	Zheng et al. (2018)
	Syngas (CO, CO_2, H_2, etc.)	Pakpour et al. (2014)
Aromatic compound	Coumaric acid, benzoic acid, acetophenic acid, caffeic acid, cinnamic acid, cyclohexanoic acid, ferulic acid, ρ-hydroxybenzoic acid, vanillic acid, syringic acid, etc.	Dutton and Evans (1969), Harwood and Gibson (1988), Harwood et al. (1998), Austin et al. (2015)

(**Table 1**). *R. palustris* can absorb light as an energy source to produce ATP. Therefore, *R. palustris* has great advantages as a chassis organism in terms of carbon and energy sources.

First, *R. palustris* CGA009 can use inorganic matters as the carbon source, such as CO_2, which is fixed by the Calvin Bassham Benson (CBB) cycle to participate in cell growth metabolism using thiosulfate as the electron donor (Huang et al., 2010). Generally, photoautotrophic cyanobacteria have received much attention in the field of photosynthesis of valuable biofuels and chemicals because they can fix CO_2 through oxygenic photosynthesis with an higher efficiency than plant (Melis, 2009). PNSB, another group of photoautotrophic organisms, have received increasing attention in recent years. PNSB can capture CO_2 under anaerobic conditions, a photoautotrophic mechanism very different from cyanobacteria (Grattieri, 2020). Furthermore, ribulose 1,5-bisphosphate (RuBP) carboxylase/oxygenase (RubisCO) is responsible for CO_2 fixation by catalyzing the carboxylation of RuBP *via* the CBB cycle. Usually, the form I RubisCOs are phylogenetically divided into a green type, which is present in cyanobacteria, and a red type (Tabita, 1999; Badger and Bek, 2008; Tabita et al., 2008). Several red-type RubisCOs were demonstrated to have higher CO_2/O_2 specificity than green-type RubisCOs (Read and Tabita, 1994; Tabita, 1999). Most PNSB species, including *R. palustris*, contain the red-type form I RubisCO with higher CO_2/O_2 specificity (Swingley et al., 2009). Moreover, in *R. palustris*, a proportion of CO_2 and electrons can be directly catalyzed by remodeled nitrogenases to produce methane (Fixen et al., 2016). In total, except for cyanobacteria, PNSB including *R. palustris* has garnered considerable attention for photosynthetic conversion of CO_2 into value-added chemicals in recent years.

Second, *R. palustris* can degrade and utilize most short-chain organic acids such as acetate, butyrate, fumarate, succinate and lactate, which are often present in agricultural and industrial wastewater. The metabolism of acetate and butyrate assimilation is initiated by converting to acetyl-CoA, which is mainly assimilated by the glyoxylate shunt, with a few carbon flux entering into the TCA cycle and into pyruvate catalyzed by pyruvate dehydrogenase (McKinlay and Harwood, 2010a; McKinlay and Harwood, 2011). Fumarate and succinate are assimilated directly through the TCA cycle (McKinlay and Harwood, 2011). The assimilation pathway of lactate in *R. palustris* has not been reported; however, a gene (*RPA3503*) encoding D-lactate dehydrogenase and a gene (*RPA1136*) encoding lactate permease were predicated in the genome of *R. palustris* CGA009 (Larimer et al., 2003). Under different organic acid conditions, the growth of *R. palustris* and its productivity are different. Seven different organic acid salts were individually added into the culture medium of methane-producing *R. palustris* as carbon sources, and the highest yield of methane was obtained when fumarate was added (Fixen et al., 2016). *R. palustris* cannot readily use lactate as a sole carbon source, and coutilization with other substrates stimulated its consumption (Govindaraju et al., 2019). When different concentrations (2–10 mmol/L) of lactate were added into the culture medium, different hydrogen yields were obtained (Lazaro et al., 2017). Therefore, when *R. palustris* is utilized as a microbial cell factory, screen of the optimal carbon source is necessary.

Third, *R. palustris* can also use alcohols such as ethanol, crude glycerol and butanol as carbon sources. Crude glycerol is the main byproduct in biodiesel industry (Habe et al., 2009). Due to the rapid development of the biodiesel market, large amounts of crude glycerol are produced and treated as industrial waste (Sabourin-Provost and Hallenbeck, 2009). In *R. palustris*, crude glycerol can be converted to hydrogen at a conversion efficiency nearing 90% (Pott et al., 2013; Pott et al., 2014). Based on environmental and economic considerations, efficient utilization of crude glycerol in *R. palustris* is beneficial for its application as a microbial cell factory.

Last, *R. palustris* can also use multiple aromatic compounds as carbon sources. Utilization of lignocellulosic biomass hydrolysates, an abundant and renewable resource, is the research hotspot in recent years; however, the toxic aromatic compounds in the hydrolysates limit the utilization (Austin et al., 2015). *R. palustris* harbors a benzoate-degrading benzoyl-CoA pathway (**Figure 2**), through which the aromatic compounds in the hydrolysates are catabolized (Harwood and Gibson, 1988; Egland et al., 1997; Harwood et al., 1998). Conversion of lignocellulosic biomass to valuable chemicals in *R. palustris* is of great value in industrial application.

In summary, due to the diversity of available carbon sources, *R. palustris* has great potential to be utilized as a microbial cell factory for valuable chemicals production, and environmental and economic factors can be considered at the same time.

2.2 Exploration of Genetic Engineering Strategies

Development of genetic engineering tools is necessary for manipulation at the genetic level, such as gene knockout and gene overexpression, which can modify the organism as desired.

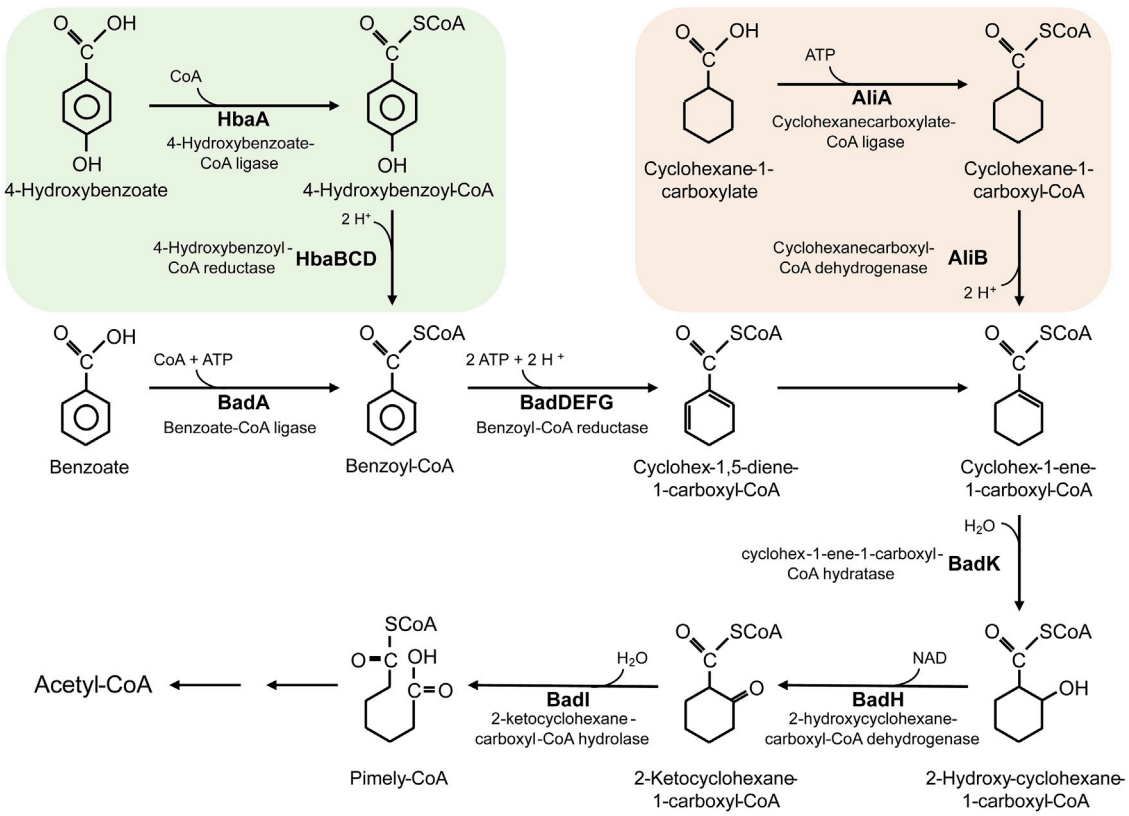

FIGURE 2 | The metabolic pathway for degradation of benzoate, 4-hydroxybenzoate and cyclohexane-1-carboxylate in *R. palustris*.

In *R. palustris*, a few gene editing tools have been reported up to date. A plasmid pMG101 (15 kb), which can replicate in PNSB, was obtained from *R. palustris* among 400 strains isolated from a natural environment. Then, based on pMG101, *Escherichia coli-R. palustris* shuttle vectors pMG103 (5.68 kb) and pMG105 (5.68 kb) were constructed, which were stably maintained in *R. palustris* (Inui et al., 2000). In *R. palustris* TIE-1, three genes *crtE*, *hpnD* and *dxs* were cloned into pMG103, and squalene production (15.8 mg/g DCW) was obtained (Xu et al., 2016). The pBBR1MCS series, as broad-host-range plasmids, can also be used for vector construction and gene expression in *R. palustris*. The *adhE2* gene was cloned into the pBBR1MCS-2 plasmid, which was then transformed into *R. palustris* CGA009 for *n*-butyrate production (Doud et al., 2017). The overexpression of *fix* gene cluster in *R. palustris* was realized by cloning into the pBBR1MCS-5 plasmid (Huang et al., 2010). Other plasmids in the pBBR1MCS series with different antibiotic selectors, including pBBR1MCS-1, pBBR1MCS-3, and pBBR1MCS-4, can also be used for gene expression in *R. palustris* (Obranic et al., 2013). The pMG103 and pBBR1MCS harbor different origin of replication (*ori*) sources, and co-transformation of pMG103 and pBBR1MCS into *R. palustris* is promising, which is beneficial for overexpression of several genes in the same strain, broadening the application of *R. palustris* as a microbial cell factory.

In addition to gene overexpression, gene mutations mediated by suicide plasmid have also been reported in *R. palustris*. pJQ200SK is a suicide vector that is widely applied in Gram-negative bacteria, featuring the P15A *ori*, a gentamicin selection marker and the gene *sacB* from *Bacillus subtilis*, encoding sucrose-6-fructosyltransferase, which can catalyze the decomposition of sucrose to high-molecular fructan, which has a lethal effect on Gram-negative bacteria (Quandt and Hynes, 1993). The suicide plasmid pJQ200SK was used to insert the mutated $nifA^{*571}$, $nifA^{*574}$, and $nifD^{V75AH201Q}$ into the chromosome of *R. palustris* CGA009 to study the function of nitrogenase (Fixen et al., 2016).

To perform more molecular research of *R. palustris* for its further application and characterization, exploring more genetic editing tools is necessary and urgent. In another PNSB, *Rhodobacter sphaeroides*, several other vectors have also been used for gene expression aside from the pBBR1MCS series. The broad-host-range plasmids of the RK2 family, including pRK310, have been widely utilized in *R. sphaeroides* (Keen et al., 1988; Scott et al., 2003; Ryu et al., 2014). The strain harboring pRK310 showed a higher growth rate and higher gene expression levels than the strain harboring pBBR1MCS-2 (Scott et al., 2003). An IPTG-inducible plasmid (pIND4) was also constructed based on plasmid pMG160, and applied for gene expression (Ind et al., 2009; Qiang et al., 2019). In another PNSB, *R. capsulatus*, a set of novel broad-host-range vectors (pRho) with T7 promoters were constructed and further utilized for heterogeneous gene expression for sesquiterpenoids synthesis (Katzke et al., 2010; Troost et al., 2019). Application of

TABLE 2 | Summary of biopolymers and their building blocks production in *R. palustris*.

Product	Characteristics of main strategies	Yield/titer	Culture conditions	References
3-hydroxybutyrate-co-3-hydroxyvalerate) (PHBV)	Overexpression of *phaP1* from *Cupriavidus necator* H16	0.7 g/L	In PM with 1 mM *p*-coumarate and 10 mM sodium bicarbonate as the carbon courses in sealed 14 ml tubes	Brown et al. (2021)
PHB	An integrated experimental and computational approach to identify novel design strategies	0.41 g/L	In PM with 1 mM *p*-coumarate or coniferyl alcohol supplemented with 10 mM sodium bicarbonate as the carbon sources	Alsiyabi et al. (2021)
PHB	—	0.41 g/L	In PM with 1 mM *p*-coumarate as the carbon source	Brown et al. (2020)
PHB	CdS-*R. palustris* hybrid system.	4% of dry mass	In 50 ml MMN medium with pure CO_2 gas at the headspace.	Wang et al. (2019)
PHB	Assessment of PHB production under various conditions	5.49 mg/L 6.06×10^{-14} mg/cell/h	Photoelectroautotrophy using N_2 as the nitrogen source	Ranaivoarisoa et al. (2019)
PHB	Effect of volatile fatty acids mixtures	16.4 mg/g/day	1,370 mg/L acetic acid, 618 mg/L propionic acid, and 133 mg/L butyric acid	Cardena et al. (2017)
PHB	Assessment of PHB production from agroindustrial residues and energy crops	11.53% TS	In 100 ml photobioreactors with 100 ml olive pomace effluent under anaerobic conditions	Corneli et al. (2016)
PHB	Assessment of PHB production from acetate, propionate, malate, lactate, glucose, and lactose	11.6–17.1% substrate conversion efficiency.	1 g/L acetate	Wu et al. (2012)
Polysaccharide	*R. palustris* contains a functional unipolar polysaccharide biosynthesis gene cluster for polysaccharide production	—	Photoheterotrophic Conditions	Fritts et al. (2017)
Carotenoids	CdS-*R. palustris* hybrid system.	2.5 mg/g dry mass	In 50 ml MMN medium with pure CO_2 gas at the headspace.	Wang et al. (2019)
Carotenoids	Effect of light sources on growth and carotenoid production	1782 μg/g biomass	In NS medium with 5 g/L sodium succinate as carbon source under LED blue light conditions	Kuo et al. (2012)
Carotenoids	Effect of light intensity and light/dark cycle on carotenoid production	1.94 mg/g biomass	In 0317 medium with volatile fatty acids wastewater under light intensity of 150 μmol-photons/m^2/s and light/dark cycle of 4/2 (16 h/8 h).	Liu et al. (2019)
Carotenoids	Effect of light intensity and different culturing conditions on carotenoids production and composition	1.5 mg/g biomass (79% lycopene)	In RPP medium with 4 g/L malate and 0.5 g/L NH_4Cl under hydrogen-production conditions with low light intensity	Muzziotti et al. (2017)
Carotenoids	Effect of hydraulic retention time (HRT) and organic loading rate (OLR) on carotenoid production	3.91 mg/g biomass	Produced from acidic food industry wastewater treated under HRT of 48 h and OLR of 2.51 g/L/d.	Liu et al. (2016)
Squalene	Deletion of the *shc* gene (encoding the squalene hopene cyclase), fusion of two consecutive enzymes (CrtE and HpnD) and overexpression of the *dxs* gene	15.8 mg/g biomass	In medium with 0.2% sodium succinate, 1% glucose, 0.3% peptone, 0.3% yeast extract.	Xu et al. (2016)
Hopanoids	Different growth conditions: chemoheterotrophic, photoheterotrophic and pH shock	36.7 mg/g biomass	Photoheterotrophic growth condition: in anaerobic bicarbonate-buffered freshwater medium with 2 mM sodium acetate	Welander et al. (2009)

these vectors in *R. palustris* is promising, satisfying the requirement of special expression mode in *R. palustris*.

In *R. palustris*, even though the tools for gene overexpression and gene deletion have been reported, the time-consuming genetic editing process limits the widespread application of *R. palustris*. Exploration of novel genetic editing tools is necessary. A SpCas9-sgRNA-based genomic DNA targeting system for *R. sphaeroides* was developed for gene knock-out, knock-in and single nucleotide substitutions, which indicates the development of a similar Cas9-based genome editing tool in *R. palustris* in future research (Mougiakos et al., 2019). In 2020, base editing systems for *R. sphaeroides*, cytosine base editors (CBEs) and adenine base editors (ABEs), all based on CRISPR/Cas9 systems, were also generated (Luo et al., 2020). Development of novel genetic modification tools in *R. palustris* would promote the application of *R. palustris* as a microbial cell factory.

3 APPLICATIONS OF *R. PALUSTRIS*

3.1 Application in Biopolymers and Their Building Blocks

Biopolymers are biodegradable polymers that are synthesized from renewable resources by living organisms, which allow them to replace the fossil fuel–based polymers. *R. palustris* is rich in valuable compounds such as PHB, polysaccharide and isoprenoid, building blocks for biopolymers production, making it a promising microbial cell factory (**Table 2**).

3.1.1 Poly-Beta-Hydroxybutyrate Production

Biodegradable polymers, such as polyhydroxyalkanoates (PHAs), have been identified as potential alternatives to traditional plastics, which have been a heavy burden to the environment due to their recalcitrant nature (Kalia et al., 2021). Depending on the carbon atoms per monomer, PHAs can be classified as short-chain-length PHAs (scl-PHAs, C_3–C_5) and medium-chain-length PHAs (mcl-PHAs, C_6–C_{14}) (Li et al., 2016). PHAs are accumulated by many bacteria as a carbon- and energy- storage compound, and the most accumulated PHA is PHB, a polymer composed of 3-hydroxybutyrate, belonging to scl-PHAs (Lee, 1996). Although PHB is the most studied PHA in literature, the bioplastic products derived solely from it are typically brittle and stiff, which are undesirable in many applications (McAdam et al., 2020). Nonetheless, the material properties could be improved by adding 3-hydroxyvalerate units into a PHB biopolymer, obtaining copolymer poly(3-hydroxybutyrate-co-3-hydroxyvalerate), also named PHBV (Li et al., 2016). Due to their inherent biodegradability, excellent biocompatibility and non-toxicity, PHAs have been widely applied in the fields of agriculture, aquaculture, and human health sectors (Kalia et al., 2021).

PHB is produced as an energy- and carbon-storage compound by PNSB under special stress conditions (Monroy and Buitrón, 2020). Production of PHB from CO_2 (carbon source) *via* photoautotrophy in *R. palustris* is considered to be sustainable and environmental-friendly. When the electron donor was a poised electrode (photoelectroautotrophy) or a ferrous iron (photoferroautotrophy), it showed the highest PHB electron yield (7.34%) and specific productivity (8.4×10^{-14} mg/cell/h) in *R. palustris* TIE-1 (Ranaivoarisoa et al., 2019). In the CdS-*R. palustris* hybrid system, the CdS nanoparticles cotaded on the surface of *R. palustris* formed by Cd^{2+} bioprecipitation through the cysteine desulfurase can absorb solar energy and release electrons, and the biomass, PHB and carotenoid production were improved by 148%, 147%, and 122%, respectively (Wang et al., 2019). PHB production in *R. palustris* from lignocellulosic biomass which is considered to be the most economic carbon source in the world has received much attention. *R. palustris* can utilize *p*-coumarate, the major lignin breakdown product, to produce PHB (Brown et al., 2020; Alsiyabi et al., 2021). *R. palustris* can produce a copolymer of PHB called PHBV, which has more ideal thermomechanical properties than PHB alone (Li et al., 2016). Phasin has been shown to control the size and number of granules in the cell, affect PHB accumulation, and promote localization of granules, and heterologous expression of phasin in *R. palustris* resulted in a significantly higher PHBV titer (0.7 g/L) from *p*-coumarate (Brown et al., 2021). PHB production from other carbon sources have also been researched, and PHB of different level are obtained with different substrates. Among the different short-chain organic acids utilized, only acetate and propionate can lead to the production of PHB in *R. palustris*, achieving 17.1% and 11.8% substrate conversion efficiency, respectively (Wu et al., 2012). Moreover, mixtures of acetate, propionate and butyrate as substrates had a significant effect on PHB production, 16.4 mg/g/day (Cardena et al., 2017). When acetate was used as the carbon source, under limiting ammonium concentrations, acetate was consumed through the glyoxylate pathway to produce PHB; however, under nitrogen starvation conditions, acetate was consumed through the TCA cycle and PHB production was increased by 30% (McKinlay et al., 2014). Some agroindustrial residues and energy crops were also investigated for PHB formation, and the highest PHB production, 11.53% TS, was obtained in olive pomace effluent (Corneli et al., 2016). In summary, PHB production in *R. palustris* from different carbon sources, like CO_2, lignocellulosic biomass, short-chain organic acids, agroindustrial residues and energy crops, has been focused. However, in *R. palustris*, hydrogen production competes for the reducing equivalents and metabolites with PHB (Wu et al., 2012), genetic engineering to redirect more metabolic flux from hydrogen to PHB is proposed in future study.

3.1.2 Polysaccharide Production

Polysaccharide biopolymers are composed of mono saccharides linked together by O-glycosidic bonds (Hangasky et al., 2019). Due to their versatile properties like thickening, crosslinking and adsorption, polysaccharide biopolymers have been widely applied in the petroleum industry (Xia et al., 2020). Moreover, based on its properties of low production cost, nontoxicity and biocompatibility, polysaccharides is considered as green biopolymer for *in situ* gel formulation for drug delivery (Chowhan and Giri, 2020). *R. palustris* was reported to produce unipolar polysaccharide for biofilm formation under diverse conditions (Fritts et al., 2017). In the genome of *R. palustris* CGA009, *uppE* (RPA2750) and *uppC* (RPA4833) were identified to be responsible for unipolar polysaccharide production (Fritts et al., 2017). Unipolar polysaccharide production was enhanced in response to three photoheterotrophic conditions, including nutrient limitation, less-preferred nutrients and high salinity; however, cell growth rate was affected (Fritts et al., 2017). Design of the culture conditions of *R. palustris* is of critical importance to balance the cell growth and unipolar polysaccharide production, which affects the overall process economics. Further genetical modification would improve polysaccharide production.

3.1.3 Production of Building Blocks Belonging to Isoprenoids

Among the chemicals belonging to isoprenoids, isoprene and squalene are building blocks for biopolymer production. *R. palustris* is rich in carotenoids, another kind of isoprenoids, which include lycopene, rhodopin, 3,4-didehydro-rhodopin, anhydro-rhodovibrin, rhodovibrin, hydroxy-spirilloxanthin and spirilloxanthin (Chi et al., 2015). The produced carotenoids are connected to the transmembrane proteins through a noncovalent bond, which can stabilize the transmembrane proteins and capture light for the light harvesting complex in the cell membrane (Lang and Hunter, 1994; Takaichi, 2004). The precursors for isoprenoids production, isopentenyl diphosphate (IPP) and dimethylallyl diphosphate (DMAPP), are supplied by the methylerythritol phosphate (MEP)

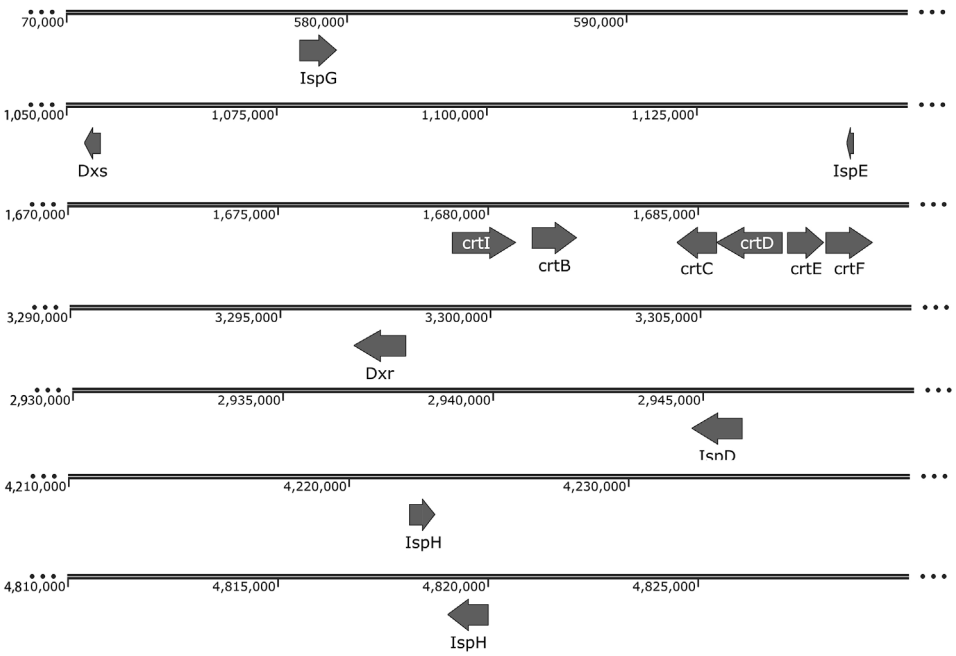

FIGURE 3 | Genome distribution of genes in the carotenoid synthetic pathway in *R. palustris*. Abbreviations: 1-deoxy-D-xylulose-5-phosphate synthase (DXS); 1-deoxy-D-xylulose 5-phosphate reductoisomerase (DXR); 2-C-methyl-D-erythritol 4-phosphate cytidylyltransferase (IspD); 4-diphosphocytidyl-2-C-methyl-D-erythritol kinase (IspE); 4-hydroxy-3-methylbut-2-enyl diphosphate synthase (IspG); 4-hydroxy-3-methylbut-2-enyl diphosphate reductase (IspH); amine oxidase/Phytoene desaturase (crtI), squalene/phytoene synthase (crtB), hydroxyneurosporene synthase (crtC), FAD dependent oxidoreductase (crtD), polyprenyl synthetase (crtE), O-methyltransferase family 2 (crtF).

pathway or the mevalonate (MVA) pathway (Li et al., 2019). Genes of the MEP pathway and carotenoid synthetic pathway were identified in the genome of *R. palustris* (**Figure 3**). The high carotenoids content indicates that *R. palustris* has great potential to be developed as a microbial cell factory for isoprenoids production.

Carotenoids, such as lycopene and β-carotene, have great application value as food additives and in the pharmaceutical industry. Research about carotenoids production by *R. palustris* have been mainly focused on the changes in the culture conditions, such as light sources, light intensity, pH, carbon and nitrogen sources. Among the tested light sources, blue LED showed the highest growth, the highest carotenoid content (1,782 μg/g biomass) and the highest carotenoid productivity (1,800 μg/g/Watt) (Kuo et al., 2012). The light/dark cycle ratio and light intensities also influence the carotenoid yield, and light/dark cycle of 16 h/8 h and light intensity of 150 μmol-photons/m^2/s were proven to be the best light parameters in *R. palustris* (Liu et al., 2019). Moreover, the composition of the carotenoids are different under different light illumination conditions (Muzziotti et al., 2017). Among the various carotenoids in *R. palustris*, the content of lycopene is the highest, which can reach 79% of the total carotenoids under certain light conditions (Muzziotti et al., 2017). Therefore, lycopene production in *R. palustris* is very promising. Considering the high total carotenoids production in *R. palustris*, further engineering at the gene level would enhance the metabolic flux to a specific carotenoid and isoprenoid.

Squalene production in *R. palustris* has been reported. Due to its antioxidant properties and unique structure, squalene is usually utilized extensively in the pharmaceutical, food, cosmetic and biofuel industries (Kim and Karadeniz, 2012). Squalene derivatives, such as tetramethylsqualene epoxides, botryoxanthins and braunixanthins, could be incorporated to resistant biopolymers by condensation with polyaldehydes (Okada et al., 2000). In *R. palustris* TIE-1, through deletion of the *shc* gene (encoding the squalene hopene cyclase), fusion of two consecutive enzymes (CrtE and HpnD) and overexpression of the *dxs* gene, squalene yield reached 15.8 mg/g (Xu et al., 2016). In another study, the yield of hopanoids, a downstream product of squalene, was more than 36.7 mg/g DCW in wild-type *R. palustris* TIE-1 under certain culture conditions (Welander et al., 2009), which indicates the high potential of further improvement of squalene production.

Isoprene is a platform chemical for natural rubber (*cis*-1,4-polyisoprene) production. Studies on the production of isoprene in *R. palustris* has not been reported; however, our group found that the wild type *R. palustris* can produce isoprene, which was usually produced in plant. Due to its high carotenoids-producing capacity, high isoprene production is promising in *R. palustris*. Isoprene is produced from precursor DMAPP catalyzed by isoprene synthase (Li et al., 2018). Except for the utilization of the native MEP pathway to accumulate DMAPP, heterologous expression of the MVA pathway in *R. palustris* would improve isoprenoid production dramatically. The plasmid harboring the enzymes of the MVA pathway in the vector pBBR1MCS-2 was transformed into another PNSB, *R. sphaeroides*, resulting in an 8-fold increase in

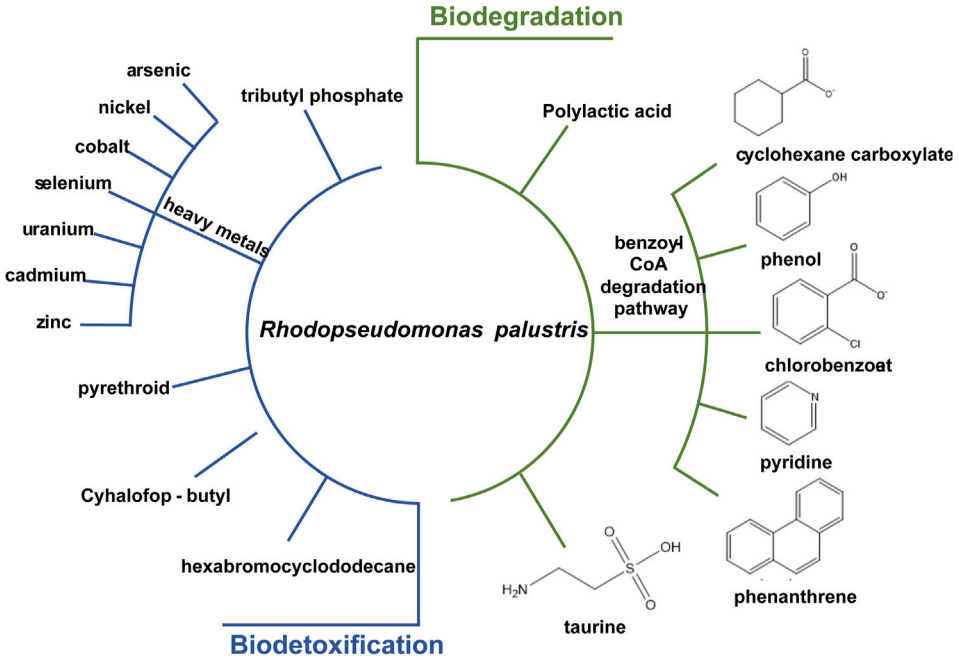

FIGURE 4 | Substrates which can be biodetoxified or biodegraded in *R. palustris*.

amorphadiene production (Orsi et al., 2019). Transformation of the same plasmid into *R. palustris* is expected in future research.

In conclusion, *R. palustris* has great potential to produce biopolymers and their building blocks. *R. palustris* can accumulate biopolymers naturally, such as PHB and polysaccharide, under various conditions. Another beneficial property of *R. palustris* as a microbial cell factory is that industry waste, CO_2 and lignocellulosic biomass can be converted to valuable biopolymers. The light-harvesting system in the cell membrane of *R. palustris* can capture light as an energy source, contributing to photosynthesis in *R. palustris*. Bioproduction of these valuable chemicals using many traditional chassis organisms, such as *E. coli*, *Saccharomyces cerevisiae*, and *Corynebacterium glutamicum*, has been researched in recent years, and high production has been realized. However, carbon and energy sources of these chassis organisms limit its sustainable and cost-effective application in industry. Therefore, in terms of economy of the fermentation process, *R. palustris* is more suitable as a microbial cell factory for valuable chemicals production. However, bioproduction in *R. palustris* suffers from the low growth rate, and improvement of growth rate is urgently required. Moreover, most research of *R. palustris* has focused on the optimization of culture conditions to improve chemicals accumulation in *R. palustris*; but genetic manipulation of *R. palustris* is seldomly executed due to its complicated genetical engineering process.

3.2 Traditional Application

3.2.1 Application in Wastewater Treatment and Bioremediation

R. palustris is widely applied in wastewater treatment and bioremediation as a model organism for its biodetoxification and biodegradation properties (**Figure 4**). Aromatic compounds in the wastewater, such as 3-chlorobenzoate (3-CBA), can be consumed by *R. palustris* as the sole carbon source through the innate benzoate-degrading pathway (Harwood et al., 1998). *R. palustris* WS17 was found to degrade 3-CBA anaerobically in the light; then, *R. palustris* DCP3 was found to degrade not only 3-CBA but also 2-CBA, 4-CBA and 3,5-CBA (Kamal and Wyndham, 1990; van der Woude et al., 1994; Krooneman et al., 1999). The degradation mechanism of 3-CBA in *R. palustris* RCB100 was deciphered, which includes three steps, reductive dechlorination of 3-CBA to 3-chlorobenzoyl coenzyme A, dehalogenation of 3-chlorobenzoyl-CoA to benzoyl-CoA, and degradation of benzoyl-CoA to acetyl-CoA (Egland et al., 2001). *R. palustris* can also grow on cyclohexane carboxylate (CHC), the simplest alicyclic acids, which is degraded to cyclohex-1-enecarboxyl-CoA (CHene-CoA), an intermediate of the benzoate-degrading pathway (**Figure 2**) (Küver et al., 1995; Hirakawa et al., 2015). Two transcription factors, BadR and BadM, were proven to regulate two operons expression related to the benzoate-degrading pathway (Hirakawa et al., 2015). Additionally, pyridine, a heterocyclic aromatic compound released into the environment as industrial waste, can be degraded by *R. palustris* JA1 as a sole carbon source for growth (Ramana et al., 2002). Another aromatic compound, phenol, is a toxic compound from the chemical industry and human activity, and it can be converted to 4-hydroxyphenylacetate in *R. palustris* PL1 (Noh et al., 2002). *R. palustris* CQV97 was isolated and identified as a microorganism that has the ability to degrade phenanthrene, a polycyclic aromatic compound (Zhao et al., 2011). In addition to aromatic compounds, utilization of taurine, a sulfonate, and

degradation of polylactic acid (PLA), have also been reported (Novak et al., 2004; Hajighasemi et al., 2016). The biodegradable PLA is a promising candidate for the replacement of traditional petroleum-based plastics, and depolymerization and recycling utilization of PLA is essential to relieve environment pressure and save resources. The protein RPA1511 from *R. palustris* was identified to have the hydrolytic activity toward PLA (Hajighasemi et al., 2016).

R. palustris also has the capability of heavy metal tolerance and assimilation. Heavy metals are released in industrial processes, leading to contaminants in soils and water bodies. *R. palustris* is recognized as a model organism for heavy metal detoxification, especially for arsenic (As), a common soil contaminant. An As-redox transformation system exists in *R. palustris* that can reduce the highly toxic As^{5+} to As^{3+} and oxidize As^{3+} to methylated arsenic (low-toxic) (Batool et al., 2017). The As^{5+} resistance of *R. palustris* is up to 100 mM; and 62.9% of the toxic As^{5+} in the medium can be reduced (Batool et al., 2017). In the genome of *R. palustris*, three *ars* operons and four *arsR* genes related to As metabolism were identified (Zhao et al., 2015). Moreover, cobalt (Co) and nickel (Ni), serious pollutants with the development of industry, can also be assimilated by *R. palustris*. The Co-Ni transporter from *R. palustris* CGA009 was introduced into *Deinococcus radiodurans* R1, resulting in nearly 60% Co removal from the contaminated effluents within 90 min and was introduced into *Nicotiana tabacum* leading to a 5-fold Co acquisition and 2-fold Ni accumulation (Nair et al., 2012; Gogada et al., 2015). In addition, the biodetoxification of other heavy metals, including selenium (Se), uranium (U), cadmium (Cd) and zinc (Zn), have also been reported. After 9 days of cultivation, 99.9% of SeO_3^{2-} was reduced to red elemental selenium in *R. palustris* strain N (Li et al., 2014). U can be reduced to U(IV)-phosphate or U(IV)-carboxylate compounds or accumulate in the cytoplasm and the cell wall in *R. palustris* (Llorens et al., 2012). Removal of Cd and Zn by 84% and 55%, respectively, were detected in *R. palustris* TN110 (Sakpirom et al., 2017).

In addition to heavy metals, *R. palustris* has high tolerance and degradation effects toward pesticides and herbicides, which are widely applied in agriculture and forestry. The residual pesticides and herbicides in the agro-ecosystem have caused significant environmental and human health concerns in recent years (Katsuda, 1999; Ray and Fry, 2006). Among them, pyrethroid pesticides have been extensively utilized for 30 years. *R. palustris* JSC-3b has the ability to degrade pyrethroid effectively; and the gene *est3385*, encoding a pyrethroid degradation ester, was identified in strain PSB-S (Zhang et al., 2014; Luo et al., 2018). Cyhalofop-butyl herbicides remaining in the soil can also cause serious environmental pollution and risk. The cyhalofop-butyl in soybean processing wastewater can be completely degraded after 5 days by *R. palustris* (Wu et al., 2019). Other toxic compounds detected in various environmental matrixes, such as hexabromocyclododecane and tributyl phosphate, which can cause serious human health problems, can also be degraded by *R. palustris* (Berne et al., 2005; Chang et al., 2020).

Food waste generated from restaurants and schools has caused many management problems in recent years. *R. palustris* CGA009 was reported to remove a wide variety of organic compounds, ammonia, nitrate and starch from food waste, and BOD and COD were reduced by 70% and 33%, respectively (Mekjinda and Ritchie, 2015).

An obvious characteristic of *R. palustris* is the possibility of simultaneous wastewater treatment and valuable chemicals bioproduction. When soybean processing wastewater was adopted as a carbon source, the toxic cyhalofop-butyl in the wastewater was degraded and the production of single cell protein, carotenoid and bacteriochlorophyll were enhanced (Wu et al., 2019). A maximum of 80 ml H_2/g COD/day hydrogen was concurrently produced with efficient removal of BOD, COD, ammonia, nitrate, starch in the food waste (Mekjinda and Ritchie, 2015).

These outstanding functions make *R. palustris* a potential organism to be applied in wastewater treatment and bioremediation. However, due to the cell washout and unstable biodegradation, these traditional use of suspended *R. palustris* is inefficient. Immobilization microorganism technology, which loads bacteria into a solid carrier to enhance the abundance of bacteria in the wastewater, is attempted in recent years. The immobilized *R. palustris* with alginate, polyvinyl alcohol or agar beads showed 30%~40% higher ammonia removal rate than that by free *R. palustris* (Zhan and Liu, 2013). *R. palustris* P1 was immobilized to glass pumice with a high adsorption capacity of 4.02×10^8 cells g^{-1}, and the maximum NH_4^+-N and NO_2^--N removal rates were 134.82 ± 0.67% and 93.68 ± 0.14% higher than those of free *R. palustris* P1, respectively (Xiao et al., 2019). The immobilized technology showed properties like high removal stability, easy to use in continuous reactors, high cell densities, and protecting the bacteria from predation by plankton, contributing to its highly effective aquaculture wastewater treatment.

3.2.2 Applications in Agriculture, Aquaculture and Livestock Breeding

R. palustris is traditionally utilized as a biofertilizer in agriculture, and as food additives and water purification microbes in aquaculture and livestock breeding. In agriculture, due to the detoxification and degradation properties of *R. palustris* mentioned above, it can be utilized to clean up the pollutants in the soil and improve the soil quality. An alternative method is to clone the specific genes from *R. palustris* into plants, which process endows the plants with the ability to tolerate and degrade heavy metals and pesticides in the soil. *R. palustris* also has the capability to promote plant growth due to its function of nitrogen fixation (Oda et al., 2005) and the production of two phytohormones, indole-3-acetic acid and ALA (Koh and Song, 2007). Plant *Vigna mungo* treated with *R. palustris* CS2 showed a 17% increase in shoot length and a 21.7% increase in root length (Batool et al., 2017). Additionally, *R. palustris* has the ability to induce resistance against plant disease, such as tobacco mosaic virus (TMV), one of the most destructive plant viruses. The Rhp-PSP protein with inhibitory activities against TMV *in vivo* and *in vitro* was isolated and purified from *R. palustris* JSC-3b (Su et al., 2015). An *R. palustris* GJ22 suspension was sprayed on tobacco, which induced tobacco resistance against TMV and enhanced the immune response under subsequent TMV

infection (Su et al., 2017). The growth and germination of the tobacco were also promoted at the same time (Su et al., 2017). These outstanding properties, detoxification and degradation functions, plant growth promoting effects and anti-virus abilities, make *R. palustris* a potential candidate as a biofertilizer in agriculture.

R. palustris is also widely applied in aquaculture and livestock breeding in terms of its probiotic properties as feed additives and its wastewater treatment ability. Supplementing the drinking water of broiler chickens with *R. palustris* resulted in the growth promotion and the improvement of meat quality (Xu et al., 2014). The growth performance and immune response of tilapia (*Oreochromis niloticus*) were also improved by using *R. palustris* as a water additive (Zhou et al., 2010). In addition, the probiotic properties of *R. palustris* were further demonstrated in a model animal, rats (Fang et al., 2012). Tissue damage and bacteria translocation were not detected in rats, and no *R. palustris* remained in the feces of the rats 3 days after the termination of intake, indicating the biological safety of *R. palustris* as a probiotic bacterium (Fang et al., 2012). However, the molecular mechanism of its probiotic properties is not very clear. In 2019, an extracellular polysaccharide RPEPS-30 from *R. palustris* was found to enhance the host immune system and improve the growth of beneficial microbes in the gut (Zhang et al., 2019). As we mentioned above, *R. palustris* is suitable for wastewater treatment, which is generated from the aquaculture and livestock breeding industries. *R. palustris* WKU-KDNS3 was isolated from an animal waste lagoon, and its capability to eliminate skatole, a major contributor to the malodor emission from feces, was proven (Sharma et al., 2015). In another study, the isolated *R. palustris* from eutrophicated ponds can remove the odorous organic acids and phosphate swine wastewater (Kim et al., 2004). At present, research about the applications of *R. palustris* in the aquaculture and livestock industries have focused on the isolation of strains and demonstrations of their activity. Further analysis of the molecular basis of its probiotic properties is necessary, and subsequent genetic manipulation of *R. palustris* would improve its probiotic properties.

3.3 Application in Other Fields

3.3.1 Application in Biofuel Production

Considering the environmental pollution caused by the consumption of large amounts of nonrenewable fossil fuels, it is urgent to find alternative clean energy sources. Numerous studies have shown that *R. palustris* can produce biofuels, such as hydrogen, methane, ammonia and butanol (**Table 3**).

Ammonia is a clean fuel with features like high energy density, no carbon emission, low storage cost, difficult to explode (Bélanger-Chabot et al., 2015; Jiao and Xu, 2019). Ammonia is particularly considered as a strong option for long-haul shipping (Phillips et al., 2010; Zhao et al., 2021). Ammonia is chemically produced from hydrogen and nitrogen by the Haber-Bosch process that is conducted at a high temperature and high pressure in industry (Kandemir et al., 2013). In nature, ammonia can be produced by biological nitrogen fixation catalyzed by nitrogenase (**Figure 5**, Eqs 1–3), which is highly sensitive to oxygen (Oelze and Klein, 1996; Vitousek et al., 1997). In *R. palustris*, three different nitrogenase gene clusters, *anf*, *vnf* and *nif*, encoding three nitrogenase isozymes, were identified by genomic analysis, and further functional analysis demonstrated their function (Larimer et al., 2003; Oda et al., 2005). Different from algae and cyanobacteria, in which the inhibitory effect of oxygen on nitrogenase limits its wide application, *R. palustris* is an anoxygenic photosynthetic bacteria and the inhibitory effect of oxygen is absent (McKinlay and Harwood, 2010b). Hydrogen and methane production catalyzed by nitrogenase in *R. palustris* have also been reported. Actually, researchers have focused more on hydrogen and methane production than ammonia production by *R. palustris*.

Hydrogen has been recognized as promising alternative due to properties like high conversion efficiency, renewability, clean burning nature and high mass-based energy density (Patel et al., 2012; Hu et al., 2018). Biological hydrogen production has significant potential in the hydrogen economy (Christopher and Dimitrios, 2012). Photo-fermentative hydrogen production by photosynthetic bacteria can be using energy directly from sunlight and reduced organic compounds (Hallenbeck and Ghosh, 2009). In *R. palustris*, hydrogen is produced as an obligate product during the nitrogen reduction process catalyzed by nitrogenase (McKinlay and Harwood, 2010b; Heiniger et al., 2012) (**Figure 5**, Eqs 1–3), even in the condition of nitrogen deficiency (**Figure 5**, Eq. 4) (McKinlay and Harwood, 2010b). In this process, electrons are obtained from organic or inorganic compounds and then transported to ferredoxin through the photosynthetic electron transport chain, which is utilized for hydrogen production *via* nitrogenase in combination with generated ATP (McKinlay and Harwood, 2010b). In *R. palustris*, the wide type nitrogenase consumed 75% reductant (ferredoxin) for ammonia production and the hydrogen production is at a low level (Rey et al., 2007). Moreover, the nitrogenase activity is inhibited by ammonia at the transcriptional and posttranslational level and is also inhibited by ADP, which competes with ATP for binding to the enzyme (Dixon and Kahn, 2004; Heiniger et al., 2012; Zheng and Harwood, 2019). Moreover, in *R. palustris*, PHB is synthesized as an energy- and carbon-storage compound, which competes with the metabolites and reducing equivalents for hydrogen production (Vincenzini et al., 1997). Some genetic engineering strategies were explored to improve hydrogen production efficiency, such as improvement of ammonium tolerance of the nitrogenase, elimination of PHB synthesis and disruption of the Calvin cycle. Regulatory gene *nifA* mutants, which lead to high nitrogenase expression even in the presence of ammonium, were screened, and up to five times hydrogen production (332 μmol/mg protein) relative to the wild type was detected (Rey et al., 2007). Disruption of the PHB synthesis gene *phbC* was performed in *R. palustris* WP3-5, and a 1.7-fold increase in hydrogen content (70%) was obtained (Yang and Lee, 2011). Hydrogen production can be improved by 4.6-fold to 145 μmol/mg protein in a *ΔcbbLS ΔcbbM ΔcbbP* mutant strain, in which electrons entering the Calvin cycle were blocked and redirected to hydrogen production (Zheng and Harwood, 2019). An obvious increase of hydrogen production has been obtained after genetic engineering strategies were applied.

TABLE 3 | Summary of biofuels production in *R. palustris*.

Product	Characteristics of main strategies	Yield/titer	Culture conditions	References
Hydrogen	Screening of mutants that produce hydrogen constitutively, even in the presence of ammonium.	332 μmol/mg protein	In PM medium with 4.5 mM *p*-coumarate by *R. palustris* mutant CGA574	Rey et al. (2007)
Hydrogen	Disruption of the PHB synthesis gene *phbC*	457 ml/L/day	In a 2.5 L bioreactor using organic acid synthetic wastewater	Yang and Lee (2011)
Hydrogen	Influence of light energy and electron availability on CH_4 production, including providing cells with different substrates, using nongrowing cells, blocking electrons from entering the Calvin cycle, or blocking H_2 uptake	500 μmol/mg protein	Nongrowing cell suspensions were incubated in light for 10 days in PM with 20 mM acetate and 10 mM $NaHCO_3$; *R. palustris* strain *nifA* nifD*^{V75AH201Q}	Zheng and Harwood (2019)
Hydrogen	Evaluation of lighting systems, carbon sources	4.92 mol H_2/mol substrate	In 30 mM medium with 2 g/L butyrate under incandescent light	Hu et al. (2018)
Hydrogen	Effect of volatile fatty acids mixtures	391 ml/g/day	1.2 g/L acetic acid, 0.2 g/L propionic acid, and 0.05 g/L butyric acid	Cardena et al. (2017)
Hydrogen	—	34 ml/g/h	10 mM glycerol and 5 mM glutamate	Pott et al. (2013)
Hydrogen	Effects of light intensity, the concentrations of crude glycerol and glutamate	6.69 mol/mol glycerol	A light intensity of 175 W/m2, 30 mM glycerol, and 4.5 mM glutamate,	Ghosh et al. (2012)
Hydrogen	Effect of different liming nitrogen regimes	6 mol/mol glycerol	In RCV medium with 10 mM crude glycerol and 2 mM glutamate	Sabourin-Provost and Hallenbeck, (2009)
Hydrogen	Assessment of hydrogen production from agroindustrial residues and energy crops	648.6 mg/L	In 100 ml photobioreactors with 100 ml wheat bran effluent under anaerobic conditions	Corneli et al. (2016)
Hydrogen	Application of immobilized-cell technology	11.2 mmol/m_2/h 70 ml/h flow rate 0.25 mol/mol glucose	Biofilm formed under 590 nm and 5,000 lx illumination	Liao et al. (2010)
Hydrogen	Application of a cell immobilization technique to a biofilm-based photobioreactor	38.9 ml/L/h 0.2 mol/mol glucose	Illumination condition of 5,000 lux and 590 nm wavelength; glucose concentration is 0.12 M, the optimal pH = 7 and optimal temperature of influent liquid 25°C.	Tian et al. (2010)
Hydrogen	Latex coating immobilization on chromatography paper	0.47 ± 0.04 mmol/m^2/h	Incubated in the head-space of the Balch tubes	Gosse et al. (2012)
Hydrogen	Effect of osmoprotectants, temperature, humidity and O_2 on H_2 production in *R. palustris* coatings	69.1% headspace	*R. palustris* coatings containing glycerol and sucrose after storage for 8–12 weeks at <5% relative humidity; production under argon 10 days post rehydration in PM (NF) medium	Piskorska et al. (2013)
Hydrogen	Blocking of the calvin cycle flux; effect of different substrate	80 mol/mol C consumed	In PM with 10 mM butyrate in front of a 60-W light bulb at 30°C; strain *R. palustris* CGA679	McKinlay and Harwood (2011)
Methane	*nifD*$^{V75A\ and\ H201Q}$ encoding a Mo-dependent nitrogenase; calvin cycle through genetic mutation*ΔcbbMLS*; using nongrowing cells; effect of different substrates	800 nmol/mg total protein	Nongrowing cell suspensions were incubated in light for 10 days in PM with 20 mM acetate and 10 mM $NaHCO_3$; *R. palustris* strain *nifA* nifD*$^{V75A\ H201Q}$	Fixen et al. (2016)
Methane	Influence of light energy and electron availability on CH_4 production	900 nmol/mg total protein	Nongrowing cell suspensions were incubated in light for 10 days in PM with 10 mM succinate and 10 mM $NaHCO_3$; *R. palustris* strain *nifA* nifD*$^{V75A\ H201Q}$	Zheng and Harwood (2019)
Methane	V-dependent nitrogenase (*VnfD*$^{V57A\ H180Q}$); Fe-only nitrogenase	150 nmol/mg total protein (V); 400 nmol/mg total protein (Fe)	Non-growing cell suspensions incubated in light for 10 days in 10 ml NFM medium supplemented with 20 mM acetate and 10 mM $NaHCO_3$	Zheng et al. (2018)
Butanol	Overexpression of *adhE2* gene	1.5 mM; 0.03 g/L/day	Cultured in anaerobic butyrate Rhodospirillaceae medium	Doud et al. (2017)

Photo-fermentation of hydrogen suffers from the low light conversion efficiency and high energy demand by nitrogenase, leading to the low hydrogen yield. Most research on the improvement of hydrogen production in *R. palustris* has mainly focused on optimization of basic cultivation parameters, including the substrate, light intensity, pH, temperature and immobilization of the cells. Organic acids, such as acetate, propionate, malate and lactate, can be utilized as substrates to produce hydrogen by *R. palustris* WP3-5 (Wu et al., 2012). Four different carbon sources were evaluated for hydrogen production by *R. palustris* DSM127, and the highest hydrogen yield, 1.69, 2.38, 2.57, and 4.92 mol H_2/mol substrate, were obtained using acetate (3 g/L), malate (2 g/L), lactate (2.5 g/L), and butyrate (2 g/L), respectively (Hu et al., 2018). However, when butyrate (2 g/L) was utilized as the carbon source, hydrogen production started after 400 h, longer than other carbon sources (Hu et al., 2018). Mixtures of different substrates were evaluated for the distribution of hydrogen and PHB production, and mixtures of propionate and acetate showed the highest hydrogen production, 391 ml/g/day (Cardena et al., 2017). The possibility of using various industrial and agricultural wastewater for hydrogen production has been widely investigated.

Mo-nitrogenase $N_2 + 8H^+ + 8e^- + 16ATP \rightarrow 2NH_3 + H_2 + 16ADP + 16Pi$ (1)

V-nitrogenase $N_2 + 12H^+ + 12e^- + 24ATP \rightarrow 2NH_3 + 3H_2 + 24ADP + 24Pi$ (2)

Fe - nitrogenase $N_2 + 20H^+ + 20e^- + 40ATP \rightarrow 2NH_3 + 7H_2 + 48ADP + 40Pi$ (3)

Mo-nitrogenase(absence of N_2): $8H^+ + 8e^- + 16ATP \rightarrow 4H_2 + 16ADP + 16Pi$ (4)

Mo-nitrogenase (Remodeled) $CO_2 + 8H^+ + 16ATP + 8e^- \rightarrow CH_4 + 2H_2O + 16ADP + 16Pi$ (5)

FIGURE 5 | Stoichiometries of production of ammonia, hydrogen and methane through nitrogenase in *R. palustris*. The references were (McKinlay and Harwood, 2010b; Yang et al., 2012; Fixen et al., 2016; Harwood, 2020).

Photofermentation of crude glycerol, a major side product of the biodiesel industry, to hydrogen was also studied in *R. palustris*, and the conversion rate was improved through adjusting the cultivation conditions (Sabourin-Provost and Hallenbeck, 2009; Ghosh et al., 2012; Pott et al., 2013). Agroindustrial residues and energy crops were also investigated for hydrogen production in *R. palustris*. For instance, a *R. palustris* CGA676 mutant cultured with wheat bran and maize effluent produced 648.6 and 320.3 ml/L hydrogen, respectively (Corneli et al., 2016). Light systems are also essential for hydrogen production. Two light systems, the fluorescent and incandescent, were investigated for cell growth and hydrogen production, and the incandescent system was proven to be more effective (Hu et al., 2018). Immobilization of *R. palustris* through biofilm formation and latex coatings formation can concentrate its biological reactivity and stabilize the microbes, which is beneficial for hydrogen production and light conversion efficiency (Liao et al., 2010; Tian et al., 2010). *R. palustris* CQK 01 was immobilized on the surface of baked glass beads to form a biofilm, and the bioreactor showed high hydrogen production, 38.9 ml/L/h and 0.2 mol/mol glucose (Tian et al., 2010). Latex coatings of *R. palustris* CGA009 were constructed in both dry and wet conditions, and high-level hydrogen production was detected (Gosse et al., 2012; Piskorska et al., 2013). In summary, hydrogen production by *R. palustris* has been widely studied, and abundant genetic engineering strategies and optimization of culture conditions have been performed.

Moreover, the intracellular redox balance can also influence hydrogen production in *R. palustris*. During photoheterotrophic conditions, *R. palustris* will produce a large amount of reducing equivalents, a part of which are consumed by nitrogenase for hydrogen production for intracellular redox balance (McKinlay and Harwood, 2011). However, the native Calvin cycle can also absorb a large section of the reducing equivalents (McKinlay and Harwood, 2010a; McKinlay and Harwood, 2011). The CbbRRS system in the Calvin cycle can respond to the redox signal and regulate the carbon flux (Romagnoli and Tabita, 2007; Laguna et al., 2010). Therefore, the Calvin cycle competes for reducing equivalents with hydrogen production. When the Calvin cycle was blocked in *R. palustris*, the hydrogen produced was enhanced on all substrates (McKinlay and Harwood, 2011). Hence, for hydrogen production, attention should be paid to the oxidation state of substrates and the Calvin cycle flux to avoid redox imbalance.

The efficiency of hydrogen production can be further improved *via* complementation of photo-fermentation and dark-fermentation. In this sequential two-stage dark- and photo-fermentation process, dark hydrogen production was conducted using acidogenic bacteria like *Clostridium butyricum* (Su et al., 2009a), *C. pasteurianum* (Chen et al., 2008), *Caldicellulosiruptor saccharolyticus* (Özgür et al., 2010), and *E. coli* (Sangani et al., 2019), and photo hydrogen production was conducted using photosynthetic bacteria, like *R. palustris*. A sequential dark- and photo-fermentation system including *C. pasteurianum* and *R. palustris* has been constructed for hydrogen production using sucrose as a feedstock (Chen et al., 2008). The overall hydrogen yield increased from the maximum of 3.8 mol H_2/mol sucrose in dark fermentation to 10.02 mol H_2/mol sucrose by sequential dark and photofermentation (Chen et al., 2008). In the sequential dark- and photo-fermentation system, photo-fermentation can utilize the resulting effluent from dark fermentation, mainly consisting of butyric and acetic acid. It is reported that the sequential dark- and photo-fermentation system could achieve a theoretically maximum hydrogen yield (Su et al., 2009b); therefore, is has been considered as an efficient system to increase hydrogen production yield.

Methane is a commonly used energy source, and nearly half of hydrogen production in industry is from methane. A purified Mo-dependent nitrogenase from *Azotobacter vinelandii* with two mutations, V70A and H195Q, in *NifD* near the FeMo cofactor, was proven to be capable of reducing carbon dioxide to methane *in vitro* (Yang et al., 2012). Then, homologous mutations, V75A and H201Q, in *NifD* from *R. palustris*, were produced and methane production from carbon dioxide was also detected *in vivo* (**Figure 5**, Eq. 5) (Fixen et al., 2016; Zheng and Harwood, 2019). Further optimization indicated that utilization of nongrowing cells which are not carrying out the competing biosynthesis can enhance the yield of methane by 9-fold to 900 nmol/mg total protein using fumarate as the substrate (Zheng and Harwood, 2019). The analogous mutation of the V-dependent nitrogenase ($VnfD^{V57AH180Q}$) can also catalyze the synthesis of methane in *R. palustris* (Zheng et al., 2018). The wild type of another Fe-only nitrogenase in *R. palustris* also has the ability to synthesize methane, ammonia and hydrogen simultaneously, but the proportion of methane is relatively low (Zheng et al., 2018). With in-depth study of the mechanisms of nitrogenase, improving the ability of nitrogenase to synthesize

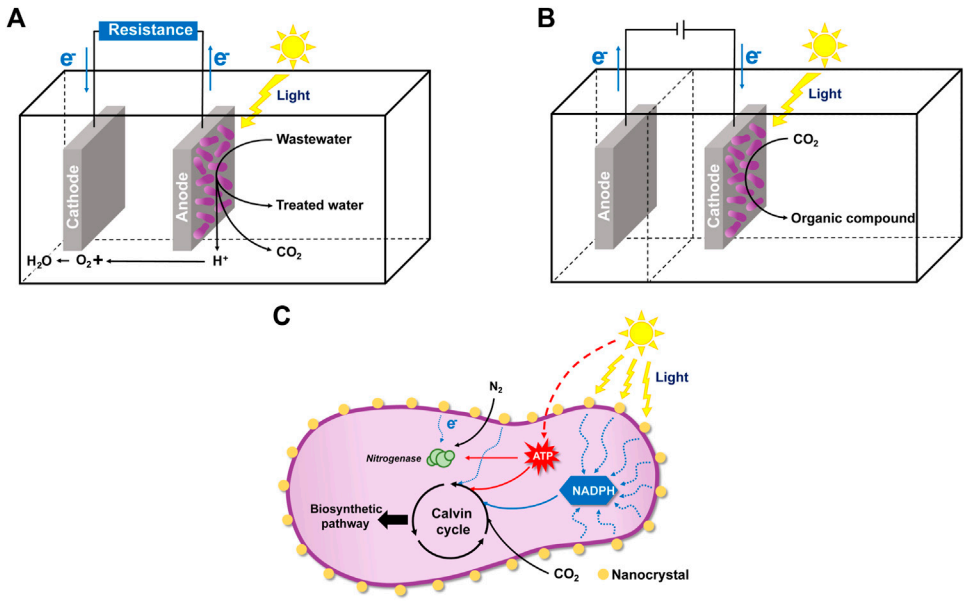

FIGURE 6 | Illustration of the microbial fuel cell (MFC) and microbial electrosynthesis (MES) of *R. palustris* and CdS-*R. palustris* hybrid system. **(A)** In the MFC system, *R. palustris* in the anode can oxidize organic substrates in the wastewater and release electrons and protons. Electricity current is generated, and the protons are transferred to the cathode and react with oxygen to generate water. **(B)** In the MES system, the electrons from the cathode is absorbed by *R. palustris* for organic chemicals production from inorganic carbon dioxide and light energy. **(C)** In the CdS-*R. palustris* hybrid system, *R. palustris* can absorb electrons from the CdS nanoparticles (NPs) coated on its cell surface.

hydrogen and methane through genetic engineering and synthetic biology methods are the direction of further research.

In addition, the production of butanol by *R. palustris* has also been reported. Compared to ethanol, butanol is an attractive renewable biofuel with a higher energy content, lower volatility, higher viscosity and higher intersolubility with traditional fuels (Jin et al., 2011). The *adhE2* gene from *Clostridium acetobutylicum* ATCC 824 encodes alcohol-aldehyde dehydrogenase, which catalyzes the synthesis of *n*-butanol from *n*-butyrate, was expressed in *R. palustris* (Doud et al., 2017). A selectivity (butanol production from butyrate) up to 40%, close to the theoretical maximum selectivity 45%, was achieved in the engineered *R. palustris* (Doud et al., 2017). However, a very low *n*-butanol production rate, 0.03 g L^{-1} d^{-1}, was obtained as a result of the slow growth of *R. palustris*, and the redox flux is speculated to be the limiting factor (Doud et al., 2017). Further engineering to improve its growth rate and metabolic rate is proposed to improve butanol and other biofuels production.

Biofuel production, mostly hydrogen, in *R. palustris* has been widely researched in the fields of diverse substrates and genetical modification to improve the metabolic flux. However, the low production yield still limits its application in industry. Combination of biofuel production with industrial and agricultural wastewater treatment or biodegradation might be a promising strategy to reduce cost.

3.3.2 Application in Microbial Fuel Cells, Microbial Electrosynthesis and Photocatalytic Synthesis

In recent years, some novel application fields were reported for *R. palustris*, utilizing its electron exchange ability with solid-phase materials, such as MCF, MES and photocatalytic synthesis (**Figure 6**). Construction of MFC has attracted much attention in recent years due to its electricity generation ability. In the MFC system, microbes can oxidize organic substrates in the anode and release electrons and protons, which are transferred to the cathode and react with oxygen to generate water, while generating electricity at the same time (**Figure 6A**) (Slate et al., 2019). Photo-microbial fuel cells (PMFC), which can convert light energy to electricity due to the photosynthetic activity of the photosynthetic microorganisms, are also being developed. *R. palustris* has been utilized as a model organism in PMFC. The power density of *R. palustris* DX-1 achieved 2,720 mW/m^2 under light with acetate as the electron donor (Xing et al., 2008). Carbon sources from wastewater and contaminated sites can also be utilized as electron donors in the PMFC system. *R. palustris* RP2 can produce a current (power density 720 μW/m^2) using petroleum hydrocarbons from oil contaminated sites as the energy source (Venkidusamy and Megharaj, 2016). In another study, *R. palustris* G11 could accumulate polyphosphate and PHB when a sufficient carbon source was provided, and the stored polyphosphate and PHB were further used for electricity production in a carbon source-insufficient condition (Lai et al., 2017). Power production under carbon source-insufficient conditions indicates the simultaneous application of PMFC for energy production and wastewater treatment, in which the carbon source is not enriched. Recently, a novel hybrid hydrogen-photosynthetic microbial fuel cell was constructed, which can produce hydrogen and a maximum power density of 2.39 mW/m^2 in *R. palustris* ATCC 17007 at the same time (Pankan et al., 2020). The performance of

PMFC may be affected by the electrode material, reactor, membrane, substrate and operating conditions (Aghababaie et al., 2015). Application of PMFC is mostly limited by its low power generation and expensive electrode materials, and research should be focused on improving the rate of electron transfer to/from the electrode and the exploration of advanced materials as the electrode.

Microorganisms applied in MCF can release electrons to the solid-phase material and generate electricity. However, microorganisms can also absorb electrons from the cathode for MES, a bioelectrochemical process (Rabaey et al., 2011). In an MES system, desired chemicals are produced from an inorganic substrate and the absorbed electrons at the cathode-microbe interface (**Figure 6B**) (Karthikeyan et al., 2019). Photoautotrophic iron-oxidizing *R. palustris* TIE-1 can accept electrons from a solid-phase electrode, with carbon dioxide as the sole carbon source and electron acceptor (Bose et al., 2014). In *R. palustris* TIE-1, the *pio* operon is responsible for electron uptake from the electrode, and electron uptake stimulates *ruBisCo* form I expression, indicating the enhancement of carbon fixation during MES (Jiao and Newman, 2007; Bose et al., 2014). The major obstacle for using *R. palustris* TIE-1 for MES is the low electron uptake efficiency from cathode, which is reflected by the low maximum current density values (Ranaivoarisoa et al., 2019). To further enhance the electron uptake ability by *R. palustris* TIE-1, several iron-based redox mediators coated cathodes were tested and the immobilized Prussian blue (PB)-coated cathode was proven to be the best (Rengasamy et al., 2018). In another study, to enhance the electron uptake rates of *R. palustris* TIE-1, a photobioelectrochemical system with two uncoupled reactors, an electrochemical system and a photobioreactor, was developed, which had an electron uptake rate 56-fold higher than the single system (Doud and Angenent, 2014). In summary, the application of *R. palustris* in MES has been reported in recent years, but electron transfer efficiency is still the key factor limiting its efficiency. Actually, even after a decade of development, using MES for chemical synthesis cannot compete with the traditional fossil-fuel-derived production (Prevoteau et al., 2020). However, MES is still promising for chemical production from carbon dioxide, and the performance of MES can be improved.

R. palustris can also absorb electrons from the nanoparticles (NPs) coated on its cell surface. An inorganic-biological hybrid system, a CdS-*R. palustris* hybrid system, was constructed, in which CdS NPs coated on the cell surface can absorb solar energy, release electrons, then participate in various biosynthetic pathways (**Figure 6C**) (Wang et al., 2019). In this semiartificial photosynthetic platform, solar energy is directly utilized for the chemical production. CdS NPs on the surface of *R. palustris* are formed by Cd^{2+} bioprecipitation through the cysteine desulfurase (Bai et al., 2009). In the CdS-*R. palustris* hybrid system, carbon dioxide reduction was enhanced and the production of solid biomass, carotenoids and PHB were increased to 148%, 122%, and 147%, respectively (Wang et al., 2019). The synthesized CdS NPs can also locate to the cytoplasm, absorb solar energy, and enhance the nitrogen fixation catalyzed by nitrogenase (Sakpirom et al., 2019). Research about the nanoparticles-photosynthetic hybrid system is still in the initial stage. Further research on different nanomaterials and the genetic modification of *R. palustris* are expected to improve its catalytic efficiency.

4 CHALLENGES AND POSSIBLE SOLUTIONS

R. palustris has great potential for application in many fields: valuable chemicals production as a chassis organism; wastewater treatment and bioremediation for its biodetoxification and biodegradation properties; agriculture, aquaculture and livestock breeding as food additives; MCF, MES and photocatalytic synthesis for its electron exchange ability with solid materials. However, some properties of *R. palustris* limit its wide application. First, even though the versatile *R. palustris* can use a variety of carbon sources, its metabolic efficiency and growth rate are very low. Random mutation and screening are expected to improve its metabolic efficiency. Second, to our knowledge, except for a few gene expression vectors (pMG103 and pBBR1MCS series) and a gene knockout vector (pJQ200SK), no other genetic manipulation tools available in *R. palustris* have been reported. Exploring more genetic tools for *R. palustris* is necessary. Genetic manipulation tools, such as pRK404 and pIND4, which are available in other PNSBs, may be suitable for *R. palustris*. In addition, the implementation of some novel gene manipulation technologies, such as CRISPR-Cas and antisense RNA, in *R. palustris* is promising. Third, most of the research about *R. palustris* is at the physiological and biochemical levels, and genetic manipulation to enhance its efficiency is rarely reported. For example, for hydrogen production, most of the research has focused on the optimization of culture conditions to improve its production, and only limited research about the genetic manipulation of *R. palustris* has been reported. However, genetic manipulation could improve the properties of *R. palustris* significantly. Development of genetic engineering tools would facilitate genetic manipulation of *R. palustris* to improve its performance.

AUTHOR CONTRIBUTIONS

ML and PN searched for the literatures and prepared the manuscript. YS helped to polish the manuscript. JL and JY put forward the concept of the manuscript and revised the manuscript. All authors have read and agreed to the published version of the manuscript.

FUNDING

This work was supported by grants from the "First class grassland science discipline" program in Shandong Province, the National Natural Science Foundation of China (31860011), Key Laboratory of Biobased Materials, Qingdao Institute of Bioenergy and Bioprocess Technology, Chinese Academy of Sciences (BMF-2020-01), the Talents of High Level Scientific

Research Foundation (grants 6651120032, 6651117005, and 6651119011) of Qingdao Agricultural University, Natural Science Foundation of Shandong Province (Grant No. ZR2020QC069), and Key Laboratory of Biofuels, Qingdao Institute of Bioenergy and Bioprocess Technology, Chinese Academy of Sciences (CASKLB201805).

REFERENCES

Adessi, A., Concato, M., Sanchini, A., Rossi, F., and De Philippis, R. (2016). Hydrogen Production under Salt Stress Conditions by a Freshwater *Rhodopseudomonas palustris* Strain. *Appl. Microbiol. Biotechnol.* 100 (6), 2917–2926. doi:10.1007/s00253-016-7291-4

Aghababaie, M., Farhadian, M., Jeihanipour, A., and Biria, D. (2015). Effective Factors on the Performance of Microbial Fuel Cells in Wastewater Treatment - a Review. *Environ. Technol. Rev.* 4 (1), 71–89. doi:10.1080/09593330.2015.1077896

Alsiyabi, A., Brown, B., Immethun, C., Long, D., Wilkins, M., and Saha, R. (2021). Synergistic Experimental and Computational Approach Identifies Novel Strategies for Polyhydroxybutyrate Overproduction. *Metab. Eng.* 68, 1–13. doi:10.1016/j.ymben.2021.08.008

Austin, S., Kontur, W. S., Ulbrich, A., Oshlag, J. Z., Zhang, W., Higbee, A., et al. (2015). Metabolism of Multiple Aromatic Compounds in Corn Stover Hydrolysate by *Rhodopseudomonas palustris*. *Environ. Sci. Technol.* 49 (14), 8914–8922. doi:10.1021/acs.est.5b02062

Badger, M. R., and Bek, E. J. (2008). Multiple Rubisco Forms in Proteobacteria: Their Functional Significance in Relation to CO2 Acquisition by the CBB Cycle. *J. Exp. Bot.* 59 (7), 1525–1541. doi:10.1093/jxb/erm297

Bai, H. J., Zhang, Z. M., Guo, Y., and Yang, G. E. (2009). Biosynthesis of Cadmium Sulfide Nanoparticles by Photosynthetic Bacteria *Rhodopseudomonas palustris*. *Colloids Surfaces B Biointerf.* 70 (1), 142–146. doi:10.1016/j.colsurfb.2008.12.025

Batool, K., Tuz Zahra, F., and Rehman, Y. (2017). Arsenic-Redox Transformation and Plant Growth Promotion by Purple Nonsulfur Bacteria *Rhodopseudomonas palustris* CS2 and *Rhodopseudomonas faecalis* SS5. *BioMed Res. Int.* 2017, 1–8. doi:10.1155/2017/6250327

Bélanger-Chabot, G., Rahm, M., Haiges, R., and Christe, K. O. (2015). Ammonia-(Dinitramido)boranes: High-Energy-Density Materials. *Angew. Chem. Int. Ed.* 54 (40), 11730–11734. doi:10.1002/anie.201505684

Berne, C., Allainmat, B., and Garcia, D. (2005). Tributyl Phosphate Degradation by *Rhodopseudomonas palustris* and Other Photosynthetic Bacteria. *Biotechnol. Lett.* 27 (8), 561–566. doi:10.1007/s10529-005-2882-7

Bose, A., Gardel, E. J., Vidoudez, C., Parra, E. A., and Girguis, P. R. (2014). Electron Uptake by Iron-Oxidizing Phototrophic Bacteria. *Nat. Commun.* 5, 3391. doi:10.1038/ncomms4391

Brown, B., Immethun, C., Alsiyabi, A., Long, D., Wilkins, M., and Saha, R. (2022). Heterologous Phasin Expression in *Rhodopseudomonas palustris* CGA009 for Bioplastic Production from Lignocellulosic Biomass. *Metab. Eng. Commun.* 14, e00191. doi:10.1016/j.mec.2021.e00191

Brown, B., Immethun, C., Wilkins, M., and Saha, R. (2020). *Rhodopseudomonas palustris* CGA009 Polyhydroxybutyrate Production from a Lignin Aromatic and Quantification via Flow Cytometry. *Bioresour. Technol. Rep.* 11, 100474. doi:10.1016/j.biteb.2020.100474

Cardeña, R., Valdez-Vazquez, I., and Buitrón, G. (2017). Effect of Volatile Fatty Acids Mixtures on the Simultaneous Photofermentative Production of Hydrogen and Polyhydroxybutyrate. *Bioprocess Biosyst. Eng.* 40 (2), 231–239. doi:10.1007/s00449-016-1691-9

Chang, T.-H., Wang, R., Peng, Y.-H., Chou, T.-H., Li, Y.-J., and Shih, Y.-h. (2020). Biodegradation of Hexabromocyclododecane by *Rhodopseudomonas palustris* YSC3 Strain: A Free-Living Nitrogen-Fixing Bacterium Isolated in Taiwan. *Chemosphere* 246, 125621. doi:10.1016/j.chemosphere.2019.125621

Chen, C.-Y., Yang, M.-H., Yeh, K.-L., Liu, C.-H., and Chang, J.-S. (2008). Biohydrogen Production Using Sequential Two-Stage Dark and Photo Fermentation Processes. *Int. J. Hydrogen Energy* 33 (18), 4755–4762. doi:10.1016/j.ijhydene.2008.06.055

Chi, S. C., Mothersole, D. J., Dilbeck, P., Niedzwiedzki, D. M., Zhang, H., Qian, P., et al. (2015). Assembly of Functional Photosystem Complexes in *Rhodobacter sphaeroides* Incorporating Carotenoids from the Spirilloxanthin Pathway. *Biochim. Biophys. Acta Bioenerg.* 1847 (2), 189–201. doi:10.1016/j.bbabio.2014.10.004

Chowhan, A., and Giri, T. K. (2020). Polysaccharide as Renewable Responsive Biopolymer for *In Situ* Gel in the Delivery of Drug through Ocular Route. *Int. J. Biol. Macromol.* 150, 559–572. doi:10.1016/j.ijbiomac.2020.02.097

Christopher, K., and Dimitrios, R. (2012). A Review on Exergy Comparison of Hydrogen Production Methods from Renewable Energy Sources. *Energy Environ. Sci.* 5 (5), 6640–6651. doi:10.1039/C2EE01098D

Corneli, E., Adessi, A., Dragoni, F., Ragaglini, G., Bonari, E., and De Philippis, R. (2016). Agroindustrial Residues and Energy Crops for the Production of Hydrogen and Poly-β-Hydroxybutyrate via Photofermentation. *Bioresour. Technol.* 216, 941–947. doi:10.1016/j.biortech.2016.06.046

Dixon, R., and Kahn, D. (2004). Genetic Regulation of Biological Nitrogen Fixation. *Nat. Rev. Microbiol.* 2 (8), 621–631. doi:10.1038/nrmicro954

Doud, D. F. R., and Angenent, L. T. (2014). Toward Electrosynthesis with Uncoupled Extracellular Electron Uptake and Metabolic Growth: Enhancing Current Uptake with *Rhodopseudomonas palustris*. *Environ. Sci. Technol. Lett.* 1 (9), 351–355. doi:10.1021/ez500244n

Doud, D. F. R., Holmes, E. C., Richter, H., Molitor, B., Jander, G., and Angenent, L. T. (2017). Metabolic Engineering of *Rhodopseudomonas palustris* for the Obligate Reduction of *N*-Butyrate to *N*-Butanol. *Biotechnol. Biofuels* 10 (1), 178. doi:10.1186/s13068-017-0864-3

Dutton, P. L., and Evans, W. C. (1969). The Metabolism of Aromatic Compounds by *Rhodopseudomonas palustris*. A New, Reductive, Method of Aromatic Ring Metabolism. *Biochem. J.* 113, 525–536. doi:10.1042/bj1130525

Egland, P. G., Gibson, J., and Harwood, C. S. (2001). Reductive, Coenzyme A-Mediated Pathway for 3-Chlorobenzoate Degradation in the Phototrophic Bacterium *Rhodopseudomonas palustris*. *Appl. Environ. Microbiol.* 67 (3), 1396–1399. doi:10.1128/aem.67.3.1396-1399.2001

Egland, P. G., Pelletier, D. A., Dispensa, M., Gibson, J., and Harwood, C. S. (1997). A Cluster of Bacterial Genes for Anaerobic Benzene Ring Biodegradation. *Proc. Natl. Acad. Sci. U.S.A.* 94, 6484–6489. doi:10.1073/pnas.94.12.6484

Fang, L. C., Li, Y., Cheng, P., Deng, J., Jiang, L. L., Huang, H., et al. (2012). Characterization of *Rhodopseudomonas palustris* Strain 2C as a Potential Probiotic. *Apmis* 120 (9), 743–749. doi:10.1111/j.1600-0463.2012.02902.x

Fixen, K. R., Zheng, Y., Harris, D. F., Shaw, S., Yang, Z.-Y., Dean, D. R., et al. (2016). Light-driven Carbon Dioxide Reduction to Methane by Nitrogenase in a Photosynthetic Bacterium. *Proc. Natl. Acad. Sci. U.S.A.* 113 (36), 10163–10167. doi:10.1073/pnas.1611043113

Fritts, R. K., LaSarre, B., Stoner, A. M., Posto, A. L., and McKinlay, J. B. (2017). A Rhizobiales-Specific Unipolar Polysaccharide Adhesin Contributes to *Rhodopseudomonas palustris* Biofilm Formation across Diverse Photoheterotrophic Conditions. *Appl. Environ. Microbiol.* 83 (4), e03035–03016. doi:10.1128/AEM.03035-16

Ghosh, D., Sobro, I. F., and Hallenbeck, P. C. (2012). Stoichiometric Conversion of Biodiesel Derived Crude Glycerol to Hydrogen: Response Surface Methodology Study of the Effects of Light Intensity and Crude Glycerol and Glutamate Concentration. *Bioresour. Technol.* 106, 154–160. doi:10.1016/j.biortech.2011.12.021

Gogada, R., Singh, S. S., Lunavat, S. K., Pamarthi, M. M., Rodrigue, A., Vadivelu, B., et al. (2015). Engineered Deinococcus Radiodurans R1 with NiCoT Genes for Bioremoval of Trace Cobalt from Spent Decontamination Solutions of Nuclear Power Reactors. *Appl. Microbiol. Biotechnol.* 99 (21), 9203–9213. doi:10.1007/s00253-015-6761-4

Gosse, J. L., Chinn, M. S., Grunden, A. M., Bernal, O. I., Jenkins, J. S., Yeager, C., et al. (2012). A Versatile Method for Preparation of Hydrated Microbial-Latex Biocatalytic Coatings for Gas Absorption and Gas Evolution. *J. Ind. Microbiol. Biotechnol.* 39 (9), 1269–1278. doi:10.1007/s10295-012-1135-8

Govindaraju, A., McKinlay, J. B., and LaSarre, B. (2019). Phototrophic Lactate Utilization by *Rhodopseudomonas palustris* is Stimulated by Coutilization with Additional Substrates. *Appl. Environ. Microbiol.* 85 (11), e00048–00019. doi:10.1128/AEM.00048-19

Grattieri, M. (2020). Purple Bacteria Photo-Bioelectrochemistry: Enthralling Challenges and Opportunities. *Photochem. Photobiol. Sci.* 19 (4), 424–435. doi:10.1039/c9pp00470j

Guan, C.-j., Ji, Y.-j., Hu, J.-l., Hu, C.-n., Yang, F., and Yang, G.-e. (2017). Biotransformation of Rutin Using Crude Enzyme from *Rhodopseudomonas palustris*. *Curr. Microbiol.* 74 (4), 431–436. doi:10.1007/s00284-017-1204-3

Habe, H., Fukuoka, T., Kitamoto, D., and Sakaki, K. (2009). Biotechnological Production of D-Glyceric Acid and its Application. *Appl. Microbiol. Biotechnol.* 84 (3), 445–452. doi:10.1007/s00253-009-2124-3

Hajighasemi, M., Nocek, B. P., Tchigvintsev, A., Brown, G., Flick, R., Xu, X., et al. (2016). Biochemical and Structural Insights into Enzymatic Depolymerization of Polylactic Acid and Other Polyesters by Microbial Carboxylesterases. *Biomacromolecules* 17 (6), 2027–2039. doi:10.1021/acs.biomac.6b00223

Hallenbeck, P. C., and Ghosh, D. (2009). Advances in Fermentative Biohydrogen Production: The Way Forward? *Trends Biotechnol.* 27 (5), 287–297. doi:10.1016/j.tibtech.2009.02.004

Hangasky, J. A., Detomasi, T. C., and Marletta, M. A. (2019). Glycosidic Bond Hydroxylation by Polysaccharide Monooxygenases. *Trends Chem.* 1 (2), 198–209. doi:10.1016/j.trechm.2019.01.007

Harwood, C. S., Burchhardt, G., Herrmann, H., and Fuchs, G. (1998). Anaerobic Metabolism of Aromatic Compounds via the Benzoyl-CoA Pathway. *FEMS Microbiol. Rev.* 22 (5), 439–458. doi:10.1111/j.1574-6976.1998.tb00380.x

Harwood, C. S., and Gibson, J. (1988). Anaerobic and Aerobic Metabolism of Diverse Aromatic Compounds by the Photosynthetic Bacterium *Rhodopseudomonas palustris*. *Appl. Environ. Microbiol.* 54, 712–717. doi:10.1128/aem.54.3.712-717.1988

Harwood, C. S. (2020). Iron-Only and Vanadium Nitrogenases: Fail-Safe Enzymes or Something More? *Annu. Rev. Microbiol.* 74 (1), 247–266. doi:10.1146/annurev-micro-022620-014338

Heiniger, E. K., Oda, Y., Samanta, S. K., and Harwood, C. S. (2012). How Posttranslational Modification of Nitrogenase is Circumvented in *Rhodopseudomonas palustris* Strains that Produce Hydrogen Gas Constitutively. *Appl. Environ. Microbiol.* 78 (4), 1023–1032. doi:10.1128/aem.07254-11

Hirakawa, H., Hirakawa, Y., Greenberg, E. P., and Harwood, C. S. (2015). BadR and BadM Proteins Transcriptionally Regulate Two Operons Needed for Anaerobic Benzoate Degradation by *Rhodopseudomonas palustris*. *Appl. Environ. Microbiol.* 81 (13), 4253–4262. doi:10.1128/aem.00377-15

Hu, C., Choy, S.-Y., and Giannis, A. (2018). Evaluation of Lighting Systems, Carbon Sources, and Bacteria Cultures on Photofermentative Hydrogen Production. *Appl. Biochem. Biotechnol.* 185 (1), 257–269. doi:10.1007/s12010-017-2655-5

Huang, J. J., Heiniger, E. K., McKinlay, J. B., and Harwood, C. S. (2010). Production of Hydrogen Gas from Light and the Inorganic Electron Donor Thiosulfate by *Rhodopseudomonas palustris*. *Appl. Environ. Microbiol.* 76 (23), 7717–7722. doi:10.1128/aem.01143-10

Ind, A. C., Porter, S. L., Brown, M. T., Byles, E. D., de Beyer, J. A., Godfrey, S. A., et al. (2009). Inducible-Expression Plasmid for *Rhodobacter sphaeroides* and *Paracoccus denitrificans*. *Appl. Environ. Microbiol.* 75 (20), 6613–6615. doi:10.1128/AEM.01587-09

Inui, M., Roh, J. H., Zahn, K., and Yukawa, H. (2000). Sequence Analysis of the Cryptic Plasmid pMG101 from *Rhodopseudomonas palustris* and Construction of Stable Cloning Vectors. *Appl. Environ. Microbiol.* 66 (1), 54–63. doi:10.1128/aem.66.1.54-63.2000

Jiao, F., and Xu, B. (2019). Electrochemical Ammonia Synthesis and Ammonia Fuel Cells. *Adv. Mat.* 31, 1805173. doi:10.1002/adma.201805173

Jiao, Y., and Newman, D. K. (2007). The *Pio* Operon is Essential for Phototrophic Fe(II) Oxidation in *Rhodopseudomonas palustris* TIE-1. *J. Bacteriol.* 189 (5), 1765–1773. doi:10.1128/JB.00776-06

Jin, C., Yao, M., Liu, H., Lee, C.-f. F., and Ji, J. (2011). Progress in the Production and Application of *N*-Butanol as a Biofuel. *Renew. Sustain. Energy Rev.* 15 (8), 4080–4106. doi:10.1016/j.rser.2011.06.001

Kalia, V. C., Singh Patel, S. K., Shanmugam, R., and Lee, J.-K. (2021). Polyhydroxyalkanoates: Trends and Advances Toward Biotechnological Applications. *Bioresour. Technol.* 326, 124737. doi:10.1016/j.biortech.2021.124737

Kamal, V. S., and Wyndham, R. C. (1990). Anaerobic Phototrophic Metabolism of 3-Chlorobenzoate by *Rhodopseudomonas palustris* WS17. *Appl. Environ. Microbiol.* 56 (12), 3871–3873. doi:10.1128/aem.56.12.3871-3873.1990

Kandemir, T., Schuster, M. E., Senyshyn, A., Behrens, M., and Schlögl, R. (2013). The Haber-Bosch Process Revisited: On the Real Structure and Stability of "Ammonia Iron" Under Working Conditions. *Angew. Chem. Int. Ed.* 52 (48), 12723–12726. doi:10.1002/anie.201305812

Karthikeyan, R., Singh, R., and Bose, A. (2019). Microbial Electron Uptake in Microbial Electrosynthesis: A Mini-Review. *J. Ind. Microbiol. Biotechnol.* 46 (9–10), 1419–1426. doi:10.1007/s10295-019-02166-6

Katsuda, Y. (1999). Development of and Future Prospects for Pyrethroid Chemistry. *Pestic. Sci.* 55 (8), 775–782. doi:10.1002/(sici)1096-9063(199908)55:8<775:aid-ps27>3.0.co;2-n

Katzke, N., Arvani, S., Bergmann, R., Circolone, F., Markert, A., Svensson, V., et al. (2010). A Novel T7 RNA Polymerase Dependent Expression System for High-Level Protein Production in the Phototrophic Bacterium *Rhodobacter capsulatus*. *Protein Expr. Purif.* 69 (2), 137–146. doi:10.1016/j.pep.2009.08.008

Keen, N. T., Tamaki, S., Kobayashi, D., and Trollinger, D. (1988). Improved Broad-Host-Range Plasmids for DNA Cloning in Gram-Negative Bacteria. *Gene* 70 (1), 191–197. doi:10.1016/0378-1119(88)90117-5

Kim, M. K., Choi, K.-M., Yin, C.-R., Lee, K.-Y., Im, W.-T., Lim, J. H., et al. (2004). Odorous Swine Wastewater Treatment by Purple Non-sulfur Bacteria, *Rhodopseudomonas palustris*, Isolated from Eutrophicated Ponds. *Biotechnol. Lett.* 26 (10), 819–822. doi:10.1023/b:bile.0000025884.50198.67

Kim, S.-K., and Karadeniz, F. (2012). "Biological Importance and Applications of Squalene and Squalane," in *Advances in Food and Nutrition Research*. Editor S.-K. Kim (Waltham, MA: Academic Press), 223–233. doi:10.1016/b978-0-12-416003-3.00014-7

Koh, R. H., and Song, H. G. (2007). Effects of Application of *Rhodopseudomonas* spp. On Seed Germination and Growth of Tomato under Axenic Conditions. *J. Microbiol. Biotechnol.* 17 (11), 1805–1810.

Krooneman, J., van den Akker, S., Pedro Gomes, T. M., Forney, L. J., and Gottschal, J. C. (1999). Degradation of 3-Chlorobenzoate under Low-Oxygen Conditions in Pure and Mixed Cultures of the Anoxygenic Photoheterotroph *Rhodopseudomonas palustris* DCP3 and an Aerobic *Alcaligenes* Species. *Appl. Environ. Microbiol.* 65 (1), 131–137. doi:10.1128/AEM.65.1.131-137.1999

Kuo, F.-S., Chien, Y.-H., and Chen, C.-J. (2012). Effects of Light Sources on Growth and Carotenoid Content of Photosynthetic Bacteria *Rhodopseudomonas palustris*. *Bioresour. Technol.* 113, 315–318. doi:10.1016/j.biortech.2012.01.087

Küver, J., Xu, Y., and Gibson, J. (1995). Metabolism of Cyclohexane Carboxylic Acid by the Photosynthetic bacteriumRhodopseudomonas Palustris. *Arch. Microbiol.* 164 (5), 337–345. doi:10.1007/BF02529980

Laguna, R., Joshi, G. S., Dangel, A. W., Luther, A. K., and Tabita, F. R. (2010). Integrative Control of Carbon, Nitrogen, Hydrogen, and Sulfur Metabolism: the Central Role of the Calvin-Benson-Bassham Cycle. *Adv. Exp. Med. Biol.* 675, 265–271. doi:10.1007/978-1-4419-1528-3_15

Lai, Y.-C., Liang, C.-M., Hsu, S.-C., Hsieh, P.-H., and Hung, C.-H. (2017). Polyphosphate Metabolism by Purple Non-sulfur Bacteria and its Possible Application on Photo-Microbial Fuel Cell. *J. Biosci. Bioeng.* 123 (6), 722–730. doi:10.1016/j.jbiosc.2017.01.012

Lang, H. P., and Hunter, C. N. (1994). The Relationship Between Carotenoid Biosynthesis and the Assembly of the Light-Harvesting LH2 Complex in *Rhodobacter sphaeroides*. *Biochem. J.* 298, 197–205. doi:10.1042/bj2980197

Larimer, F. W., Chain, P., Hauser, L., Lamerdin, J., Malfatti, S., Do, L., et al. (2003). Complete Genome Sequence of the Metabolically Versatile Photosynthetic Bacterium *Rhodopseudomonas palustris*. *Nat. Biotechnol.* 22 (1), 55–61. doi:10.1038/nbt923

Lazaro, C. Z., Hitit, Z. Y., and Hallenbeck, P. C. (2017). Optimization of the Yield of Dark Microaerobic Production of Hydrogen from Lactate by *Rhodopseudomonas palustris*. *Bioresour. Technol.* 245 (Pt A), 123–131. doi:10.1016/j.biortech.2017.08.207

Lee, S. Y. (1996). Bacterial Polyhydroxyalkanoates. *Biotechnol. Bioeng.* 49 (1), 1–14. doi:10.1002/(SICI)1097-0290(19960105)49:1<1::AID-BIT1>3.0.CO;2-P

Li, B., Liu, N., Li, Y., Jing, W., Fan, J., Li, D., et al. (2014). Reduction of Selenite to Red Elemental Selenium by *Rhodopseudomonas palustris* Strain N. *PLoS One* 9 (4), e95955. doi:10.1371/journal.pone.0095955

Li, M., Hou, F., Wu, T., Jiang, X., Li, F., Liu, H., et al. (2019). Recent Advances of Metabolic Engineering Strategies in Natural Isoprenoid Production Using Cell Factories. *Nat. Prod. Rep.* 37 (1), 80–99. doi:10.1039/c9np00016j

Li, M., Nian, R., Xian, M., and Zhang, H. (2018). Metabolic Engineering for the Production of Isoprene and Isopentenol by *Escherichia coli*. *Appl. Microbiol. Biotechnol.* 102 (18), 7725–7738. doi:10.1007/s00253-018-9200-5

Li, Z., Yang, J., and Loh, X. J. (2016). Polyhydroxyalkanoates: Opening Doors for a Sustainable Future. *NPG Asia Mater* 8 (4), e265. doi:10.1038/am.2016.48

Liao, Q., Wang, Y.-J., Wang, Y.-Z., Zhu, X., Tian, X., and Li, J. (2010). Formation and Hydrogen Production of Photosynthetic Bacterial Biofilm under Various Illumination Conditions. *Bioresour. Technol.* 101 (14), 5315–5324. doi:10.1016/j.biortech.2010.02.019

Liu, S., Daigger, G. T., Kang, J., and Zhang, G. (2019). Effects of Light Intensity and Photoperiod on Pigments Production and Corresponding Key Gene Expression of *Rhodopseudomonas palustris* in a Photobioreactor System. *Bioresour. Technol.* 294, 122172. doi:10.1016/j.biortech.2019.122172

Liu, S., Zhang, G., Zhang, J., Li, X., and Li, J. (2016). Performance, Carotenoids Yield and Microbial Population Dynamics in a Photobioreactor System Treating Acidic Wastewater: Effect of Hydraulic Retention Time (HRT) and Organic Loading Rate (OLR). *Bioresour. Technol.* 200, 245–252. doi:10.1016/j.biortech.2015.10.044

Liu, Y., Ghosh, D., and Hallenbeck, P. C. (2015). Biological Reformation of Ethanol to Hydrogen by *Rhodopseudomonas palustris* CGA009. *Bioresour. Technol.* 176, 189–195. doi:10.1016/j.biortech.2014.11.047

Llorens, I., Untereiner, G., Jaillard, D., Gouget, B., Chapon, V., and Carriere, M. (2012). Uranium Interaction with Two Multi-Resistant Environmental Bacteria: Cupriavidus Metallidurans CH34 and *Rhodopseudomonas palustris*. *PLoS One* 7 (12), e51783. doi:10.1371/journal.pone.0051783

Luo, X., Zhang, D., Zhou, X., Du, J., Zhang, S., and Liu, Y. (2018). Cloning and Characterization of a Pyrethroid Pesticide Decomposing Esterase Gene, *Est3385*, from *Rhodopseudomonas palustris* PSB-S. *Sci. Rep.* 8 (1), 7384. doi:10.1038/s41598-018-25734-9

Luo, Y., Ge, M., Wang, B., Sun, C., Wang, J., Dong, Y., et al. (2020). CRISPR/Cas9-deaminase Enables Robust Base Editing in *Rhodobacter sphaeroides* 2.4.1. *Microb. Cell. Fact.* 19 (1), 93. doi:10.1186/s12934-020-01345-w

Madigan, M. T., and Jung, D. O. (2009). "An Overview of Purple Bacteria: Systematics, Physiology, and Habitats," in *The Purple Phototrophic Bacteria*. Editors C. N. Hunter, F. Daldal, M. C. Thurnauer, and J. T. Beatty (Dordrecht: Springer Netherlands), 1–15. doi:10.1007/978-1-4020-8815-5_1

McAdam, B., Brennan Fournet, M., McDonald, P., and Mojicevic, M. (2020). Production of Polyhydroxybutyrate (PHB) and Factors Impacting its Chemical and Mechanical Characteristics. *Polymers* 12 (12), 2908. doi:10.3390/polym12122908

McKinlay, J. B., and Harwood, C. S. (2011). Calvin Cycle Flux, Pathway Constraints, and Substrate Oxidation State Together Determine the H 2 Biofuel Yield in Photoheterotrophic Bacteria. *mBio* 2 (2), e00323–10. doi:10.1128/mBio.00323-10

McKinlay, J. B., and Harwood, C. S. (2010a). Carbon Dioxide Fixation as a Central Redox Cofactor Recycling Mechanism in Bacteria. *Proc. Natl. Acad. Sci. U.S.A.* 107 (26), 11669–11675. doi:10.1073/pnas.1006175107

McKinlay, J. B., and Harwood, C. S. (2010b). Photobiological Production of Hydrogen Gas as a Biofuel. *Curr. Opin. Biotechnol.* 21 (3), 244–251. doi:10.1016/j.copbio.2010.02.012

McKinlay, J. B., Oda, Y., Rühl, M., Posto, A. L., Sauer, U., and Harwood, C. S. (2014). Non-growing *Rhodopseudomonas palustris* Increases the Hydrogen Gas Yield from Acetate by Shifting from the Glyoxylate Shunt to the Tricarboxylic Acid Cycle. *J. Biol. Chem.* 289 (4), 1960–1970. doi:10.1074/jbc.M113.527515

Mekjinda, N., and Ritchie, R. J. (2015). Breakdown of Food Waste by Anaerobic Fermentation and Non-Oxygen Producing Photosynthesis Using a Photosynthetic Bacterium. *Waste Manag.* 35, 199–206. doi:10.1016/j.wasman.2014.10.018

Melis, A. (2009). Solar Energy Conversion Efficiencies in Photosynthesis: Minimizing the Chlorophyll Antennae to Maximize Efficiency. *Plant Sci.* 177 (4), 272–280. doi:10.1016/j.plantsci.2009.06.005

Monroy, I., and Buitrón, G. (2020). Production of Polyhydroxybutyrate by Pure and Mixed Cultures of Purple Non-Sulfur Bacteria: A Review. *J. Biotechnol.* 317, 39–47. doi:10.1016/j.jbiotec.2020.04.012

Mougiakos, I., Orsi, E., Ghiffary, M. R., Post, W., de Maria, A., Adiego-Perez, B., et al. (2019). Efficient Cas9-Based Genome Editing of *Rhodobacter sphaeroides* for Metabolic Engineering. *Microb. Cell. Fact.* 18 (1), 204. doi:10.1186/s12934-019-1255-1

Muzziotti, D., Adessi, A., Faraloni, C., Torzillo, G., and De Philippis, R. (2017). Acclimation Strategy of *Rhodopseudomonas palustris* to High Light Irradiance. *Microbiol. Res.* 197, 49–55. doi:10.1016/j.micres.2017.01.007

Nair, S., Joshi-Saha, A., Singh, S., V., R., Singh, S., Thorat, V., et al. (2012). Evaluation of Transgenic Tobacco Plants Expressing a Bacterial Co-ni Transporter for Acquisition of Cobalt. *J. Biotechnol.* 161 (4), 422–428. doi:10.1016/j.jbiotec.2012.07.191

Noh, U., Heck, S., and Kohring, G.-W. (2002). Phototrophic Transformation of Phenol to 4-Hydroxyphenylacetate by *Rhodopseudomonas palustris*. *Appl. Microbiol. Biotechnol.* 58 (6), 830–835. doi:10.1007/s00253-002-0954-3

Novak, R. T., Gritzer, R. F., Leadbetter, E. R., and Godchaux, W. (2004). Phototrophic Utilization of Taurine by the Purple Nonsulfur Bacteria *Rhodopseudomonas palustris* and *Rhodobacter sphaeroides*. *Microbiology* 150 (6), 1881–1891. doi:10.1099/mic.0.27023-0

Obranić, S., Babić, F., and Maravić-Vlahoviček, G. (2013). Improvement of pBBR1MCS Plasmids, a Very Useful Series of Broad-Host-Range Cloning Vectors. *Plasmid* 70 (2), 263–267. doi:10.1016/j.plasmid.2013.04.001

Oda, Y., Samanta, S. K., Rey, F. E., Wu, L., Liu, X., Yan, T., et al. (2005). Functional Genomic Analysis of Three Nitrogenase Isozymes in the Photosynthetic Bacterium *Rhodopseudomonas palustris*. *J. Bacteriol.* 187 (22), 7784–7794. doi:10.1128/JB.187.22.7784-7794.2005

Oelze, J. X. R., and Klein, G. (1996). Control of Nitrogen Fixation by Oxygen in Purple Nonsulfur Bacteria. *Archives Microbiol.* 165 (4), 219–225. doi:10.1007/s002030050319

Okada, S., Devarenne, T. P., and Chappell, J. (2000). Molecular Characterization of Squalene Synthase from the Green Microalga *Botryococcus braunii*, Race B. *Archives Biochem. Biophys.* 373 (2), 307–317. doi:10.1006/abbi.1999.1568

Orsi, E., Folch, P. L., Monje-López, V. T., Fernhout, B. M., Turcato, A., Kengen, S. W. M., et al. (2019). Characterization of Heterotrophic Growth and Sesquiterpene Production by *Rhodobacter sphaeroides* on a Defined Medium. *J. Ind. Microbiol. Biotechnol.* 46 (8), 1179–1190. doi:10.1007/s10295-019-02201-6

Özgür, E., Mars, A. E., Peksel, B., Louwerse, A., Yücel, M., Gündüz, U., et al. (2010). Biohydrogen Production from Beet Molasses by Sequential Dark and Photofermentation. *Int. J. Hydrogen Energy* 35 (2), 511–517. doi:10.1016/j.ijhydene.2009.10.094

Pakpour, F., Najafpour, G., Tabatabaei, M., Tohidfar, M., and Younesi, H. (2014). Biohydrogen Production from CO-rich Syngas via a Locally Isolated *Rhodopseudomonas palustris* PT. *Bioprocess Biosyst. Eng.* 37 (5), 923–930. doi:10.1007/s00449-013-1064-6

Pankan, A. O., Yunus, K., and Fisher, A. C. (2020). Mechanistic Evaluation of the Exoelectrogenic Activity of *Rhodopseudomonas palustris* under Different Nitrogen Regimes. *Bioresour. Technol.* 300, 122637. doi:10.1016/j.biortech.2019.122637

Patel, S. K. S., Kumar, P., and Kalia, V. C. (2012). Enhancing Biological Hydrogen Production through Complementary Microbial Metabolisms. *Int. J. Hydrogen Energy* 37 (14), 10590–10603. doi:10.1016/j.ijhydene.2012.04.045

Peirong, Z., and Wei, L. (2013). Use of Fluidized Bed Biofilter and Immobilized *Rhodopseudomonas palustris* for Ammonia Removal and Fish Health Maintenance in a Recirculation Aquaculture System. *Aquac. Res.* 44 (3), 327–334. doi:10.1111/j.1365-2109.2011.03038.x

Phillips, C. J. C., Pines, M. K., Latter, M., Muller, T., Petherick, J. C., Norman, S. T., et al. (2010). The Physiological and Behavioral Responses of Steers to Gaseous Ammonia in Simulated Long-Distance Transport by Ship. *J. Anim. Sci.* 88 (11), 3579–3589. doi:10.2527/jas.2010-3089

Piskorska, M., Soule, T., Gosse, J. L., Milliken, C., Flickinger, M. C., Smith, G. W., et al. (2013). Preservation of H2production Activity in Nanoporous Latex Coatings of *Rhodopseudomonas palustris* CGA009 During Dry Storage at Ambient Temperatures. *Microb. Biotechnol.* 6 (5), 515–525. doi:10.1111/1751-7915.12032

Pott, R. W. M., Howe, C. J., and Dennis, J. S. (2013). Photofermentation of Crude Glycerol from Biodiesel Using *Rhodopseudomonas palustris*: Comparison with Organic Acids and the Identification of Inhibitory Compounds. *Bioresour. Technol.* 130, 725–730. doi:10.1016/j.biortech.2012.11.126

Pott, R. W. M., Howe, C. J., and Dennis, J. S. (2014). The Purification of Crude Glycerol Derived from Biodiesel Manufacture and its Use as a Substrate by *Rhodopseudomonas palustris* to Produce Hydrogen. *Bioresour. Technol.* 152, 464–470. doi:10.1016/j.biortech.2013.10.094

Prévoteau, A., Carvajal-Arroyo, J. M., Ganigué, R., and Rabaey, K. (2020). Microbial Electrosynthesis from CO2: Forever a Promise? *Curr. Opin. Biotechnol.* 62, 48–57. doi:10.1016/j.copbio.2019.08.014

Qiang, S., Su, A. P., Li, Y., Chen, Z., Hu, C. Y., and Meng, Y. H. (2019). Elevated β-Carotene Synthesis by the Engineered Rhodobacter Sphaeroides with Enhanced CrtY Expression. *J. Agric. Food Chem.* 67 (34), 9560–9568. doi:10.1021/acs.jafc.9b02597

Quandt, J., and Hynes, M. F. (1993). Versatile Suicide Vectors Which Allow Direct Selection for Gene Replacement in Gram-Negative Bacteria. *Gene* 127 (1), 15–21. doi:10.1016/0378-1119(93)90611-6

Rabaey, K., Girguis, P., and Nielsen, L. K. (2011). Metabolic and Practical Considerations on Microbial Electrosynthesis. *Curr. Opin. Biotechnol.* 22 (3), 371–377. doi:10.1016/j.copbio.2011.01.010

Ramana, C. V., Arunasri, K., and Sasikala, C. (2002). Photobiodegradation of Pyridine by *Rhodopseudomonas palustris* JA1. *Indian J. Exp. Biol.* 40 (8), 967–970.

Ranaivoarisoa, T. O., Singh, R., Rengasamy, K., Guzman, M. S., and Bose, A. (2019). Towards Sustainable Bioplastic Production Using the Photoautotrophic Bacterium *Rhodopseudomonas palustris* TIE-1. *J. Ind. Microbiol. Biotechnol.* 46 (9), 1401–1417. doi:10.1007/s10295-019-02165-7

Ray, D. E., and Fry, J. R. (2006). A Reassessment of the Neurotoxicity of Pyrethroid Insecticides. *Pharmacol. Ther.* 111 (1), 174–193. doi:10.1016/j.pharmthera.2005.10.003

Read, B. A., and Tabita, F. R. (1994). High Substrate Specificity Factor Ribulose Bisphosphate Carboxylase/oxygenase from Eukaryotic Marine Algae and Properties of Recombinant Cyanobacterial Rubisco Containing "algal" Residue Modifications. *Arch. Biochem. Biophys.* 312 (1), 210–218. doi:10.1006/abbi.1994.1301

Rengasamy, K., Ranaivoarisoa, T., Singh, R., and Bose, A. (2018). An Insoluble Iron Complex Coated Cathode Enhances Direct Electron Uptake by *Rhodopseudomonas palustris* TIE-1. *Bioelectrochemistry* 122, 164–173. doi:10.1016/j.bioelechem.2018.03.015

Rey, F. E., Heiniger, E. K., and Harwood, C. S. (2007). Redirection of Metabolism for Biological Hydrogen Production. *Appl. Environ. Microbiol.* 73 (5), 1665–1671. doi:10.1128/aem.02565-06

Romagnoli, S., and Tabita, F. R. (2007). Phosphotransfer Reactions of the CbbRRS Three-Protein Two- Component System from Rhodopseudomonas Palustris CGA010 Appear to Be Controlled by an Internal Molecular Switch on the Sensor Kinase. *J. Bacteriol.* 189 (2), 325–335. doi:10.1128/jb.01326-06

Ryu, M.-H., Hull, N. C., and Gomelsky, M. (2014). Metabolic Engineering of *Rhodobacter sphaeroides* for Improved Hydrogen Production. *Int. J. Hydrogen Energy* 39 (12), 6384–6390. doi:10.1016/j.ijhydene.2014.02.021

Sabourin-Provost, G., and Hallenbeck, P. C. (2009). High Yield Conversion of a Crude Glycerol Fraction from Biodiesel Production to Hydrogen by Photofermentation. *Bioresour. Technol.* 100 (14), 3513–3517. doi:10.1016/j.biortech.2009.03.027

Sakpirom, J., Kantachote, D., Nunkaew, T., and Khan, E. (2017). Characterizations of Purple Non-Sulfur Bacteria Isolated from Paddy Fields, and Identification of Strains with Potential for Plant Growth-Promotion, Greenhouse Gas Mitigation and Heavy Metal Bioremediation. *Res. Microbiol.* 168 (3), 266–275. doi:10.1016/j.resmic.2016.12.001

Sakpirom, J., Kantachote, D., Siripattanakul-Ratpukdi, S., McEvoy, J., and Khan, E. (2019). Simultaneous Bioprecipitation of Cadmium to Cadmium Sulfide Nanoparticles and Nitrogen Fixation by *Rhodopseudomonas palustris* TN110. *Chemosphere* 223, 455–464. doi:10.1016/j.chemosphere.2019.02.051

Sangani, A. A., McCully, A. L., LaSarre, B., and McKinlay, J. B. (2019). Fermentative *Escherichia coli* Makes a Substantial Contribution to H2 Production in Coculture with Phototrophic *Rhodopseudomonas palustris*. *FEMS Microbiol. Lett.* 366 (14), fnz162. doi:10.1093/femsle/fnz162

Scott, H. N., Laible, P. D., and Hanson, D. K. (2003). Sequences of Versatile Broad-Host-Range Vectors of the RK2 Family. *Plasmid* 50 (1), 74–79. doi:10.1016/S0147-619X(03)00030-1

Sharma, N., Doerner, K. C., Alok, P. C., and Choudhary, M. (2015). Skatole Remediation Potential of *Rhodopseudomonas palustris* WKU-KDNS3 Isolated from an Animal Waste Lagoon. *Lett. Appl. Microbiol.* 60 (3), 298–306. doi:10.1111/lam.12379

Slate, A. J., Whitehead, K. A., Brownson, D. A. C., and Banks, C. E. (2019). Microbial Fuel Cells: An Overview of Current Technology. *Renew. Sustain. Energy Rev.* 101, 60–81. doi:10.1016/j.rser.2018.09.044

Su, H., Cheng, J., Zhou, J., Song, W., and Cen, K. (2009a). Combination of Dark- and Photo-Fermentation to Enhance Hydrogen Production and Energy Conversion Efficiency. *Int. J. Hydrogen Energy* 34 (21), 8846–8853. doi:10.1016/j.ijhydene.2009.09.001

Su, H., Cheng, J., Zhou, J., Song, W., and Cen, K. (2009b). Improving Hydrogen Production from Cassava Starch by Combination of Dark and Photo Fermentation. *Int. J. Hydrogen Energy* 34 (4), 1780–1786. doi:10.1016/j.ijhydene.2008.12.045

Su, P., Feng, T., Zhou, X., Zhang, S., Zhang, Y., Cheng, J. e., et al. (2015). Isolation of Rhp-PSP, a Member of YER057c/YjgF/UK114 Protein Family with Antiviral Properties, from the Photosynthetic Bacterium *Rhodopseudomonas palustris* Strain JSC-3b. *Sci. Rep.* 5, 16121. doi:10.1038/srep16121

Su, P., Tan, X., Li, C., Zhang, D., Cheng, J. e., Zhang, S., et al. (2017). Photosynthetic Bacterium *Rhodopseudomonas palustris* GJ-22 Induces Systemic Resistance Against Viruses. *Microb. Biotechnol.* 10 (3), 612–624. doi:10.1111/1751-7915.12704

Swingley, W. D., Blankenship, R. E., and Raymond, J. (2009). "Evolutionary Relationships Among Purple Photosynthetic Bacteria and the Origin of Proteobacterial Photosynthetic Systems," in *The Purple Phototrophic Bacteria*. Editors C. N. Hunter, F. Daldal, M. C. Thurnauer, and J. T. Beatty (Dordrecht: Springer Netherlands), 17–29. doi:10.1007/978-1-4020-8815-5_2

Tabita, F. R. (1999). Microbial Ribulose 1,5-bisphosphate Carboxylase/Oxygenase: A Different Perspective. *Photosyn. Res.* 60 (1), 1–28. doi:10.1023/A:1006211417981

Tabita, F. R., Satagopan, S., Hanson, T. E., Kreel, N. E., and Scott, S. S. (2008). Distinct Form I, II, III, and IV Rubisco Proteins from the Three Kingdoms of Life Provide Clues about Rubisco Evolution and Structure/function Relationships. *J. Exp. Bot.* 59 (7), 1515–1524. doi:10.1093/jxb/erm361

Takaichi, S. (2004). "Carotenoids and Carotenogenesis in Anoxygenic Photosynthetic Bacteria," in *The Photochemistry of Carotenoids*. Editors H. A. Frank, A. J. Young, G. Britton, and R. J. Cogdell (Dordrecht: Springer), 39–69.

Tian, X., Liao, Q., Zhu, X., Wang, Y., Zhang, P., Li, J., et al. (2010). Characteristics of a Biofilm Photobioreactor as Applied to Photo-Hydrogen Production. *Bioresour. Technol.* 101 (3), 977–983. doi:10.1016/j.biortech.2009.09.007

Troost, K., Loeschcke, A., Hilgers, F., Özgür, A. Y., Weber, T. M., Santiago-Schübel, B., et al. (2019). Engineered *Rhodobacter capsulatus* as a Phototrophic Platform Organism for the Synthesis of Plant Sesquiterpenoids. *Front. Microbiol.* 10, 1998. doi:10.3389/fmicb.2019.01998

Venkidusamy, K., and Megharaj, M. (2016). A Novel Electrophototrophic Bacterium *Rhodopseudomonas palustris* Strain RP2, Exhibits Hydrocarbonoclastic Potential in Anaerobic Environments. *Front. Microbiol.* 7, 1071. doi:10.3389/fmicb.2016.01071

Vincenzini, M., Marchini, A., Ena, A., and De Philippis, R. (1997). H and Poly-β-Hydroxybutyrate, Two Alternative Chemicals from Purple Non Sulfur Bacteria. *Biotechnol. Lett.* 19 (8), 759–762. doi:10.1023/A:1018336209252

Vitousek, P. M., Aber, J. D., Howarth, R. W., Likens, G. E., Matson, P. A., Schindler, D. W., et al. (1997). Human Alteration of the Global Nitrogen Cycle: Sources and Consequences. *Ecol. Appl.* 7 (3), 737–750. doi:10.1890/1051-0761(1997)007[0737:haotgn]2.0.co;2

Wang, B., Jiang, Z., Yu, J. C., Wang, J., and Wong, P. K. (2019). Enhanced CO2 Reduction and Valuable C2+ Chemical Production by a CdS-Photosynthetic Hybrid System. *Nanoscale* 11 (19), 9296–9301. doi:10.1039/c9nr02896j

Welander, P. V., Hunter, R. C., Zhang, L., Sessions, A. L., Summons, R. E., and Newman, D. K. (2009). Hopanoids Play a Role in Membrane Integrity and pH Homeostasis in *Rhodopseudomonas palustris* TIE-1. *J. Bacteriol.* 191 (19), 6145–6156. doi:10.1128/jb.00460-09

Woude, B. J., Boer, M., Put, N. M. J., Geld, F. M., Prins, R. A., and Gottschal, J. C. (1994). Anaerobic Degradation of Halogenated Benzoic Acids by Photoheterotrophic Bacteria. *FEMS Microbiol. Lett.* 119 (1-2), 199–207. doi:10.1111/j.1574-6968.1994.tb06889.x

Wu, P., Chen, Z., Zhang, Y., Wang, Y., Zhu, F., Cao, B., et al. (2019). *Rhodopseudomonas palustris* Wastewater Treatment: Cyhalofop-Butyl Removal, Biochemicals Production and Mathematical Model Establishment. *Bioresour. Technol.* 282, 390–397. doi:10.1016/j.biortech.2018.11.087

Wu, S. C., Liou, S. Z., and Lee, C. M. (2012). Correlation between Bio-Hydrogen Production and Polyhydroxybutyrate (PHB) Synthesis by *Rhodopseudomonas palustris* WP3-5. *Bioresour. Technol.* 113, 44–50. doi:10.1016/j.biortech.2012.01.090

Xia, S., Zhang, L., Davletshin, A., Li, Z., You, J., and Tan, S. (2020). Application of Polysaccharide Biopolymer in Petroleum Recovery. *Polymers* 12 (9), 1860. doi:10.3390/polym12091860

Xiao, L., Zhao, Z., Ma, Z., Chen, J., and Song, Z. (2019). Immobilization of Rhodopseudomonas Palustris P1 on Glass Pumice to Improve the Removal of NH_4^+ -N and NO_2^- -N from Aquaculture Pond Water. *Biotechnol. Appl. Biochem.* 67 (3), 323–329. doi:10.1002/bab.1863

Xing, D., Zuo, Y., Cheng, S., Regan, J. M., and Logan, B. E. (2008). Electricity Generation by *Rhodopseudomonas palustris* DX-1. *Environ. Sci. Technol.* 42 (11), 4146–4151. doi:10.1021/es800312v

Xu, Q. Q., Yan, H., Liu, X. L., Lv, L., Yin, C. H., and Wang, P. (2014). Growth Performance and Meat Quality of Broiler Chickens Supplemented with *Rhodopseudomonas palustris* in Drinking Water. *Br. Poult. Sci.* 55 (3), 360–366. doi:10.1080/00071668.2014.903326

Xu, W., Chai, C., Shao, L., Yao, J., and Wang, Y. (2016). Metabolic Engineering of *Rhodopseudomonas palustris* for Squalene Production. *J. Ind. Microbiol. Biotechnol.* 43 (5), 719–725. doi:10.1007/s10295-016-1745-7

Yang, C.-F., and Lee, C.-M. (2011). Enhancement of Photohydrogen Production Using phbC Deficient Mutant *Rhodopseudomonas palustris* Strain M23. *Bioresour. Technol.* 102 (9), 5418–5424. doi:10.1016/j.biortech.2010.09.078

Yang, Z.-Y., Moure, V. R., Dean, D. R., and Seefeldt, L. C. (2012). Carbon Dioxide Reduction to Methane and Coupling with Acetylene to Form Propylene Catalyzed by Remodeled Nitrogenase. *Proc. Natl. Acad. Sci. U.S.A.* 109, 19644–19648. doi:10.1073/pnas.1213159109

Zhan, P. R., and Liu, W. (2013). Immobilization and Ammonia Removal of Photosynthetic Bacteria. *Adv. Mat. Res.* 610–613, 311–314. doi:10.4028/www.scientific.net/AMR.610-613.311

Zhang, P., Sun, F., Cheng, X., Li, X., Mu, H., Wang, S., et al. (2019). Preparation and Biological Activities of an Extracellular Polysaccharide from *Rhodopseudomonas palustris*. *Int. J. Biol. Macromol.* 131, 933–940. doi:10.1016/j.ijbiomac.2019.03.139

Zhang, S., Luo, X., Cheng, J. e., Peng, J., Zhang, D., and Liu, Y. (2014). Genome Sequence of Pyrethroid-Degrading Bacterium *Rhodopseudomonas palustris* Strain JSC-3b. *Genome Announc.* 2 (1), e01228–13. doi:10.1128/genomeA.01228-13

Zhao, C., Zhang, Y., Chan, Z., Chen, S., and Yang, S. (2015). Insights into Arsenic Multi-Operons Expression and Resistance Mechanisms in *Rhodopseudomonas palustris* CGA009. *Front. Microbiol.* 6, 986. doi:10.3389/fmicb.2015.00986

Zhao, J., Wei, Q., Wang, S., and Ren, X. (2021). Progress of Ship Exhaust Gas Control Technology. *Sci. Total Environ.* 799, 149437. doi:10.1016/j.scitotenv.2021.149437

Zhao, L., Zhao, C., Han, D., Yang, S., Chen, S., and Yu, C.-P. (2011). Anaerobic Utilization of Phenanthrene by *Rhodopseudomonas palustris*. *Biotechnol. Lett.* 33 (11), 2135–2140. doi:10.1007/s10529-011-0681-x

Zheng, Y., Harris, D. F., Yu, Z., Fu, Y., Poudel, S., Ledbetter, R. N., et al. (2018). A Pathway for Biological Methane Production Using Bacterial Iron-Only Nitrogenase. *Nat. Microbiol.* 3 (3), 281–286. doi:10.1038/s41564-017-0091-5

Zheng, Y., and Harwood, C. S. (2019). Influence of Energy and Electron Availability on *In Vivo* Methane and Hydrogen Production by a Variant Molybdenum Nitrogenase. *Appl. Environ. Microbiol.* 85 (9), e02671–02618. doi:10.1128/AEM.02671-18

Zhou, X., Tian, Z., Wang, Y., and Li, W. (2010). Effect of Treatment with Probiotics as Water Additives on Tilapia (*Oreochromis niloticus*) Growth Performance and Immune Response. *Fish. Physiol. Biochem.* 36 (3), 501–509. doi:10.1007/s10695-009-9320-z

Conflict of Interest: The authors declare that the research was conducted in the absence of any commercial or financial relationships that could be construed as a potential conflict of interest.

Publisher's Note: All claims expressed in this article are solely those of the authors and do not necessarily represent those of their affiliated organizations, or those of the publisher, the editors and the reviewers. Any product that may be evaluated in this article, or claim that may be made by its manufacturer, is not guaranteed or endorsed by the publisher.

frontiers | Frontiers in Bioengineering and Biotechnology

BRIEF RESEARCH REPORT
published: 23 June 2022
doi: 10.3389/fbioe.2022.919969

Class I Polyhydroxyalkanoate (PHA) Synthase Increased Polylactic Acid Production in Engineered Escherichia Coli

Mengxun Shi[1,2], *Mengdi Li*[1], *Anran Yang*[1], *Xue Miao*[1], *Liu Yang*[1], *Jagroop Pandhal*[2] *and Huibin Zou*[1,3]*

[1]State Key Laboratory Base of Eco-Chemical Engineering, College of Chemical Engineering, Qingdao University of Science and Technology, Qingdao, China, [2]Department of Chemical and Biological Engineering, The University of Sheffield, Sheffield, United Kingdom, [3]CAS Key Laboratory of Bio-based Materials, Qingdao Institute of Bioenergy and Bioprocess Technology, Chinese Academy of Sciences, Qingdao, China

Polylactic acid (PLA), a homopolymer of lactic acid (LA), is a bio-derived, biocompatible, and biodegradable polyester. The evolved class II PHA synthase ($PhaC1_{Ps6\text{-}19}$) was commonly utilized in the *de novo* biosynthesis of PLA from biomass. This study tested alternative class I PHA synthase ($PhaC_{Cs}$) from *Chromobacterium* sp. USM2 in engineered *Escherichia coli* for the *de novo* biosynthesis of PLA from glucose. The results indicated that $PhaC_{Cs}$ had better performance in PLA production than that of class II synthase $PhaC1_{Ps6\text{-}19}$. In addition, the *sulA* gene was engineered in PLA-producing strains for morphological engineering. The morphologically engineered strains present increased PLA production. This study also tested fused propionyl-CoA transferase and lactate dehydrogenase A (fused Pct_{Cp}/LdhA) in engineered *E. coli* and found that fused Pct_{Cp}/LdhA did not apparently improve the PLA production. After systematic engineering, the highest PLA production was achieved by *E. coli* MS6 (with $PhaC_{Cs}$ and *sulA*), which could produce up to 955.0 mg/L of PLA in fed-batch fermentation with the cell dry weights of 2.23%, and the average molecular weight of produced PLA could reach 21,000 Da.

Keywords: class I polyhydroxyalkanoate synthase, engineered *E. coli*, polylactic acid, biopolyester, degradable polymer

OPEN ACCESS

Edited by:
Xinglin Jiang,
Technical University of Denmark, Denmark

Reviewed by:
Liangzhi Li,
Suzhou University of Science and Technology, China
Tingting Huang,
Shanghai Jiao Tong University, China

***Correspondence:**
Huibin Zou
zouhb@qibebt.ac.cn
huibinzou@hotmail.com

Specialty section:
This article was submitted to Industrial Biotechnology, a section of the journal Frontiers in Bioengineering and Biotechnology

Received: *14 April 2022*
Accepted: *09 May 2022*
Published: *23 June 2022*

Citation:
Shi M, Li M, Yang A, Miao X, Yang L, Pandhal J and Zou H (2022) Class I Polyhydroxyalkanoate (PHA) Synthase Increased Polylactic Acid Production in Engineered Escherichia Coli. Front. Bioeng. Biotechnol. 10:919969. doi: 10.3389/fbioe.2022.919969

INTRODUCTION

Biopolyesters have been developed in recent years as alternatives to petroleum-based synthetic polyesters (Nduko and Taguchi, 2021). As a commercialized biopolyester, polylactic acid (PLA) can be prepared from renewable biomass with promising physical performance, biocompatibility, and biodegradability (Taguchi et al., 2008; Yang et al., 2010; Paço et al., 2019). The industrial preparation of PLA is accomplished through several steps: first, the monomer of lactic acid (LA) is prepared from biomass through fermentation; then LA is converted to lactide followed by the ring-opening polymerization of lactide to PLA (Maharana et al., 2009).

With the fast development of biotechnology, PLA homopolymer and LA-containing copolymers can be *de novo* biosynthesized from renewable biomass by engineered strains (Taguchi et al., 2008; Yang et al., 2010; Choi et al., 2016; Zou et al., 2021). However, compared with the efficient bioproduction of LA-containing copolymers, the microbial production of PLA homopolymers is still

TABLE 1 | Strains and plasmids used in this study.

Names	Description	Reference/ Source
Strains		
E. coli χ7213	Donor strain for gene deletion	Laboratory-stored
E. coli MS1	Δ*ackA* from *E. coli* BL21	This study
E. coli MS2	Express *ldhA* gene in *E. coli* MS1	This study
E. coli MS3	Express the evolved Pct_{Cp} gene and the evolved $PhaC1_{Ps6\text{-}19}$ gene in *E. coli* MS2	This study
E. coli MS4	Express *sulA* gene in *E. coli* MS3	This study
E. coli MS5	Express the evolved Pct_{Cp} gene and the evolved $PhaC1_{Cs}$ gene in *E. coli* MS2	This study
E. coli MS6	Express *sulA* gene in *E. coli* MS5	This study
E. coli MS7	Express the gene of fused enzyme of Pct_{Cp}/LdhA, the evolved $PhaC1_{Ps6\text{-}19}$ gene, and *sulA* gene in *E. coli* MS1	This study
Plasmids		
pTrcHis2B	Ap^R	Laboratory-stored
pACYCDuet-1	Cm^R	Laboratory-stored
pET30a	Kan^R	Laboratory-stored
pRE112-ΔackA	Cm^R	This study
ldhA-pTrcHis2B	*ldhA* from *E. coli* inserted into the pTrcHis2B vector under trc promoter	This study
ldhA-sulA-pTrcHis2B	*ldhA* from *E. coli* BL21 and *sulA* from *E. coli* str. K-12 inserted into the pTrcHis2B vector under trc promoter	This study
Pct_{Cp}-pACYCDuet-1	Evolved Pct_{Cp} (V193A) inserted into the pACYCDuet-1 vector under T7 promoters	This study
Pct_{Cp}-$PhaC_{Ps6\text{-}19}$-pACYCDuet-1	Evolved Pct_{Cp} (V193A) and evolved $PhaC1_{Ps6\text{-}19}$ (E130D, S325T, S477G, and Q481K) inserted into the pACYCDuet-1 vector under T7 promoters	This study
Fused-Pct/ldhA-pET30a	LdhA and Pct fusion enzyme under flexible linker $(GGGGS)_3$	This study
Pct_{cp}-$PhaC_{Cs}$-pACYCDuet-1	Evolved Pct_{Cp} (V193A) and $PhaC1_{Cs}$ inserted into the pACYCDuet-1 vector under T7 promoters	This study

Ap^R, ampicillin resistance; Cm^R,chloramphemicol resistance; Kan^R, kanamycin resistance.

challenging with low productivity. One of the barriers in the biosynthesis of the PLA homopolymer is that the PHA synthases involved exhibit higher activities toward other substrates than LA monomer (Park et al., 2012).

Based on the primary structure, subunit compositions, and substrate specificity, four classes of PHA synthases have been found in nature (Yang et al., 2010; Zou et al., 2017; Chek et al., 2019). Class I, III, and IV PHA synthases prefer short-chain length (SCL) monomers, whereas class II PHA synthases exhibit higher activities toward medium-chain length (MCL) monomers (Rehm, 2003; Tsuge et al., 2015; Zou et al., 2017). Class II synthase from *Pseudomonas* sp. was engineered (E130D, S325T, S477G, and Q481K) to gain the ability to synthesize PLA and LA-containing copolymers. Although the engineered strains (with engineered class II synthase) can efficiently produce LA-containing copolymers (Jung et al., 2010; Yang et al., 2010; Choi et al., 2016; Li et al., 2016), PLA homopolymer productivity was as low as 0.5 wt% of dry cell weight (Yang et al., 2010; Park et al., 2012). The low productivity of the PLA homopolymer was presumably due to the low substrate specificity of PHA synthase (Park et al., 2012), low mobility of the generated PLA, and low concentration of LA-CoA in the engineered strains (Matsumoto et al., 2018). Robust PHA synthases with higher substrate specificity toward LA monomer need to be discovered or engineered for the enhancement of the biosynthesis of PLA homopolymers (Taguchi and Matsumoto, 2021).

Morphological engineering is another trend in the biosynthesis of biopolymers, which aims at larger cell space for the storage of the produced biopolymers *in vivo*. FtsZ, a bacterial tubulin homolog, is one of the targets in the morphological engineering of bacteria strains (Erickson et al., 2010; Chen et al., 2012; Wang et al., 2014). The inhibition of FtsZ can affect the formation of the Z ring during bacteria division and hence enlarge cell space (Dajkovic et al., 2008; Adams and Errington, 2009; Chen et al., 2012). Higher expression of SulA can inhibit FtsZ and reduce the cell division rate (Dajkovic et al., 2008; Chen et al., 2012). For example, morphologically engineered *E. coli* JM109 exhibits the increased production of poly (3-hydroxybutyrate) (PHB) (from 8 to 9 g/L) and poly (3HB-co-4HB) (from 8.2 to 9.2 g/L) (Wang et al., 2014; Wu et al., 2016).

In this study, to screen robust PHA synthase in PLA biosynthesis, we selected the class I PHA synthase from *Chromobacterium* sp. USM2, which has been used in the polymerization of 3-hydroxypropionic acid (3HP, an isomer of LA) (Linares-Pastén et al., 2015), and evaluated its performance in PLA homopolymer production by engineered *E. coli*. In addition, we additionally expressed the *sulA* gene and evaluated the PLA production of morphologically engineered strains.

MATERIALS AND METHODS

Strains and Engineering Methods

All the information on strains and plasmids is listed in **Table 1**. The information of key plasmids is provided in **Supplemental Figure S1**. The primers are summarized in **Supplemental Table S1**. Engineered strains were constructed using the following methods.

The suicide plasmid–mediated genome editing method (Gao et al., 2014) was utilized in the deletion of the *ackA* gene from the genome of *E. coli* BL21 (DE3). The homolog arms (600 bp upstream and downstream of the *ackA* gene) were cloned into

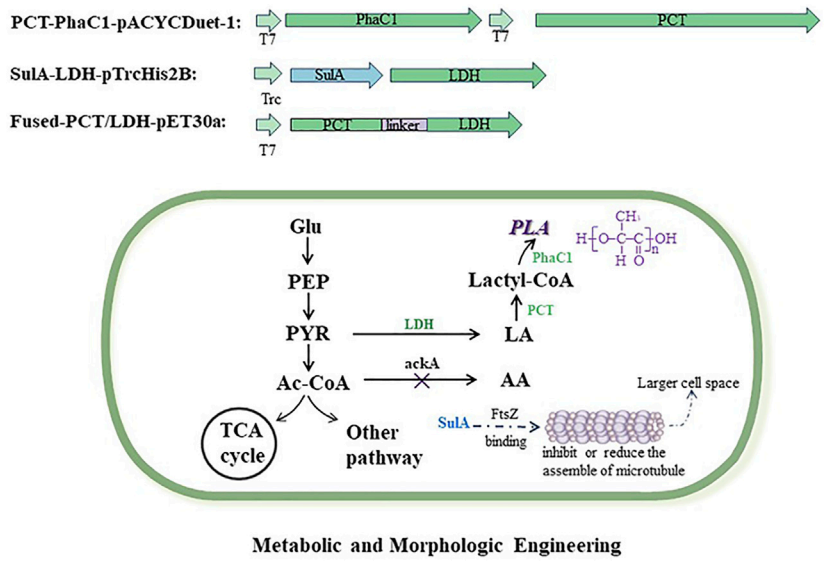

FIGURE 1 | Metabolic and morphologic engineering of *E. coli* strains for polylactic acid production. Exogenous vectors expressed the genes of key enzymes which are involved in the biosynthesis pathway of polylactic acid. The gene of *ackA* was deleted in the engineered strains to reduce the competitive by-product of acetic acid. The gene of *sulA* was expressed in engineered stains for larger cell space. Full names of abbreviations are as follows: PLA, polylactic acid; PhaC, PHA synthase; PCT, propionyl-CoA transferase; LDH, lactate dehydrogenase; Glu, glucose; PEP, phosphoenolpyruvate; PYR, pyruvate; Ac-CoA, acetyl co-enzyme A; AA, acetic acid; LA, lactic acid.

the suicide plasmid of pRE112. The constructed pRE112-△*ackA* was transformed into *E. coli* χ7213 to construct the donor strain of *E. coli* χ7213/pRE112-△*ackA*. Then, the conjugation occurred between the donor strain and the receptor strain of *E. coli* BL21 (DE3) for the deletion of the *ackA* gene. The strain of *E. coli* MS1 (**Table 1**) was constructed after knocking off *ackA*.

Based on the chassis strain of *E. coli* MS1, other engineered strains (MS2–MS7) were constructed using the following methods. As shown in **Figure 1**, the biosynthetic pathway of PLA was engineered in PLA-producing strains; in addition, the *sulA* gene was expressed in strains for larger cell space.

From *E. coli* MS1, *E. coli* MS2 additionally expressed the *ldhA* gene from *E. coli* BL21 (lactate dehydrogenase, NCBI No. NC_012892.2). From *E. coli* MS2, *E. coli* MS3 additionally expressed the evolved Pct_{Cp} gene (propionyl-CoA transferase, NCBI No. CAB77207.1, with mutation of V193A) from *Clostridium propionicum* DSM 1682 and the evolved $PhaC1_{Ps6\text{-}19}$ gene (class II PHA synthase, NCBI No. ACM68707.1, with mutations of E130D, S325T, S477G, and Q481K) from *Pseudomonas* sp. MBEL 6-19. From *E. coli* MS3, *E. coli* MS4 additionally expressed the *sulA* gene from *E. coli* str. K-12 substr. MG1655 (NCBI No. NC_000913.3).

From *E. coli* MS2, *E. coli* MS5 additionally expressed the evolved Pct_{Cp} gene from *C. propionicum* and the $PhaC_{Cs}$ gene (class I PHA synthase, NCBI No. ADL70203.1) from *Chromobacterium* sp. USM2. From *E. coli* MS5, *E. coli* MS6 additionally expressed the *sulA* gene from *E. coli* str. K-12.

From *E. coli* MS1, *E. coli* MS7 additionally expressed the gene of the fused enzyme of Pct_{Cp}/LdhA (**Supplemental Figure S2**). A flexible linker $(Gly–Gly–Gly–Gly–Ser)_3$ was inserted between Pct_{Cp} and LdhA; in addition, *E. coli* MS7 expressed the evolved $PhaC1_{Ps6\text{-}19}$ gene from *C. propionicum* and the *sulA* gene from *E. coli* str. K-12.

Flask and Fed-Batch Fermentation

All strains utilized in this study are cultivated in the Luria–Bertani (LB) medium (flask-level) or M9 medium (fermenter-level). The LB medium contains (per liter) 10 g tryptone, 5 g yeast extract, and 10 g NaCl. The M9 medium consists of (per liter) 1 g $(NH_4)_2SO_4$, 3 g $K_2HPO_4.3H_2O$, 1.9 g KCl, 5 g yeast extract, 1 g sodium citrate, 1 g citric acid, 1 g glycine betaine, 0.24 g $MgSO_4$, and 1 ml of the stored solution of trace element. The stored solution of trace element consists of (per liter) 3.7 g $(NH_4)_6Mo_7O_{24}{\cdot}4H_2O$, 2.9 g $ZnSO_4$ $7H_2O$, 24.7 g H_3BO_3, 2.5 g $CuSO_4$ $5H_2O$, and 15.8 g $MnCl_2$ $4H_2O$. Variable antibiotics were supplemented in the cultivation medium for different strains (**Table 1**). The concentration of antibiotics in the medium is as follows: ampicillin 48 mg/L, chloramphenicol 24 mg/L, and kanamycin 45 mg/L. The sucrose-containing (10% w/w) LB medium was utilized to screen the strain of *E. coli* MS1.

For fermentation of PLA, individual strains were cultivated in 10 ml LB medium at 37°C overnight in a rotary shaker at 220 rpm. Then, 5% (V/V) seed cultures were added into 100 ml LB medium (in a flask) and cultivated at 37°C overnight in a rotary shaker at 220 rpm. The secondary seed cultures were inoculated into a 5-L fermenter (Bailun Inc., China) containing 2 L M9 medium, and 20 g/L glucose was added as a starting carbon source. Fed-batch fermentation starts at 37°C. During the fermentation process, ammonium hydroxide solution (6M) was automatically added to maintain the pH at 7. The dissolved oxygen concentration (DOC) was maintained at 10–20% by changing the agitation speed and ventilatory capacity (VC). Ten hours after inoculation, 0.5 mM of

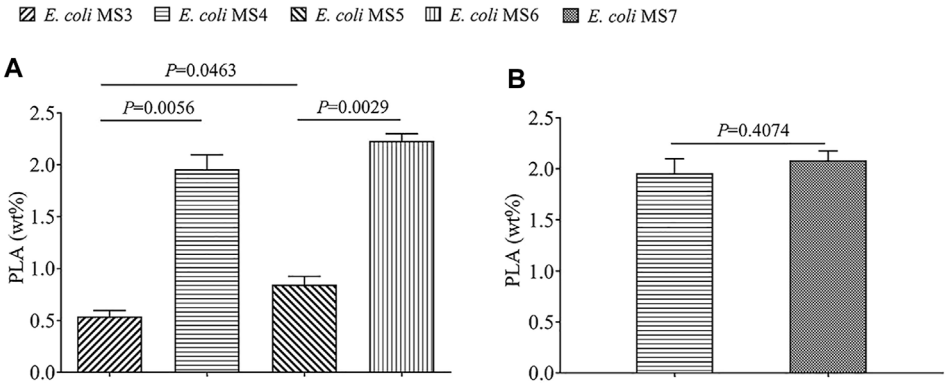

FIGURE 2 | Comparison of the PLA production by five different engineered strains. The PLA production was recorded by wt% (weight of PLA/dry cell weight). The data shown are expressed as means of three repeated experiments, and the error bars present their standard deviation. Statistical difference (*p* value) between different groups is also present. **(A)** Strains which express the gene of $PhaC1_{Cs}$ (class I PHA synthase) and *sulA* (for morphological engineering) have higher PLA production. **(B)** Strain which expresses the fused enzyme of Pct_{Cp}/LdhA has similar PLA production with the control strain.

TABLE 2 | Gel permeation chromatography (GPC) of PLA synthesized by strains with different PHA synthases.

PHA synthase	M_n[a] (Da)	M_w[b] (Da)	M_w/M_n[c]
$PhaC1_{Ps6\text{-}19}$	10,642	23,436	2.202
$PhaC_{Cs}$	16,515	21,088	1.277

[a]M_n: *number-average molecular weight.*
[b]M_w: *weight-average molecular weight.*
[c]M_w/M_n: *molecular weight dispersion index, denotes the molecular weight distribution width of the polymer.*

isopropyl-*β*-D-thiogalactopyranoside (IPTG) was added in the fermenter, and then the cultivation temperature was decreased to 30°C. Then, 100 ml of 50% glucose (w/v) was supplemented every 12 h. The cell growth value of OD_{600} was monitored using the spectrophotometer at 600 nm. The duration time of fermentation was 72 h.

Analytical Methods

The solvent extraction method (Jung et al., 2010) was utilized for the purification of PLA products from the cells. After fermentation, the cells were harvested by centrifugation at 4000 rpm for 20 min. The harvested cells were washed twice with absolute ethanol and distilled water before lyophilization. Then, the cells were lyophilized for 24 h and the cell dry weights (CDW) of different samples were measured and recorded. PLA was extracted from dried cells by chloroform in the Soxhlet apparatus at 80°C for 16 h. Excessive chloroform was removed using a rotary evaporator, and cell debris was removed by passing through a PTFE filter. PLA was precipitated by adding five-fold ice-cold methanol. Weights of purified and dried PLA was measured and recorded.

To qualitatively determine the polymer structure, the samples were analyzed by ^{1}H and ^{13}C nuclear magnetic resonance (NMR) spectra using a Bruker AM-500 MHz spectrometer at 500 and 125 MHz, respectively. The sample was solved in $CDCl_3$ with tetramethylsilane (TMS) as an internal chemical shift standard. The number-average molecular weight (M_n) and the weight-average molecular weight (M_w) of PLA were determined by gel permeation chromatography (GPC) equipped with TSKgel SuperMutipore HZ-M*2 column and GPC data processing software. The PLA sample (1 mg/ml) was eluted using tetrahydrofuran (THF) before injection (20 μl), and GPC was operated at a flow rate of 0.35 ml/min at 40°C. Polystyrene with a narrow range of polydispersity (1.03-1.05) was used for calibration.

The morphological form of engineered *E. coli* was characterized using a scanning electron microscope (SEM) on a Hitachi S-4800 instrument. The cells were harvested by centrifugation at 5000 rpm for 5 min and subsequently washed with phosphate-buffered saline (PBS) (pH 7.4) three times. Then, the washed cells were fixed with 2.5% (V/V) glutaraldehyde overnight at 4°C. The fixed cells were washed again with phosphate-buffered saline (PBS) (pH 7.4) three times (30 min each). Afterward, ethanol gradients of 30%, 50%, 70%, 80%, 90%, and 95% (V/V) solutions were used to dehydrate the fixed cells in a sequential way. The cell samples were further dehydrated with 100% ethanol three times. After that, tertiary butyl alcohol was mixed with ethanol in a ratio of 1:1 and pure tertiary butyl alcohol was used to achieve metathesis of ethanol in the cells (Wang et al., 2014). At last, the cells were mixed in with tertiary butyl alcohol and lyophilized for imaging.

The PLA granules in *E. coli* cells were characterized using a transmission electron microscope (TEM) on a Hitachi H-7650 instrument. The cells were harvested by centrifugation at 5000 rpm for 5 min and subsequently washed with phosphate-buffered saline (PBS) (pH 7.4) three times. Then, the washed cells were fixed with 2.5% (V/V) glutaraldehyde overnight at 4°C. The fixed cells were washed again with phosphate-buffered saline (PBS) (pH 7.4) three times (30 min each), and then 1% (V/V) osmic acid was added to fix the cell for 1 h. The fixed cells were washed again with PBS (pH 7.4) three times (30 min each). Afterward, acetone gradient solutions of 30%, 50%, 70%, 80%, 90%, and 95% (V/V) were used to dehydrate the fixed cells in a

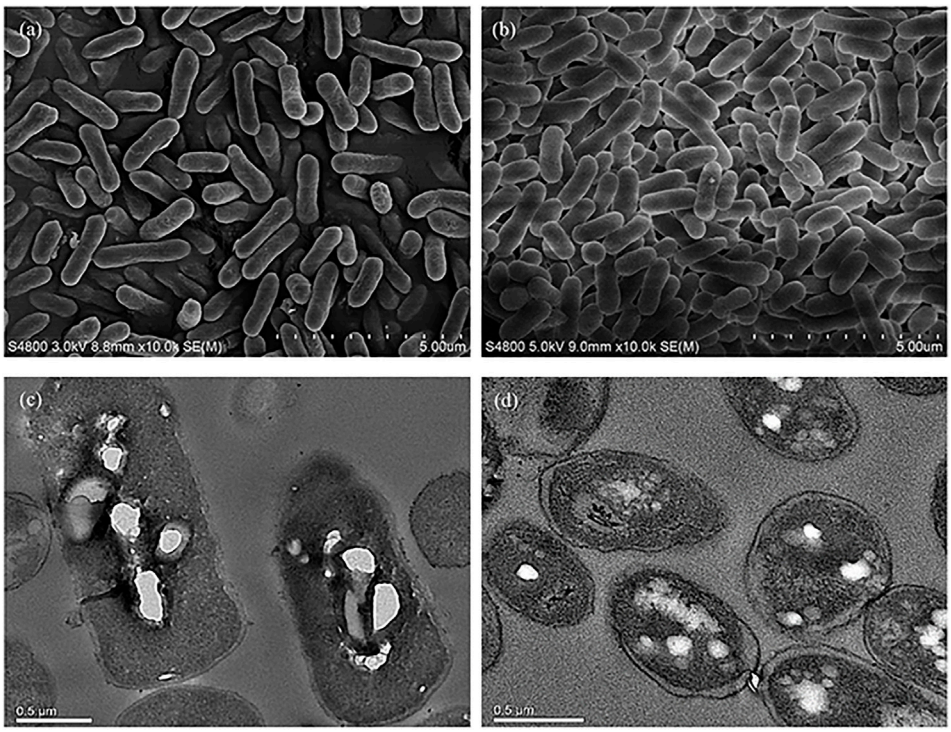

FIGURE 3 | Morphological comparison of strains with or without morphological engineering using SEM and TEM assays. **(A)** SEM assay of cells from the morphologically engineered strain (with the expression of *sulA*). **(B)** SEM assay of cells from the control strain without expressing *sulA*. **(C)** TEM assay of cells from the morphologically engineered strain (with the expression of *sulA*). **(D)** TEM assay of cells from the control strain without expressing *sulA*.

sequential way. The resulting cell samples were further dehydrated with 100% acetone three times. Finally, the cell samples are embedded with Spurr resin for imaging.

Statistical Methods

The significance of differences between the mean values of testing samples was compared using Student's t-test. Differences were considered statistically obvious if $p < 0.05$ and significant if $p < 0.01$.

RESULTS AND DISCUSSION

Biosynthesis of PLA *via* Class I PHA Synthase (From *Chromobacterium* sp. USM2)

The qualitative ^{1}H and ^{13}C assay of polymer product (**Supplemental Figure S3**) confirmed that PLA homopolymer was *de novo*–biosynthesized from glucose by the engineered strains of *E. coli*, and the ^{1}H assay also indicated the presence of oligomeric PLA or LA monomer indicated the hydrolysis of PLA during analysis processing. The quantitative comparison of PLA production by different strains (**Figure 2**) showed that *E. coli* MS5 (with *PhaCcs*) could produce up to 323.4 mg/L of PLA (0.85% of CDW), obviously higher ($p < 0.05$) than the PLA production (189.5 mg/L, 0.54% of CDW) by the control strain of *E. coli* MS3 (with evolved $PhaC1_{Ps6\text{-}19}$). The results indicated that class I PHA synthase (from *Chromobacterium* sp. USM2) exhibited better performance in the biosynthesis of the PLA homopolymer. This study further compared the M_w of the produced PLA with the strains of MS5 and MS3 (**Table 2**). Although the PLA products with two strains present a similar average M_w (around 21,000 Da), the lower M_w/M_n value of MS5 indicated that the PLA produced with MS5 has more centralized molecular weight distribution than that of MS3.

As described in earlier studies, only engineered class II PHA synthases were utilized in the biosynthesis of PLA homopolymer and LA-containing copolymers, and the mutation of several residues (E130D, S325T, S477G, and Q481K) can improve their substrate specificities toward LA monomers (Taguchi et al., 2008; Yamada et al., 2009; Jung et al., 2010; Yang et al., 2010; Choi et al., 2016). Class I PHA synthases present higher substrate specificity toward SCL monomers (Zou et al., 2017), but have not been utilized in the biosynthesis of the PLA homopolymer and LA-containing copolymers before. The results of this study confirmed that class I PHA synthase could also be utilized in PLA production (**Figure 2**). Moreover, the same synthase ($PhaC_{Cs}$) could catalyze the polymerization of 3-hydroxypropionic acid (3HP, an isomer of LA), and the CDW of the produced P (3HP) can reach 40% (Linares-Pastén et al., 2015), indicating that class I $PhaC_{Cs}$ shows

promising substrate specificity toward the SCL hydroxypropionic acids.

Increased PLA Production by Morphologically Engineered *E. coli*

At the time point of 36 h after inoculation, the cells of *E. coli* MS4 (morphological engineering via *sulA*) and MS3 (control strain without *sulA*) were harvested for SEM/TEM analysis. The SEM results revealed that *E. coli* MS4 has an elongated rod cell shape (**Figure 3A**), which presents a longer cell shape than the control strain of *E. coli* MS3 (**Figure 3B**). Moreover, TEM results showed that the intracellular PLA granules in *E. coli* MS4 (**Figure 3C**) occupied larger cell space than in the control strain of *E. coli* MS3 (**Figure 3D**), indicating the increased PLA production in *E. coli* MS4. The results of fed-batch fermentation (**Figure 2**) confirmed that *E. coli* MS4 significantly ($p < 0.01$) had higher production of PLA (CDW of 1.96%) than *E. coli* MS3 (CDW of 0.54%). The highest PLA production was achieved by *E. coli* MS6 (contains both $PhaC_{Cs}$ and *sulA*), which can produce up to 955.0 mg/L of PLA in fed-batch fermentation with the CDW of 2.23%.

The significantly increased PLA production in *E. coli* MS4 and MS6 than their control strains of *E. coli* MS3 and MS5 (**Figure 2**) indicated that the overexpression of the *sulA* gene in *E. coli* strains could morphologically affect the strains to achieve improved production of intracellular polymers. Similar to this study, *E. coli* strains have been morphologically engineered to achieve the increased production of poly (3-hydroxybutyrate-co-4-hydroxybutyrate) (Wang et al., 2014). It has been demonstrated that SulA could bind the tubulin of FtsZ to inhibit the formation of Z loop in the cell division of *E. coli* strains (Pichoff and Lutkenhaus, 2002, 2005; Chen et al., 2012). The SulA/FtsZ interaction was also found in *Pseudomonas* (Chen et al., 2012), indicating that this strategy can be more broadly applied in the biosynthesis of biopolymers by variable chassis strains.

Fused Pct_{Cp}/LdhA Did Not Increase the PLA Production

As shown in **Figure 1**, LdhA and Pct_{Cp} are two key enzymes in the biosynthetic pathway of lactyl-CoA. In order to supply the increased level of lactyl-CoA for PLA biosynthesis, the fused Pct_{Cp}/LdhA enzyme was engineered in *E. coli* MS7 (**Supplemental Figure S2**). Compared with the PLA production of the control strain of *E. coli* MS4 (CDW of 1.96%), the PLA production of *E. coli* MS7 (CDW of 2.08%) was not apparently increased ($p > 0.05$). In addition, *E. coli* MS7 (containing Pct_{Cp} and LdhA fusion enzyme) had a lower dry cell weight (28.9 g/L, 72 h) than *E. coli* MS4 (31.6 g/L, 72 h), which indicated that the presence of fused enzyme exhibits growth stress toward the engineered strain of MS7.

Similar to other fused proteins and enzymes (Yu et al., 2015), the tandem fusion of Pct_{Cp} and LdhA can spatially restrain multiple catalytic domains in one fused enzyme. The results of this study indicated that fused Pct_{Cp}/LdhA enzyme retained the biocatalytic functions of individual Pct_{Cp} and LdhA. However, fused Pct_{Cp}/LdhA did not apparently improve the general biosynthesis of PLA, which indicated that the final step (polymerization of lactyl-CoA into PLA by PHA synthase) could be the bottleneck step in the biosynthesis of the PLA homopolymer, as reported by earlier studies (Park et al., 2012; Matsumoto et al., 2018).

CONCLUSION

The present study demonstrated that class I PHA synthase from *Chromobacterium* sp. USM2 ($PhaC_{Cs}$) is feasible to catalyze the polymerization of the PLA homopolymer from lactyl-CoA. In *de novo* PLA fermentation from glucose, engineered *E. coli* strains having $PhaC_{Cs}$ present improved PLA production than control strains, which expressed the evolved class II PHA synthase $PhaC1_{Ps6\text{-}19}$. In addition, *sulA*-mediated morphological engineering could enlarge the cell space and further improve PLA production of the engineered *E. coli* strains.

DATA AVAILABILITY STATEMENT

The original contributions presented in the study are included in the article/**Supplementary Material**; further inquiries can be directed to the corresponding author.

AUTHOR CONTRIBUTIONS

HZ, MS, and LY conceived and presented the idea. MS, ML, and AY performed the experiment. MS, HZ, and JP wrote the manuscript in consultation with others. All authors read and approved the final manuscript.

FUNDING

The present study was supported by the Talent Foundation and the Province and Ministry Co-construction Collaborative Innovation Center of Eco-chemical Engineering (STHGYX2221).

SUPPLEMENTARY MATERIAL

The Supplementary Material for this article can be found online at: https://www.frontiersin.org/articles/10.3389/fbioe.2022.919969/full#supplementary-material

REFERENCES

Adams, D. W., and Errington, J. (2009). Bacterial Cell Division: Assembly, Maintenance and Disassembly of the Z Ring. *Nat. Rev. Microbiol.* 7, 642–653. doi:10.1038/nrmicro2198

Chek, M. F., Hiroe, A., Hakoshima, T., Sudesh, K., and Taguchi, S. (2019). PHA Synthase (Phac): Interpreting the Functions of Bioplastic-Producing Enzyme from a Structural Perspective. *Appl. Microbiol. Biotechnol.* 103, 1131–1141. doi:10.1007/s00253-018-9538-8

Chen, Y., Milam, S. L., and Erickson, H. P. (2012). SulA Inhibits Assembly of FtsZ by a Simple Sequestration Mechanism. *Biochemistry* 51, 3100–3109. doi:10.1021/bi201669d

Choi, S. Y., Park, S. J., Kim, W. J., Yang, J. E., Lee, H., Shin, J., et al. (2016). One-Step Fermentative Production of Poly(Lactate-Co-Glycolate) from Carbohydrates in *Escherichia coli*. *Nat. Biotechnol.* 34, 435–440. doi:10.1038/nbt.3485

Dajkovic, A., Mukherjee, A., and Lutkenhaus, J. (2008). Investigation of Regulation of FtsZ Assembly by SulA and Development of a Model for FtsZ Polymerization. *J. Bacteriol.* 190, 2513–2526. doi:10.1128/JB.01612-07

Erickson, H. P., Anderson, D. E., and Osawa, M. (2010). FtsZ in Bacterial Cytokinesis: Cytoskeleton and Force Generator All in One. *Microbiol. Mol. Biol. Rev.* 74, 504–528. doi:10.1128/mmbr.00021-10

Gao, Y., Liu, C., Ding, Y., Sun, C., Zhang, R., Xian, M., et al. (2014). Development of Genetically Stable *Escherichia coli* Strains for Poly(3-Hydroxypropionate) Production. *PLoS One* 9, e97845. doi:10.1371/journal.pone.0097845

Jung, Y. K., Kim, T. Y., Park, S. J., and Lee, S. Y. (2010). Metabolic Engineering of *Escherichia Coli* for the Production of Polylactic Acid and its Copolymers. *Biotechnol. Bioeng.* 105, 161–171. doi:10.1002/bit.22548

Li, Z.-J., Qiao, K., Shi, W., Pereira, B., Zhang, H., Olsen, B. D., et al. (2016). Biosynthesis of Poly(Glycolate-Co-Lactate-Co-3-Hydroxybutyrate) from Glucose by Metabolically Engineered *Escherichia coli*. *Metab. Eng.* 35, 1–8. doi:10.1016/j.ymben.2016.01.004

Linares-Pastén, J. A., Sabet-Azad, R., Pessina, L., Sardari, R. R. R., Ibrahim, M. H. A., and Hatti-Kaul, R. (2015). Efficient Poly(3-Hydroxypropionate) Production From Glycerol Using Lactobacillus Reuteri And Recombinant *Escherichia Coli* Harboring L. Reuteri Propionaldehyde Dehydrogenase And Chromobacterium Sp. PHA Synthase Genes. *Bioresour. Technol.* 180, 172–176. doi:10.1016/j.biortech.2014.12.099

Maharana, T., Mohanty, B., and Negi, Y. S. (2009). Melt-Solid Polycondensation of Lactic Acid and its Biodegradability. *Prog. Polym. Sci.* 34, 99–124. doi:10.1016/j.progpolymsci.2008.10.001

Matsumoto, K. i., Hori, C., Fujii, R., Takaya, M., Ooba, T., Ooi, T., et al. (2018). Dynamic Changes of Intracellular Monomer Levels Regulate Block Sequence of Polyhydroxyalkanoates in Engineered *Escherichia coli*. *Biomacromolecules* 19, 662–671. doi:10.1021/acs.biomac.7b01768

Nduko, J. M., and Taguchi, S. (2021). Microbial Production of Biodegradable Lactate-Based Polymers and Oligomeric Building Blocks from Renewable and Waste Resources. *Front. Bioeng. Biotechnol.* 8, 1–18. doi:10.3389/fbioe.2020.618077

Paço, A., Jacinto, J., da Costa, J. P., Santos, P. S. M., Vitorino, R., Duarte, A. C., et al. (2019). Biotechnological Tools for the Effective Management of Plastics in the Environment. *Crit. Rev. Environ. Sci. Technol.* 49, 410–441. doi:10.1080/10643389.2018.1548862

Park, S. J., Lee, S. Y., Kim, T. W., Jung, Y. K., and Yang, T. H. (2012). Biosynthesis of Lactate-Containing Polyesters by Metabolically Engineered Bacteria. *Biotechnol. J.* 7, 199–212. doi:10.1002/biot.201100070

Pichoff, S., and Lutkenhaus, J. (2002). Unique and Overlapping Roles for ZipA and FtsA in Septal Ring Assembly in *Escherichia coli*. *EMBO J.* 21, 685–693. doi:10.1093/emboj/21.4.685

Pichoff, S., and Lutkenhaus, J. (2005). Tethering the Z Ring to the Membrane through a Conserved Membrane Targeting Sequence in FtsA. *Mol. Microbiol.* 55, 1722–1734. doi:10.1111/j.1365-2958.2005.04522.x

Rehm, B. H. A. (2003). Polyester Synthases: Natural Catalysts for Plastics. *Biochem. J.* 376, 15–33. doi:10.1042/BJ20031254

Taguchi, S., and Matsumoto, K. i. (2021). Evolution of Polyhydroxyalkanoate Synthesizing Systems toward a Sustainable Plastic Industry. *Polym. J.* 53, 67–79. doi:10.1038/s41428-020-00420-8

Taguchi, S., Yamada, M., Matsumoto, K. i., Tajima, K., Satoh, Y., Munekata, M., et al. (2008). A Microbial Factory for Lactate-Based Polyesters Using a Lactate-Polymerizing Enzyme. *Proc. Natl. Acad. Sci. U.S.A.* 105, 17323–17327. doi:10.1073/pnas.0805653105

Tsuge, T., Hyakutake, M., and Mizuno, K. (2015). Class IV Polyhydroxyalkanoate (PHA) Synthases and PHA-Producing *Bacillus*. *Appl. Microbiol. Biotechnol.* 99, 6231–6240. doi:10.1007/s00253-015-6777-9

Wang, Y., Wu, H., Jiang, X., and Chen, G.-Q. (2014). Engineering *Escherichia coli* for Enhanced Production of Poly(3-Hydroxybutyrate-Co-4-Hydroxybutyrate) in Larger Cellular Space. *Metab. Eng.* 25, 183–193. doi:10.1016/j.ymben.2014.07.010

Wu, H., Chen, J., and Chen, G.-Q. (2016). Engineering the Growth Pattern and Cell Morphology for Enhanced PHB Production by *Escherichia coli*. *Appl. Microbiol. Biotechnol.* 100, 9907–9916. doi:10.1007/s00253-016-7715-1

Yamada, M., Matsumoto, K. i., Nakai, T., and Taguchi, S. (2009). Microbial Production of Lactate-Enriched Poly[(R)-lactate-co-(R)-3-hydroxybutyrate] with Novel Thermal Properties. *Biomacromolecules* 10, 677–681. doi:10.1021/bm8013846

Yang, T. H., Kim, T. W., Kang, H. O., Lee, S.-H., Lee, E. J., Lim, S.-C., et al. (2010). Biosynthesis of Polylactic Acid and its Copolymers Using Evolved Propionate CoA Transferase and PHA Synthase. *Biotechnol. Bioeng.* 105, 150–160. doi:10.1002/bit.22547

Yu, K., Liu, C., Kim, B.-G., and Lee, D.-Y. (2015). Synthetic Fusion Protein Design and Applications. *Biotechnol. Adv.* 33, 155–164. doi:10.1016/j.biotechadv.2014.11.005

Zou, H., Shi, M., Zhang, T., Li, L., Li, L., and Xian, M. (2017). Natural and Engineered Polyhydroxyalkanoate (PHA) Synthase: Key Enzyme in Biopolyester Production. *Appl. Microbiol. Biotechnol.* 101, 7417–7426. doi:10.1007/s00253-017-8485-0

Zou, H., Taguchi, S., and Levin, D. B. (2021). Editorial: Microbial Production of Biopolyesters and Their Building Blocks: Opportunities and Challenges. *Front. Bioeng. Biotechnol.* 9, 777265. doi:10.3389/fbioe.2021.777265

Conflict of Interest: The authors declare that the research was conducted in the absence of any commercial or financial relationships that could be construed as a potential conflict of interest.

frontiers | Frontiers in Bioengineering and Biotechnology

ORIGINAL RESEARCH
published: 30 June 2022
doi: 10.3389/fbioe.2022.908431

Engineering Glucose-to-Glycerol Pathway in *Klebsiella pneumoniae* and Boosting 3-Hydroxypropionic Acid Production Through CRISPR Interference

Hexin Liu[1], *Peng Zhao*[2] *and Pingfang Tian*[1]*

[1]College of Life Science and Technology, Beijing University of Chemical Technology, Beijing, China, [2]College of Bioscience and Resources Environment, Beijing University of Agriculture, Beijing, China

OPEN ACCESS

Edited by:
Guang Zhao,
Shandong University, China

Reviewed by:
Fei Tao,
Shanghai Jiao Tong University, China
Mingfeng Cao,
Xiamen University, China
Zhen Kang,
Jiangnan University, China

***Correspondence:**
Pingfang Tian
tianpf@mail.buct.edu.cn

Specialty section:
This article was submitted to Industrial Biotechnology, a section of the journal Frontiers in Bioengineering and Biotechnology

Received: 30 March 2022
Accepted: 23 May 2022
Published: 30 June 2022

Citation:
Liu H, Zhao P and Tian P (2022) Engineering Glucose-to-Glycerol Pathway in Klebsiella pneumoniae and Boosting 3-Hydroxypropionic Acid Production Through CRISPR Interference. Front. Bioeng. Biotechnol. 10:908431. doi: 10.3389/fbioe.2022.908431

The recent decline of the international biodiesel industry has led to decreased production and therefore increased the price of glycerol, which is a major by-product of biodiesel but a substrate for production of 3-hydroxypropionic acid (3-HP), that is, glycerol as a feedstock has no advantage over glucose in price. Hence, we engineered glucose to the glycerol pathway and improved 3-HP production by CRISPR interference (CRISPRi). To begin with, we cloned the genes encoding glycerol 3-phosphate dehydrogenase (*gpd1*) and glycerol 3-phosphatase (*gpp2*) from *Saccharomyces cerevisiae*, which jointly catalyze glucose into glycerol. The genes *gpd1* and *gpp2* were co-expressed in *K. pneumoniae* with the dCas9 gene integrated in genome, and this recombinant strain produced 2 g/L glycerol in the shake flask. To minimize the glucose consumption by competing pathways including the EMP pathway, glycerol oxidation pathway, and by-products pathways, we developed an CRISPRi system in aforementioned recombinant *K. pneumoniae* strain to inhibit the expression of the glyceraldehyde-3-phosphate dehydrogenase gene (*gapA*) and 2,3-butanediol production gene (*budA*), resulting in a bi-functional strain harboring both glucose-to-glycerol pathway and CRISPRi system. Reverse transcription and quantitative PCR (RT-qPCR) results showed that this engineered CRISPRi system transcriptionally inhibited *gapA* and *budA* by 82% and 24%, respectively. In shake flask cultivation, this bi-functional strain produced 2.8 g/L glycerol using glucose as the carbon source, which was 46.6% increase compared to the strain without the engineered CRISPRi system. Moreover, this bi-functional strain produced 0.78 g/L 3-HP using glucose as the sole carbon source. In fed-batch cultivation, this bi-functional strain produced 1.77 g/L 3-HP. This study provides insights for co-utilization of distinct carbon sources.

Keywords: *Klebsiella pneumoniae*, glucose, glycerol, 3-hydroxypropionic acid, CRISPR interference

INTRODUCTION

As an isomer of lactic acid, 3-hydroxypropionic acid (3-HP) is chemically active (de Fouchecour et al., 2018; Matsakas et al., 2018). As such, 3-HP is a versatile platform compound from which a variety of economically important chemicals can be derived. Currently, industrial production of 3-HP relies mainly on chemical synthesis (Della Pina et al., 2011). However, chemical synthesis not only relies on non-renewable resources but also leads to excessive by-products and severe environmental pollution (Della Pina et al., 2011). In recent years, microbial fermentation has emerged as an alternative to chemical synthesis. For instance, 3-HP can be produced by diverse wild-type or engineered strains, including *Escherichia coli* (Mohan Raj et al., 2009), *S. cerevisiae* (Semkiv et al., 2017), *Corynebacterium glutamicum* (Chen et al., 2017), *Lactobacillus reuteri* (Luo et al., 2011), and *K. pneumoniae* (Li et al., 2016). In aforementioned host microbes, 3-HP biosynthesis can be roughly divided into three types: glycerol-based (Kumar and Park, 2018), glucose-based (Straathof et al., 2005), and acetate-based 3-HP pathways (Zhao and Tian, 2021). The glycerol-based 3-HP synthesis involves coenzyme A-dependent pathway and coenzyme A-independent pathway (Jers et al., 2019). The CoA-independent 3-HP production from glycerol requires only two-step catalysis by glycerol dehydrogenase (GDH) (EC 4.2.1.30) and acetaldehyde dehydrogenase (ALDH) (EC 1.2.1.3). Therefore, this 3-HP pathway is of great attractiveness. However, the ALDHs in wild-type strains show low activity, and only trace amount of 3-HP can be generated (Raj et al., 2010; Ko et al., 2012). Fortunately, when the *tac* promoter was used to express PuuC, an ALDH native to *K. pneumoniae*, 3-HP was overproduced from glycerol (Li et al., 2016; Zhao et al., 2019). To produce 3-HP from glucose through the CoA-independent pathway, a glucose-to-glycerol pathway needs to be engineered. To do so, it is necessary to clone the genes encoding glycerol 3-phosphate dehydrogenase (GPD1, EC 1.1.1.8) and glycerol 3-phosphatase (GPP2, EC 3.1.3.21) from *S. cerevisiae* (Zheng et al., 2008). In addition, a host strain tolerant to glycerol is required. Of candidate host strains, *K. pneumoniae* is promising in this regard (Zhao et al., 2019), as it can efficiently metabolize glycerol. Although glycerol is the most used carbon source for production of 3-HP (Nguyen-Vo et al., 2018), its price is high due to the recent decline of the biodiesel industry.

In *S. cerevisiae*, glucose is catalyzed into glycerol by GPD1 and GPP2 (Chen et al., 2014; Kildegaard et al., 2016). In wild-type microbes, glucose conversion to glycerol is rather limited and high-level production of 3-HP is thus challenging. The reason behind is that glucose uptake is mainly accomplished by the phosphoenolpyruvate-dependent glucose uptake system (PTS), and glycolysis pathway (EMP) consumes a large amount of glucose (Chen et al., 2017). Moreover, in the presence of glucose, the Crabtree effect inhibits the conversion of glycerol to 3-HP (Joseph et al., 1981). When metabolic pathways were optimized and glucose was used as the carbon source, the maximum 3-HP titer of engineered *E. coli* reached 37.6 g/L (Heo et al., 2019). Despite a lot of studies, the low 3-HP production constrains its commercialization (Ashok et al., 2011). Hence, global regulation is required to improve the conversion rate of glucose to 3-HP.

CRISPR interference (CRISPRi, **Figure 1B**) is a powerful tool for modulation of multiple genes (Qi et al., 2013). In fact, fermentation titer is a quantitative trait controlled by multiple genes. The guide RNAs in the CRISPR system can direct dCas9 to user-defined genetic loci, leading to suppression of single or multiple genes and alternation of metabolites formation (Jakounas et al., 2015; Liu et al., 2019; Xu and Qi, 2019). For instance, lactic acid production can be attenuated by an engineered CRISPRi system targeting D-lactate dehydrogenase gene in *K. pneumoniae* (Wang et al., 2018). Conversely, aconitic acid production can be improved by an engineered CRISPRi system that simultaneously targeting pyruvate kinase (PK) in the glycolytic pathway (EMP pathway) and isocitrate dehydrogenase (IDH) in the tricarboxylic acid cycle (TCA cycle) pathway in *E. coli* (Li et al., 2020). These studies highlight the potential of the CRISPRi system in allocating metabolic flux.

Given aforementioned information, we conjecture that engineering a glucose-to-glycerol pathway in *K. pneumoniae* enables 3-HP production using glucose as carbon source. In addition, the CRISPRi system might be engineered to reallocate the metabolic flux toward 3-HP and other metabolites (**Figure 1A**). In doing so, based on the previous work, two genes, *gpd1* (GenBank accession No. Z74071.1) and *gpp2* (GenBank accession No. DQ332890.1) were used to construct the shortest pathway for conversion of glucose to 3-HP. In addition, the CRISPRi system was developed to regulate the pathways affecting 3-HP production. To boost glucose conversion to glycerol, we engineered a CRISPRi system targeting glyceraldehyde-3-phosphate dehydrogenase gene (*gapA*) and α-acetolactate decarboxylase gene (*budA*). Reverse transcription and quantitative PCR (RT-qPCR) was performed to examine the expression of *gpd1*, *gpp2*, *gapA*, and *budA*. Shake flask cultivation of the recombinant strains were to determine the production of glycerol, 3-HP, acetic acid, lactic acid, 1,3-propanediol (1,3-PDO), and 2,3-butanediol (2,3-BDO). Fed-batch cultivation of the strain was to examine the production of 3-HP.

MATERIALS AND METHODS

Strains, Vectors, and Medium

The recombinant *K. pneumoniae* strain with dCas9 integrated in genome (KP-dCas9) and plasmid ptac-15A was preserved in laboratory (Zhao et al., 2021). The plv plasmid was provided by Professor George Guoqiang Chen from Tsinghua University (Lv et al., 2015). *E. coli* Top 10 was purchased from Biomed, China. The recombinant *K. pneumoniae* strain with dCas9 integrated in genome was used as the host strain for the development of the CRISPRi system and co-overexpression of *gpd1* and *gpp2* genes for the conversion of glucose-to-glycerol (**Supplementary Table S1**). *E. coli* Top 10 was employed for vector construction. The primers used in this study are listed in **Supplementary Table S2**. *S. cerevisiae* was used as the donor strain of genes *gpd1* and *gpp2*. The original T7 promoter in vector

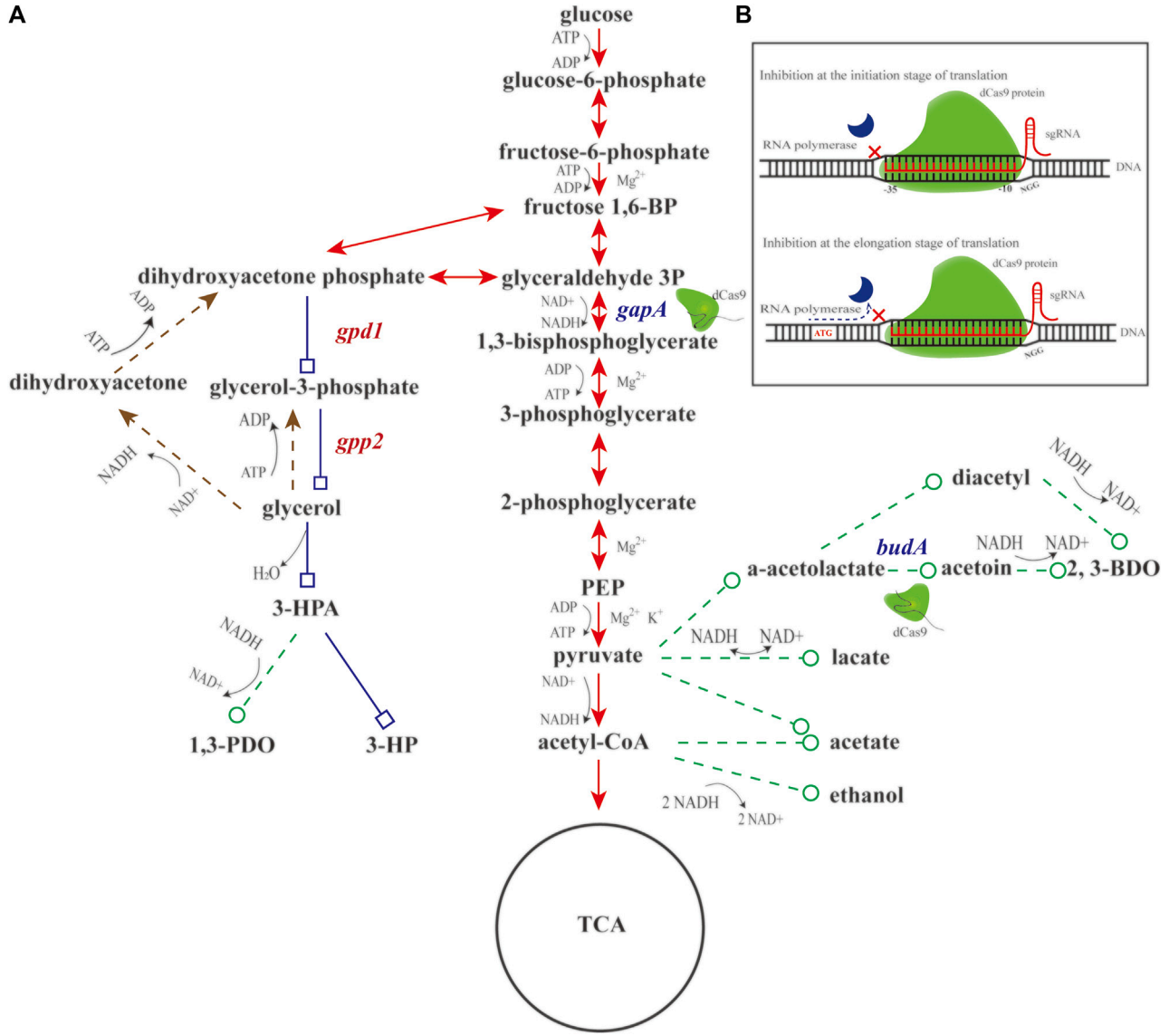

FIGURE 1 | Schematic diagram of engineering glucose-to-glycerol pathway and CRISPRi system in *K. pneumoniae*. **(A)** Diagram of engineering glucose-to-glycerol pathway. **(B)** Diagram of the CRISPRi system. Triangular arrow of solid line denotes the EMP pathway. Triangular arrow of dotted line denotes the glycerol oxidation pathway. Square arrow of solid line denotes the engineered glucose to 3-hydroxypropionic acid (3-HP) pathway, and circular arrow of dotted line denotes by-product pathways. *gapA* and *budA* are two native genes inhibited by CRISPRi. *gpd1* and *gpp2* are two heterologous genes introduced for glycerol production. Fructose 1,6-BP, fructose 1,6-diphosphate; glyceraldehyde 3P, glyceraldehyde-3-phosphate; PEP, phosphoenolpyruvate; 3-HPA, 3-hydroxypropionaldehyde; 3-HP, 3-hydroxypropionic acid; 1,3-PDO, 1,3-propanediol; 2,3-BDO, 2,3-butanediol; *gpd1*, glycerol 3-phosphate dehydrogenase; *gpp2*, glycerol 3-phosphatase; *gapA*, glyceraldehyde-3-phosphate dehydrogenase; and *budA*, α-acetolactate decarboxylase.

pET-28A was replaced by the *tac* promoter, resulting in a vector designated ptac-15A, which was used to overexpress *gpd1* and *gpp2*. In vector construction experiments, *E. coli* Top 10 was grown in Luria-Bertani (LB) medium containing the following components per liter: NaCl 10 g, tryptone 10 g, yeast extract 5 g, and chloramphenicol 34 mg. In CRISPRi and fermentation experiments, *K. pneumoniae* strain was grown in fermentation medium containing the following components per liter: glucose, 20 g; $(NH_4)_2SO_4$, 4 g; $K_2HPO_4{\cdot}3H_2O$, 3.4 g; KH_2PO_4, 1.3 g; $MgSO_4{\cdot}7H_2O$, 0.5 g; yeast extract, 3 g; $CaCO_3$, 0.1 g; 1.25 ml of trace element solution; and chloramphenicol 34 mg. The trace element solution contained the following components per liter: $CuCl_2{\cdot}2H_2O$, 1.88 g; $FeSO_4$, 32 g; $CoCl_2{\cdot}6H_2O$, 1.88 g; $ZnCl_2{\cdot}6H_2O$, 2.72 g; Na_2MoO_4, 0.02 g; $MnCl_2{\cdot}4H_2O$, 0.68 g; H_3BO_3, 0.24 g; and 40 ml concentrated HCl. Restriction enzymes, Taq DNA polymerase, and T4 DNA ligase were purchased from New England Biolabs (Beijing, China). Primer synthesis and DNA sequencing were performed by Biomed Co., Ltd. RT-qPCR was completed by RuiBiotech Co., Ltd.

TABLE 1 | sgRNAs used in this study.

sgRNA name	Sequence (5′–3′)	Targeting site
budA-sg1-F	AAATTCGTAAACCCCGCTCAGCA	113–132
budA-sg1-R	AACTGCTGAGCGGGGTTTACGAA	
budA-sg2-F	AAACACGCTCTCGGGATGCTGCG	65–84
budA-sg2-R	AACCGCAGCATCCCGAGAGCGTG	
budA-sg3-F	AAAGTTGCTGGCGGCTCACCGGA	339–358
budA-sg3-R	AACTCCGGTGAGCCGCCAGCAAC	
gapA-sg1-F	AAAGGTACACTCCACAATCACCT	272–291
gapA-sg1-R	AACAGGTGATTGTGGAGTGTACC	
gapA-sg2-F	AAACGTTGATAGCCACCACTTCC	81–100
gapA-sg2-R	AACGGAAGTGGTGGCTATCAACG	
gapA-sg3-F	AAAATCGTTGACGTTGTAGACGA	386–405
gapA-sg3-R	AACTCGTCTACAACGTCAACGAT	

F, forward; R, reverse.

Construction of Recombinants

To overexpress GPD1 and GPP2 in KP-dCas9, their coding genes *gpd1* (GenBank accession No. Z74071.1) and *gpp2* (GenBank accession No. DQ332890.1) genes were cloned by PCR from *S. cerevisiae* genome. Next, the *gpd1* gene was cloned into ptac-15A at *Noc* I/*Nde* I sites, leading to a vector designated ptac-G1; the *gpp2* gene was cloned into ptac-15A at *Nde* I/*Nhe* I sites, leading to a vector designated ptac-G2. Ligating *gpd1* with the tac promoter and the RBS sequence from ptac-G1 to vector ptac-G2 at *Not* I/*Xho* I sites led to a vector designated ptac-G12 (**Supplementary Figure S2**). Transformation of vectors ptac-15A and ptac-G12 into competent KP-dCas9 cells led to recombinant strains KP-15A and KP-G12, respectively (**Supplementary Table S1**). KP-dCas9 was transformed with the constructed plasmid by electro-transformation (0.2 cm, 2.5 kV, and time duration >0.5 ms). *E. coli* was transformed with the constructed plasmid by heat shock. Positive clones were confirmed by colony PCR and DNA sequencing.

To develop the CRISPRi system in KP-dCas9, the CRISPRi vectors targeting *gapA* or *budA* were constructed by replacement of the sgRNA sequence in vector plv-sgRNA (**Supplementary Table S1**, plv-*gapA*-1, plv-*gapA*-2, plv-*gapA*-3, plv-*budA*-1, plv-*budA*-2, and plv-*budA*-3). Briefly, two complementary single-stranded target sequences were chemically synthesized and annealed to form a 23 bp double-stranded DNA owning cohesive ends matching the *Bsp*Q I-digested vector (**Table 1**). Subsequent ligation resulted in desired CRISPRi vectors. For each *gapA* or *budA*, three candidate guide RNAs targeting the different regions were synthesized to ensure efficient inhibition, and the sgRNA sequences, *tet* promoter and an RBS sequence from plv-vector were cloned into ptac-G12 at *Eag* I/*Bmt* I sites (**Supplementary Table S1**, ptac-GS, ptac-GG1, ptac-GG2, ptac-GG3, ptac-GB1, ptac-GB2, and ptac-GB3). Transforming vectors ptac-GS, ptac-GG1, ptac-GG2, ptac-GG3, ptac-GB1, ptac-GB2, and ptac-GB3 into competent KP-dCas9 led to recombinant strains KP-GS, KP-GG1, KP-GG2, KP-GG3, KP-GB1, KP-GB2, and KP-GB3, respectively (**Supplementary Table S1**). Last, RT-qPCR was conducted to determine the most inhibited gene. The best-performing *gapA* and *budA* sgRNAs were cloned using isocaudamers *Ngo*M IV and *Xma* I and then ligated in tandem. The sgRNA expression cassettes were digested by *Eag* I and *Ngo*M IV, while the plasmid was digested by *Eag* I and *Xma* I, leading to vector named ptac-GGB. Transforming the vector ptac-GGB into competent KP-dCas9 led to the recombinant strain KP-GGB (**Supplementary Table S1**; **Supplementary Figure S3**).

RT-qPCR Analysis of CRISPR Interference

To examine the transcription levels of *gpd1*, *gpp2*, *gapA*, and *budA*, RT-qPCR was performed. Briefly, strains including KP-dCas9, KP-G12, KP-GS, KP-GG1, KP-GG2, KP-GG3, KP-GB1, KP-GB2, KP-GB3, and KP-GGB were cultivated in medium for 24 h and harvested by centrifugation at 4°C, 12,000 rpm. Then, the harvested bacteria were lysed with TRIzol reagent. The RNA samples were used as template to synthesize cDNAs through reverse transcription. RT-qPCR was carried out by Applied Biosystems™ 7900HT Fast Real-Time PCR System (Thermo Fisher) with SYBR Green addition. The RT-qPCR data were analyzed using the ΔΔCT method with 16S rRNA as an internal control. All experiments were performed in triplicate.

Shake Flask and Bioreactor Cultivation

In shake flask cultivation, strains KP-dCas9, KP-15A, KP-GS, KP-GG1, KP-GB2, and KP-GGB were pre-cultured in 4 ml LB medium overnight. Next, these strains were independently grown in 250-ml shake flasks each containing 100 ml 3-HP–producing medium and 8.5 mg chloramphenicol at 37°C and 150 rpm. After 3 h cultivation, IPTG at a final concentration of 0.5 mM was added to induce the expression of *gpd1* and *gpp2*. Dehydrated tetracycline (aTc) at a final concentration of 2 μM was added to induce sgRNA expression. Fermentation broth was sampled every 3 h to examine cell growth, glucose consumption, and metabolites formation.

In fed-batch cultivation, the recombinant strain was grown in a 5 L bioreactor (Baoxing, China) containing 3 L fermentation medium to produce 3-HP. The strain KP-GB2 was pre-cultured in 100 ml of LB medium overnight at 37°C and subsequently inoculated into a bioreactor, containing antibiotics and IPTG. Air was supplied at 1.5 vvm, and agitation speed was set at 400 rpm. The temperature was set at 37°C, and the pH was maintained at 7.0 by adding 5 M NaOH. A total of 700 ml of 500 g/L glucose solution was added at a rate of 4.5 g/h to maintain cell growth after the glucose in medium was exhausted. The samples were taken out every 6 h to examine cell growth, glucose consumption, and metabolites formation.

Analytical Methods

Cell concentrations were measured by using microplate reader at 600 nm with 200 μL fermentation broth and 1,800 μL ddH_2O added in a cuvette. To measure metabolites, fermentation broth was centrifuged at 12,000 rpm for 10 min to remove bacteria. Major metabolites including 3-HP, lactic acid, and acetic acid in supernatant were analyzed by using the high-performance liquid chromatography (HPLC) system (Shimadzu, Kyoto, Japan) equipped with a C_{18} column and an SPD-20A UV detector at 210 nm. The column was maintained at 25°C. The mobile phase was 0.05% phosphoric acid at a flow rate of 0.8 ml/min. 1,3-PDO and 2,3-BDO were analyzed by GC (Persee). Analytically pure 1,3-PDO and 2,3-BDO were used as standard for quantification. Residual glucose concentration was measured by an SBA-40E biosensor analyzer (Biology Institute of Shandong Academy of

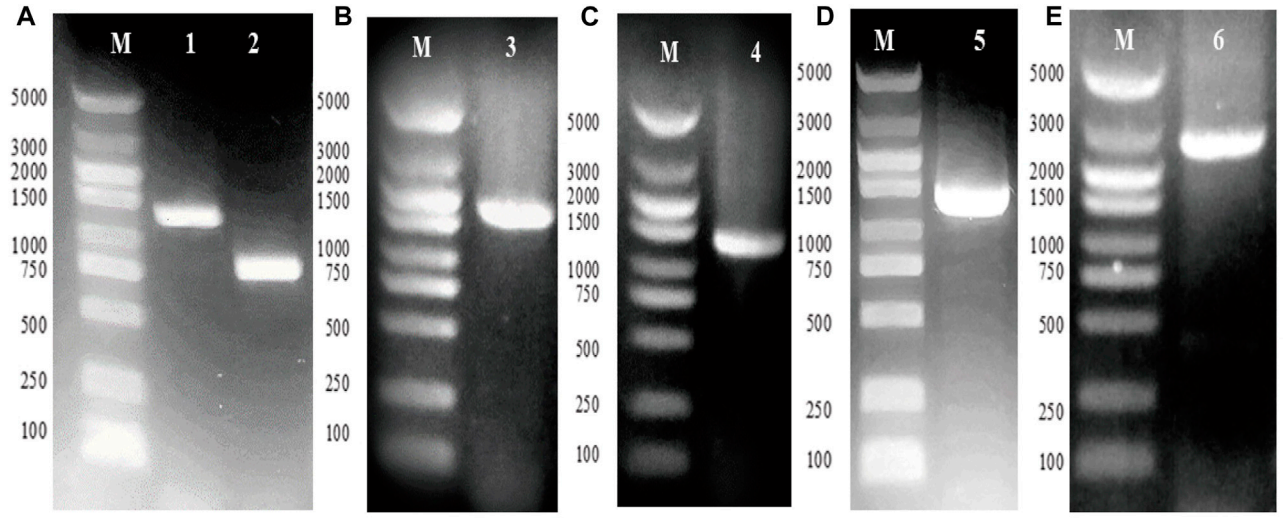

FIGURE 2 | Construction of plasmid ptac-G12 that co-expressing *gpd1* and *gpp2* under tac promoter. G1 denotes *gpd1* gene encoding glycerol 3-phosphate dehydrogenase; G2 denotes *gpp2* gene encoding glycerol 3-phosphatase; and G12 denotes co-expression of *gpd1* and *gpp2*. **(A)** PCR amplification of the *gpd1* and *gpp2* genes from *S. cerevisiae*. **(B)** Colony PCR of plasmid ptac-*gpd1*. **(C)** Colony PCR of plasmid ptac-*gpp2*. **(D)** PCR amplification of ptac-*gpd1* expression cassette. **(E)** Colony PCR of *gpd1* and *gpp2*. M, Marker; lane 1, *gpd1* gene; lane 2, *gpp2* gene; lane 3, plasmid ptac-*gpd1* expression cassette; lane 4, plasmid ptac-*gpp2* expression cassette; lane 5, plasmid ptac-*gpd1* expression cassette; and lane 6, colony PCR of the co-expressed *gpd1* and *gpp2* in tandem.

Science, China). A new immobilized enzyme membrane was installed on the electrode, 500 ml standard buffer was prepared with ddH_2O, and the three-in-one standard solution of SBA was prepared (three materials mentioned earlier are provided by the instrument manufacturer). Glucose concentration in the supernatant was diluted to less than 1 g/L. After 25 μL standard solution was injected into the sampling port stabilization instrument with a microinjector, the glucose content in the sample was measured successively, and each sample was measured three times. Glycerol concentration was measured by the glycerin test kit (APPLYGEN Beijing). All samples were filtered through a 0.22 μm membrane filter.

RESULT

Determination of Plasmids

The genes *gpd1* and *gpp2* were cloned from *S. cerevisiae* and independently subcloned into vector ptac-15A, resulting in vectors ptac-G1 and ptac-G2, respectively (**Figures 2A–C**). Next, PCR was conducted to obtain ptac-G1 as template, *gpd1* fragment, *tac* promoter, and operon (**Figure 2D**). These fragments were then inserted into ptac-G2 to construct ptac-G12 (**Figure 2E**). The two genes *gpd1* and *gpp2* were expressed using respective *tac* promoter, and their expression was induced by IPTG.

Glycerol Production by Engineered *K. pneumoniae*

The recombinant *K. pneumoniae* strain was cultured in a shake flask to verify glycerol production. To construct glucose-to-glycerol pathway, *gpd1* and *gpp2* were co-expressed in strain KP-dCas9, which harbored the engineered CRISPRi system. In doing so, we constructed a recombinant strain named KP-G12, and the strains KP-15A and KP-dCas9 were used as controls. RT-qPCR results showed that the transcription levels of *gpd1* and *gpp2* were significantly increased in KP-G12 compared to KP-dCas9 (**Figures 3A,B**). In 24 h cultivation, glucose consumption was slowed down due to the expression of heterologous genes (**Figure 3C**), and the strain KP-G12 showed a significant decrease in OD_{600} (**Figure 3D**). The strain containing vector ptac-G12 produced 2 g/L glycerol, with 0.1 g/g yield on glycerol (g of glucose)$^{-1}$. In contrast, no glycerol was produced by strains KP-dCas9 and KP-15A (**Figure 3E,F**), indicating that *gpd1* and *gpp2* catalyzed glucose into glycerol in *K. pneumoniae*.

CRISPR Interference System Inhibiting EMP Downstream Pathway and 2,3-BDO Production

To optimize the CRISPRi system, we prepared several guide RNAs named G1, G2, G3, B1, B2, and B3 that target the different regions of *gapA* and *budA* (**Supplementary Figures S1A,B,G**). The aforementioned six sgRNAs and one non-target sgRNA were independently ligated to vector ptac-G12 (**Supplementary Figures S1C,D**; **Figure 4A**). Transforming these vectors into KP-dCas9 led to recombinant strains KP-GG1, KP-GG2, KP-GG3, KP-GB1, KP-GB2, KP-GB3, and KP-GS, respectively. The strain KP-GS was used as the control. RT-qPCR results showed that compared to KP-GS, the strains KP-GG1 and KP-GB2 showed significant decrease in the expression of target genes (**Figures 4A,B**). The *gapA* gene in strain KP-GG1was transcriptionally inhibited by 60%, and the *budA* gene in

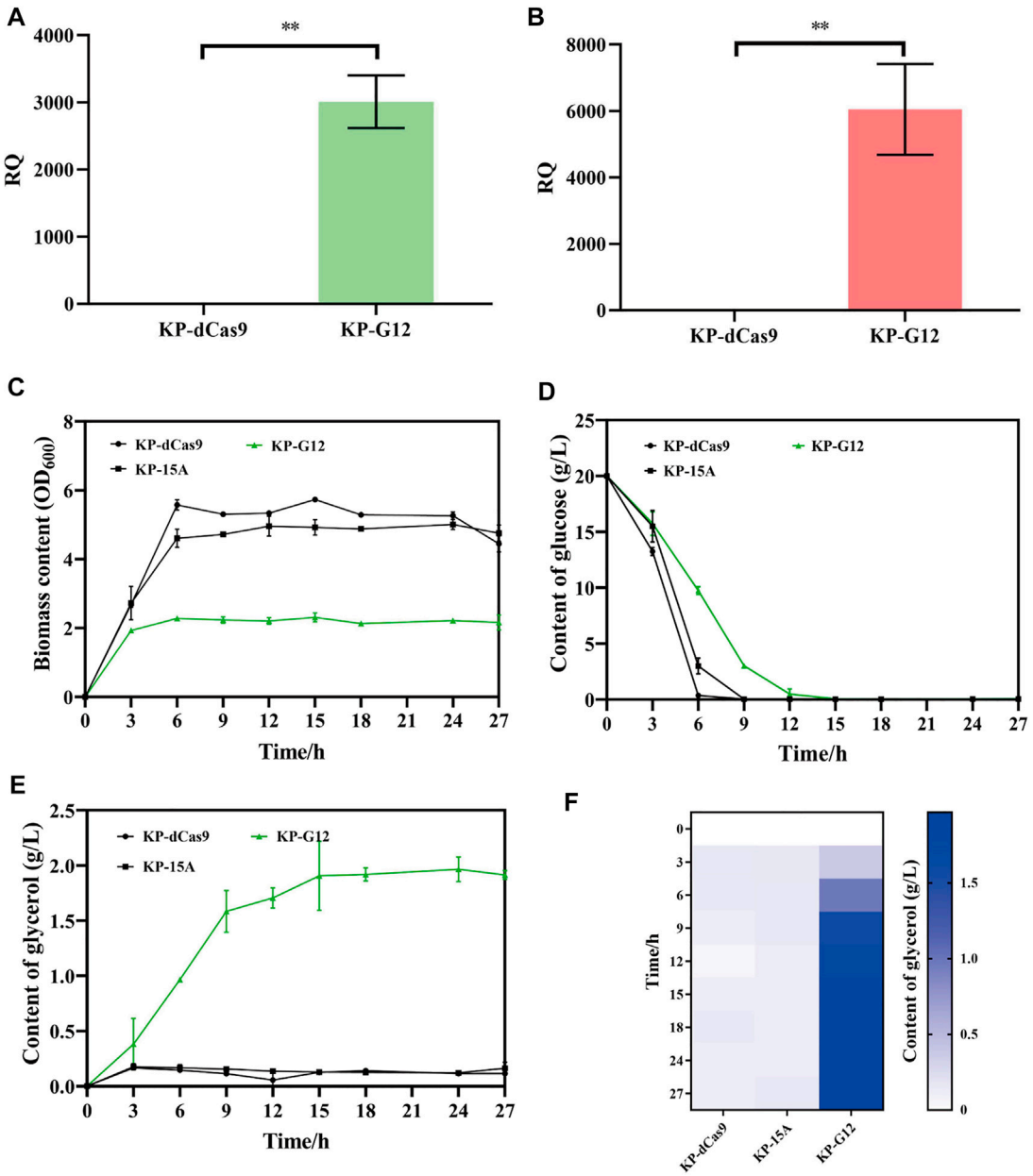

FIGURE 3 | Performance of strains in shake flasks. **(A)** Relative quantity of *gpd1* gene transcription. **(B)** Relative quantity of *gpp2* gene transcription. KP-dCas9 indicates the recombinant *K. pneumoniae* with dCas9 integrated in genome, and its 16S rRNA serves as the internal reference gene. **(C)** Glucose level after 24 h fermentation. **(D)** OD_{600} after 24 h fermentation. **(E)** Line chart represents the glycerol level. **(F)** Heatmap of the glycerol level. KP-dCas9 indicates the recombinant *K. pneumoniae* with dCas9 integrated in genome. KP-15A indicates the recombinant *K. pneumoniae* harboring plasmid ptac-15A and serves as a control. KP-G12 indicates the recombinant *K. pneumoniae* harboring plasmid ptac-G12 co-expressing *gpd1* and *gpp2* genes. RQ, relative quantity of transcription. $^{*}p < 0.05$ and $^{**}p < 0.01$.

strain KP-GB2 was transcriptionally inhibited by 54%. When *budA*-2 was connected in series with *gapA*-1, *gpd1*, and *gpp2* (**Supplementary Figures S1E,F**), the resulting plasmid was named GGB, and the corresponding recombinant strain was named KP-GGB. In strain KP-GGB, the inhibitory rates of the CRISPRi system on genes *gapA* and *budA* reached 82 and 24%, respectively.

Shake Flask Cultivation of the CRISPR Interference Strains

To maximize 3-HP and minimize 2,3-BDO, the glycerol synthesis genes *gpd1* and *gpp2* were co-expressed, and two genes *gapA* and *budA* were inhibited by the CRISPRi system. RT-qPCR results showed that the strains KP-GG1, KP-GB2, and KP-GGB demonstrated the strongest CRISPR inhibition under micro-

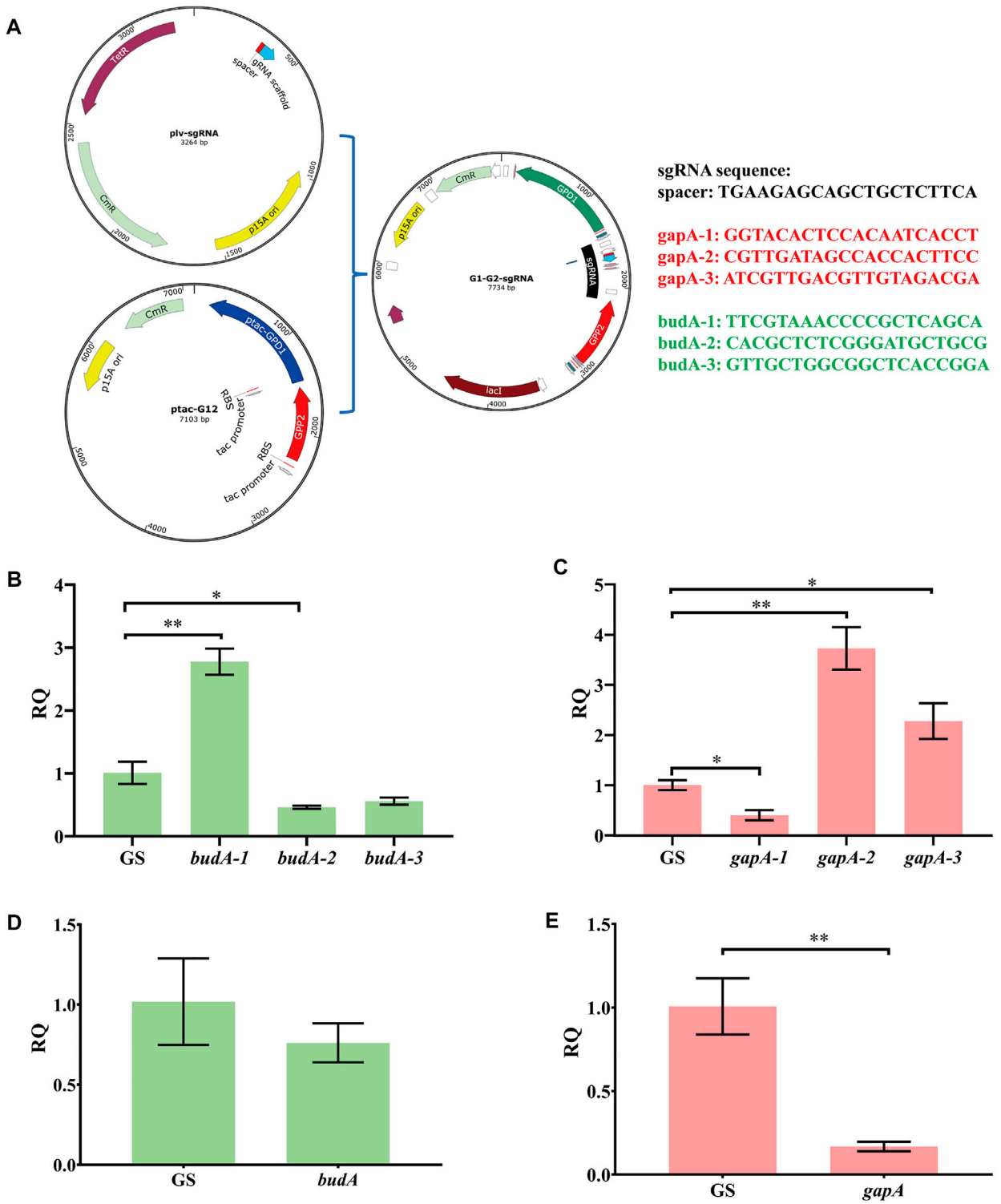

FIGURE 4 | Relative transcription quantity of *K. pneumoniae* with dCas9 integrated in genome and an engineered CRISPRi system. **(A)** Schematic diagram of linking sgRNA to plasmid ptac-G12 co-expressing *gpd1* and *gpp2*. **(B)** RT-qPCR analysis of CRISPRi inhibition on different regions of the *budA* gene. *budA*-1, *budA*-2, and *budA*-3 represent different regions of *budA* gene. GS, recombinant *K. pneumoniae* harboring the non-targeting CRISPRi system. **(C)** RT-qPCR analysis of CRISPRi inhibition on different regions of *gapA* gene. *gapA*-1, *gapA*-2, and *gapA*-3 represent different regions of the *budA* gene. **(D)** RT-qPCR analysis of transcription inhibition on the *budA* gene by the CRISPRi system carrying the sgRNAs for both *budA* and *gapA*. **(E)** RT-qPCR analysis of transcription inhibition on the *gapA* gene by the CRISPRi system carrying the sgRNAs for both *budA* and *gapA*. *gapA*-1, *gapA*-2, and *gapA*-3 denote different regions of the *gapA* gene. RQ, relative quantity of transcription. $^{*}p < 0.05$ and $^{**}p < 0.01$.

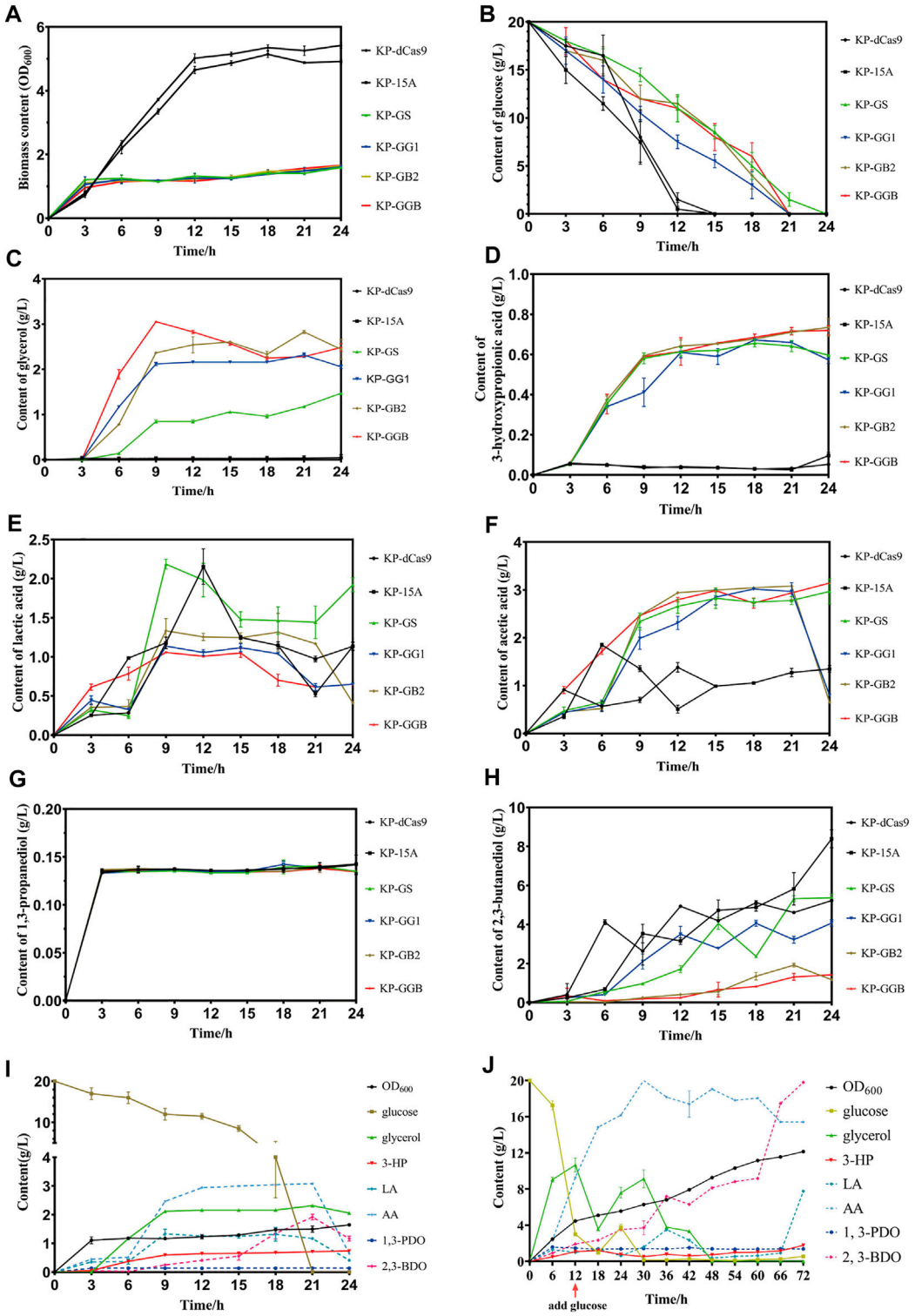

FIGURE 5 | Fermentation of strain harboring CRISPRi system to repress by-product pathways. **(A)** Biomass (OD_{600}) of the CRISPRi strain in the shake flask. **(B)** Glucose consumption of CRISPRi strain in the shake flask. **(C)** Glycerol production by CRISPRi strain in the shake flask. **(D)** 3-Hydroxypropionic acid production by CRISPRi strain in the shake flask. **(E)** Lactic acid production by CRISPRi strain in the shake flask. **(F)** Acetic acid production by CRISPRi strain in the shake flask. **(G)** 1,3-Propanediol production of CRISPRi strain in the shake flask. **(H)** 2,3-Butanediol production by CRISPRi strain in the shake flask. **(I)** Metabolites of CRISPRi strain KP-GB2 in the shake flask. **(J)** Metabolites of CRISPRi strain KP-GB2 in fed-batch culture. KP-dCas9, the recombinant *K. pneumoniae* strain with dCas9 integrated in genome; KP-15A, the recombinant *K. pneumoniae* strain harboring empty vector ptac-15A; KP-GS, the recombinant *K. pneumoniae* with dCas9 integrated in genome, (*Continued*)

FIGURE 5 | and harboring vector ptac-GS co-expressing non-target sgRNA, *gpd1* and *gpp2*; KP-GG1, recombinant *K. pneumoniae* with dCas9 integrated in genome of and ptac-GG1 plasmid co-expressing *gpd1*, *gpp2*, and *gapA*-targeting sgRNA; KP-GB2, the recombinant *K. pneumoniae* with dCas9 integrated in genome and vector ptac-GB2 co-expressing *gpd1*, *gpp2*, and *budA*-targeting sgRNA; KP-GGB, the recombinant *K. pneumoniae* with dCas9 integrated in genome and plasmid ptac-GGB co-expressing *gpd1*, *gpp2*, and sgRNAs targeting *gapA* and *budA*. 3-HP, 3-hydroxypropionic acid; LA, lactic acid; AA, acetic acid; 1,3-PDO, 1,3-propanediol; and 2,3-BDO, 2,3-butanediol.

oxygen conditions as compared to the strains KP-GS, KP-dCas9, and KP-15A. In 24 h cultivation, these engineered strains showed retarded cell growth and reduced glucose consumption. All engineered *K. pneumoniae* strains produced glycerol, but the difference was not significant. For 2,3-BDO production, the strain KP-15A presented the highest titer (8.39 ± 0.33 g/L), while the strain KP-GB2 presented the lowest titer (1.185 ± 0.045 g/L). In addition, the strain KP-GB2 produced the highest 3-HP (0.734 ± 0.032 g/L). Interestingly, no significant differences were observed in the production of acetic acid, lactic acid, and 1,3-PDO in all strains.

Fed-Batch Cultivation of CRISPR Interference Strains

Now that the strain co-expressing *gpd1* and *gpp2* was able to synthesize glycerol from glucose and the strain KP-GB2 showed the highest 3-HP level in the shake flask, the strain was then cultivated in a 5 L bioreactor. Results showed that the strain did not consume glycerol until 12 h fermentation, at this time the glucose was exhausted. When glucose was supplemented, the glycerol level was further improved, indicating that the strain did not consume glycerol until glucose was exhausted. In addition, only a small amount of 2,3-BDO was produced in the initial stage of fermentation. However, in the middle and late stages of fermentation, 2,3-BDO production was increased presumably due to the rising pH value of medium and the failure of aTc induction in an alkaline environment, which hampered the inhibition of the CRISPRi system on by-product pathways. Due to the engineered glycerol synthesis pathway, the strain KP-GB2 produced 1.77 ± 0.04 g/L 3-HP in 72 h, with productivity of 0.025 g/L/h. This low productivity may be ascribed to the engineered CRISPRi system and genes *gpd1* and *gpp2*, which imposed a heavy burden on cell growth. Indeed, the maximum OD_{600} was only 12.135 ± 0.005.

DISCUSSION

In this study, the glycerol synthesis pathway was engineered in *K. pneumoniae*, and the resulting strain was subjected to CRISPRi-dependent gene regulation (**Figure 2**). By co-expressing *gpd1* and *gpp2* and simultaneously inhibiting *gapA* and *budA*, the levels of both glycerol and 3-HP were improved (**Figure 4**, **Figure 5**). In addition, the by-products and glucose flux in the EMP pathway were reduced. The aforementioned results confirmed the engineered glucose to the 3-HP pathway in *K. pneumoniae*. In *K. pneumoniae*, glycerol-based 3-HP synthesis requires only two reactions, and the theoretical conversion rate is therefore high. After introducing *gpd1* and *gpp2* into *K. pneumoniae*, glucose-based production of 3-HP requires only four enzyme genes including *gpd*, *gpp2*, *gdh*, and *aldH* (e.g., *puuC*). As for the low 3-HP production, it was ascribed to the presence of glucose. In particular, the Crabtree effect hindered glycerol utilization. Future studies may focus on how to attenuate the Crabtree effect. To address this issue, an orthogonal expression system could be engineered to express glycerol utilization genes and minimize the Crabtree effect so that glycerol can be efficiently converted to 3-HP while cell growth is not compromised. Clearly, profound understanding of the *dha* regulon and Crabtree effect is a prerequisite for achieving this goal.

The Crabtree effect and Pasteur effect (Winkler et al., 2003) are two important regulatory mechanisms affecting glucose metabolism. The Crabtree effect is a common problem encountered by mixed carbon source fermentation. Removal of the Crabtree effect enables bacteria to co-utilize glucose and other carbon sources. The Pasteur effect entangles the choice of aeration during fermentation. Aerobic respiration increases bacterial growth but reduces the activity of phosphofructokinase through feedback inhibition, thereby inhibiting the EMP pathway. In fed-batch cultivation, it is necessary to maintain different oxygen levels in bioreactor for different purposes. If the Crabtree effect can be attenuated and aeration can be adjusted in fed-batch cultivation, the strain will use glucose as a carbon source for growth, which will in turn improve the production of glycerol and 3-HP. However, it is extremely challenging to completely decouple glucose pathways from glycerol pathways, and co-utilization of different carbon sources may be feasible to maintain active cell growth.

CRISPRi is usually not lethal to host cell, as it does not digest DNA. In contrast, gene knockout tools such as CRISPR editing, RecA homologous recombination, and Red homologous recombination are in most cases lethal to host cells. In present study, CRISPRi was developed to inhibit *gapA*, an enzyme catalyzes 3-glyceraldehyde triphosphate into 1,3-diphosphoglyceric acid. CRISPRi was also used to inhibit *budA*, an enzyme required for 2,3-BDO production in *K. pneumoniae* (Yang et al., 2014). RT-qPCR results showed that the engineered CRISPRi systems could significantly inhibit the expression of *budA* and *gapA*. In shake flask cultivation, the CRISPRi strain demonstrated slight enhancement in the glycerol level but significant decrease in 2,3-BDO production. However, the inhibitory effect on *bud*A was significantly reduced when two groups of sgRNAs were linked in tandem. This might be ascribed to the low expression of dCas9, which was insufficient for binding two target genes simultaneously. Plasmid-based overexpression of dCas9 and multi-copy integration of dCas9 into genome may

be feasible solutions. Overall, this study demonstrated the feasibility of glucose-to-glycerol as well as CRISPRi-dependent gene regulation in *K. pneumoniae*. We anticipate that better understanding of the metabolic networks is crucial for high-level production of 3-HP, 1,3-PDO, 2,3-BDO, and beyond.

DATA AVAILABILITY STATEMENT

The original contributions presented in the study are included in the article/Supplementary Material; further inquiries can be directed to the corresponding author.

AUTHOR CONTRIBUTIONS

PT conceived the protocol. HL and PZ performed experiments. HL and PT wrote the manuscript. All authors read and approved the manuscript.

FUNDING

This study was funded by grants from the National Key Research and Development Program of China (2018YFA0901800) and Hebei Program for the Development of Science and Technology Guided by Central Universities (206Z2902G).

ACKNOWLEDGMENTS

We thank Professor Guoqiang Chen in Tsinghua University for providing CRISPRi plasmid plv.

SUPPLEMENTARY MATERIAL

The Supplementary Material for this article can be found online at: https://www.frontiersin.org/articles/10.3389/fbioe.2022.908431/full#supplementary-material

REFERENCES

Ashok, S., Raj, S. M., Rathnasingh, C., and Park, S. (2011). Development of Recombinant *Klebsiella pneumoniae dhaT* Strain for the Co-production of 3-hydroxypropionic Acid and 1,3-Propanediol from Glycerol. *Appl. Microbiol. Biotechnol.* 90, 1253–1265. doi:10.1007/s00253-011-3148-z

Chen, Y., Bao, J., Kim, I.-K., Siewers, V., and Nielsen, J. (2014). Coupled Incremental Precursor and Co-factor Supply Improves 3-Hydroxypropionic Acid Production in *Saccharomyces cerevisiae*. *Metab. Eng.* 22, 104–109. doi:10.1016/j.ymben.2014.01.005

Chen, Z., Huang, J., Wu, Y., Wu, W., Zhang, Y., and Liu, D. (2017). Metabolic Engineering of *Corynebacterium Glutamicum* for the Production of 3-hydroxypropionic Acid from Glucose and Xylose. *Metab. Eng.* 39, 151–158. doi:10.1016/j.ymben.2016.11.009

de Fouchecour, F., Sanchez-Castaneda, A. K., Saulou-Berion, C., and Spinnler, H. E. (2018). Process Engineering for Microbial Production of 3-hydroxypropionic Acid. *Biotechnol. Adv.* 36, 1207–1222. doi:10.1016/j.biotechadv.2018.03.020

Della Pina, C., Falletta, E., and Rossi, M. (2011). A Green Approach to Chemical Building Blocks. The Case of 3-hydroxypropanoic Acid. *Green Chem.* 13, 1624–1632. doi:10.1039/c1gc15052a

Heo, W., Kim, J. H., Kim, S., Kim, K. H., Kim, H. J., and Seo, J.-H. (2019). Enhanced Production of 3-hydroxypropionic Acid from Glucose and Xylose by Alleviation of Metabolic Congestion Due to Glycerol Flux in Engineered *Escherichia coli*. *Bioresour. Technol.* 285, 121320. doi:10.1016/j.biortech.2019.121320

Jakočiūnas, T., Bonde, I., Herrgård, M., Harrison, S. J., Kristensen, M., Pedersen, L. E., et al. (2015). Multiplex Metabolic Pathway Engineering Using CRISPR/Cas9 in *Saccharomyces cerevisiae*. *Metab. Eng.* 28, 213–222. doi:10.1016/j.ymben.2015.01.008

Jers, C., Kalantari, A., Garg, A., and Mijakovic, I. (2019). Production of 3-hydroxypropanoic Acid from Glycerol by Metabolically Engineered Bacteria. *Front. Bioeng. Biotechnol.* 7, 124. doi:10.3389/fbioe.2019.00124

Joseph, E., Danchin, A., and Ullmann, A. (1981). Regulation of Galactose Operon Expression: Glucose Effects and Role of Cyclic Adenosine 3',5'-monophosphate. *J. Bacteriol.* 146, 149–154. doi:10.1128/jb.146.1.149-154.1981

Kildegaard, K. R., Jensen, N. B., Schneider, K., Czarnotta, E., Özdemir, E., Klein, T., et al. (2016). Engineering and Systems-Level Analysis of *Saccharomyces cerevisiae* for Production of 3-Hydroxypropionic Acid via Malonyl-CoA Reductase-Dependent Pathway. *Microb. Cell Fact.* 15, 53. doi:10.1186/s12934-016-0451-5

Ko, Y., Ashok, S., Zhou, S., Kumar, V., and Park, S. (2012). Aldehyde Dehydrogenase Activity Is Important to the Production of 3-hydroxypropionic Acid from Glycerol by Recombinant *Klebsiella pneumoniae*. *Process Biochem.* 47, 1135–1143. doi:10.1016/j.procbio.2012.04.007

Kumar, V., and Park, S. (2018). Potential and Limitations of *Klebsiella pneumoniae* as a Microbial Cell Factory Utilizing Glycerol as the Carbon Source. *Biotechnol. Adv.* 36, 150–167. doi:10.1016/j.biotechadv.2017.10.004

Li, Y., Wang, X., Ge, X., and Tian, P. (2016). High Production of 3-hydroxypropionic Acid in *Klebsiella pneumoniae* by Systematic Optimization of Glycerol Metabolism. *Sci. Rep.* 6, 26932. doi:10.1038/srep26932

Li, Q., Zhao, P., Yin, H., Liu, Z., Zhao, H., and Tian, P. (2020). CRISPR Interference-Guided Modulation of Glucose Pathways to Boost Aconitic Acid Production in *Escherichia coli*. *Microb. Cell Fact.* 19, 174. doi:10.1186/s12934-020-01435-9

Liu, K., Yuan, X., Liang, L., Fang, J., Chen, Y., He, W., et al. (2019). Using CRISPR/Cas9 for Multiplex Genome Engineering to Optimize the Ethanol Metabolic Pathway in *Saccharomyces cerevisiae*. *Biochem. Eng. J.* 145, 120–126. doi:10.1016/j.bej.2019.02.017

Luo, L. H., Seo, J.-W., Baek, J.-O., Oh, B.-R., Heo, S.-Y., Hong, W.-K., et al. (2011). Identification and Characterization of the Propanediol Utilization Protein PduP of *Lactobacillus Reuteri* for 3-hydroxypropionic Acid Production from Glycerol. *Appl. Microbiol. Biotechnol.* 89, 697–703. doi:10.1007/s00253-010-2887-6

Lv, L., Ren, Y.-L., Chen, J.-C., Wu, Q., and Chen, G.-Q. (2015). Application of CRISPRi for Prokaryotic Metabolic Engineering Involving Multiple Genes, a Case Study: Controllable P(3HB-co-4HB) Biosynthesis. *Metab. Eng.* 29, 160–168. doi:10.1016/j.ymben.2015.03.013

Matsakas, L., Hrůzová, K., Rova, U., and Christakopoulos, P. (2018). Biological Production of 3-hydroxypropionic Acid: An Update on the Current Status. *Fermentation* 4, 13. doi:10.3390/fermentation4010013

Mohan Raj, S., Rathnasingh, C., Jung, W.-C., and Park, S. (2009). Effect of Process Parameters on 3-hydroxypropionic Acid Production from Glycerol Using a Recombinant *Escherichia coli*. *Appl. Microbiol. Biotechnol.* 84, 649–657. doi:10.1007/s00253-009-1986-8

Nguyen-Vo, T. P., Ainala, S. K., Kim, J.-R., and Park, S. (2018). Analysis and Characterization of Coenzyme B-12 Biosynthetic Gene Clusters and Improvement of B-12 Biosynthesis in *Pseudomonas Denitrificans* ATCC 13867. *Fems Microbiol. Lett.* 365 (21), 1–7. doi:10.1093/femsle/fny211

Qi, L. S., Larson, M. H., Gilbert, L. A., Doudna, J. A., Weissman, J. S., Arkin, A. P., et al. (2013). Repurposing CRISPR as an RNA-Guided Platform for Sequence-specific Control of Gene Expression. *Cell* 152, 1173–1183. doi:10.1016/j.cell.2013.02.022

Raj, S. M., Rathnasingh, C., Jung, W.-C., Selvakumar, E., and Park, S. (2010). A Novel NAD(+)-dependent Aldehyde Dehydrogenase Encoded by the *puuC* Gene of *Klebsiella pneumoniae* DSM 2026 that Utilizes 3-

Hydroxypropionaldehyde as a Substrate. *Biotechnol. Bioproc E* 15, 131–138. doi:10.1007/s12257-010-0030-2

Semkiv, M. V., Dmytruk, K. V., Abbas, C. A., and Sibirny, A. A. (2017). Metabolic Engineering for High Glycerol Production by the Anaerobic Cultures of *Saccharomyces cerevisiae*. *Appl. Microbiol. Biotechnol.* 101, 4403–4416. doi:10.1007/s00253-017-8202-z

Straathof, A. J. J., Sie, S., Franco, T. T., and Van Der Wielen, L. A. M. (2005). Feasibility of Acrylic Acid Production by Fermentation. *Appl. Microbiol. Biotechnol.* 67, 727–734. doi:10.1007/s00253-005-1942-1

Wang, J., Zhao, P., Li, Y., Xu, L., and Tian, P. (2018). Engineering CRISPR Interference System in *Klebsiella pneumoniae* for Attenuating Lactic Acid Synthesis. *Microb. Cell Fact.* 17, 56. doi:10.1186/s12934-018-0903-1

Winkler, B. S., Sauer, M. W., and Starnes, C. A. (2003). Modulation of the Pasteur Effect in Retinal Cells: Implications for Understanding Compensatory Metabolic Mechanisms. *Exp. Eye Res.* 76, 715–723. doi:10.1016/s0014-4835(03)00052-6

Xu, X., and Qi, L. S. (2019). A CRISPR-dCas Toolbox for Genetic Engineering and Synthetic Biology. *J. Mol. Biol.* 431, 34–47. doi:10.1016/j.jmb.2018.06.037

Yang, T. H., Rathnasingh, C., Lee, H. J., and Seung, D. (2014). Identification of Acetoin Reductases Involved in 2,3-butanediol Pathway in *Klebsiella Oxytoca*. *J. Biotechnol.* 172, 59–66. doi:10.1016/j.jbiotec.2013.12.007

Zhao, P., and Tian, P. (2021). Biosynthesis Pathways and Strategies for Improving 3-hydroxypropionic Acid Production in Bacteria. *World J. Microbiol. Biotechnol.* 37, 117. doi:10.1007/s11274-021-03091-6

Zhao, P., Ma, C., Xu, L., and Tian, P. (2019). Exploiting Tandem Repetitive Promoters for High-Level Production of 3-hydroxypropionic Acid. *Appl. Microbiol. Biotechnol.* 103, 4017–4031. doi:10.1007/s00253-019-09772-5

Zhao, P., Li, Q., Tian, P., and Tan, T. (2021). Switching Metabolic Flux by Engineering Tryptophan Operon-Assisted CRISPR Interference System in *Klebsiella pneumoniae*. *Metab. Eng.* 65, 30–41. doi:10.1016/j.ymben.2021.03.001

Zheng, Y., Zhao, L., Zhang, J., Zhang, H., Ma, X., and Wei, D. (2008). Production of Glycerol from Glucose by Coexpressing Glycerol-3-Phosphate Dehydrogenase and Glycerol-3-Phosphatase in *Klebsiella pneumoniae*. *J. Biosci. Bioeng.* 105, 508–512. doi:10.1263/jbb.105.508

Conflict of Interest: The authors declare that the research was conducted in the absence of any commercial or financial relationships that could be construed as a potential conflict of interest.

Publisher's Note: All claims expressed in this article are solely those of the authors and do not necessarily represent those of their affiliated organizations, or those of the publisher, the editors, and the reviewers. Any product that may be evaluated in this article, or claim that may be made by its manufacturer, is not guaranteed or endorsed by the publisher.

frontiers | Frontiers in Bioengineering and Biotechnology

TYPE Mini Review
PUBLISHED 19 July 2022
DOI 10.3389/fbioe.2022.966598

OPEN ACCESS

EDITED BY
Xinjun Feng,
Qingdao Institute of Bioenergy and Bioprocess Technology (CAS), China

REVIEWED BY
Zheng-Jun Li,
Beijing University of Chemical Technology, China
Dan Tan,
Xi'an Jiaotong University, China

*CORRESPONDENCE
Markus Neureiter,
markus.neureiter@boku.ac.at
Yina Lin,
linyina2021@163.com
Jian-Wen Ye,
yejianwen@scut.edu.cn

†These authors have contributed equally to this work

SPECIALTY SECTION
This article was submitted to Bioprocess Engineering, a section of the journal Frontiers in Bioengineering and Biotechnology

RECEIVED 11 June 2022
ACCEPTED 01 July 2022
PUBLISHED 19 July 2022

CITATION
Gao Q, Yang H, Wang C, Xie X-Y, Liu K-X, Lin Y, Han S-Y, Zhu M, Neureiter M, Lin Y and Ye J-W (2022), Advances and trends in microbial production of polyhydroxyalkanoates and their building blocks.
Front. Bioeng. Biotechnol. 10:966598.
doi: 10.3389/fbioe.2022.966598

Advances and trends in microbial production of polyhydroxyalkanoates and their building blocks

Qiang Gao[1†], Hao Yang[2†], Chi Wang[2†], Xin-Ying Xie[2], Kai-Xuan Liu[2], Ying Lin[2], Shuang-Yan Han[2], Mingjun Zhu[2], Markus Neureiter[3*], Yina Lin[2*] and Jian-Wen Ye[2*]

[1]Key Laboratory of Plateau Ecology and Agriculture, Qinghai University, Xining, QH, China, [2]School of Biology and Biological Engineering, South China University of Technology, Guangzhou, China, [3]Institute for Environmental Biotechnology, Department of Agrobiotechnology, University of Natural Resources and Life Sciences, Tulln, Austria

With the rapid development of synthetic biology, a variety of biopolymers can be obtained by recombinant microorganisms. Polyhydroxyalkanoates (PHA) is one of the most popular one with promising material properties, such as biodegradability and biocompatibility against the petrol-based plastics. This study reviews the recent studies focusing on the microbial synthesis of PHA, including chassis engineering, pathways engineering for various substrates utilization and PHA monomer synthesis, and PHA synthase modification. In particular, advances in metabolic engineering of dominant workhorses, for example *Halomonas, Ralstonia eutropha, Escherichia coli* and *Pseudomonas,* with outstanding PHA accumulation capability, were summarized and discussed, providing a full landscape of diverse PHA biosynthesis. Meanwhile, we also introduced the recent efforts focusing on structural analysis and mutagenesis of PHA synthase, which significantly determines the polymerization activity of varied monomer structures and PHA molecular weight. Besides, perspectives and solutions were thus proposed for achieving scale-up PHA of low cost with customized material property in the coming future.

KEYWORDS

polyhydroxyalkanoates, synthetic pathway, metabolic engineering, PHA synthase, microbial production

Introduction

Polyhydroxyalkanoates (PHAs) is a series of polyesters synthesized by different microbes (Steinbüchel, 2001), which have been widely used as bio-plastics for replacing petrol-based plastic due to their outstanding biodegradability and biocompatibility. Accordingly, PHA can be divided into three categories (Sudesh et al., 2000) including short-, medium- and long- chain-length PHAs, namely SCL-, MCL- and LCL-PHA, respectively. Of which, the monomers of SCL-, MCL- and LCL-

PHA generally contain 2–5, 6–14 and over 15 carbon atoms, respectively. Because of the competitive material properties, PHA has attracted growing attentions of commercial interests in different application areas, such as medical implant (Chen and Wu, 2005), cosmetic beads (Choi et al., 2020), packaging (Chen and Patel, 2012), agricultural film (Chen, 2009), textile (Chen, 2009), feeding additives (Chen, 2009) and so on. In the past decades, intensive efforts have been made to generate various PHA productions consisting of diverse polymerized units with different carbon-chain-length and structures by genetically modified bacterial (Chen and Jiang, 2017), such as *Halomonas spp.* (Tan et al., 2011; Fu X. Z. et al., 2014), *Ralstonia eutropha* (Antonio et al., 2000; Raberg et al., 2018; Xiong et al., 2018), *Escherichia coli* (Park et al., 2001; Linares-Pastén et al., 2015; Sudo et al., 2020), *Pseudomonas* spp (Chanasit et al., 2016; Liang et al., 2020; Li M. et al., 2021) and so on (Hyakutake et al., 2014; Tariq et al., 2015). Therefore, over 150 types of PHAs have been obtained including homopolymers (PHB, poly-3-hydroxybutyrate) (Tan et al., 2011), random- and/or block-copolymers such as poly(3-hydroxybutyrate-*co*-4-hydroxybutyrate) (P34HB), poly(3-hydroxybutyrate-*co*-3-hydroxyvalerate) (PHBV) (Fu X. Z. et al., 2014), poly(3-hydroxybutyrate-*co*-3-hydroxyhexonate) (PHBHHx) (Park et al., 2001), etc. (Li M. et al., 2021). To date, many building blocks, including rational designed enzymes (Chek et al., 2019; Lim et al., 2021), fine-tuned metabolic pathways towards monomer synthesis (Pacholak et al., 2021) and genetically engineered chassis of predominant PHA accumulation performance (Liang et al., 2020; Ye and Chen, 2021), have been developed for sufficient PHA synthesis using a variate of substrates.

In particular, scale-up industrial production lines for various PHA manufacturing have been recently launched or established by several companies, for example, MedPHA (operating production line of 1,000 ton/year PHB and/or P34HB, China) (Obruča et al., 2022), PhaBuilder (10,000 ton/year, under construction, China) (Yang et al., 2010), Tianan (3,000 ton/year PHBV, China) (Modi et al., 2011), Tepha (P4HB for medical uses, United States) (Martin and Williams, 2003), Danimer Scientific (6,000 ton/year PHBHHx, United State) (Mehrpouya et al., 2021), Keneka (5,000 ton/year PHBHHx, Japan) (Tanaka et al., 2021). However, the production cost of PHA still challenges for wide range commercial uses. Therefore, many solutions have been proposed and developed to reduce the industrial cost of PHA, including high cell density fermentation based on optimized feeding solution (Silva et al., 2017), non-sterile open fermentation process based on recombinant halophiles (Tan et al., 2011), cell factory engineering for effective utilization of low-cost carbon sources (Murugan et al., 2017; Panich et al., 2021), carbon fixation engineering for the improved conversion rate from glucose to PHA (Salehizadeh et al., 2020), co-production of PHA and value-added chemicals (Lan et al., 2016; Li et al., 2016) and so on.

Therefore, this study summarized recent advances of various PHA production and industrial trends thereof. Additionally, major building blocks, including representative workhorses, metabolic pathways and critical enzymes, for PHA synthesis have been reviewed and discussed. This study provides an entire landscape of PHA productions powered by synthetic biology, as well as perspectives focusing on cost-effective PHA manufacturing in the coming future.

Workhorses for PHA production

Halomonas bluephagenesis TD01

Halomonas bluephagenesis TD01 (*H. bluephagenesis*), a natural PHB producer isolated from salt lake (Tan et al., 2011), has been recently developed as a versatile chassis for PHA productions and value added chemicals, which exemplifies a cost-effective biomanufacturing paradigm based on next generation industrial biotechnology (NGIB) enabling non-sterile open fermentation process under high salt and high pH condition (Ye and Chen, 2021). Currently, the genetically reprogrammed *H. bluephagenesis* can produce various PHA polymers, including PHB (Tan et al., 2011), PHBV (Fu X. Z. et al., 2014), P34HB (Chen et al., 2017) and PHBP (poly-3-hydroxybutyrate-*co*-3-hydroxypropionate) (Jiang et al., 2021) using glucose, starch, gluconate and structural related carbon sources for corresponding monomer synthesis whenever necessary, for example, 4HB from γ-butyrolactone (GBL), 3HP from 1,3-propanediol, 3HV from propionate, etc. Notably, pilot-scale production of PHB and P34HB have succeeded in a 5,000-L bioreactor, yielding up to 100 g/L dry cell mass (DCM) containing 60–70 wt% PHA content with over 30% cost reduction (Ye et al., 2018). Besides, engineering electron transport system could significantly improve the supplementation of NADH (Ling et al., 2018), overexpression of Vitreoscilla hemoglobin (VHb) protein led to improved oxygen uptake efficiency (Ouyang et al., 2018), deficiency of outer membrane synthesis enabled sufficient production yield of PHA from glucose and simplified cell lysis (Wang Z. et al., 2021), manipulation of cell morphology also resulted in self-flocculation separation process (Ling et al., 2019). Moreover, different genetic parts and tools have been established allowing for rational engineering of *H. bluephagenesis* (Zhang et al., 2020). These efforts have proved successful in building a high-performing workhorse for PHA production based on NGIB. Additionally, many other *Halomonas* strains were also successfully developed for PHA synthesis, such as *Halomonas campanesis* LS21 (Yue et al., 2014), *Halomonas*

elongate DSM2581 (Ilham et al., 2014), *Halomonas pacifica* ASL10 (Abd El-malek et al., 2020) and so on, illustrating the great potential of halophiles used as PHA producers.

Ralstonia eutropha

Ralstonia eutropha H16 (*Cupriavidus necator*) is a well-studied PHA producer from glucose, glycerol, palm oil and other fatty acids (FAs) (Murugan et al., 2017). In addition to short chain length PHA synthesis, *R. eutropha* H16 has been engineered to produce varied copolymers consisting of SCL-monomer (3HB) and MCL-monomers, such as 3HHx, 3HO (3-hydroxyoctanoate), 3HDD (3-hydroxydodecanoate) and so on (Antonio et al., 2000). In previous studies, genetic editing tools for chromosomal engineering was established based on CRISPR/Cas9 system and Cre/LoxP integrase system (Park et al., 2001). An electroporation approach was developed in recombinant *R. eutropha* H16 allowing for sufficient and high-through clone construction (Xiong et al., 2018). More importantly, over 200 g/L DCM with over 70 wt% PHA accumulation can be obtained by *R. eutropha* H16 and its derivates during fed-batch fermentation conducted in the lab- (<10-L) and/or pilot- (>100-L) scale bioreactors under strictly sterilized conditions (Ryu et al., 1997). Moreover, industrial productions of PHB, PHBV and PHBHHx based on recombinant *R. eutropha* H6 have been achieved by several companies. Therefore, *R. eutropha* H16 is expected to be a prominent chassis for PHA productions, especially for PHBHHx, however, high production cost remains challenging (Raberg et al., 2018).

Escherichia coli

Escherichia coli (*E. coli*), such BL21, JM109, etc., are well-studied model chassis that have clear genetic background and effective genetic tools for cell factory engineering of varied purposes, such as PHA biosynthesis. Even though *E. coli* is not a natural PHA producer, the heterogonous expression of *phaCAB* gene cluster from *R. eutropha* could efficiently boost carbon flux from pyruvate towards PHB synthesis. Therefore, intensive studies focusing on CO_2 fixation (Lee et al., 2021), pathway engineering (Chen and Jiang, 2017) and feeding solution design of fed-batch fermentation (Yang et al., 2014) have been performed to generate enhanced production yield of PHB. Besides, *E. coli* is an ideal workhorse for studying the novel-type PHA synthesis, such as copolymers of 3HB and lactate, glycolic acid, 4-hydroxybutyrate, 5-hydroxyvalerate and other monomers with functional groups (Scheel et al., 2021). Specifically, the DCM and PHA content reached up to 194 g/L and 73 wt% by recombinant *E. coli* grown in fed-batch fermentation condition (JONG-IL CHOI, 1998), which shows promising performance in PHA accumulation.

Pseudomonas

Pseudomonas, including *P. putida* KT2440, *P. entomophila*, etc. have been recently engineered to be dominant producers of PHA copolymers consist of 3HB and MCL- and LCL-3HAs due to their strong FAs metabolism involved in β-oxidation cycle and *de novo* FAs synthesis pathways. Currently, PHA copolymers are composed of 3HB, 4HB, 3HV, 3HHx, 3HHp (3-hydroxyheptanoate), 3HO (3-hydroxyoctanoate), 3HD (3-hydroxydecanoate), etc. could be obtained by metabolically engineered *Pseudomonas* strains (Prieto et al., 2016). Many PHA synthases able to polymerize MCL- and LCL-3HA into polymers were thus identified from different *Pseudomonas* strains (Chung et al., 2011; Li et al., 2019; Tan et al., 2020; Li M. et al., 2021). Notably, an effective platform was developed for producing full spectrum of PHAs, which contain SCl-, MCL, LCL- 3HAs and monomers carrying carbon-carbon double bones, with over 90% increase in production yield based on recombinant *P. entomophila* (Li M. et al., 2021). Moreover, higher DCM, reaching over 70 g/L, was also achieved by *Pseudomonas* leveraging fed-batch fermentation process optimization (Cerrone et al., 2014). These efforts demonstrate proven success in scalable tailor-made PHA synthesis of varied functions by reprogrammed *Pseudomonas*.

Additionally, various attempts have been carried out to achieve PHA synthesis based on different hosts, such as *Alcaligenes* (H W Ryu 1996), *Bacillus* (Sathiyanarayanan et al., 2013), *Burkholderia* (Miranda De Sousa Dias et al., 2017), *microalgae* (Costa et al., 2019), *Salinivibrio* (Van Thuoc et al., 2019; Van Thuoc et al., 2020), *Marinobacterium* (Wang et al., 2022), *Vibrio alginolyticus* (Li H. F. et al., 2021) and so on, using diverse carbon sources including sucrose, propionate, carbon dioxide, volatile fatty acids, etc. It is important to note that the highest resultant DCM reached up to 281 g/L with 232 g/L PHB accumulation by *Alcaligenes eutrophus*, a natural PHB producer of high cell density growth and effective PHA accumulation, during a 74 h fed-batch fermentation conducted in a 60-L bioreactor (H W Ryu 1996).

Metabolic pathways for PHA synthesis

The biosynthesis pathways of most PHA monomers from varied carbon sources like glucose, fatty acids, etc. are mainly related to essential carbon metabolic pathways, such as glycolysis, β-oxidation and *de novo* fatty acid synthesis (Figure 1). Besides, using structurally related carbon sources as precursors is an alternative strategy to generate diverse PHA copolymers

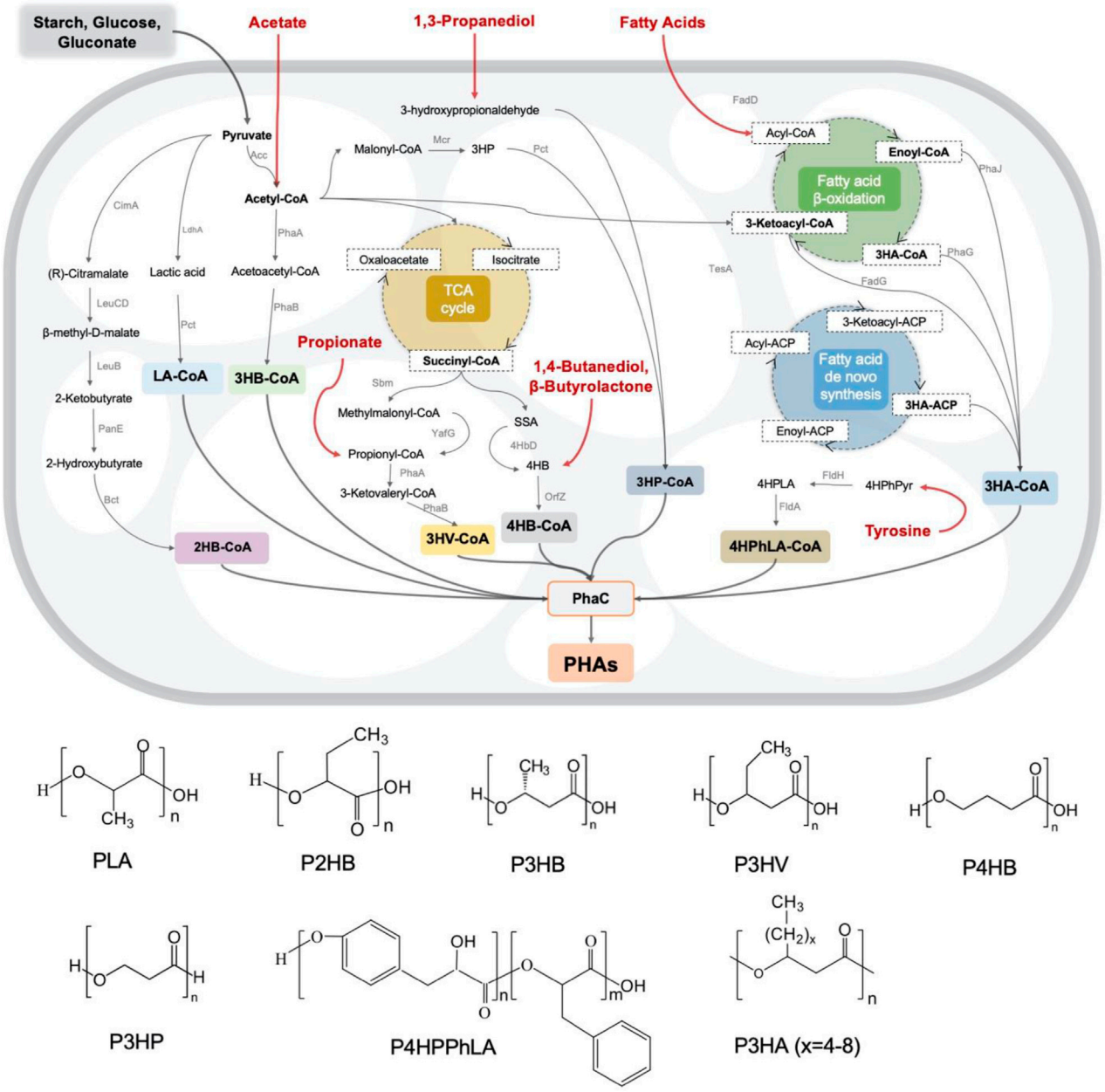

FIGURE 1
Metabolic pathways and monomer structures of different microbial synthesized PHAs.

consist of different monomers, including 4HB from γ-butyrolactone (GBL)/1,4-butanediol (BDO), 3HV from propionate, 3HP from 1,3-propionediol (PDO), middle- and long-chain length 3HA from different fatty acids with corresponding carbon atoms and so on, which have significant impact on the material property (Chen et al., 2016). Therefore, a wide variety of PHA homo- and co-polymers can be obtained by engineered microbes by feeding customized feedstocks (Figure 1).

PHA from structure-unrelated carbon sources

Glucose is a widely used feedstock in biomanufacturing. Similarly, intensive studies have been carried out for generating different PHA using glucose as the sole carbon source by metabolically engineered microorganisms. To date, many metabolic pathways have been mined and refined as significant building blocks for rewiring glucose-derived fluxes

towards various monomers, such as converting pyruvate into2HB-CoA (Park et al., 2012c) and LA-CoA (Park et al., 2012b), acetyl-CoA into 3HB-CoA and 3HP-CoA (Meng et al., 2015), succinyl-CoA into 3HV-CoA (Bhatia et al., 2015) and 4HB-CoA (Lv et al., 2015), respectively. Interestingly, starch (Yang et al., 2020), volatile fatty acids like acetate (Yang et al., 2019), waste gluconate (Ciesielski et al., 2010), the byproduct of glucose processing, were also used to culture engineered *Halomonas* and *Pseudomonas* to achieve cost-effective PHA productions (Figure 1).

In addition to glucose, building blocks for many other carbon sources metabolism, such as glycerol, sucrose, xylose, C1 compounds, etc., have been constructed to synthesize PHA. Specifically, the highest PHA accumulation, reaching 38.9 wt% with 0.34 g/L/h of productivity have been achieved by engineered *P. putida* KT2440 (Borrero-de Acuna et al., 2021). Fu et al. produced MCL-PHA also could be obtained by grown on chemical-grade glycerol (PG) and biodiesel-derived waste glycerol (WG) as sole carbon sources (Fu J. et al., 2014). Moreover, recombinant strains including *P. putida S12* and *R. eutropha* harboring expression vessel containing isomerase (XylA) and xylulokinase (XylB) have been constructed by Meijnen et al. (2008) and Kim et al. (2017), respectively, to produce PHA using xylose as sole carbon source (Meijnen et al., 2008). Similarly, a sucrose-favored *P. putida* strain was also developed for PHA synthesis from sucrose only (Hobmeier et al., 2020). More importantly, due to the growing interests of global carbon neutral, many bacterial like *P. furiosus* and *R. eutropha* B8562 were engineered to produce PHA polymers containing 3HP and 3HB units, respectively, using CO_2 as carbon source (Volova et al., 2006; Keller et al., 2013). Besides, biosynthesis pathways for PHA synthesis from CH_4 were also established based on many hydrogen-oxidizing bacteria (Khosravi-Darani et al., 2013). In summary, metabolic engineering of microbes is able to achieve targeted PHA synthesis from different structure-unrelated carbon sources.

PHA from structure-related carbon sources

For most MCL- and LCL-PHA synthesis, supplementation of structure-related fatty acids in the medium is a commonly used strategy to grow recombinant cells with defected β-oxidation cycle or reprogramed *de novo* fatty acids synthesis pathways (Gutierrez-Gomez et al., 2019). For instance, a wide range of PHA copolymers composed of 3HB and MCL-/LCL-3HA units containing carbon atoms numbered from 6 to 18, even with carbon-carbon double bone, have been achieved by engineered *Pseudomonas*, yielding over 100% increase of production titer (Yao J, 1999). Besides, many short chain length (SCL) PHA units were also produced from structure-related carbon sources used as precursors, such as 4HB synthesis from 1,4-propanediol (PDO) and β-butyrolactone (GBL) (Cavalheiro et al., 2012), 3HP synthesis from 1,3-propionediol (PDO) (Zhou et al., 2011), 5HV synthesis from 1,5-pentanediol (Yan et al., 2022), as well as functional group monomer like 4HPhLA synthesized from tyrosine (Yang et al., 2018), etc. Recently, high production yield of P34HB with 4HB molar ratio from 5 mol% to 26 mol% has been achieved by recombinant *H. bluephagenesis* based on NGIB platform, which also demonstrated the success in scale-up production of low cost conducted in 5-to-200 m^3 fermenters (Ling et al., 2018). Notably, Lee et al. (2021) used engineered *Escherichia coli* to synthesize aromatic polyester, P(3HB-*co*-D-phenylacetate), from tyrosine, of which the molar ratio of D-phenylacetate monomer reaches up to 47.7 mol% (Yang et al., 2018). Moreover, tailor-made copolymers, as well as block copolymers, consisting of two, three and even more units could be easily obtained by designing the supplementation formula of target precursors and feeding strategy thereof (Yu et al., 2020).

Engineering tools and strategies for sufficient PHA synthesis

In addition to the biosynthesis pathway construction for diverse PHA productions, many metabolic engineering tools including high resolution gene expression tuning (Ye et al., 2020), high throughput library construction (Zhou et al., 2015; Young et al., 2018), constitutive and inducible promoter design (Shen et al., 2018; Ma et al., 2020) and so on have been developed for constructing effective PHA producing strains. Moreover, a carbon fixation of CO_2 was established in *E. coli* to generate an increased bioconversion rate of glucose towards PHB (Lin et al., 2015). Modulating the NADH levels and its regeneration pathways could also show proven effects on PHA accumulation in both *E. coli* and *Halomonas* strains with PHA content increased up to 90 wt% (Ling et al., 2018). Interestingly, cell morphology control is an efficient strategy to obtain enhanced PHA accumulation with significantly improved substrate conversion rate (Wang X. et al., 2021). Manipulation of PHA granule size also demonstrated strong significance for downstream processing, which dramatically reduce the energy consumption of cell separation and PHA purification (Kourmentza et al., 2017). Therefore, the downstream-inspired engineering of microbes also displays great significance in cost-reduction for industrial PHA biomanufacturing.

PHA synthase

PHA synthase (PhaC) is an important building block for PHA synthesis. Generally, there are four major types of PhaC, namely Class-I/II/III/IV (Możejko-Ciesielska and Kiewisz, 2016), which have been identified from different PHA producing strains (Table 1). Of which, Class-I, -III and IV generally show higher activity on short-chain-length (SCL) monomers (C3-C5) polymerization, while Class-II has higher specificity to

TABLE 1 Different PHA synthases identified from natural PHA producing strains.

Class	Source	Expression host	PHA	PHA content	DCM (g/L)	References
I	*Ralstonia eutropha*	*A. eutrophus* (NCIMB 11599)	PHB	83 wt%	281	Ryu et al. (1997)
I	*Ralstonia eutropha*	*C. necator* Re2133	P (3HB-*co*-18.5 mol% 3HHx)	52 wt%	1.1	Bhatia et al. (2019)
I	*Ralstonia eutropha*	*Ralstonia eutropha* PHB-4	P (3HB-*co*-5 mol% 3HP-*co*-10 mol % 5HV)	12 wt%	0.3	Chuah et al. (2013)
I	*Ralstonia eutropha*	*E. coli* JM109SGIK	P (3HB-*co*-7.89 mol% 4HB)	78 wt%	11.6	Wang et al. (2014)
I	*Ralstonia eutropha H16*	*Pseudomonas putida* KTOY08ΔGC	P (3HB-*b*-80.31 mol% 4HB)	50 wt%	5.5	Hu et al. (2011)
I	*Ralstonia eutropha*	*E. coli*	P (3HB-*co*-84 mol% 3HP)	42 wt%	5	Meng et al. (2015)
I	*Aeromonas caviae*	*Ralstonia eutropha* PHB-4	P (3HB-*co*-35 mol% 3HV-*co*-3HHx)	80 wt%	7.1	Wang et al. (2014)
I	*Chromobacterium sp*	*E. coli*	P3HP	40 wt%	-	Linares-Pastén et al. (2015)
I	*Aeromonas caviae*	*Burkholderia* sp. USM (JCM15050)	P (3HB-*co*-34 mol% 3HV-*co*-6 mol% 3HHx)	86 wt%	1.5	Chee et al. (2012)
II	*Pseudomonas sp. 61–3*	*Pseudomonas entomophila*	P (3HB-*co*-14 mol% 3HPD)	60 wt%	9	Li et al. (2021b)
II	*Pseudomonas sp. 61–3*	*E. coli* W3110	P (11 mol% 3HHx-*co*-39 mol% 3HO-*co*-50 mol% 3HD)	4.8 wt%	1.7	Park et al. (2002)
II	*Pseudomonas sp. MBEL 6–19*	*E. coli* XL1-Blue	P (38.1 mol% PhLA-*co*-3HB)	55 wt%	13.9	Yang et al. (2018)
II	*Pseudomonas sp. MBEL 6–19*	*E. coli* XL1-Blue	P (88.2 mol%LA-*co*-11.8 mol%GA)	12.6 wt%	-	Choi et al. (2016)
II	*Pseudomonas*	*E. coli*	P (8.2 mol%GA-*co*-16.3 mol%GA-*co*-66.1 mol%3HB-*co*-9.4 mol%4HB)	72.89 wt%	19.6	Li et al. (2017)
II	*Pseudomonas mendocina*	*Pseudomonas mendocina*	P (3HB-*co*-3HO-*co*-3HD)	77 wt%	3.7	Chanasit et al. (2016)
II	*Pseudomonas oleovorans ATCC 29347*	*Pseudomonas oleovorans* ATCC 29347	mcl-PHA	63 wt%	18	Jung et al. (2001)
III	*Thiocapsa pfennigii*	*Pseudomonas putida* GPp104	P (3HB-*co*-3HV-*co*-15.4 mol% 4HV)	52 wt%	20	Gorenflo et al. (2001)
IV	*Bacillus cereus FA11*	*Bacillus cereus* FA11	P (3HB-*co*-6.49 mol% 3HV)	49 wt%	6.2	Tariq et al. (2015)
IV	*Bacillus cereus YB-4*	*E. coli* JM109	PHB	36 wt%	3.0	Hyakutake et al. (2014)
-	*Halomonas bluephagenesis TD01*	*Halomonas bluephagenesis* TD01	P (3HB-*co*-16.1 mol% 4HB)	61 wt%	82.6	Chen et al. (2017)
-	*Burkholderia sacchari DSM 17165*	*Burkholderia sacchari* DSM 17165	P (3HB-*co*-1.6 mol% 4HB)	73 wt%	72.9	Miranda De Sousa Dias et al. (2017)
-	*Cupriavidus malaysiensis USMAA2-4*	*Cupriavidus malaysiensis* USMAA1020	P (3HB-*co*-99 mol% 4HB)	92 wt%	50.4	Norhafini et al. (2019)

-Not classified PHA synthase.

medium- and long- chain-length (M/LCL) monomers containing 6–18 carbon atoms, namely C6-C18 (Chek et al., 2017). Specifically, most Class-I PHA synthases, such as PhaCs from *R. eutropha* (Ushimaru et al., 2014), *Alcaligenes latus* (Park et al., 2012a), *Aeromonas Caviae* and *Chromobacterium sp.* (Choi et al., 2020), not only show effective activity on SCL PHA accumulation including 3HB, 3HP, 4HB and 3HV units, but also display polymerization capability of MCL PHA like 3HHx (Antonio et al., 2000).

Recently, many efforts have been made to modified the polymerization activity of PHA synthase, including protein structure analysis (Chek et al., 2017), mutagenesis (Zou et al., 2017) and fusion of functional domains from different PhaCs (Matsumoto et al., 2009), to generate high-performing PHA synthase. For instance, Kim et al. (2017) report the first crystal structure of *Ralstonia eutropha* PHA synthase at 1.8 Å resolution and structure-based mechanisms for PHA polymerization, RePhaC1 contains two distinct domains, the N-terminal (RePhaC1ND) and C-terminal domains (RePhaC1CD), and exists as a dimer (Kim et al., 2017). Furthermore, site-directed mutation was employed to generate PhaC mutants, namely $PhaC_{61-3}$ and $PhaC_{1437}$, based on PHA synthases from *Pseudomonas* sp. 61–3 and *Pseudomonas* sp. MBEL 6–19, respectively, which show wide substrate specificity to both SCL and M/LCL monomers (Yang et al., 2010), as well as monomers with a particular structure like benzene ring (Mizuno et al., 2018).

Moreover, an artificial PHA synthase, $PhaC_{AR}$, was constructed by hybridizing the C-terminal of $PhaC_{AC}$ from *Aermonas Caviae* and N-terminal of $PhaC_{RE}$ from *R. eutropha* (*Cupriavidus necator*), enabling effective accumulation for block copolymers containing 2-hydroxybutyrate (2HB) (Sudo et al., 2020);

Conclusion and perspective

In this study, we highlighted the global trends of industrial PHA productions reported by different companies and start-up teams, and briefly summarized and discussed the advances of different building blocks focusing on PHA synthase, biosynthesis pathways of SCL-, MCL- and LCL-PHA, dominant PHA workhorses of industrial potential and optimization strategies for effective PHA synthesis. This study provides an overview of PHA biosynthesis from enzyme engineering, cell factory design, towards scale-up bio-manufacturing. However, more attempts are still required to achieve further cost-reduction and improved material properties of tailor-made PHAs against the petrol-based plastics.

Author contributions

QG, HY, and CW contributed equally in this study. X-YX, K-XL, YgL, S-YH, MN, YaL, and J-WY wrote the manuscript, J-WY, YaL, and MN proposed the idea and revised the manuscript.

Funding

This research is supported by National Natural Science Foundation of China (Grant No. 32001029), National Natural Science Foundation of Qinghai Province (Grant No. 2020-ZJ-759), Guangdong Basic and Applied Basic Research Foundation (Grant No. 2020A1515111079), State Key Laboratory of Plateau Ecology and Agriculture, Qinghai University (Grant No. 2021-KF-09), and Tsinghua University-INDITEX Sustainable Development Fund (Grant No. TISD201907).

Conflict of interest

The authors declare that the research was conducted in the absence of any commercial or financial relationships that could be construed as a potential conflict of interest.

Publisher's note

References

Abd El-Malek, F., Farag, A., Omar, S., and Khairy, H. (2020). Polyhydroxyalkanoates (PHA) from Halomonas pacifica ASL10 and Halomonas salifodiane ASL11 isolated from Mariout salt lakes. *Int. J. Biol. Macromol.* 161, 1318–1328. doi:10.1016/j.ijbiomac.2020.07.258

Antonio, R. V., Steinbüchel, A., and Rehm, B. H. A. (2000). Analysis of *in vivo* substrate specificity of the PHA synthase from Ralstonia eutropha: Formation of novel copolyesters in recombinant *Escherichia coli*. *FEMS Microbiol. Lett.* 182, 111–117. doi:10.1111/j.1574-6968.2000.tb08883.x

Bhatia, S. K., Gurav, R., Choi, T.-R., Jung, H.-R., Yang, S.-Y., Song, H.-S., et al. (2019). Poly(3-hydroxybutyrate-co-3-hydroxyhexanoate) production from engineered Ralstonia eutropha using synthetic and anaerobically digested food waste derived volatile fatty acids. *Int. J. Biol. Macromol.* 133, 1–10. doi:10.1016/j.ijbiomac.2019.04.083

Bhatia, S. K., Yi, D. H., Kim, H. J., Jeon, J. M., Kim, Y. H., Sathiyanarayanan, G., et al. (2015). Overexpression of succinyl-CoA synthase for poly (3-hydroxybutyrate-co-3-hydroxyvalerate) production in engineered *Escherichia coli* BL21(DE3). *J. Appl. Microbiol.* 119, 724–735. doi:10.1111/jam.12880

Borrero-De Acuna, J. M., Rohde, M., Saldias, C., and Poblete-Castro, I. (2021). Fed-batch mcl- polyhydroxyalkanoates production in Pseudomonas putida KT2440 and DeltaphaZ mutant on biodiesel-derived crude glycerol. *Fron t Bioeng. Biotechnol.* 9, 642023. doi:10.3389/fbioe.2021.642023

Cavalheiro, J. M., De Almeida, M. C., Da Fonseca, M. M., and De Carvalho, C. C. (2012). Adaptation of Cupriavidus necator to conditions favoring polyhydroxyalkanoate production. *J. Biotechnol.* 164, 309–317. doi:10.1016/j.jbiotec.2013.01.009

Cerrone, F., Duane, G., Casey, E., Davis, R., Belton, I., Kenny, S. T., et al. (2014). Fed-batch strategies using butyrate for high cell density cultivation of Pseudomonas putida and its use as a biocatalyst. *Appl. Microbiol. Biotechnol.* 98, 9217–9228. doi:10.1007/s00253-014-5989-8

Chanasit, W., Hodgson, B., Sudesh, K., and Umsakul, K. (2016). Efficient production of polyhydroxyalkanoates (PHAs) from Pseudomonas mendocina PSU using a biodiesel liquid waste (BLW) as the sole carbon source. *Biosci. Biotechnol. Biochem.* 80, 1440–1450. doi:10.1080/09168451.2016.1158628

Chee, J.-Y., Lau, N.-S., Samian, M.-R., Tsuge, T., and Sudesh, K. (2012). Expression of Aeromonas caviae polyhydroxyalkanoate synthase gene in Burkholderia sp. USM (JCM15050) enables the biosynthesis of SCL-MCL PHA from palm oil products. *J. Appl. Microbiol.* 112, 45–54. doi:10.1111/j.1365-2672.2011.05189.x

Chek, M. F., Hiroe, A., Hakoshima, T., Sudesh, K., and Taguchi, S. (2019). PHA synthase (PhaC): Interpreting the functions of bioplastic-producing enzyme from a structural perspective. *Appl. Microbiol. Biotechnol.* 103, 1131–1141. doi:10.1007/s00253-018-9538-8

Chek, M. F., Kim, S. Y., Mori, T., Arsad, H., Samian, M. R., Sudesh, K., et al. (2017). Structure of polyhydroxyalkanoate (PHA) synthase PhaC from Chromobacterium sp. USM2, producing biodegradable plastics. *Sci. Rep.* 7, 5312. doi:10.1038/s41598-017-05509-4

Chen, G.-Q., and Patel, M. K. (2012). Plastics derived from biological sources: Present and future: A technical and environmental review. *Chem. Rev.* 112, 2082–2099. doi:10.1021/cr200162d

Chen, G.-Q., and Wu, Q. (2005). The application of polyhydroxyalkanoates as tissue engineering materials. *Biomaterials* 26, 6565–6578. doi:10.1016/j.biomaterials.2005.04.036

Chen, G. Q. (2009). A microbial polyhydroxyalkanoates (PHA) based bio- and materials industry. *Chem. Soc. Rev.* 38, 2434. doi:10.1039/b812677c

Chen, G. Q., and Jiang, X. R. (2017). Engineering bacteria for enhanced polyhydroxyalkanoates (PHA) biosynthesis. *Synth. Syst. Biotechnol.* 2, 192–197. doi:10.1016/j.synbio.2017.09.001

Chen, G. Q., Jiang, X. R., and Guo, Y. (2016). Synthetic biology of microbes synthesizing polyhydroxyalkanoates (PHA). *Synth. Syst. Biotechnol.* 1, 236–242. doi:10.1016/j.synbio.2016.09.006

Chen, X., Yin, J., Ye, J., Zhang, H., Che, X., Ma, Y., et al. (2017). Engineering Halomonas bluephagenesis TD01 for non-sterile production of poly(3-hydroxybutyrate-co-4-hydroxybutyrate). *Bioresour. Technol.* 244, 534–541. doi:10.1016/j.biortech.2017.07.149

Choi, S. Y., Cho, I. J., Lee, Y., Kim, Y.-J., Kim, K.-J., Lee, S. Y., et al. (2020). Bacterial polyesters: Microbial polyhydroxyalkanoates and nonnatural polyesters (adv. Mater. 35/2020). *Adv. Mat.* 32, 2070264. doi:10.1002/adma.202070264

Choi, S. Y., Park, S. J., Kim, W. J., Yang, J. E., Lee, H., Shin, J., et al. (2016). One-step fermentative production of poly(lactate-co-glycolate) from carbohydrates in *Escherichia coli*. *Nat. Biotechnol.* 34, 435–440. doi:10.1038/nbt.3485

Chuah, J.-A., Yamada, M., Taguchi, S., Sudesh, K., Doi, Y., Numata, K., et al. (2013). Biosynthesis and characterization of polyhydroxyalkanoate containing 5-hydroxyvalerate units: Effects of 5HV units on biodegradability, cytotoxicity, mechanical and thermal properties. *Polym. Degrad. Stab.* 98, 331–338. doi:10.1016/j.polymdegradstab.2012.09.008

Chung, A. L., Jin, H. L., Huang, L. J., Ye, H. M., Chen, J. C., Wu, Q., et al. (2011). Biosynthesis and characterization of poly(3-hydroxydodecanoate) by beta-oxidation inhibited mutant of Pseudomonas entomophila L48. *Biomacromolecules* 12, 3559–3566. doi:10.1021/bm200770m

Ciesielski, S., Mozejko, J., and Przybylek, G. (2010). The influence of nitrogen limitation on mcl-PHA synthesis by two newly isolated strains of Pseudomonas sp. *J. Ind. Microbiol. Biotechnol.* 37, 511–520. doi:10.1007/s10295-010-0698-5

Costa, S. S., Miranda, A. L., De Morais, M. G., Costa, J. a. V., and Druzian, J. I. (2019). Microalgae as source of polyhydroxyalkanoates (PHAs) - a review. *Int. J. Biol. Macromol.* 131, 536–547. doi:10.1016/j.ijbiomac.2019.03.099

Fu, J., Sharma, U., Sparling, R., Cicek, N., and Levin, D. B. (2014a). Evaluation of medium-chain-length polyhydroxyalkanoate production by Pseudomonas putida LS46 using biodiesel by-product streams. *Can. J. Microbiol.* 60, 461–468. doi:10.1139/cjm-2014-0108

Fu, X. Z., Tan, D., Aibaidula, G., Wu, Q., Chen, J. C., Chen, G. Q., et al. (2014b). Development of Halomonas TD01 as a host for open production of chemicals. *Metab. Eng.* 23, 78–91. doi:10.1016/j.ymben.2014.02.006

Gorenflo, V., Schmack, G., Vogel, R., and Steinbüchel, A. (2001). Development of a process for the biotechnological large-scale production of 4-hydroxyvalerate-containing polyesters and characterization of their physical and mechanical properties. *Biomacromolecules* 2, 45–57. doi:10.1021/bm0000992

Gutierrez-Gomez, U., Servin-Gonzalez, L., and Soberon-Chavez, G. (2019). Role of beta-oxidation and de novo fatty acid synthesis in the production of rhamnolipids and polyhydroxyalkanoates by *Pseudomonas aeruginosa*. *Appl. Microbiol. Biotechnol.* 103, 3753–3760. doi:10.1007/s00253-019-09734-x

Hobmeier, K., Lowe, H., Liefeldt, S., Kremling, A., and Pfluger-Grau, K. (2020). A nitrate-blind P. Putida strain boosts PHA production in a synthetic mixed culture. *Front. Bioeng. Biotechnol.* 8, 486. doi:10.3389/fbioe.2020.00486

Hu, D., Chung, A.-L., Wu, L.-P., Zhang, X., Wu, Q., Chen, J.-C., et al. (2011). Biosynthesis and characterization of polyhydroxyalkanoate block copolymer P3HB-b-P4HB. *Biomacromolecules* 12, 3166–3173. doi:10.1021/bm200660k

Hyakutake, M., Tomizawa, S., Mizuno, K., Abe, H., and Tsuge, T. (2014). Alcoholytic cleavage of polyhydroxyalkanoate chains by class IV synthases induced by endogenous and exogenous ethanol. *Appl. Environ. Microbiol.* 80, 1421–1429. doi:10.1128/aem.03576-13

Ilham, M., Nakanomori, S., Kihara, T., Hokamura, A., Matsusaki, H., Tsuge, T., et al. (2014). Characterization of polyhydroxyalkanoate synthases from Halomonas sp. O-1 and Halomonas elongata DSM2581: Site-directed mutagenesis and recombinant expression. *Polym. Degrad. Stab.* 109, 416–423. doi:10.1016/j.polymdegradstab.2014.04.024

Jiang, X. R., Yan, X., Yu, L. P., Liu, X. Y., and Chen, G. Q. (2021). Hyperproduction of 3-hydroxypropionate by Halomonas bluephagenesis. *Nat. Commun.* 12, 1513. doi:10.1038/s41467-021-21632-3

Jong-Il Choi, S. Y. L., Lee, S. Y., and Han, K. (1998). Kyuboem HanCloning of the Alcaligenes latus polyhydroxyalkanoate biosynthesis genes and use of these genes for enhanced production of poly(3-hydroxybutyrate) in *Escherichia coli*. *Appl. Environ. Microbiol.* 1, 4897–4903. doi:10.1128/aem.64.12.4897-4903.1998

Jung, K., Hazenberg, W., Prieto, M., and Witholt, B. (2001). Two-stage continuous process development for the production of medium-chain-length poly(3-hydroxyalkanoates). *Biotechnol. Bioeng.* 72, 19–24. doi:10.1002/1097-0290(20010105)72:1<19::aid-bit3>3.0.co;2-b

Keller, M. W., Schut, G. J., Lipscomb, G. L., Menon, A. L., Iwuchukwu, I. J., Leuko, T. T., et al. (2013). Exploiting microbial hyperthermophilicity to produce an industrial chemical, using hydrogen and carbon dioxide. *Proc. Natl. Acad. Sci. U. S. A.* 110, 5840–5845. doi:10.1073/pnas.1222607110

Khosravi-Darani, K., Mokhtari, Z. B., Amai, T., and Tanaka, K. (2013). Microbial production of poly(hydroxybutyrate) from C(1) carbon sources. *Appl. Microbiol. Biotechnol.* 97, 1407–1424. doi:10.1007/s00253-012-4649-0

Kim, J., Kim, Y. J., Choi, S. Y., Lee, S. Y., and Kim, K. J. (2017). Crystal structure of Ralstonia eutropha polyhydroxyalkanoate synthase C-terminal domain and reaction mechanisms. *Biotechnol. J.* 1, 1600648. doi:10.1002/biot.201600648

Kourmentza, C., Plácido, J., Venetsaneas, N., Burniol-Figols, A., Varrone, C., Gavala, H. N., et al. (2017). Recent advances and challenges towards sustainable polyhydroxyalkanoate (PHA) production. *Bioengineering* 4, 55. doi:10.3390/bioengineering4020055

Lan, L.-H., Zhao, H., Chen, J.-C., and Chen, G.-Q. (2016). Engineering Halomonas spp. as A low-cost production host for production of bio-surfactant protein PhaP. *Biotechnol. J.* 11, 1595–1604. doi:10.1002/biot.201600459

Lee, J., Park, H. J., Moon, M., Lee, J.-S., and Min, K. (2021). Recent progress and challenges in microbial polyhydroxybutyrate (PHB) production from CO2 as a sustainable feedstock: A state-of-the-art review. *Bioresour. Technol.* 339, 125616. doi:10.1016/j.biortech.2021.125616

Li, H. F., Wang, M. R., Tian, L. Y., and Li, Z. J. (2021a). Production of polyhydroxyalkanoates (PHAs) by Vibrio alginolyticus strains isolated from salt fields. *Molecules* 26 (20), 6283. doi:10.3390/molecules26206283

Li, M., Chen, X., Che, X., Zhang, H., Wu, L. P., Du, H., et al. (2019). Engineering Pseudomonas entomophila for synthesis of copolymers with defined fractions of 3-hydroxybutyrate and medium-chain-length 3-hydroxyalkanoates. *Metab. Eng.* 52, 253–262. doi:10.1016/j.ymben.2018.12.007

Li, M., Ma, Y., Zhang, X., Zhang, L., Chen, X., Ye, J. W., et al. (2021b). Tailor-made polyhydroxyalkanoates by reconstructing Pseudomonas entomophila. *Adv. Mat.* 33, e2102766. doi:10.1002/adma.202102766

Li, T., Guo, Y.-Y., Qiao, G.-Q., and Chen, G.-Q. (2016). Microbial synthesis of 5-aminolevulinic acid and its coproduction with polyhydroxybutyrate. *ACS Synth. Biol.* 5, 1264–1274. doi:10.1021/acssynbio.6b00105

Li, Z. J., Qiao, K., Che, X. M., and Stephanopoulos, G. (2017). Metabolic engineering of *Escherichia coli* for the synthesis of the quadripolymer poly(glycolate-co-lactate-co-3-hydroxybutyrate-co-4-hydroxybutyrate) from glucose. *Metab. Eng.* 44, 38–44. doi:10.1016/j.ymben.2017.09.003

Liang, P., Zhang, Y., Xu, B., Zhao, Y., Liu, X., Gao, W., et al. (2020). Deletion of genomic islands in the Pseudomonas putida KT2440 genome can create an optimal chassis for synthetic biology applications. *Microb. Cell. Fact.* 19, 70. doi:10.1186/s12934-020-01329-w

Lim, H., Chuah, J.-A., Chek, M. F., Tan, H. T., Hakoshima, T., Sudesh, K., et al. (2021). Identification of regions affecting enzyme activity, substrate binding, dimer stabilization and polyhydroxyalkanoate (PHA) granule morphology in the PHA synthase of Aquitalea sp. USM4. *Int. J. Biol. Macromol.* 186, 414–423. doi:10.1016/j.ijbiomac.2021.07.041

Lin, Z., Zhang, Y., Yuan, Q., Liu, Q., Li, Y., Wang, Z., et al. (2015). Metabolic engineering of *Escherichia coli* for poly (3-hydroxybutyrate) production via threonine bypass. *Microb. Cell. Fact.* 14, 185. doi:10.1186/s12934-015-0369-3

Linares-Pastén, J. A., Sabet-Azad, R., Pessina, L., Sardari, R. R. R., Ibrahim, M. H. A., Hatti-Kaul, R., et al. (2015). Efficient poly(3-hydroxypropionate) production from glycerol using Lactobacillus reuteri and recombinant *Escherichia coli* harboring L. reuteri propionaldehyde dehydrogenase and Chromobacterium sp. PHA synthase genes. *Bioresour. Technol.* 180, 172–176. doi:10.1016/j.biortech.2014.12.099

Ling, C., Qiao, G.-Q., Shuai, B.-W., Song, K.-N., Yao, W.-X., Jiang, X.-R., et al. (2019). Engineering self-flocculating Halomonas campaniensis for wastewaterless open and continuous fermentation. *Biotechnol. Bioeng.* 116, 805–815. doi:10.1002/bit.26897

Ling, C., Qiao, G. Q., Shuai, B. W., Olavarria, K., Yin, J., Xiang, R. J., et al. (2018). Engineering NADH/NAD(+) ratio in Halomonas bluephagenesis for enhanced production of polyhydroxyalkanoates (PHA). *Metab. Eng.* 49, 275–286. doi:10.1016/j.ymben.2018.09.007

Lv, L., Ren, Y. L., Chen, J. C., Wu, Q., and Chen, G. Q. (2015). Application of CRISPRi for prokaryotic metabolic engineering involving multiple genes, a case study: Controllable P(3HB-co-4HB) biosynthesis. *Metab. Eng.* 29, 160–168. doi:10.1016/j.ymben.2015.03.013

Ma, H., Zhao, Y., Huang, W., Zhang, L., Wu, F., Ye, J., et al. (2020). Rational flux-tuning of Halomonas bluephagenesis for co-production of bioplastic PHB and ectoine. *Nat. Commun.* 11, 3313. doi:10.1038/s41467-020-17223-3

Martin, D. P., and Williams, S. F. (2003). Medical applications of poly-4-hydroxybutyrate: A strong flexible absorbable biomaterial. *Biochem. Eng. J.* 16, 97–105. doi:10.1016/s1369-703x(03)00040-8

Matsumoto, K. I., Takase, K., Yamamoto, Y., Doi, Y., and Taguchi, S. (2009). Chimeric enzyme composed of polyhydroxyalkanoate (PHA) synthases from Ralstonia eutropha and Aeromonas caviae enhances production of PHAs in

recombinant *Escherichia coli*. *Biomacromolecules* 10, 682–685. doi:10.1021/bm801386j

Mehrpouya, M., Vahabi, H., Barletta, M., Laheurte, P., and Langlois, V. (2021). Additive manufacturing of polyhydroxyalkanoates (PHAs) biopolymers: Materials, printing techniques, and applications. *Mater. Sci. Eng. C* 127, 112216. doi:10.1016/j.msec.2021.112216

Meijnen, J. P., De Winde, J. H., and Ruijssenaars, H. J. (2008). Engineering Pseudomonas putida S12 for efficient utilization of D-xylose and L-arabinose. *Appl. Environ. Microbiol.* 74, 5031–5037. doi:10.1128/aem.00924-08

Meng, D. C., Wang, Y., Wu, L. P., Shen, R., Chen, J. C., Wu, Q., et al. (2015). Production of poly(3-hydroxypropionate) and poly(3-hydroxybutyrate-co-3-hydroxypropionate) from glucose by engineering *Escherichia coli*. *Metab. Eng.* 29, 189–195. doi:10.1016/j.ymben.2015.03.015

Miranda De Sousa Dias, M., Koller, M., Puppi, D., Morelli, A., Chiellini, F., and Braunegg, G. (2017). Fed-batch synthesis of poly(3-hydroxybutyrate) and poly(3-hydroxybutyrate-co-4-hydroxybutyrate) from sucrose and 4-hydroxybutyrate precursors by Burkholderia sacchari strain DSM 17165. *Bioengineering* 4, 36. doi:10.3390/bioengineering4020036

Mizuno, S., Enda, Y., Saika, A., Hiroe, A., and Tsuge, T. (2018). Biosynthesis of polyhydroxyalkanoates containing 2-hydroxy-4-methylvalerate and 2-hydroxy-3-phenylpropionate units from a related or unrelated carbon source. *J. Biosci. Bioeng.* 125, 295–300. doi:10.1016/j.jbiosc.2017.10.010

Modi, S., Koelling, K., and Vodovotz, Y. (2011). Assessment of PHB with varying hydroxyvalerate content for potential packaging applications. *Eur. Polym. J.* 47, 179–186. doi:10.1016/j.eurpolymj.2010.11.010

Możejko-Ciesielska, J., and Kiewisz, R. (2016). Bacterial polyhydroxyalkanoates: Still fabulous? *Microbiol. Res.* 192, 271–282. doi:10.1016/j.micres.2016.07.010

Murugan, P., Gan, C.-Y., and Sudesh, K. (2017). Biosynthesis of P(3HB-co-3HHx) with improved molecular weights from a mixture of palm olein and fructose by Cupriavidus necator Re2058/pCB113. *Int. J. Biol. Macromol.* 102, 1112–1119. doi:10.1016/j.ijbiomac.2017.05.006

Norhafini, H., Huong, K.-H., and Amirul, A. A. (2019). High PHA density fed-batch cultivation strategies for 4HB-rich P(3HB-co-4HB) copolymer production by transformant Cupriavidus malaysiensis USMAA1020. *Int. J. Biol. Macromol.* 125, 1024–1032. doi:10.1016/j.ijbiomac.2018.12.121

Obruča, S., Dvořák, P., Sedláček, P., Koller, M., Sedlář, K., Pernicová, I., et al. (202210790). Polyhydroxyalkanoates synthesis by halophiles and thermophiles: Towards sustainable production of microbial bioplastics. *Biotechnol. Adv.* 58, 107906. doi:10.1016/j.biotechadv.2022.107906

Ouyang, P., Wang, H., Hajnal, I., Wu, Q., Guo, Y., Chen, G. Q., et al. (2018). Increasing oxygen availability for improving poly(3-hydroxybutyrate) production by Halomonas. *Metab. Eng.* 45, 20–31. doi:10.1016/j.ymben.2017.11.006

Pacholak, A., Gao, Z.-L., Gong, X.-Y., Kaczorek, E., and Cui, Y.-W. (2021). The metabolic pathways of polyhydroxyalkanoates and exopolysaccharides synthesized by Haloferax mediterranei in response to elevated salinity. *J. Proteomics* 232, 104065. doi:10.1016/j.jprot.2020.104065

Panich, J., Fong, B., and Singer, S. W. (2021). Metabolic engineering of cupriavidus necator H16 for sustainable biofuels from CO2. *Trends Biotechnol.* 39, 412–424. doi:10.1016/j.tibtech.2021.01.001

Park, S. J., Ahn, W. S., Green, P. R., and Lee, S. Y. (2001). Production of poly(3-hydroxybutyrate-co-3-hydroxyhexanoate) by metabolically engineered *Escherichia coli* strains. *Biomacromolecules* 2, 248–254. doi:10.1021/bm000105u

Park, S. J., Kim, T. W., Kim, M. K., Lee, S. Y., and Lim, S.-C. (2012a). Advanced bacterial polyhydroxyalkanoates: Towards a versatile and sustainable platform for unnatural tailor-made polyesters. *Biotechnol. Adv.* 30, 1196–1206. doi:10.1016/j.biotechadv.2011.11.007

Park, S. J., Lee, S. Y., Kim, T. W., Jung, Y. K., and Yang, T. H. (2012b). Biosynthesis of lactate-containing polyesters by metabolically engineered bacteria. *Biotechnol. J.* 7, 199–212. doi:10.1002/biot.201100070

Park, S. J., Lee, T. W., Lim, S. C., Kim, T. W., Lee, H., Kim, M. K., et al. (2012c). Biosynthesis of polyhydroxyalkanoates containing 2-hydroxybutyrate from unrelated carbon source by metabolically engineered *Escherichia coli*. *Appl. Microbiol. Biotechnol.* 93, 273–283. doi:10.1007/s00253-011-3530-x

Park, S. J., Park, J. P., and Lee, S. Y. (2002). Metabolic engineering of *Escherichia coli* for the production of medium-chain-length polyhydroxyalkanoates rich in specific monomers. *FEMS Microbiol. Lett.* 214, 217–222. doi:10.1111/j.1574-6968.2002.tb11350.x

Prieto, A., Escapa, I. F., Martinez, V., Dinjaski, N., Herencias, C., De La Pena, F., et al. (2016). A holistic view of polyhydroxyalkanoate metabolism in Pseudomonas putida. *Environ. Microbiol.* 18, 341–357. doi:10.1111/1462-2920.12760

Raberg, M., Volodina, E., Lin, K., and Steinbuchel, A. (2018). Ralstonia eutropha H16 in progress: Applications beside PHAs and establishment as production platform by advanced genetic tools. *Crit. Rev. Biotechnol.* 38, 494–510. doi:10.1080/07388551.2017.1369933

Ryu, H. W., S, K. H., Chang, Y. K., and Chang, H. N. (1996). Production of poly(3-hydroxybutyrate) by high cell density fed-batch culture of Alcaligenes eutrophus with phospate limitation. *Biotechnol. Bioeng.* 55 (51), 28–32. doi:10.1002/(sici)1097-0290(19970705)55:1<28::aid-bit4>3.0.co;2-z

Ryu, H. W., Hahn, S. K., Chang, Y. K., and Chang, H. N. (1997). Production of poly(3-hydroxybutyrate) by high cell density fed-batch culture of Alcaligenes eutrophus with phospate limitation. *Biotechnol. Bioeng.* 55, 28–32. doi:10.1002/(sici)1097-0290(19970705)55:1<28::aid-bit4>3.0.co;2-z

Salehizadeh, H., Yan, N., and Farnood, R. (2020). Recent advances in microbial CO2 fixation and conversion to value-added products. *Chem. Eng. J.* 390, 124584. doi:10.1016/j.cej.2020.124584

Sathiyanarayanan, G., Kiran, G. S., Selvin, J., and Saibaba, G. (2013). Optimization of polyhydroxybutyrate production by marine Bacillus megaterium MSBN04 under solid state culture. *Int. J. Biol. Macromol.* 60, 253–261. doi:10.1016/j.ijbiomac.2013.05.031

Scheel, R. A., Ho, T., Kageyama, Y., Masisak, J., Mckenney, S., Lundgren, B. R., et al. (2021). Optimizing a fed-batch high-density fermentation process for medium chain-length poly(3-hydroxyalkanoates) in *Escherichia coli*. *Front. Bioeng. Biotechnol.* 9, 618259. doi:10.3389/fbioe.2021.618259

Shen, R., Yin, J., Ye, J.-W., Xiang, R.-J., Ning, Z.-Y., Huang, W.-Z., et al. (2018). Promoter engineering for enhanced P (3HB-co-4HB) production by Halomonas bluephagenesis. *ACS Synth. Biol.* 7, 1897–1906. doi:10.1021/acssynbio.8b00102

Silva, F., Campanari, S., Matteo, S., Valentino, F., Majone, M., Villano, M., et al. (2017). Impact of nitrogen feeding regulation on polyhydroxyalkanoates production by mixed microbial cultures. *N. Biotechnol.* 37, 90–98. doi:10.1016/j.nbt.2016.07.013

Steinbüchel, A. (2001). Perspectives for biotechnological production and utilization of biopolymers: Metabolic engineering of polyhydroxyalkanoate biosynthesis pathways as a successful example. *Macromol. Biosci.* 1, 1–24. doi:10.1002/1616-5195(200101)1:1<1::aid-mabi1>3.0.co;2-b

Sudesh, K., Abe, H., and Doi, Y. (2000). Synthesis, structure and properties of polyhydroxyalkanoates: Biological polyesters. *Prog. Polym. Sci.* 25, 1503–1555. doi:10.1016/s0079-6700(00)00035-6

Sudo, M., Hori, C., Ooi, T., Mizuno, S., Tsuge, T., Matsumoto, K. I., et al. (2020). Synergy of valine and threonine supplementation on poly(2-hydroxybutyrate-block-3-hydroxybutyrate) synthesis in engineered *Escherichia coli* expressing chimeric polyhydroxyalkanoate synthase. *J. Biosci. Bioeng.* 129, 302–306. doi:10.1016/j.jbiosc.2019.09.018

Tan, D., Xue, Y. S., Aibaidula, G., and Chen, G. Q. (2011). Unsterile and continuous production of polyhydroxybutyrate by Halomonas TD01. *Bioresour. Technol.* 102, 8130–8136. doi:10.1016/j.biortech.2011.05.068

Tan, I. K. P., Foong, C. P., Tan, H. T., Lim, H., Zain, N. A., Tan, Y. C., et al. (2020). Polyhydroxyalkanoate (PHA) synthase genes and PHA-associated gene clusters in Pseudomonas spp. and Janthinobacterium spp. isolated from Antarctica. *J. Biotechnol.* 313, 18–28. doi:10.1016/j.jbiotec.2020.03.006

Tanaka, K., Yoshida, K., Orita, I., and Fukui, T. (2021). Biosynthesis of poly (3-hydroxybutyrate-co-3-hydroxyhexanoate) from CO2 by a recombinant cupriavidusnecator. *Bioengineering* 8, 179. doi:10.3390/bioengineering8110179

Tariq, A., Hameed, A., Bokhari, H., and Masood, F. (2015). Is atomic rearrangement of type IV PHA synthases responsible for increased PHA production? *J. Biomol. Struct. Dyn.* 33, 1225–1238. doi:10.1080/07391102.2014.941401

Ushimaru, K., Motoda, Y., Numata, K., and Tsuge, T. (2014). Phasin proteins activate Aeromonas caviae polyhydroxyalkanoate (PHA) synthase but not Ralstonia eutropha PHA synthase. *Appl. Environ. Microbiol.* 80, 2867–2873. doi:10.1128/aem.04179-13

Van Thuoc, D., Loan, T. T., Trung, T. A., Van Quyen, N., Tung, Q. N., Tien, P. Q., et al. (2020). Genome mining reveals the biosynthetic pathways of polyhydroxyalkanoate and ectoines of the halophilic strain Salinivibrio proteolyticus M318 isolated from fermented shrimp paste. *Mar. Biotechnol. (NY).* 22, 651–660. doi:10.1007/s10126-020-09986-z

Van Thuoc, D., My, D. N., Loan, T. T., and Sudesh, K. (2019). Utilization of waste fish oil and glycerol as carbon sources for polyhydroxyalkanoate production by Salinivibrio sp. M318. *Int. J. Biol. Macromol.* 141, 885–892. doi:10.1016/j.ijbiomac.2019.09.063

Volova, T., Trusova, M., Kalacheva, G., and Kozhevnicov, I. (2006). Physiological–biochemical properties and the ability to synthesize polyhydroxyalkanoates of the glucose-utilizing strain of the hydrogen bacterium Ralstonia eutropha B8562. *Appl. Microbiol. Biotechnol.* 73, 429–433. doi:10.1007/s00253-006-0460-0

Wang, M. R., Li, H. F., Yi, J. J., Tao, S. Y., and Li, Z. J. (2022). Production of polyhydroxyalkanoates by three novel species of Marinobacterium. *Int. J. Biol. Macromol.* 195, 255–263. doi:10.1016/j.ijbiomac.2021.12.019

Wang, X., Han, J.-N., Zhang, X., Ma, Y.-Y., Lin, Y., Wang, H., et al. (2021a). Reversible thermal regulation for bifunctional dynamic control of gene expression in *Escherichia coli*. *Nat. Commun.* 12, 1411. doi:10.1038/s41467-021-21654-x

Wang, Y., Wu, H., Jiang, X., and Chen, G.-Q. (2014). Engineering *Escherichia coli* for enhanced production of poly(3-hydroxybutyrate-co-4-hydroxybutyrate) in larger cellular space. *Metab. Eng.* 25, 183–193. doi:10.1016/j.ymben.2014.07.010

Wang, Z., Qin, Q., Zheng, Y., Li, F., Zhao, Y., Chen, G.-Q., et al. (2021b). Engineering the permeability of Halomonas bluephagenesis enhanced its chassis properties. *Metab. Eng.* 67, 53–66. doi:10.1016/j.ymben.2021.05.010

Xiong, B., Li, Z., Liu, L., Zhao, D., Zhang, X., Bi, C., et al. (2018). Genome editing of Ralstonia eutropha using an electroporation-based CRISPR-Cas9 technique. *Biotechnol. Biofuels* 11, 172. doi:10.1186/s13068-018-1170-4

Yan, X., Liu, X., Yu, L. P., Wu, F., Jiang, X. R., Chen, G. Q., et al. (2022). Biosynthesis of diverse α, ω-diol-derived polyhydroxyalkanoates by engineered Halomonas bluephagenesis. *Metab. Eng.* 72, 275–288. doi:10.1016/j.ymben.2022.04.001

Yang, J. E., Choi, Y. J., Lee, S. J., Kang, K. H., Lee, H., Oh, Y. H., et al. (2014). Metabolic engineering of *Escherichia coli* for biosynthesis of poly(3-hydroxybutyrate-co-3-hydroxyvalerate) from glucose. *Appl. Microbiol. Biotechnol.* 98, 95–104. doi:10.1007/s00253-013-5285-z

Yang, J. E., Park, S. J., Kim, W. J., Kim, H. J., Kim, B. J., Lee, H., et al. (2018). One-step fermentative production of aromatic polyesters from glucose by metabolically engineered *Escherichia coli* strains. *Nat. Commun.* 9, 79. doi:10.1038/s41467-017-02498-w

Yang, S., Li, S., and Jia, X. (2019). Production of medium chain length polyhydroxyalkanoate from acetate by engineered Pseudomonas putida KT2440. *J. Ind. Microbiol. Biotechnol.* 46, 793–800. doi:10.1007/s10295-019-02159-5

Yang, T. H., Kim, T. W., Kang, H. O., Lee, S. H., Lee, E. J., Lim, S. C., et al. (2010). Biosynthesis of polylactic acid and its copolymers using evolved propionate CoA transferase and PHA synthase. *Biotechnol. Bioeng.* 105, 150–160. doi:10.1002/bit.22547

Yang, X., Li, S., and Jia, X. (2020). A four-microorganism three-step fermentation process for producing medium-chain-length polyhydroxyalkanoate from starch. *Biotech* 10, 352. doi:10.1007/s13205-020-02347-6

Yao J, Z., Wu, Q., Chen, G., and Zhang, R. (1999). Production of polyhydroxyalkanoates by Pseudomonas nitroreducens. *Antonie Leeuwenhoek* 75 (74), 345–349. doi:10.1023/a:1002082303615

Ye, J., Hu, D., Yin, J., Huang, W., Xiang, R., Zhang, L., et al. (2020). Stimulus response-based fine-tuning of polyhydroxyalkanoate pathway in Halomonas. *Metab. Eng.* 57, 85–95. doi:10.1016/j.ymben.2019.10.007

Ye, J., Huang, W., Wang, D., Chen, F., Yin, J., Li, T., et al. (2018). Pilot scale-up of poly(3-hydroxybutyrate-co-4-hydroxybutyrate) production by Halomonas bluephagenesis via cell growth adapted optimization process. *Biotechnol. J.* 13, 1800074. doi:10.1002/biot.201800074

Ye, J. W., and Chen, G. Q. (2021). Halomonas as a chassis. *Essays Biochem.* 65, 393–403. doi:10.1042/ebc20200159

Young, E. M., Zhao, Z., Gielesen, B. E., Wu, L., Gordon, D. B., Roubos, J. A., et al. (2018). Iterative algorithm-guided design of massive strain libraries, applied to itaconic acid production in yeast. *Metab. Eng.* 48, 33–43. doi:10.1016/j.ymben.2018.05.002

Yu, L. P., Yan, X., Zhang, X., Chen, X. B., Wu, Q., Jiang, X. R., et al. (2020). Biosynthesis of functional polyhydroxyalkanoates by engineered Halomonas bluephagenesis. *Metab. Eng.* 59, 119–130. doi:10.1016/j.ymben.2020.02.005

Yue, H., Ling, C., Yang, T., Chen, X., Chen, Y., Deng, H., et al. (2014). A seawater-based open and continuous process for polyhydroxyalkanoates production by recombinant Halomonas campaniensis LS21 grown in mixed substrates. *Biotechnol. Biofuels* 7, 108. doi:10.1186/1754-6834-7-108

Zhang, X., Lin, Y., Wu, Q., Wang, Y., and Chen, G. Q. (2020). Synthetic biology and genome-editing tools for improving PHA metabolic engineering. *Trends Biotechnol.* 38, 689–700. doi:10.1016/j.tibtech.2019.10.006

Zhou, H., Vonk, B., Roubos, J. A., Bovenberg, R. A., and Voigt, C. A. (2015). Algorithmic co-optimization of genetic constructs and growth conditions: Application to 6-ACA, a potential nylon-6 precursor. *Nucleic Acids Res.* 43, 10560–10570. doi:10.1093/nar/gkv1071

Zhou, Q., Shi, Z. Y., Meng, D. C., Wu, Q., Chen, J. C., Chen, G. Q., et al. (2011). Production of 3-hydroxypropionate homopolymer and poly(3-hydroxypropionate-co-4-hydroxybutyrate) copolymer by recombinant *Escherichia coli*. *Metab. Eng.* 13, 777–785. doi:10.1016/j.ymben.2011.10.002

Zou, H., Shi, M., Zhang, T., Li, L., Li, L., Xian, M., et al. (2017). Natural and engineered polyhydroxyalkanoate (PHA) synthase: Key enzyme in biopolyester production. *Appl. Microbiol. Biotechnol.* 101, 7417–7426. doi:10.1007/s00253-017-8485-0

frontiers | Frontiers in Bioengineering and Biotechnology

TYPE Original Research
PUBLISHED 25 July 2022
DOI 10.3389/fbioe.2022.951583

OPEN ACCESS

EDITED BY
Xinglin Jiang,
Technical University of Denmark, Denmark

REVIEWED BY
Martin Koller,
University of Graz, Austria
Christian Kennes,
University of A Coruña, Spain
Yongqiang Gao,
Harvard Medical School, United States

*CORRESPONDENCE
Justyna Mozejko-Ciesielska,
justyna.mozejko@uwm.edu.pl

SPECIALTY SECTION
This article was submitted to Industrial Biotechnology, a section of the journal Frontiers in Bioengineering and Biotechnology

RECEIVED 24 May 2022
ACCEPTED 27 June 2022
PUBLISHED 25 July 2022

CITATION
Szacherska K, Moraczewski K, Czaplicki S, Oleskowicz-Popiel P and Mozejko-Ciesielska J (2022), Effect of short- and medium-chain fatty acid mixture on polyhydroxyalkanoate production by Pseudomonas strains grown under different culture conditions.
Front. Bioeng. Biotechnol. 10:951583.
doi: 10.3389/fbioe.2022.951583

Effect of short- and medium-chain fatty acid mixture on polyhydroxyalkanoate production by *Pseudomonas* strains grown under different culture conditions

Karolina Szacherska[1], Krzysztof Moraczewski[2], Sylwester Czaplicki[3], Piotr Oleskowicz-Popiel[4] and Justyna Mozejko-Ciesielska[1]*

[1]Department of Microbiology and Mycology, Faculty of Biology and Biotechnology, University of Warmia and Mazury in Olsztyn, Olsztyn, Poland, [2]Institute of Materials Engineering, Kazimierz Wielki University, Bydgoszcz, Poland, [3]Department of Plant Food Chemistry and Processing, Faculty of Food Sciences, University of Warmia and Mazury in Olsztyn, Olsztyn, Poland, [4]Water Supply and Bioeconomy Division, Faculty of Environmental Engineering and Energy, Poznan University of Technology, Poznan, Poland

Short- and medium-chain fatty acids (SMCFAs) derived from the acidogenic anaerobic mixed culture fermentation of acid whey obtained from a crude cheese production line and their synthetic mixture that simulates a real SMCFA-rich stream were evaluated for polyhydroxyalkanoate (PHA) production. Three individual *Pseudomonas* sp. strains showed different capabilities of growing and producing PHAs in the presence of a synthetic mixture of SMCFAs. *Pseudomonas* sp. GL06 exhibited the highest SMCFA tolerance and produced PHAs with the highest productivity (2.7 mg/L h). Based on these observations, this strain was selected for further investigations on PHA production in a fed-batch bioreactor with a SMCFA-rich stream extracted from the effluent. The results showed that PHA productivity reached up to 4.5 mg/L h at 24 h of fermentation together with the ammonium exhaustion in the growth medium. Moreover, the PHA monomeric composition varied with the bacterial strain and the type of the growth medium used. Furthermore, a differential scanning calorimetric and thermogravimetric analysis showed that a short- and medium-chain-length PHA copolymer made of 3-hydroxybutyric, -hexanoic, -octanoic, -decanoic, and -dodecanoic has promising properties. The ability of *Pseudomonas* sp. to produce tailored PHA copolymers together with the range of possible applications opens new perspectives in the development of PHA bioproduction as a part of an integrated valorization process of SMCFAs derived from waste streams.

KEYWORDS

biopolymers, medium-chain fatty acids, polyhydroxyalkanoates, *Pseudomonas* sp., short-chain fatty acids

1 Introduction

The negative impact of petrochemical plastics on the environment has prompted a growing interest in environmentally friendly alternative materials. Polyhydroxyalkanoates (PHAs) are especially attractive because of their unique material properties such as biodegradability, non-toxicity, and biocompatibility and the similarity of their physical properties to those of synthetic polymers (Zubairi et al., 2016). Moreover, PHAs have many advantages over petrochemical-derived polymers, such as hydrophobicity, thermoplastic processability, relatively high melting point, and optical purity. They are natural polyesters synthesized by various microorganisms under unbalanced growth conditions as intracellular energy compounds in the form of granules in the cytoplasm (Akaraonye et al., 2010). Generally, PHAs are classified according to the carbon-chain-length of the constituent monomers into short-chain-length (PHA_{SCL}) containing 3–5 carbon atoms in the molecule, medium-chain-length (PHA_{MCL}) with 6–14 carbon atoms in the molecule, and long-chain-length (PHA_{LCL}) which contains more than 15 carbon atoms (Tan et al., 2014). It is known that the monomeric composition of PHAs depend mainly on the carbon source used for bacterial culture and the bacterium that is able to synthesize and accumulate PHAs (Koller and Braunegg, 2015). The applicability of bacterial PHAs is directly related to their properties. PHA_{SCL}, such as poly-3-hydroxybutyrate [P(3HB)], shows high crystallinity, stiffness, and brittleness with poor elastic properties, limiting its use as a stable material. PHA_{MCL} shows more favorable and useful properties. They are elastomers with a low degree of crystallinity, melting point, and tensile strength as well as high elongation to break. They are synthesized mainly by bacteria of the *Pseudomonas* genus. Due to their useful properties, PHAs have great potential in biomedical, agricultural, and industrial applications (Tan et al., 2021). Nevertheless, the commercialization of PHAs in the world market is currently limited, mainly due to the high production costs compared to synthetic polymers. Despite the fact that the fermentation technology and polymer extraction process have considerably improved over the past decade, the cost of the carbon source still accounts for half of the cost of producing PHAs. Consequently, there is a growing need to develop novel microbial processes using renewable and inexpensive carbon sources. Short and medium chain fatty acids (SMCFAs) generated by acidogenic anaerobic mixed culture fermentation (MCF) are an interesting alternative to the expensive substrates. Recycling waste into desirable and valuable products is a revolutionary path in waste management and an environmentally friendly process (Martinez et al., 2015). Various renewable wastes converted into SMCFAs such as sugarcane molasses (Albuquerque et al., 2007), paper mill wastewater (Bengtsson et al., 2008), olive oil wastewater (Beccari et al., 2009), food waste (Venkateswar Reddy and Venkata Mohan, 2012; Aremu et al., 2021; Thomas et al., 2022), and pea shells (Patel et al., 2012) have been used to produce environmentally friendly PHAs. In contrast, few scientific publications have evaluated the potential of pure bacterial cultures to convert SMCFA-rich streams from MCF using organic waste into PHAs (Venkateswar Reddy et al., 2012; Cerrone et al., 2014; Martinez et al., 2015; Vu et al., 2021). It should also be mentioned that none of these studies evaluated, in detail, the properties of the extracted PHAs.

An important aspect in the cost-effective production of PHAs is also the selection of a microorganism that has the ability to efficiently intracellularly accumulate this biopolymer using renewable carbon sources. Bacteria belonging to the *Pseudomonas* genus meet these criteria by transforming post-fermentative carbon sources into multipurpose biopolymers. They are also characterized by fast biomass growth, low production requirements, easy adaptation, and tolerance to oxidative stress (Mozejko-Ciesielska et al., 2019). *Pseudomonas* sp. Have been characterized as the producers, usually producing mcl-PHA rather than scl-PHA (Solaiman and Ashby, 2005). The synthesis of PHAs from SMCFAs has been described for several *Pseudomonas* spp., including: *Pseudomonas* sp. ST2 (Reddy et al., 2008; Munir and Jamil, 2018), *Pseudomonas* sp. H9 (Liu et al., 2021), *P. putida* KT2440 (Kourmentza et al., 2009; Cerrone et al., 2014; Yang et al., 2019), *P. otitidis* (Venkateswar Reddy et al., 2012), *P. pseudoflava* (Venkateswar Reddy et al., 2017), *P. palleronii* (Venkateswar Reddy et al., 2017), and *P. oleovorans* (Aremu et al., 2021). To the best of our knowledge, none of these studies described the properties of the extracted scl-mcl-PHA copolymers.

In recent years, the amount of organic and biomass waste has been steadily increasing. Currently, sewage sludge is a burden for municipal wastewater treatment plants (Lad et al., 2022). Moreover, acid whey, a by-product of Greek yoghurt, cottage cheese production, and the like, poses a risk to the ecosystem and its disposal is associated with a fee (Erickson, 2017). Therefore, SMCFAs derived from sludge and acid whey are attractive raw materials for biopolymer synthesis by microorganisms, and this makes the bioprocess more environmentally friendly. This is the first study that reports about SMCFAs from the anaerobic mixed culture fermentation of acid whey, which is available worldwide, to produce unique scl-mcl PHAs. Three strains belonging to *Pseudomonas* genera were first evaluated to study their capability of producing PHAs while they grew on different media supplemented with a synthetic mixture of SMCFAs, that simulates a real SMCFA-rich stream, as the only carbon sources. Then, the most effective *Pseudomonas* sp. strain was cultured with SMCFAs derived from whey wastewater fermentation effluent. The extracted PHAs were characterized using GC/MS, FTIR, DSC, and TG to assess the application potential of these materials.

2 Materials and methods

2.1 Microorganisms and inoculum preparation

Pseudomonas sp. Gl01 and *Pseudomonas* sp. Gl06 strains were isolated from mixed microbial communities and belong to the Culture Collection of the Department of Microbiology and Mycology, University of Warmia and Mazury in Olsztyn. They were previously described as strains capable of synthesizing and accumulating PHA_{MCL} (Ciesielski et al., 2010). The *Pseudomonas antarctica* (DSM 15318) used in the study was purchased from the German Collection of Microorganisms and Cell Cultures GmbH at the Leibniz Institute.

2.2 Culture condition and carbon sources

Seed cultures were grown in lysogeny broth (10 g/L tryptone, 5 g/L yeast extract, 10 g/L NaCl) at 30°C, shaking at 150 rpm for 16 h. Then, the precultures were transferred to three different non-limited and nitrogen-limited mineral salt media (MSM): (MSM 1) 12.8 g/L $Na_2HPO_4{\cdot}7H_2O$, 3 g/L KH_2PO_4, 10 g/L NH_4Cl, 0.5 g/L NaCl (Poblete-Castro et al., 2012); (MSM 2) 12.8 g/L Na_2HPO_4, 3 g/L KH_2PO_4, 10 g/L $(NH_4)_2SO_4$; (MSM 3) 3.5 g/L Na_2HPO_4, 5 g/L KH_2PO_4, 10 g/L $(NH_4)SO_4$. Nitrogen-limited MSM consisted of 1 g/L of nitrogen source in each media. The media were supplemented with 1 g/L of $MgSO_4{\cdot}7H_2O$ and 2.5 ml/L of trace element solution consisting of (per liter): 20 g $FeCl_3{\cdot}6H_2O$, 10 g $CaCl_2{\cdot}H_2O$, 0.03 g $CuSO_4{\cdot}5H_2O$, 0.05 g $MnCl_2{\cdot}4H_2O$, and 0.1 g $ZnSO_4{\cdot}7H_2O$ dissolved in 0.5N HCl. The pH of each culture was adjusted to 7.0 by adding 1N NaOH and 1N HCl. All MSM components were dissolved in water and then autoclaved at 121°C. An $MgSO_4{\cdot}7H_2O$ solution was sterilized and added separately. The MSM were supplemented with 20% (v/v) of a mixture of synthetic SMCFAs ($SMCFA_{synthetic}$-rich stream) or 20% (v/v) of SMCFAs extracted from mixed culture fermentation of acid whey ($SMCFA_{extracted}$-rich stream). $SMCFA_{synthetic}$-rich stream is a mixture of synthetic carboxylic acids composed of 2.85 g/L of acetic acid, 9.86 g/L of butyric acid, 0.16 g/L of valeric acid, and 3.05 g/L of caproic acid. The effluent for PHA production was taken from the acidogenic anaerobic mixed culture fermentation of acid whey obtained from a crude cheese production line (Duber et al., 2018). It was taken from a steady-state phase and contained (except for organic acids mentioned previously) 9.31 g/L lactic acid and 1.64 g/L ethanol.

The *Pseudomonas* spp. strains were cultured in 250-ml Erlenmeyer flasks in a rotary shaker at 150 rpm, at 30°C for 48 h. Fermentation shake flasks were inoculated with 5% v/v of the precultures. The carbon source was added at the beginning of the cultivations. Three replicate cultivations were carried out. The bacterial cells were harvested at 48 h to determine the cell dry mass, PHA concentration, and composition.

2.3 Bioreactor fermentation

The preliminary cultivations in shake flasks led to the selection of MSM, consisting of 12.8 g/L Na_2HPO_4, 3 g/L KH_2PO_4, 1 g/L $(NH_4)_2SO_4$ that supported the best PHA productivity, and *Pseudomonas* sp. GL06 as the most effective PHA producer.

The PHA production of the selected *Pseudomonas* sp. strain was conducted at 30°C with an aeration rate of 4 L/min in a 7 L bioreactor (Biostat A, Sartorius, Germany) equipped with a pH controller. The pH-value was maintained at seven through the modulated addition of concentrated 1N NaOH and 1N HCl. The temperature was maintained by a thermostatic jacket. The dissolved oxygen was monitored during the whole cycle with an O_2 electrode (InPro 6800, Mettler Toledo GmbH, Switzerland) and was maintained at 50% air saturation by adjusting the agitation rate from 300 to 1,000 rpm automatically. Total fermentation time was 48 h. The inoculation size was 10% (v/v). The mineral salt medium was supplemented with a total of 20% (v/v) SMCFAs-extracted. The substrate was added in two portions: first at the beginning of the cultivation and then after 8 h of fermentation. A concentrate solution (Sigma Aldrich) was used as an antifoam in response to the antifoam controller. The samples of the culture broth were removed at several time intervals for analysis of biomass concentration, ammonium and phosphate concentration, PHA yield, the composition, and concentration of PHA monomers.

2.4 Analytical procedures

To measure cell dry mass (CDM), 100 ml of culture broth was centrifuged at 11.200 × g for 10 min and then lyophilized for 24 h using a Lyovac GT2 System (SRK Systemtechnik GmbH). Ammonium and phosphorus concentration were determined spectrophotometrically using a Hach Lange DR 2800 spectrophotometer (Hach Lange, Düsseldorf, Germany) as well as the LCK338 and LCK350 kits according to the manufacturer's instructions, respectively. Quantitative and qualitative analysis of the obtained biopolymers was performed. Biopolyesters were extracted by shaking lyophilized cells in chloroform at 50°C for 3 h. Then the mixture was filtered through No. 1 Whatman filter paper to remove the cellular debris. Biopolymers dissolved in chloroform were purified by precipitation with a 70% cold methanol solution and then allowed to evaporate at room temperature. The PHA content (% of CDM) was defined as the percentage of the ratio of biopolymer concentration to total cell concentration.

2.5 PHA analyses

2.5.1 Gas chromatography coupled with mass spectrometry

To evaluate the PHA composition, the lyophilized cells were analyzed by gas chromatography coupled with mass spectrometry (GC-MS QP2010 PLUS, Shimadzu, Japan) according to the method described by Możejko-Ciesielska and Pokój (2018). As a first step, analyzed samples were suspended in a chloroform-methanol-sulfuric acid mixture (100/97/3, v/v/v), and the methylation process was performed by heating the vials at 100°C for 20 h. After that, the sulfuric acid was neutralized with Na_2CO_3 and the resulting mixture was dried with anhydrous Na_2SO_4. After filtration, the methyl esters were analyzed using a BPX70 (25 m × 0.22 mm × 0.25 mm) capillary column (SGE Analytical Science, Victoria, Australia) with helium as a carrier gas at a flow rate of 1.38 ml/min. The column was heated from 80 to 240°C at a rate of 10°C/min. The interface and ion source temperatures of GC-MS were set at 240°C, and the electron energy was set at 70 eV. The total ion current (TIC) mode was used in 45–500 m/z range. Pure standards of methyl 3-hydroxybutyrate, 3-hydroxyvalerate, 3-hydroxyhexanoate, -octanoate, -nonanoate, -decanoate, -undecanoate, -dodecanoate, -tetradecanoate, and -hexadecanoate were purchased from Larodan Fine Chemicals (Sweden) to generate calibration curves for the methanolysis assay.

2.5.2 Fourier-transform infrared spectroscopy

The infrared spectra were recorded in the range from 4,000 to 650 cm^{-1} with a Fourier Transform Spectrophotometer (FTIR) Nicolet iS10 (ThermoScientific, United States) by the attenuated total reflection method (ATR-FTIR) on samples without prior preparation. Each spectrum analyzed was the average of 16 recorded measurements.

2.5.3 Differential scanning calorimetry and thermogravimetry

Differential scanning calorimetry (DSC) tests were carried out in a nitrogen atmosphere with a Q200 differential scanning calorimeter (TA Instruments, United States). The temperature ranged from −70 to 230°C with a heating/cooling rate of 10°C/min. Samples of approximately 1 mg were first rapidly heated to 230°C and conditioned for 1 min to remove the thermal history of the material. The samples were then cooled to −70°C and re-heated to 230°C. Thermal analysis of polymers was based on the second heating curve, where the glass transition temperature (T_g), melting point (T_m), and change in enthalpy of the melting process (ΔH_m) were recorded.

Thermogravimetry (TG) tests were performed in a nitrogen atmosphere with a Q500 thermobalance (TA Instruments, United States). The temperature ranged from 25 to 700°C with a heating rate of 10°C/min. The mass of the analyzed samples was approximately 1 mg. From the thermogravimetric curve, 5% mass loss temperature ($T_{5\%}$) was determined and used as a parameter determining the onset of thermal degradation of the material, taken as the thermal resistance of the material (T_d). The differential thermogravimetric curve (DTG) (first derivative of the TG curve) was also presented, and the T_{max} values determining the temperature of the fastest mass loss were also presented.

3 Results and discussion

3.1 Capability of *Pseudomonas* sp. strains to grow and produce PHAs in mineral salt media containing $SMCFA_{synthetic}$-rich stream

A preliminary study of the *Pseudomonas* sp. GL01, *Pseudomonas* sp. GL06, and *P. antarctica* was conducted to determine their ability to grow and synthesize PHAs in the presence of a mixture of SMCFAs ($SMCFA_{synthetic}$-rich stream) that mimicked the effluent from whey wastewater anaerobic fermentation as the carbon source.

As can be seen in Figure 1 all tested bacteria could grow in the medium supplemented with $SMCFA_{synthetic}$-rich stream under all culture conditions used. In particular, the *Pseudomonas* sp. GL06 showed the highest biomass concentration among all tested MSM media, achieving the maximum biomass value in MSM 1 (1.8 g/L of CDM). A slightly lower amount of CDM (1.7 g/L) was achieved in the cultivation of *Pseudomonas* sp. GL01 grown on MSM 2 under non-limited conditions. A 3-fold lower CDM of all *Pseudomonas putida* strains (KT2440, CA-3, and GO16) was determined by Cerrone et al. (2014) ,who cultured them using fatty acids derived from anaerobic digestion of grass. In our study, low growth was detected in the cultivation of *P. antarctica* in culture media under non-limited as well as nitrogen-limited conditions, that could suggest the inhibitory effect of the $SMCFA_{synthetic}$-rich stream used. However, higher CDM values were observed in the cultures under non-limited conditions.

In general, adequate nitrogen source is essential for bacterial cell growth. On the other hand, PHA synthesis and accumulation by bacteria belonging to *Pseudomonas* genera is induced by nitrogen limitation in the culture medium (Hoffmann and Rehm, 2005). Our results showed that PHA concentration and productivity increased under nitrogen starvation and depended on the type of MSM used. Only in the case of *P. antarctica* grown on MSM 3, PHA yield was not triggered by nitrogen limitation (Figures 2A,B). The best PHA concentration was achieved in the culture with *Pseudomonas* sp. GL06 grown on MSM 2 under N-limitation (0.13 g/L) at the PHA productivity level of 2.7 mg/L h. Aremu et al. (2021) reported a similar PHA value (0.12 g/L) in *Pseudomonas oleovorans* culture supplemented with acetic acid as the carbon source in a nitrogen-limited medium.

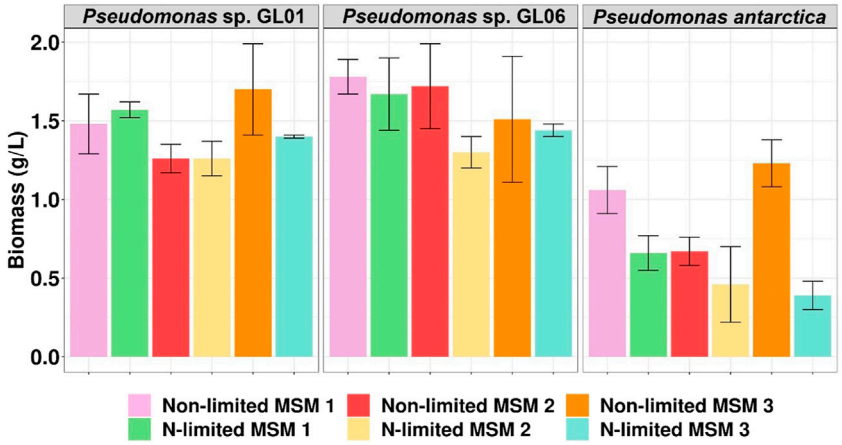

FIGURE 1
Biomass concentration (g/L) of *Pseudomonas* sp. Gl01, *Pseudomonas* sp. Gl06, and *P. antarctica* at 48 h cultured on three different growth media (MSM 1, MSM 2, and MSM 3) in shake flask experiments under non-limited and N-limited conditions using $SMCFA_{synthetic}$-rich stream.

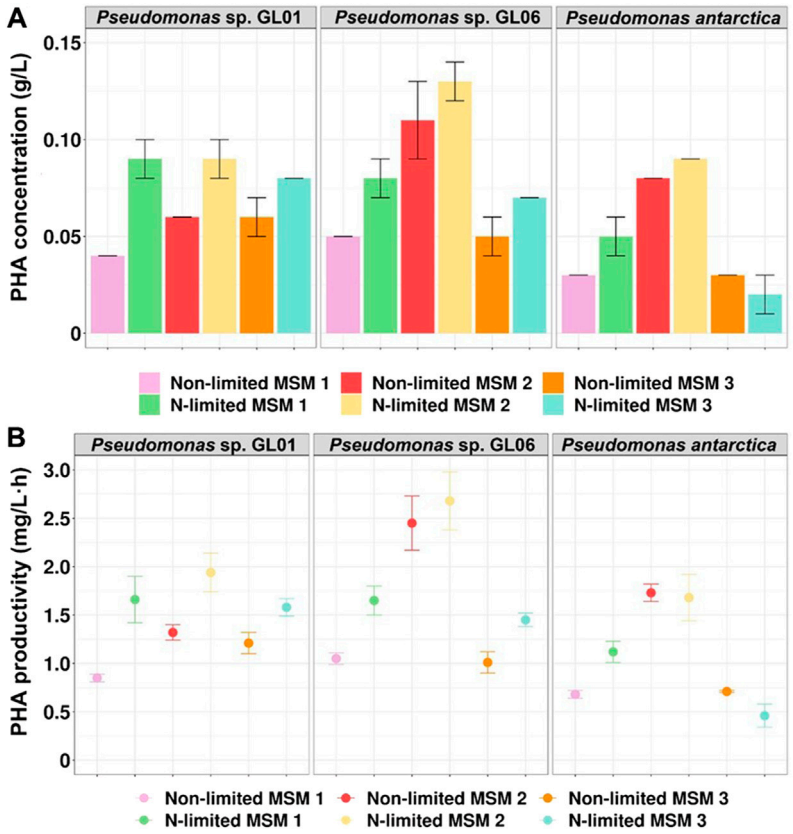

FIGURE 2
PHA production from $SMCFA_{synthetic}$-rich stream by *Pseudomonas* sp. GL01, *Pseudomonas* sp. GL06, and *P. antarctica* at 48 h cultured on three different growth media (MSM 1, MSM 2, and MSM 3) in shake flask experiments under non-limited and N-limited conditions. **(A)** PHA concentration (g/L) and **(B)** PHA productivity (mg/L h).

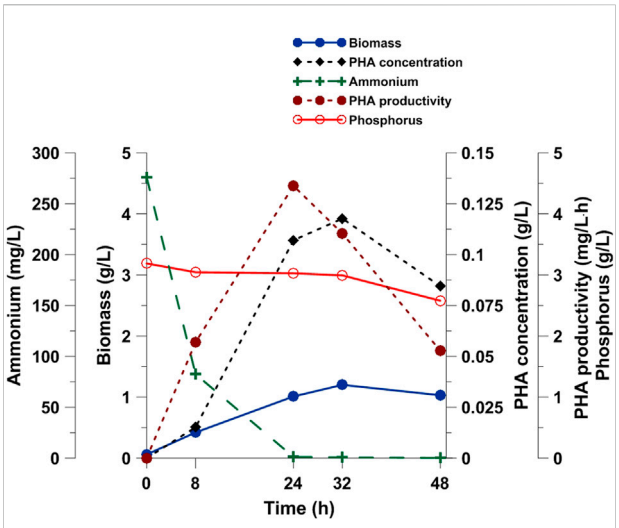

FIGURE 3
PHA production, cell, ammonium and phosphate concentration during *Pseudomonas* sp. GL06 cultivation on $SMCFA_{extracted}$-rich stream in the bioreactor fermentation.

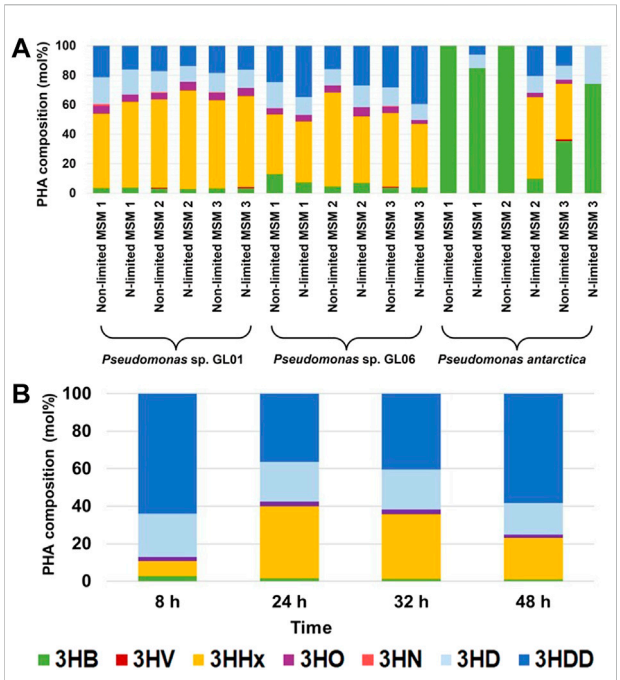

FIGURE 4
Monomeric composition of extracted PHAs from shake flasks **(A)** and bioreactor **(B)**.

Furthermore, our results suggests that PHA production could be enhanced by controlling the nitrogen source. In all tested *Pseudomonas* strains, higher PHA efficiency was observed when MSM 2 [contained $(NH_4)_2SO_4$] was used under both growth conditions compared to MSM 1 (consisted of NH_4Cl). Moreover, our data revealed that when phosphate sources ($Na_2HPO_4{\cdot}7H_2O$ and KH_2PO_4) were used in a higher concentration (MSM 2 compared to MSM 3), PHAs were synthesized and accumulated at higher yields, in particular by *Pseudomonas* sp. GL06 and *P. antarctica*. It could be concluded that the PHA concentration and productivity were dependent on the culture conditions used.

3.2 $SMCFA_{extracted}$-rich stream derived from anaerobic fermentation as the carbon source for biomass growth and PHA production

On the basis of the previously described results that *Pseudomonas* sp. GL06 produced PHAs with the highest efficiency, it was selected for further investigations into PHA production with $SMCFA_{extracted}$-rich stream from the acidogenic anaerobic mixed culture fermentation of acid whey obtained from a cheese production line. The fermentation process in a bioreactor led us to precisely monitor the bioprocess due to larger volume for sampling. As may be observed from the data reported in Figure 3, biomass concentration had been increasing for up to 32 h, and then reached 1.03 g/L at the end of the bioprocess. Comparable biomass data (1.03 g/L) were reported in *P. oleovorans* culture supplemented with volatile fatty acid streams from chicken manure where acetate was the predominant acid (Aremu et al., 2021). Higher biomass concentration was determined by our research group by supplementation of the culture medium with the same $SMCFA_{extracted}$-rich stream in the cultivation of *Paracoccus homiensis* (Szacherska et al., 2021). Moreover, our results confirmed that PHA productivity increased under nitrogen limitation, reaching a maximum value of 4.5 mg/L h at 24 h of the fermentation after ammonium exhaustion in the growth medium was reached. Similar results (4.4 mg/L h) were achieved by Kourmentza et al. (2009), who cultivated *Pseudomonas* sp. on a mixture of acetic, propionic, and butyric acids under nitrogen-limiting conditions. Goh and Tan (2012), by feeding of glucose and glycerol in the cultivation of arctic *Pseudomonas* sp. UMAB-40, determined a much lower productivity, i.e., 2.6 mg/L h and 1.6 mg/L h, respectively. Exponential nonanoic acid-limited growth of *P. putida* KT2440 resulted in a PHA content of 75.4%, giving a high cumulative PHA productivity of 1.11 g/L h (Sun et al., 2007). It should be emphasized that in our study, the PHA yield did not increase more after 24 h. The observed reduction in PHA synthesis can be explained by the consumption of the accumulated PHAs as energy reserves to extend the survival of bacteria after depletion of the carbon and nitrogen sources (Kourmentza et al., 2017). The same observation was made by Venkateswar Reddy et al. (2012) who reported that after reaching the maximum PHA concentration, the production capacity of

Pseudomonas otitidis decreased up to the end of the experiment. The authors suggested that due to the famine phase, the stored PHAs were consumed by the bacteria to maintain their cell activity in the absence of essential nutrients. Furthermore, the PHA productivity was about 60% higher than that determined in the shake flask experiments using the same culture medium. It should be noted that the difference between $SMCFA_{synthetic}$-rich stream and $SMCFA_{extracted}$-rich stream was the presence of lactic acid and ethanol in the latter. Thus, our data suggested that neither lactic acid nor ethanol affected the PHA productivity negatively.

Furthermore, quite low PHA productivity was reported in the cultivation of *P. homiensis* grown on the same (as in our study) $SMCFA_{extracted}$-rich stream, suggesting that the presence of butyric acid as the dominant component had more inhibitory effect due to the fact that a single short-chain-fatty acid in the medium resulted in the lowest PHA production efficiency compared with others (Szacherska et al., 2021).

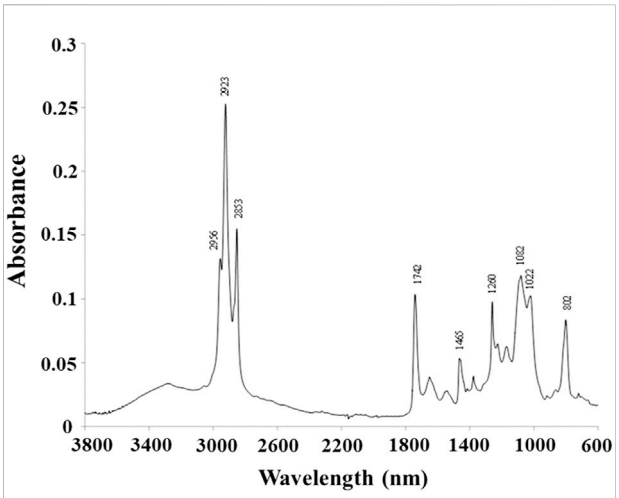

FIGURE 5
FTIR spectra of P(3HB-co-3HHx-co-3HO-co-3HD-co-3HDD) extracted from the *Pseudomonas* sp. GL06 cells at 48 h cultured in the bioreactor.

3.3 The characterization of PHAs

3.3.1 GC-MS

As shown in Figure 4, the PHA monomeric composition varied with the bacterial strain and the type of the growth medium used. Our results proved that in the cultivations supplemented with $SMCFA_{synthetic}$-rich stream that simulated a real SMCFA-rich stream, *Pseudomonas* sp. GL01 and GL06 showed the tendency to produce high amounts of 3-hydroxyhexanoate (3HHx) and 3-hydroxydodecanoate (3HDD) as the main monomers and lower content of 3-hydroxybutyrate (3HB), 3-hydroxyoctanoate (3HO), and 3-hydroxydecaonate (3HD). Interestingly, only in the cultivations of *Pseudomonas* sp. GL01 performed under non-limited growth conditions a trace amounts of 3-hydroxynonanoate was detected. This monomer was found mainly at the end of the fermentation of the same bacterial strain using saponified waste palm oil (Możejko and Ciesielski, 2013). The level of 3HB in the extracted PHAs seems to be strain dependent. Our results indicated that *P. antarctica* is able to synthesize P(3HB) homopolymer grown on MSM1 and MSM2 under non-limited conditions, whereas this bacterium cultured on MSM 3 under both conditions applied was capable of producing scl-mcl copolymers. *P. otitidis* also prefers to produce copolymers, however, consisting of 3HB and 3HV monomers (Venkateswar Reddy et al., 2012). The authors reported that the copolymer showed higher 3HB monomer content (91 mol%) when the bacteria were cultured on synthetic acids (acetate, propionate, and butyrate) compared to acidogenic effluent from the biohydrogen reactor. Furthermore, it was observed that *P. putida* KT2440 grown in the medium supplemented with acetate as the sole carbon source produced P(3HO-*co*-3HD-*co*-3HDD) terpolymer with 3HD as the principal monomer (Yang et al., 2019).

The GC/MS analysis confirmed that at the beginning of the cultivations of *Pseudomonas* sp. GL06 in the bioreactor, no PHAs were detected. The repeat-unit composition of the purified biopolymers extracted from the bioreactor at 8 h of the fermentation was found to consist mainly of 3HD and 3HDD and lesser amounts of 3HB, 3HHx, and 3HO. From 24 to 48 h of the cultivation higher content of 3HHx fraction was observed from 38.5 mol% to 22.1 mol%, respectively. 3HB and 3HO monomers were detected as minor components in extracted biomaterials. Similarly, when glucose, glycerol, and fructose were supplied as carbon sources to *Pseudomonas* sp. B14-6 by Choi et al. (2021), scl-mcl copolymer was detected. However, *P. putida* KT2440 and CA-3 synthesized mcl-copolymers cultured on the concentrated fatty acid mixture derived from the anaerobic digestion leachate. Cerrone et al. (2014) showed that these strains produced 3HD as the main constituent and 3HO and 3HDD as minor components.

3.3.2 FTIR

The FTIR spectra of the polymer produced is presented in Figure 5. The spectrum displays the typical bands for PHAs (Shamala et al., 2009; Rebocho et al., 2020; Meneses et al., 2021). Peaks at 2,956, 2,923, and 2,853 cm^{-1} can be assigned to the stretching vibration of C-H bonds of methyl (CH_3) and methylene (CH_2) groups of the PHA molecule. The high intensity of the 3,000–2,700 band (the highest in the entire spectrum) results from the presence of a large amount of medium chain length monomers in the tested polymer. The absorbance band located at 1740 cm^{-1} is attributed to the stretching vibration of the C=O group (ester carbonyl) in the

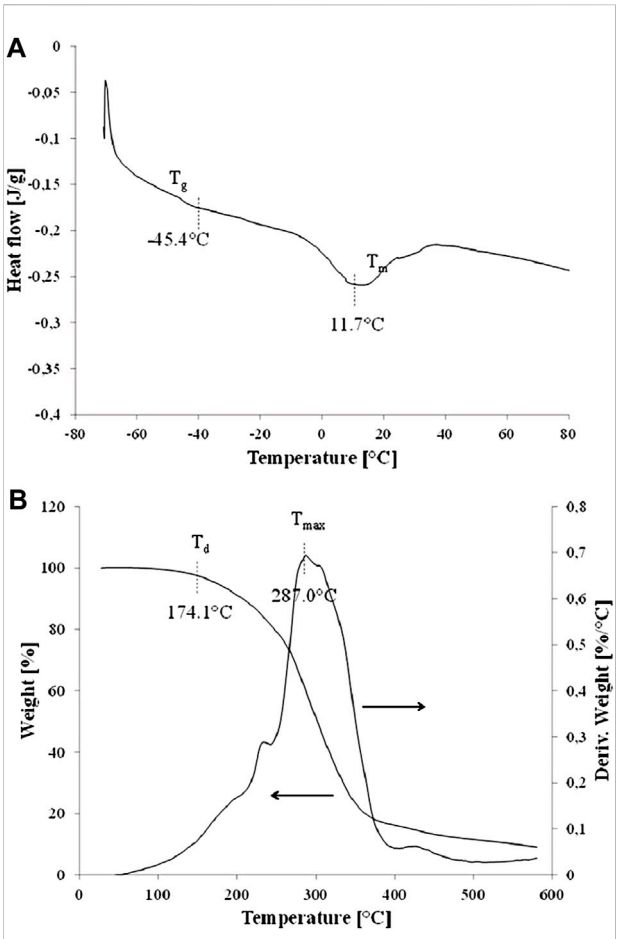

FIGURE 6
DSC curves **(A)** and TG curves **(B)** of P(3HB-co-3HHx-co-3HO-co-3HD-co-3HDD) extracted from the *Pseudomonas* sp. GL06 cells at 48 h cultured in the bioreactor.

PHA polyester. The bands between 1,022 and 1,260 cm^{-1} are related to the crystallinity of the material, with the 1,082 cm^{-1} peak attributed to C–O bonds. The band appearing at 802 cm^{-1} represents the C-C stretching bond and is also characteristic of PHA.

3.3.3 Thermal analysis

As can be shown in Figure 6A, DSC studies proved that glass transition temperature (T_g) of P(3HB-co-3HHx-co-3HO-co-3HD-co-3HDD) produced by *Pseudomonas* sp. GL01 reached −45.4°C. Furthermore, a small melting peak with a melting temperature (T_m) of 11.7°C and enthalpy change (ΔH_m) of 6.6 J/g was observed. The recorded T_g value is typical for mcl-PHAs and corresponds to the values reported in the literature (Simon-Colin et al., 2012; Basnett et al., 2017). The obtained melting point (11.7°C) is low and unusual, as in most cases the recorded T_m mcl-PHA values are in the range from 40 to 55°C. Lower T_m values are related to the low degree of crystallinity of this polymer and the predominance of the amorphous phase. The low content of the crystalline phase in the tested material is confirmed by the FTIR tests (low absorbance of peaks related to the crystalline phase) and the very low ΔH_m value obtained in the DSC tests. Nevertheless a P(3HO-*co*-3HD-*co*-3HDD-*co*-3HTD) copolymer produced by *Yarrowia lipolytica* ThYl_1,166 also possess low T_g (−39°C) and T_m (19°C) values indicating its amorphous behavior and flexibility at ambient temperature (Rigouin et al., 2019).

Moreover, the degradation temperature (T_d) of the tested scl-mcl copolymer was observed at 174.1°C (Figure 6B) and was lower than the typical T_d values recorded for mcl-PHAs (above 200°C) (Simon-Colin et al., 2012; Basnett et al., 2017) due to its low degree of crystallinity. Additionally, TG analysis showed that the beginning of the degradation process already started just above 100°C and proceeded over a fairly large temperature range with the maximum intensity (T_{max}) at 287.0°C (Figure 6B). The course of the degradation process may have been caused by a large number of macromolecules of shorter length (lower molecular weight), which are characterized by lower degradation temperatures. The fact that 3HB monomer was present in the extracted copolymer could be the reason for its lower thermal resistance.

4 Conclusion

Supplementation of synthetic SMCFAs in bacterial cultures would be expensive. Therefore using SMCFA-rich stream from the fermentation of agro-industrial waste to produce PHAs can significantly reduce the cost of the process. In this study, both variants of SMCFAs were proved to be potential substrates for PHA production by *Pseudomonas* strains. The highest PHA productivity was achieved in *Pseudomonas* sp. Gl06 cultivation in the bioreactor under N-limited with MSM 2 using $SMCFA_{extracted}$-rich stream derived from MCF using food waste. The structure and thermal properties of the PHAs were analytically verified and we proved that the extracted scl-mcl copolymers possess lower melting point and degradation temperature compared to the PHAs described in the literature. These findings indicate the possibility of feeding the *Pseudomonas* sp. GL06 with cheap $SMCFA_{extracted}$-rich stream to produce PHA copolymers with improved properties.

Data availability statement

The original contributions presented in the study are included in the article; further inquiries can be directed to the corresponding author.

Author contributions

KS participated in the design of the study and performed the cultivations and PHA extractions. KM performed and interpreted FTIR and differential scanning calorimetric and thermogravimetric analyses. SC performed and interpreted gas chromatography coupled with mass spectrometry analysis. PO-P performed waste-derived SMCFA analysis and participated in the design of the study. JM-C participated in the design of the study and supervised in study coordination. KS and JM-C wrote the manuscript with input from all the authors.

Funding

This work was supported by the University of Warmia and Mazury in Olsztyn (Poland) (Grant Number 12.620.012-300) and by the Poznan University of Technology (Grant Number 0713/SBAD/0958). KS is a recipient of a scholarship from the Programme Interdisciplinary Doctoral Studies in Bioeconomy (POWR.03.02.00-00-I034/16-00), which is funded by the European Social Funds.

Conflict of interest

The authors declare that the research was conducted in the absence of any commercial or financial relationships that could be construed as a potential conflict of interest.

Publisher's note

All claims expressed in this article are solely those of the authors and do not necessarily represent those of their affiliated organizations, or those of the publisher, the editors, and the reviewers. Any product that may be evaluated in this article, or claim that may be made by its manufacturer, is not guaranteed or endorsed by the publisher.

References

Akaraonye, E., Keshavarz, T., and Roy, I. (2010). Production of polyhydroxyalkanoates: The future green materials of choice. *J. Chem. Technol. Biotechnol.* 85, 732–743. doi:10.1002/jctb.2392

Albuquerque, M. G. E., Eiroa, M., Torres, C., Nunes, B. R., and Reis, M. A. M. (2007). Strategies for the development of a side stream process for polyhydroxyalkanoate (PHA) production from sugar cane molasses. *J. Biotechnol.* 130, 411–421. doi:10.1016/j.jbiotec.2007.05.011

Aremu, M. O., Ishola, M. M., and Taherzadeh, M. J. (2021). Polyhydroxyalkanoates (PHAs) production from volatile fatty acids (VFAs) from organic wastes by *Pseudomonas oleovorans*. *Fermentation* 7, 287. doi:10.3390/fermentation7040287

Basnett, P., Lukasiewicz, B., Marcello, E., Gura, H. K., Knowles, J. C., Roy, J., et al. (2017). Production of a novel medium chain length poly(3-hydroxyalkanoate) using unprocessed biodiesel waste and its evaluation as a tissue engineering scaffold. *Microb. Biotechnol.* 10, 1384–1399. doi:10.1111/1751-7915.12782

Beccari, M., Bertin, L., Dionisi, D., Fava, F., Lampis, S., Majone, M., et al. (2009). Exploiting olive oil mill effluents as a renewable resource for production of biodegradable polymers through a combined anaerobic–aerobic process. *J. Chem. Technol. Biotechnol.* 84, 901–908. doi:10.1002/jctb.2173

Bengtsson, S., Werker, A., Christensson, M., and Welander, T. (2008). Production of polyhydroxyalkanoates by activated sludge treating a paper mill wastewater. *Bioresour. Technol.* 99, 509–516. doi:10.1016/j.biortech.2007.01.020

Cerrone, F., Choudhari, S. K., Davis, R., Cysneiros, D., O'Flaherty, V., Duane, G., et al. (2014). Medium chain length polyhydroxyalkanoate (mcl-PHA) production from volatile fatty acids derived from the anaerobic digestion of grass. *Appl. Microbiol. Biotechnol.* 98, 611–620. doi:10.1007/s00253-013-5323-x

Choi, T. R., Park, Y. L., Song, H. S., Lee, S. M., Park, S. L., Lee, H. S., et al. (2021). Fructose-based production of short-chain-length and medium-chain-length polyhydroxyalkanoate copolymer by arctic *Pseudomonas* sp. B14-6. *Polymers* 13, 1398. doi:10.3390/polym13091398

Ciesielski, S., Możejko, J., and Przybyłek, G. (2010). The influence of nitrogen limitation on mcl-PHA synthesis by two newly isolated strains of *Pseudomonas* sp. *J. Ind. Microbiol. Biotechnol.* 37, 511–520. doi:10.1007/s10295-010-0698-5

Duber, A., Jaroszynski, Ł., Zagrodnik, R., Chwialkowska, J., Juzwa, W., Ciesielski, S., et al. (2018). Exploiting the real wastewater potential for resource recovery – N-Caproate production from acid whey. *Green Chem.* 20, 3790–3803. doi:10.1039/c8gc01759j

Erickson, B. E. (2017). Acid whey: Is the waste product an untapped goldmine? *Chem. Eng. News.* 95, 26–30. doi:10.1021/cen-09506-cover

Goh, Y. S., and Tan, I. K. P. (2012). Polyhydroxyalkanoate production by Antarctic soil bacteria isolated from casey station and signy island. *Microbiol. Res.* 167, 211–219. doi:10.1016/j.micres.2011.08.002

Hoffmann, N., and Rehm, B. H. (2005). Nitrogen-dependent regulation of medium-chain length polyhydroxyalkanoate biosynthesis genes in pseudomonads. *Biotechnol. Lett.* 27, 279–282. doi:10.1007/s10529-004-8353-8

Koller, M., and Braunegg, G. (2015). Biomediated production of structurally diverse poly(hydroxyalkanoates) from surplus streams of the animal processing industry. *Polimery* 60 (5), 298–308. doi:10.14314/polimery.2015.298

Kourmentza, C., Ntaikou, I., Kornaros, M., and Lyberatos, G. (2009). Production of PHAs from mixed and pure cultures of *Pseudomonas* sp. using short-chain fatty acids as carbon source under nitrogen limitation. *Desalination* 248, 723–732. doi:10.1016/j.desal.2009.01.010

Kourmentza, C., Plácido, J., Venetsaneas, N., Burniol-Figols, A., Varrone, C., Gavala, H. N., et al. (2017). Recent advances and challenges towards sustainable polyhydroxyalkanoate (PHA) production. *Bioeng. (Basel).* 4 (2), 55. doi:10.3390/bioengineering4020055

Lad, B. C., Coleman, S. M., and Alper, H. S. (2022). Microbial valorization of underutilized and nonconventional waste streams. *J. Ind. Microbiol. Biotechnol.* 49, kuab056. doi:10.1093/jimb/kuab056

Liu, C. H., Chen, H. Y., LeeChen, Y. L., and Sheu, D. S. (2021). The polyhydroxyalkanoate (PHA) synthase 1 of *Pseudomonas* sp. H9 synthesized a 3-hydroxybutyrate-dominant hybrid of short- and medium-chain-length PHA. *Enzyme Microb. Technol.* 143, 109719. doi:10.1016/j.enzmictec.2020.109719

Martinez, G. A., Bertin, L., Scoma, A., Rebecchi, S., Braunegg, G., Fava, F., et al. (2015). Production of polyhydroxyalkanoates from dephenolised and fermented olive mill wastewaters by employing a pure culture of *Cupriavidus necator*. *Biochem. Eng. J.* 97, 92–100. doi:10.1016/j.bej.2015.02.015

Meneses, L., Craveiro, R., Jesus, A. R., Reis, M. A. M., Freitas, F., Paiva, A., et al. (2021). Supercritical CO_2 assisted impregnation of ibuprofen on medium-chain-length polyhydroxyalkanoates (mcl-PHA). *Molecules* 26, 4772. doi:10.3390/MOLECULES26164772

Możejko, J., and Ciesielski, S. (2013). Saponified waste palm oil as an attractive renewable resource for mcl-polyhydroxyalkanoate synthesis. *J. Biosci. Bioeng.* 116, 485–492. doi:10.1016/j.jbiosc.2013.04.014

Możejko-Ciesielska, J., and Pokój, T. (2018). Exploring nutrient limitation for polyhydroxyalkanoates synthesis by newly isolated strains of *Aeromonas* sp. using biodiesel-derived glycerol as a substrate. *PeerJ* 6, e5838. doi:10.7717/peerj.5838

Mozejko-Ciesielska, J., Szacherska, K., and Marciniak, P. (2019). *Pseudomonas* species as producers of eco-friendly polyhydroxyalkanoates. *J. Polym. Environ.* 27, 1151–1166. doi:10.1007/s10924-019-01422-1

Munir, S., and Jamil, N. (2018). Polyhydroxyalkanoates (PHA) production in bacterial co-culture using glucose and volatile fatty acids as carbon source. *J. Basic Microbiol.* 58 (3), 247–254. doi:10.1002/jobm.201700276

Patel, S. K. S., Singh, M., Kumar, P., Purohit, H. J., and Kalia, V. C. (2012). Exploitation of defined bacterial cultures for production of hydrogen and polyhydroxybutyrate from pea shells. *Biomass Bioenergy* 36, 218–225. doi:10.1016/j.biombioe.2011.10.027

Poblete-Castro, I., Escapa, I., Jager, C., Puchalka, J., Lam, M. C., Schomburg, D., et al. (2012). The metabolic response of *P. putida* KT2442 producing high levels of polyhydroxyalkanoate under single- and multiple-nutrient-limited growth: Highlights from a multi-level omics approach. *Microb. Cell. Fact.* 11, 34. doi:10.1186/1475-2859-11-34

Rebocho, A. T., Pereira, J. R., Neves, L. A., Alves, V. D., Sevrin, C., and Grandfils, C. (2020). Preparation and characterization of films based on a natural P(3HB)/mcl-PHA blend obtained through the Co-culture of *cupriavidus necator* and *Pseudomonas citronellolis* in apple pulp waste. *Bioeng. (Basel).* 7, 34. doi:10.3390/BIOENGINEERING7020034

Reddy, S. V., Thirumala, M., and Mahmood, S. K. (2008). Production of PHB and P (3HB-co-3HV) biopolymers by *Bacillus megaterium* strain OU303A isolated from municipal sewage sludge. *World J. Microbiol. Biotechnol.* 25, 391–397. doi:10.1007/s11274-008-9903-3

Rigouin, C., Lajus, S., Ocando, C., Borsenberger, V., Nicaud, J. M., Marty, A., et al. (2019). Production and characterization of two medium-chain-length polydroxyalkanoates by engineered strains of *Yarrowia lipolytica*. *Microb. Cell. Fact.* 18, 99. doi:10.1186/s12934-019-1140-y

Shamala, T. R., Divyashree, M. S., Davis, R., Kumari, K. S. L., Vijayendra, S. V. N., Raj, B., et al. (2009). Production and characterization of bacterial polyhydroxyalkanoate copolymers and evaluation of their blends by Fourier transform infrared spectroscopy and scanning electron microscopy. *Indian J. Microbiol.* 49, 251–258. doi:10.1007/S12088-009-0031-Z

Simon-Colin, C., Gouin, C., Lemechko, P., Schmitt, S., Senant, A., Kervarec, N., et al. (2012). Biosynthesis and characterization of polyhydroxyalkanoates by *Pseudomonas guezennei* from alkanoates and glucose. *Int. J. Biol. Macromol.* 51, 1063–1069. doi:10.1016/J.IJBIOMAC.2012.08.018

Solaiman, D. K., and Ashby, R. D. (2005). Genetic characterization of the poly(hydroxyalkanoate) synthases of various *Pseudomonas oleovorans* strains. *Curr. Microbiol.* 50, 329–333. doi:10.1007/s00284-005-4508-7

Sun, Z., Ramsay, J. A., Guay, M., and Ramsay, B. A. (2007). Carbon-limited fed-batch production of medium-chain-length polyhydroxyalkanoates from nonanoic acid by *Pseudomonas putida* KT2440. *Appl. Microbiol. Biotechnol.* 74, 69–77. doi:10.1007/s00253-006-0655-4

Szacherska, K., Moraczewski, K., Rytlewski, P., Czaplicki, S., Ciesielski, S., Oleskowicz-Popiel, P., et al. (2021). Polyhydroxyalkanoates production from short and medium chain carboxylic acids by *Paracoccus homiensis*. *Sci. Rep.* 12 (1), 7263. doi:10.1038/s41598-022-11114-x

Tan, D., Wang, Y., Tong, Y., and Chen, G. Q. (2021). Grand challenges for industrializing polyhydroxyalkanoates (PHAs). *Trends Biotechnol.* 39 (9), 953–963. doi:10.1016/j.tibtech.2020.11.010

Tan, G. Y. A., Chen, C. L., Li, L., Ge, L., Wang, L., Razaad, I. M. N., et al. (2014). Start a research on biopolymer polyhydroxyalkanoate (PHA): A review. *Polymers* 6 (3), 706–754. doi:10.3390/polym6030706

Thomas, C. M., Kumar, D., Scheel, R., Ramarao, B., and Nomura, C. T. (2022). Production of Medium Chain Length polyhydroxyalkanoate copolymers from agro-industrial waste streams. *Biocatal. Agric. Biotechnol.* 43, 102385. doi:10.1016/j.bcab.2022.102385

Venkateswar Reddy, M., Mawatari, Y., Onodera, R., Nakamura, Y., Yuka Yajima, Y., Chang, Y. C., et al. (2017). Polyhydroxyalkanoates (PHA) production from synthetic waste using *Pseudomonas pseudoflava*: PHA synthase enzyme activity analysis from. *P. pseudoflava P. palleronii. Bioresour. Technol.* 234, 99–105. doi:10.1016/j.biortech.2017.03.008

Venkateswar Reddy, M., Nikhil, G. N., Venkata Mohan, S., Swamy, Y. V., and Sarma, P. N. (2012). *Pseudomonas otitidis* as a potential biocatalyst for polyhydroxyalkanoates (PHA) synthesis using synthetic wastewater and acidogenic effluents. *Bioresour. Technol.* 123, 471–479. doi:10.1016/j.biortech.2012.07.077

Venkateswar Reddy, M., and Venkata Mohan, S. (2012). Influence of aerobic and anoxic microenvironments on polyhydroxyalkanoates (PHA) production from food waste and acidogenic effluents using aerobic consortia. *Bioresour. Technol.* 103, 313–321. doi:10.1016/j.biortech.2011.09.040

Vu, D. H., Wainaina, S., Taherzadeh, M. J., Åkesson, D., and Ferreira, J. A. (2021). Production of polyhydroxyalkanoates (PHAs) by *Bacillus megaterium* using food waste acidogenic fermentation-derived volatile fatty acids. *Bioengineered* 12 (1), 2480–2498. doi:10.1080/21655979.2021.1935524

Yang, S., Li, S., and Jia, X. (2019). Production of medium chain length polyhydroxyalkanoate from acetate by engineered *Pseudomonas putida* KT2440. *J. Ind. Microbiol. Biotechnol.* 46 (6), 793–800. doi:10.1007/s10295-019-02159-5

Zubairi, S. I., Mantalaris, A., Bismarck, A., and Aizad, S. (2016). Polyhydroxyalkanoates (PHAs) for tissue engineering applications: Biotransformation of palm oil mill effluent (pome) to value-added polymers. *J. Teknol.* 78, 13–29. doi:10.11113/jt.v78.4042

frontiers | Frontiers in Bioengineering and Biotechnology

TYPE Original Research
PUBLISHED 16 August 2022
DOI 10.3389/fbioe.2022.966062

OPEN ACCESS

EDITED BY
Xiao-Jun Ji,
Nanjing Tech University, China

REVIEWED BY
Xin Wang,
Nanjing Tech University, China
Zhaojuan Zheng,
Nanjing Forestry University, China

*CORRESPONDENCE
Mo Xian,
xianmo@qibebt.ac.cn
Guang Zhao,
zhaoguang@sdu.edu.cn

†These authors have contributed equally to this work

SPECIALTY SECTION
This article was submitted to Industrial Biotechnology, a section of the journal Frontiers in Bioengineering and Biotechnology

RECEIVED 10 June 2022
ACCEPTED 27 July 2022
PUBLISHED 16 August 2022

CITATION
Liu M, Huo M, Liu C, Guo L, Ding Y, Ma Q, Qi Q, Xian M and Zhao G (2022), Lysine acetylation of Escherichia coli lactate dehydrogenase regulates enzyme activity and lactate synthesis. *Front. Bioeng. Biotechnol.* 10:966062. doi: 10.3389/fbioe.2022.966062

Lysine acetylation of *Escherichia coli* lactate dehydrogenase regulates enzyme activity and lactate synthesis

Min Liu[1†], Meitong Huo[1†], Changshui Liu[2], Likun Guo[1], Yamei Ding[2], Qingjun Ma[2], Qingsheng Qi[1], Mo Xian[3*] and Guang Zhao[1,3*]

[1]State Key Laboratory of Microbial Technology, Shandong University, Qingdao, China, [2]Institute of Oceanology, Chinese Academy of Sciences, Qingdao, China, [3]CAS Key Laboratory of Biobased Materials, Qingdao Institute of Bioenergy and Bioprocess Technology, Chinese Academy of Sciences, Qingdao, China

As an evolutionarily conserved posttranslational modification, protein lysine acetylation plays important roles in many physiological and metabolic processes. However, there are few reports about the applications of lysine acetylation in metabolic regulations. Lactate is a main byproduct in microbial fermentation, and itself also an important bulk chemical with considerable commercial values in many fields. Lactate dehydrogenase (LdhA) is the key enzyme catalyzing lactate synthesis from pyruvate. Here, we reported that *Escherichia coli* LdhA can be acetylated and the acetylated lysine sites were identified by mass spectrometry. The effects and regulatory mechanisms of acetylated sites on LdhA activity were characterized. Finally, lysine acetylation was successfully used to regulate the lactate synthesis. LdhA (K9R) mutant overexpressed strain improved the lactate titer and glucose conversion efficiency by 1.74 folds than that of wild-type LdhA overexpressed strain. LdhA (K154Q-K248Q) mutant can inhibit lactate accumulation and improve 3HP production. Our study established a paradigm for lysine acetylation in lactate synthesis regulation and suggested that lysine acetylation may be a promising strategy to improve the target production and conversion efficiency in microbial synthesis. The application of lysine acetylation in regulating lactate synthesis also provides a reference for the treatment of lactate-related diseases.

KEYWORDS

lysine acetylation, lactate dehydrogenase A, enzyme activity, metabolic engineering, lactate synthesis

Introduction

In order to adapt a changing environment, cells undergo complex regulations at different levels. Among them, posttranslational modification (PTM) can covalently modify amino acid by biochemical mechanism to make the protein structure more complex and the regulatory effect more precise (Liu et al., 2021). Protein lysine acetylation

is a highly conserved PTM from bacteria to higher animals (Hentchel and Escalante-Semerena, 2015; VanDrisse and Escalante-Semerena, 2019). Acetylation modification induces charge change of lysine from +1 to 0 and adds a bigger side chain of acetyl group. Lysine acetylation contains enzymatic and nonenzymatic mechanisms. In enzymatic acetylation, lysine acetyltransferase (KAT) catalyzes the transfer of an acetyl group from acetyl coenzyme A (Acetyl-CoA) to target protein lysine residues. In nonenzymatic acetylation, an acetyl group from acetyl phosphate (AcP) direct transfers to protein lysine residues. AcP- mediated nonenzymatic acetylation is the primary mechanism of *E. coli* (Liu et al., 2021).

Previously, researches on protein acetylation mainly focused on histone modification for regulating gene transcription in eukaryotes (Verdin and Ott, 2015). In recent decades, many bacterial acetylated proteins were constantly discovered with the development of high-affinity immune separation and nano-HPLC/MS/MS (Yu et al., 2008; Zhang et al., 2009; Zhang et al., 2013; Kuhn et al., 2014). Lysine acetylation is abundant in bacteria, affecting the cellular physiology and metabolism (Wang, 2010; Liu et al., 2021). Thus, lysine acetylation may become a promising tool in metabolic engineering. However, the applications of lysine acetylation in metabolic regulations are rarely reported. Furthermore, it remains unclear how lysine acetylation affects the cellular physiology and metabolism.

NAD-dependent lactate dehydrogenase (LdhA) is a conserved protein presented in many species, specific for lactate biosynthesis from pyruvate. In human, lactate has been proved to play an important role in pathogenesis of cancer and diabetes (Feng et al., 2018; Lin et al., 2022), and lysine acetylation regulates the activity of human LdhA, further affecting cell migration and proliferation in pancreatic cancer (Zhao et al., 2013). On the other hand, lactate itself is an important bulk chemical, widely used in the fields of cosmetics, herbicides and pharmaceutical (Feng et al., 2014; Choi et al., 2019). Lactate is also used as the precursor for producing the bioplastic polymers of polylactic acid (PLA). At present, the majority of lactate is produced by microbial fermentation because of some outstanding advantages over the chemical synthesis, like the environmental protection, low cost and low energy consumption (Abdel-Rahman et al., 2013; Juturu and Wu, 2016). In addition, lactate accumulation is also a main problem in bioproduction process of other chemicals, which is caused by the intracellular accumulation of pyruvate and NADH, as a consequence of the imbalance between rapid glucose catabolism and the limited respiratory capacity of microbe (Eiteman and Altman, 2006; Bernal et al., 2016). Traditionally, *ldhA* gene was deleted in engineered microorganism to repress the lactate production, that brought about some negative issues. So, regulation of lactate production is an enduring research topic in metabolic engineering.

Escherichia coli is one of the most widely used host in microbial fermentation, employed to synthesize a large amount of chemicals including lactate, but it still remains unknown whether the activity of *E. coli* LdhA is affected by lysine acetylation. In this study, we found lysine acetylation can affect LdhA function in *E. coli*. We identified the acetylated sites and explored the mechanism of LdhA acetylation on enzyme activity. Finally, we established a paradigm of lactate synthesis regulation by lysine acetylation.

Materials and methods

Plasmids and strains construction

Primers used in this study were listed in Supplementary Table S1, all plasmids and strains used in this study were listed in Table 1. *E. coli* DH5α was used as the host for plasmid construction, and *E. coli* BL21 (DE3) was used as the host for protein expression and target production. Polymerase chain reaction (PCR) combined with restriction enzyme digest were used to plasmid construction. Site-directed mutagenesis of *ldhA* was carried out according to the Stratagene protocol. The chromosomal genes of *E. coli* BL21 (DE3) were knocked out *via* P_1 vir-mediated transduction as previously described (Moore, 2011). The donor strains were purchased from the Keio collection (Baba et al., 2006). The *ldhA* (K154Q-248Q) replacement *in situ* was carried out by suicide plasmid pRE112-mediated homologous recombination (Edwards et al., 1998). The recombinant plasmids were transformed to their corresponding hosts for protein expression and fermentation.

Identification of acetylated lysine residues by mass spectrometry

The purified LdhA cultured in Luria–Bertani (LB) with 2% glucose was detected by 12% SDS-PAGE, the excised LdhA band was digested with trypsin by a standard in-gel digestion protocol. The trypsin digested product was desalted by Ziptip C18 chromatographic column and redissolved by 0.1% trifluoroacetic acid. Peptides were separated on a nanoViper C18 silica column Acclaim PepMap RSLC (75 μm × 25 cm, 2 μm, Thermo, United States) with mobile phase system of solvent A (0.1% formic acid) and B (80% ACN and 0.1% formic acid) at a flow rate of 300 nL/min, and analyzed by nano system (Thermo Scientific, EASY-nLC, United States) coupled with a 1,000,000 FWHM high-resolution Nano Orbitrap Fusion Lumos Tribrid Mass Spectrometer system (Thermo Scientific, United States). Mass spectrometric data processing used the Proteome Discoverer software 2.3 (Thermo Scientific, United States).

Protein expression and purification

E. coli cells were grown overnight at 37°C in LB medium with appropriate antibiotics. The culture was diluted 1:

TABLE 1 Plasmids and strains used in this study.

Plasmids and strains	Relevant properties	Source
Plasmids		
pACYCDuet1	*Cm*^{r} *oriP*$_{15A}$ *lacI*^{q} P$_{T7}$	Novagen
pETDuet1	Amp^r oriP$_{BR322}$ lacIq P$_{T7}$	Novagen
pCP20	reppSC101^{ts} Ap^R Cm^R cI857 λP$_R$ FLP	CGSC[a]
pRE112	oriT oriV sacB Cm^R	Dr. Roy Curtiss III
pACYCDuet1-*acc*	rep$_{p15A}$ Cm^R lacI P$_{T7}$ *accA* $_{PT7}$ *accD* $_{PT7}$ *accBC*	Liu et al. (2016)
pETDuet1-*mcr*	rep$_{pBR322}$ Amp^R lacI P$_{lac,p2\text{-}51}$ -*mcr*1-549 P$_{T7}$ *mcr*550-1,219(N940 V K1106W S1114R)	Liu et al. (2016)
pETDuet1-*ldhA*	Amp^r oriP$_{BR322}$ lacIq P$_{T7}$ ldhA	This study
Strains		
E. coli DH5α	F$^-$ *supE*44 Δ*lacU*169 (*ϕ*80 *lacZ* Δ*M15*) *hsdR*17 *recA*1 *endA*1 *gyrA*96 *thi*-1 *relA*1	Invitrogen
E. coli BL21 (DE3)	F$^-$ *ompT gal dcm lon hsdSB* (rB$^-$ mB$^-$) λ(DE3)	Invitrogen
E. coli χ7213	*thi*-1 *thr*-1 *leu*B6 *gln*V44 *fhu*A21 *lac*Y1 *rec*A1 *RP4*-2-Tc:Mu λ*pir* Δ*asd*A4 Δ*zhf*-2:*Tn*10	Dr. Roy Curtiss III
Q3685	*E. coli* BL21 (DE3)/pETDuet1-*ldhA*	This study
Q3749	*E. coli* BL21 (DE3)/pETDuet1-*ldhA* (K9R)	This study
Q3750	*E. coli* BL21 (DE3)/pETDuet1-*ldhA* (K9Q)	This study
Q3686	*E. coli* BL21 (DE3)/pETDuet1-*ldhA* (K70R)	This study
Q3687	*E. coli* BL21 (DE3)/pETDuet1-*ldhA* (K70Q)	This study
Q3688	*E. coli* BL21 (DE3)/pETDuet1-*ldhA* (K154R)	This study
Q3689	*E. coli* BL21 (DE3)/pETDuet1-*ldhA* (K154Q)	This study
Q3690	*E. coli* BL21 (DE3)/pETDuet1-*ldhA* (K248R)	This study
Q3691	*E. coli* BL21 (DE3)/pETDuet1-*ldhA* (K248Q)	This study
Q3714	*E. coli* BL21 (DE3)/pETDuet1-*ldhA* (K70Q-K154Q)	This study
Q3715	*E. coli* BL21 (DE3)/pETDuet1-*ldhA* (K154Q-K248Q)	This study
Q3719	*E. coli* BL21 (DE3)/pETDuet1-*ldhA* (D279E)	This study
Q3720	*E. coli* BL21 (DE3)/pETDuet1-*ldhA* (D279N)	This study
Q3786	*E. coli* BL21 (DE3)/pETDuet1-*ldhA* (E269D)	This study
Q3787	*E. coli* BL21 (DE3)/pETDuet1-*ldhA* (E269N)	This study
JW1375	BW25113 *ΔldhA::Km*^{R}	Keio collection
Q2326	*E. coli* BL21 (DE3) Δ*ldhA*	This study
Q3784	*E. coli* BL21 (DE3) Δ*ldhA*/pETDuet1-*ldhA*	This study
Q3785	*E. coli* BL21 (DE3) Δ*ldhA*/pETDuet1-*ldhA* (K9R)	This study
Q3790	*E. coli* BL21 (DE3) *ldhA*: *ldhA* (K154Q-K248Q)	This study
Q2191	*E. coli* BL21 (DE3)/pACYCDuet1-*acc*/pETDuet1-*mcr*	This study
Q 3824	Q2326/pACYCDuet1-*acc*/pETDuet1-*mcr*	This study
Q 3825	Q3790/pACYCDuet1-*acc*/pETDuet1-*mcr*	This study

[a]The Coli Genetic Stock Center at Yale University.

50 into fresh LB medium with 2% glucose and incubated under the same condition. When the OD_{600} of culture reached about 0.8, 100 μM isopropyl-β-D-thiogalactopyranoside (IPTG) was added for T_7 promoter induction and growth was continued for 18 h at 30°C. Cells were collected by centrifugation and resuspended in phosphate buffer saline buffer (pH 7.5), and subjected to high pressure. The cell lysates were centrifuged and purified using Ni-NTA His·Bind Column (Novagen) according to the manufacturer's instruction. The purified proteins were used for detecting the lysine acetylation and enzyme activity.

Western blotting

The concentrations of purified protein samples were determined by A280 absorption and fractionated on a 12% SDS-PAGE gel. Then, the protein samples were transferred to polyvinylidene difluoride (PVDF) membranes for 1.5 h at 15 V. The membrane was blocked at room temperature for 1 h using quick block western reagent (Beyotime, China). Acetyl lysine mouse monoclonal antibody (EasyBio, China, 1:2000) was used as the primary antibody and incubated overnight at 4°C, then Goat horseradish peroxidase-conjugated anti-mouse antibody diluted in PBST (EasyBio, China, 1:10,000) was used as the secondary antibody

and incubated for 1 h. After washing three times with PBST, an enhanced chemiluminescence (ECL) system was used for signal detection according to the manufacturer's instructions.

LdhA activity assay

The reaction mixture contained 100 mM phosphate buffer (pH 7.5), 1 mM NADH, 1 mM pyruvate, and 40 nm purified protein. The specific activity was assayed by measuring the change in absorbance at 340 nm resulting from NADH oxidation using multimode microplate reader (Spark, Tecan).

Shake-flask fermentation

The D-lactate production of Q3784 and Q3785 in shake flask cultivation were performed as previously described methods (Feng et al., 2014). Strains were cultivated in a 250 ml flask containing 100 ml medium at 37°C with 100 rpm. When OD_{600} reached about 0.8, 100 μM IPTG was added and further incubated 24 h at 30°C. The pH was maintained at 7.0 with ammonia every 12 h. The 3HP production of the Q2191, Q3824, and Q3825 strains in shake flask cultivation were referred in (Liu et al., 2016). The strains were grown overnight at 37°C in LB broth and then 1:50 diluted into 250 ml Erlenmeyer flasks with 50 ml minimal medium. When OD_{600} of the culture reached about 0.6, IPTG was added to a final concentration of 100 μM and further incubated at 30°C for 48 h. The OD_{600}, the concentrations of residual glucose and intermediates were measured during the whole fermentation course.

Analytic methods

Cell growth was assayed by measuring optical density of the culture at 600 nm using a spectrophotometer (U-2900; Hitachi). The residual glucose concentration was detected by an SBA-40ES biological sensing analyzer (Institute of Biology, Shandong Academy of sciences, China). Metabolites were analyzed by an Agilent 1,260 Infinity series HPLC system equipped with an HPX-87H column (Bio-Rad, Hercules, CA) (300 mm × 7.8 mm). All samples were filtered through 0.22 μm syringe filter. 5 mM H_2SO4 was used as the eluent at 0.5 ml/min. The oven temperature was maintained at 40°C. Concentrations of metabolites were calculated according to the standard curves.

Results and discussion

Identification of acetylated LdhA sties

In order to verify whether *E. coli* LdhA was acetylated, we firstly performed a western blot of LdhA cultivated in LB medium using an acetyl lysine monoclonal antibody. Though lysine acetylation of *E. coli* LdhA was detected by western blot, the acetylation level was weak in LB cultivated condition as shown in Figure 1A. Some previous studies have reported that different carbon source affects the acetylation status and glucose can improve the protein acetylation (Wang et al., 2010; Schilling et al., 2019). Different carbon source and concentration can affect the intracellular AcP level *via* acetate metabolism pathway, regulating protein acetylation level by AcP-mediated nonenzymatic mechanism (Schilling et al., 2019). Then, the lysine acetylation of LdhA cultivated in LB medium supplemented with 2% glucose were detected. Consistently with the previous reports, supplementation of glucose significantly improved the acetylation level of LdhA protein by 2.93-fold (Figure 1A).

Additionally, wild-type LdhA activity in *E. coli* cells grown with the presence and absence of 2% glucose were compared. LdhA activity decreased to about 71% with supplementation of 2% glucose (Figure 1B). Due to the need of positive charge of lysine residue in some interactions, improved acetylation level by 2% glucose supplementation reduced the overall activity of LdhA. For identifying more acetylated peptides, LdhA protein was purified from cells grown with 2% glucose, and analyzed by mass spectrometry. Four acetylated sites of K9, K70, K154, and K248 were detected, and all the acetylated LdhA peptides were presented in Table 2.

Effect of acetylated sites on LdhA activity

To avoid biased selection, we studied the effects of all the identified acetylated sites on LdhA activity. Each of these four lysine residues was substituted to arginine (R) and glutamine (Q) in which the substitution of arginine keeps the positive charge and avoids acetylation, whereas glutamine substitution neutralizes the positive charge and mimics the structure of acetylated lysine. Then all these mutants cultivated in LB with 2% glucose were characterized by western bolt and activity assay. For K70 mutants, neither acetylation level nor enzyme activity changed as compared to wild-type LdhA. In contrast, the acetylation levels of all other mutants decreased to varying degrees (Figure 1C), and the picture of enzyme activity change of these mutants was more complex. Specifically, the lysine acetylation level of K9 mutants, K154 mutants and K248R decreased to 0.5–0.6 folds, and the lysine acetylation level of K248Q decreased to 0.23-fold (Figure 1C). The enzyme activities of K154Q, K248R, and K248Q mutants decreased to about 30% of wild-type LdhA, while K9R mutation increased LdhA activity by 2.5 times (Figure 1D). K154R and K9Q mutations showed no obvious difference as compared to the LdhA activity, although they did lower the acetylation status of the LdhA protein (Figure 1D). Considering all these results, we speculated that K70 may be located at the non-core region of the structure and

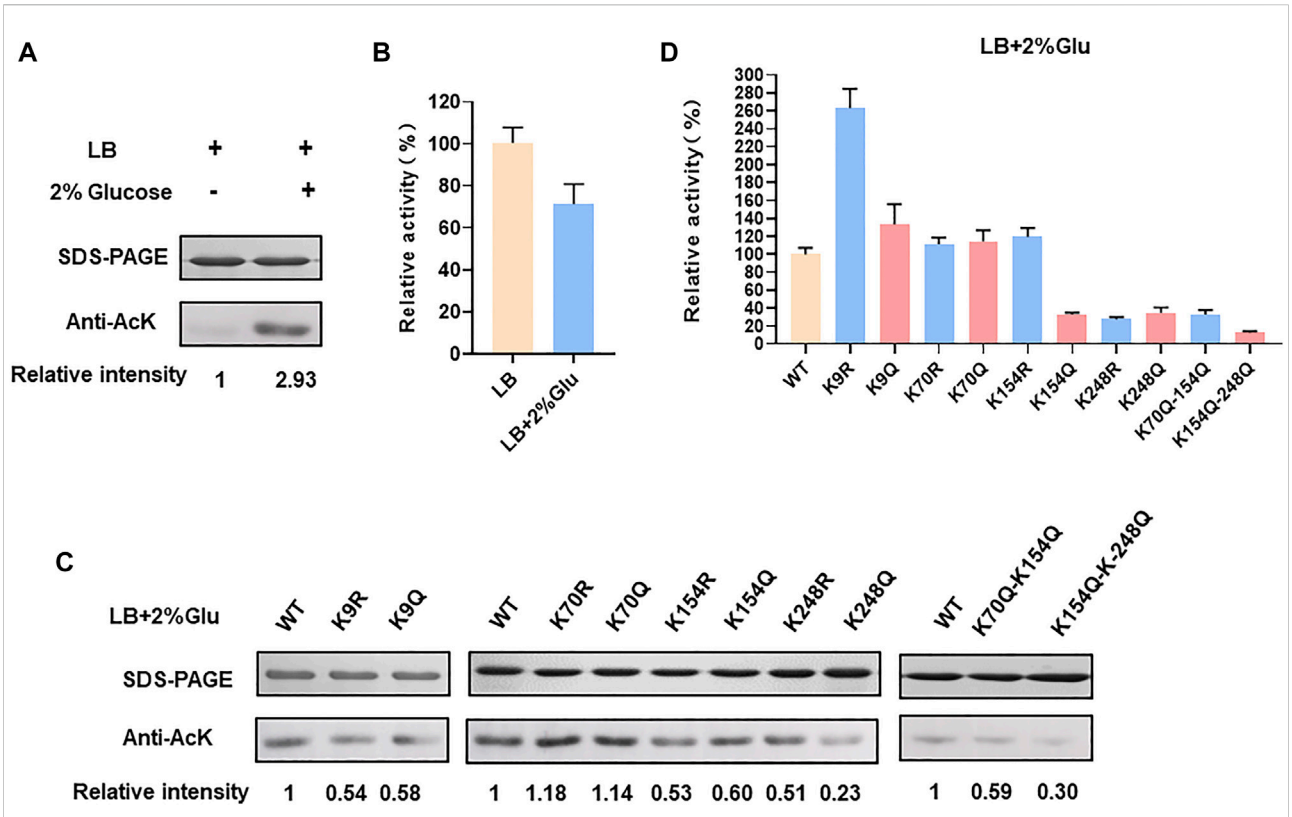

FIGURE 1
LdhA acetylation and enzyme activity in LB with 2% glucose cultivated condition. **(A)** SDS-PAGE and western blot analysis of LdhA cultivated in different conditions. **(B)** LdhA activity in cells grown in LB broth with and without 2% glucose supplementation. **(C)** SDS-PAGE and western blot analysis of LdhA variants with lysine substitution. **(D)** The enzyme activities of LdhA variants with lysine substitution.

TABLE 2 Identification of acetylated LdhA peptides by mass spectrometry.

Site	Sequence
K9	LAVYSTK(Ac)QYDK
K70	HGVK(Ac)YIALR
K154	TAGVIGTGK(Ac)IGVAMLR
K248	IDSQAAIEALK(Ac)NQKIGSLGMD

lysine acetylation did not affect the LdhA activity. While, K154 and K248 may be involved in binding the substrate and cofactor or maintaining the spatial conformation. Acetylation modification changes the charge status and adds an acetyl group to lysine residue, which may sterically block the catalytic pockets and affect the LdhA activity. Therefore, structural analysis of LdhA will help to reveal the regulation mechanism of acetylated lysine sites on enzyme activity.

Furthermore, two double mutants, K70Q-K154Q and K154Q-K248Q, were constructed and analyzed. The acetylation level and enzyme activity of K70Q-K154Q were similar to those of K154Q (Figures 1C,D), and this phenomenon is consistent with above result that K70Q cannot function on LdhA acetylation and enzyme activity. Though the acetylation level of K154Q-K248Q was similar as the single mutant K248Q, its activity was decreased to 12.6% (Figure 1D). In summary, each individual acetylated lysine residue has different effect on LdhA activity that may depend on the spatial location of each acetylated lysine. In addition, mutation of a single specific lysine or a combination of several specific lysines may achieve a desirable effect in metabolic regulation.

Mechanism of acetylation regulating LdhA enzyme activity

Previous studies found that *E. coli* LdhA (EcLdhA) functions as a homotetramer with allosteric property, and pyruvate binding activates the enzyme with a potential conformational change, displaying the positive cooperativity among the monomers (Tarmy and Kaplan, 1968a; Tarmy and Kaplan, 1968b; Furukawa et al., 2014). Structural analysis showed each

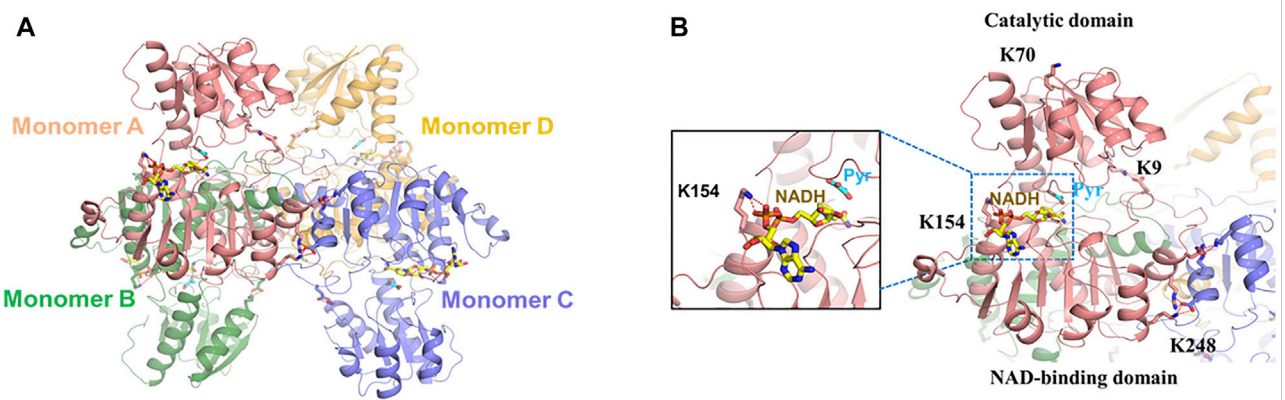

FIGURE 2
The 3D modelled structure of EcLdhA. **(A)** Quaternary structures of LdhA. **(B)** Location of the LdhA acetylated lysine sites, K70 is located at the distal region of the catalytic domain, K154 is responsible for binding the cofactor of NADH, K9 and K248 form the salt bridges with acidic amino acids, Pyr: pyruvate.

monomer of EcLdhA consists of a catalytic domain and an NAD-binding domain connected by two linkers (Furukawa et al., 2018). As known, EcLdhA belongs to the D-isomer-specific 2-hydroxyacid dehydrogenase family, in which the homolog members adopt a closed conformation when the catalytic domains bind substrates or the analogs (Taguchi and Ohta, 1991; Razeto et al., 2002; Furukawa et al., 2018). However, the complex structure of EcLdhA with pyruvate and NADH has not been reported, resulting in a limitation for our structural observation. To figure out how acetylation of each lysine residue regulates LdhA activity, it is needed to gain the complex structure of EcLdhA by homology modelling. The D-lactate dehydrogenases from *Pseudomonas aeruginosa* (PaLdhA) and *Fusobacterium nucleatum* (FnLdhA) share a high sequence identity of 54% and 47% with EcLdhA, respectively, and they both possess the ternary structures with a pyruvate analog and NADH (Furukawa et al., 2018). In contrast to PaLdhA, FnLdhA shares more similarity in the quaternary structure with EcLdhA, and they both exhibits a positive cooperativity of substrate binding compared to the negative cooperativity in the PaLdhA (Furukawa et al., 2014; Furukawa et al., 2018). Therefore, the FnLdhA ternary structure (PDB: 5Z21) was finally used as the template to simulate the complex structure of EcLdhA by Swiss-Model (Waterhouse et al., 2018).

As shown in Figure 2A, EcLdhA presents a homotetrameric structure with each monomer in the closed state, and pyruvate and NADH are located at the catalytic domain and the NAD-binding domain, respectively (Figure 2B). According to this 3D modelled structure (Figure 2B), K70 is located at the distal region of the catalytic domain and has less impact on LdhA function, which is the reason why K70 substitutions did not change LdhA activity (Figure 2B). In contrast, K154 is responsible for binding the phosphate group of NADH, and replacement of this lysine by glutamine would impair this interaction, leading to a dramatic decrease of enzyme activity.

K9 located at the catalytic domain may play an important role in maintaining the intramonomer interaction by forming a salt bridge with E269 located in NAD-binding domain (Figure 3A). To verify whether this salt bridge affects the LdhA activity, E269 was substituted to negative charged aspartic acid and neutral charged asparagine, respectively. As expected, E269 mutations didn't change the overall acetylation status of LdhA (Figure 3B). The enzyme activities of E269D and E269N mutants were decreased to 10.3% and 23.2% (Figure 3C), which is probably due that improper charge and side chain length of position 269 residue blocked the formation of salt bridge with K9. It is worth mentioned that the activity of K9R mutant was increased by 2.5 times (Figure 1D), and it was assumed this activity improvement could be caused by two reasons. On one hand, substitution of lysine by arginine avoids acetylation of this residue; on the other hand, the bifurcated guanidine group of arginine is supposed to form stronger interactions with the carboxyl group of E269, maintaining the closed conformation favorably for substrate binding and improving the enzyme activity of LdhA.

Unlike the intramonomer salt bridge between K9-E269, K248 located at the NAD-binding domain forms a salt bridge with D279 from an adjacent monomer, contributing to the intermonomer interaction (Figure 4A). Similar to E269, D279 was substituted to glutamic acid and asparagine, leading to unchanged acetylation level and significantly reduced activity of LdhA (Figures 4B,C). To be noted, differently from the K9R mutant that may reinforce salt bridges for improved activity, K248R reduced LdhA activity to 27.5% (Figure 1D). Combined with the changed activity of the D279 mutations, it was confirmed that a certain impact on the intermonomer salt

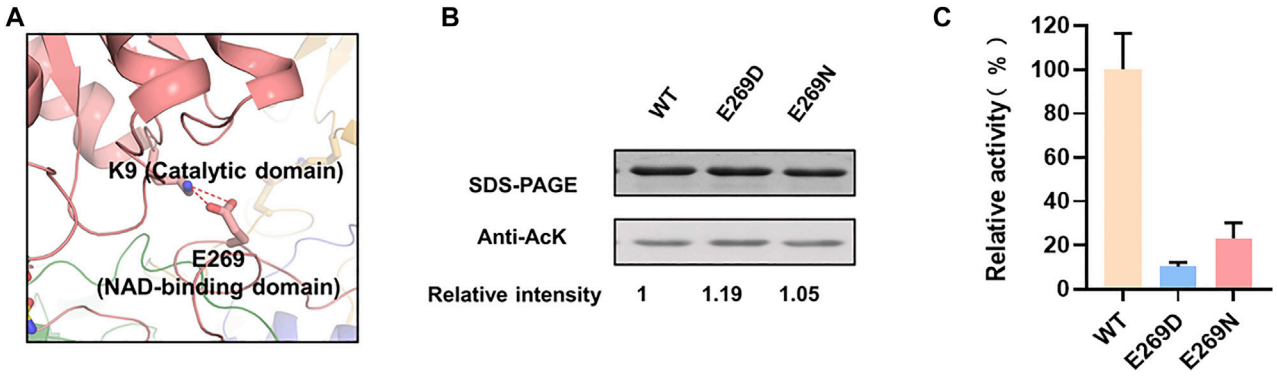

FIGURE 3
The mechanism of K9 acetylation on enzyme activity. **(A)** The salt bridge of K9-E269 in monomer. **(B)** The acetylation levels of E269 mutants. **(C)** The enzyme activities of E269 mutants.

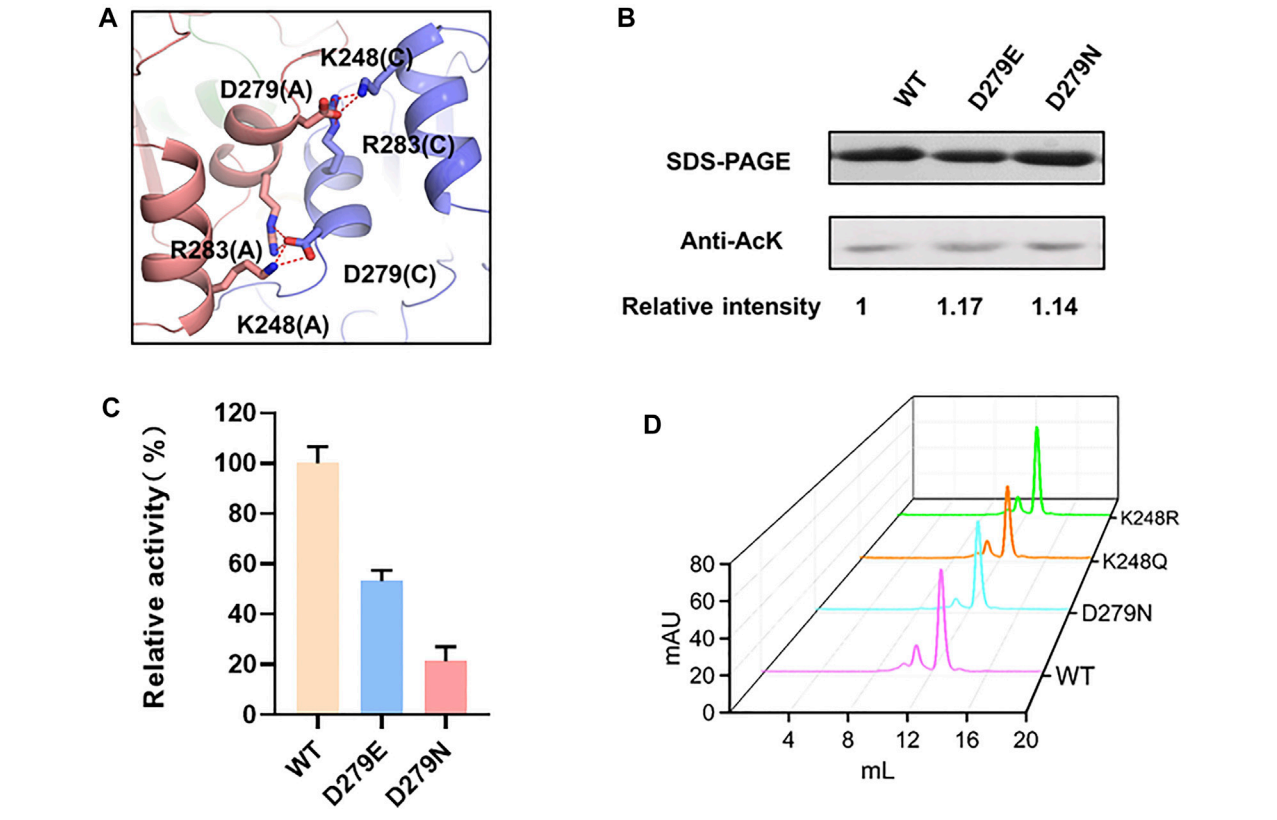

FIGURE 4
The mechanism of K248 acetylation on enzyme activity. **(A)** The intermonomer salt bridge of K248-D279. **(B)** The acetylation levels of D279 mutants. **(C)** The enzyme activities of D279 mutants. **(D)** Size exclusion chromatograph of LdhA mutants about the K248-D279 salt bridge.

bridges between K248 and D279 results in the decreased activity of LdhA, and this impact should be further involved in an interfacial change which may alter the inherent allosteric effect of the tetramer or even cause tetramer dissociation. To test this hypothesis, the wild-type LdhA protein and K248R, K248Q, and D279N mutants were subjected to gel filtration analysis. The retention volumes of the highest peaks of these mutants were same as that of the wild type (Figure 4D), proving

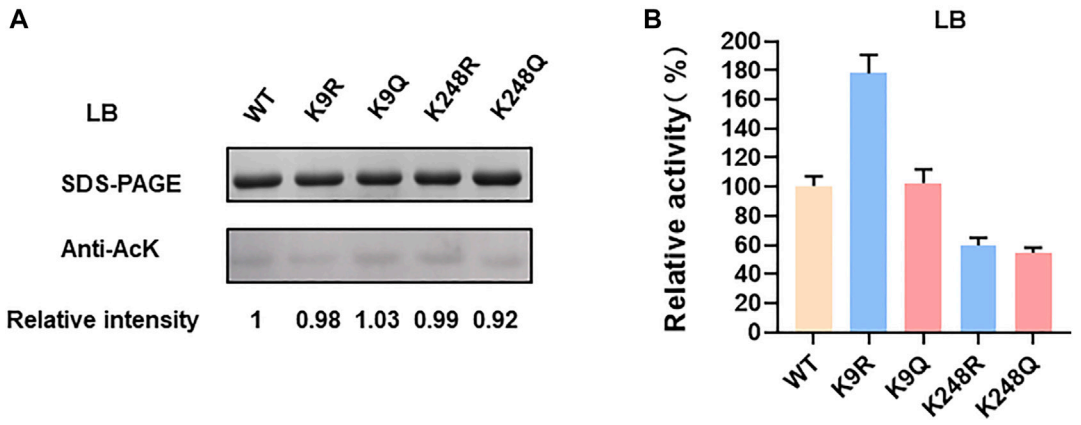

FIGURE 5
LdhA acetylation and enzyme activity in LB cultivated condition. **(A)** SDS-PAGE and western blot analysis of LdhA variants with lysine substitution. **(B)** The enzyme activities of LdhA variants with lysine substitution.

the presence of LdhA tetramer and that only preventing formation of the salt bridge between K248-D279 is not sufficient to destroy tetrameric state of LdhA. Hence, the salt bridges between K248 and D279 should be strictly required for the allosteric property of the tetramer, and the substitution by arginine may not achieve allosteric regulation to some extent. Sequence alignment further showed K248 is highly conserved in diverse bacterial species (Supplementary Figure S1), suggesting K248 should be a key residue to form the intermonomer interface and thus could be utilized as a target for regulating LdhA activity in bacteria.

K9 and K248 are not the catalytic key sites, but they both help for keeping LdhA conformation by forming salt bridges with acidic amino acids. (Figure 2B). However, the mechanisms of K9 and K248 on LdhA conformation are different, which lead to different effects of lysine acetylation on enzyme activity. In order to investigate the effect of key lysine site mutation on enzyme activity, the acetylation status and enzyme activity of K9 and K248 mutants cultivated in LB medium with and without 2% glucose were compared. The acetylation levels of LdhA and mutants in LB medium were very low as compared to that in LB medium with 2% glucose (Figure 1A and Figure 5A). The enzyme activities of K248R and K248Q mutants in LB cultivated condition decreased to about 50% of wild-type LdhA, while K9R mutation increased LdhA activity by 1.8 times (Figure 5B). Due to the very low acetylation level, we concluded that the change of LdhA activity in LB cultivated condition is mainly resulted from the mutation of lysine residues. It is worth noting that mutation of lysine residue mimics the function of acetylation modification. The substitutions of lysine residue change the side chain size and charge. Therefore, when K9 and K248 mutants cultivated in LB +2% glucose medium, the improved acetylation modification further expanded the degree of variation. K248 mutants decreased LdhA activity to about 30% of wild-type LdhA and K9R mutant increased LdhA activity by 2.5 times (Figures 1B,C). Therefore, the effect of lysine acetylation on enzyme activity is depend on the contribution of positive charge and side chain size of lysine on structure. The spatial location of each lysine and acetylation modification work together to regulate the enzyme activity.

In conclusion, the mechanisms of acetylation of each lysine regulating LdhA activity are different, which mainly depends on the interaction modes of these residues. K9 and K248 form the intramonomer and intermonomer salt bridges with acidic amino acids, while K154 binds the phosphate group of NADH. All these interactions need the positive charge of lysine. Therefore, this study provided a new perspective for rationally regulation of enzyme activity by lysine acetylation modification.

K9R mutant improves lactate production

Lactate is an important bulk chemical widely used in many fields. The strategies for improving lactate production in microbial fermentation mainly by inhibiting the byproducts accumulation, overexpressing *ldhA* gene of lactate synthetic pathway and optimizing fermentation conditions in some previous studies (Abdel-Rahman et al., 2013; Feng et al., 2014; Juturu and Wu, 2016; Feng et al., 2017). Elevating the LdhA activity by posttranslational modification may further improve the lactate production. According to the above results, LdhA (K9R) mutant significantly improved the activity of LdhA. Thus, the genes of *ldhA* and *ldhA* (K9R) mutant were respectively overexpressed in *E. coli* to produce lactate. The cell growth and glucose consumption of the two strains had no obvious difference (Figure 6A). The OD600 of wild LdhA and K9R mutant

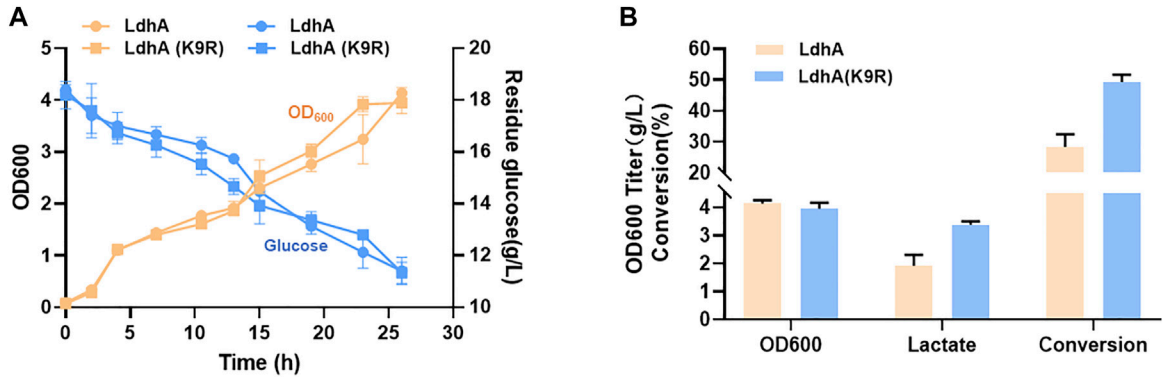

FIGURE 6
K9R mutant improves lactate production. **(A)** The cell growth and glucose consumption of wild LdhA and K9R mutant overexpressed strains. The yellow line represents the cell growth, the blue line represents the glucose consumption. **(B)** The biomass and metabolic profiles of wild LdhA and K9R mutant overexpressed strains in lactate fermentation.

overexpressed strains were 4.13 and 3.95 respectively after 24 h fermentation. The lactate titer of LdhA (K9R) overexpressed strain was 3.38 g/L, much higher than that produced in wild LdhA overexpressed strain of 1.91 g/L. The conversion efficiency of K9R mutation was 49.23%, which was improved by 1.74 folds as compared to wild LdhA overexpressed strain of 28.37% (Figure 6B).

According to these results, LdhA (K9R) mutant can effectively improve the lactate production and glucose conversion efficiency by elevating enzyme activity. Therefore, the combination of lysine acetylation regulation and the traditional engineering strategies will achieve the more efficient synthesis of lactate and promote the industrial applications.

K154Q-K248Q mutant improves 3HP production by inhibiting lactate accumulation

Lactate is one of the most byproducts in microbial fermentation. In traditional methods, *ldhA* gene is usually deleted in engineered microorganism to overcome the lactate production and thus improve other chemicals production (Wu et al., 2009; Kumar et al., 2013; Lange et al., 2017). However, *ldhA* gene deletion may affect the replenishment of NAD and further inhibit cell growth. In this study, a double mutant K154Q-K248Q presented the lowest activity (Figure 1D). To explore the applications of this mutants in metabolic engineering, the chromosomal *ldhA* gene was *in situ* replaced by K154Q-K248Q variant and the cell growth and lactate synthesis were compared between the different gene modifications. In cell culture, the lactate concentrations were below 0.5 g/L in both *ldhA*-deleted strain (Δ*ldhA*) and *ldhA* (K154Q-K248Q) strain, significantly lower than that of the wild type (Figure 7B). The cell growth rates of these two mutants were higher in exponential phase, but they soon began to decline, especially in Δ*ldhA* strain (Figures 7B,C). Finally, the wild-type strain accumulated the highest biomass.

3-hydroxypropionate (3HP) is an attractive platform chemical for a wide range of industrial applications (Rathnasingh et al., 2009; Wang et al., 2012; Liu et al., 2013). We used 3HP as a case to study the application of LdhA acetylation in chemicals production *via* overcoming lactate accumulation. 3HP biosynthesis pathway from glucose was shown in Figure 7A. In 3HP fermentation, the Δ*ldhA* and *ldhA* (K154Q-K248Q) mutants kept a very low level of lactate and 3HP titers were 1.79 g/L and 2.05 g/L respectively, clearly higher than that produced by the wild-type strain of 1.57 g/L (Figure 7D). The 3HP conversion efficiencies of these mutants were improved by 1.33 and 1.38 times than that of the wild strain. More carbon flux may be assimilated to the pathway of 3HP biosynthesis due to the inhibition of byproduct synthesis. Therefore, LdhA acetylation modification can improve the 3HP biosynthesis *via* overcoming the lactate accumulation, and the regulatory effects are slightly better than the traditional method through gene knockout.

In conclusion, manipulating the lysine acetylation level could regulate the activity of related enzyme and affect the production of the desirable chemical. Lysine acetylation modification will be a promising regulatory strategy in microbial synthesis. How does control the acetylated level or sites? On one hand, we can identify the natural acetylated sites of proteins and regulate their acetylation level by mutation. On the other hand, a genetic code expansion approach can be used to incorporate acetyllysine directly into the selected positions. This approach utilizes an engineered pyrrolysyl-tRNA synthetase (Bryson et al., 2017) and a rationally evolved

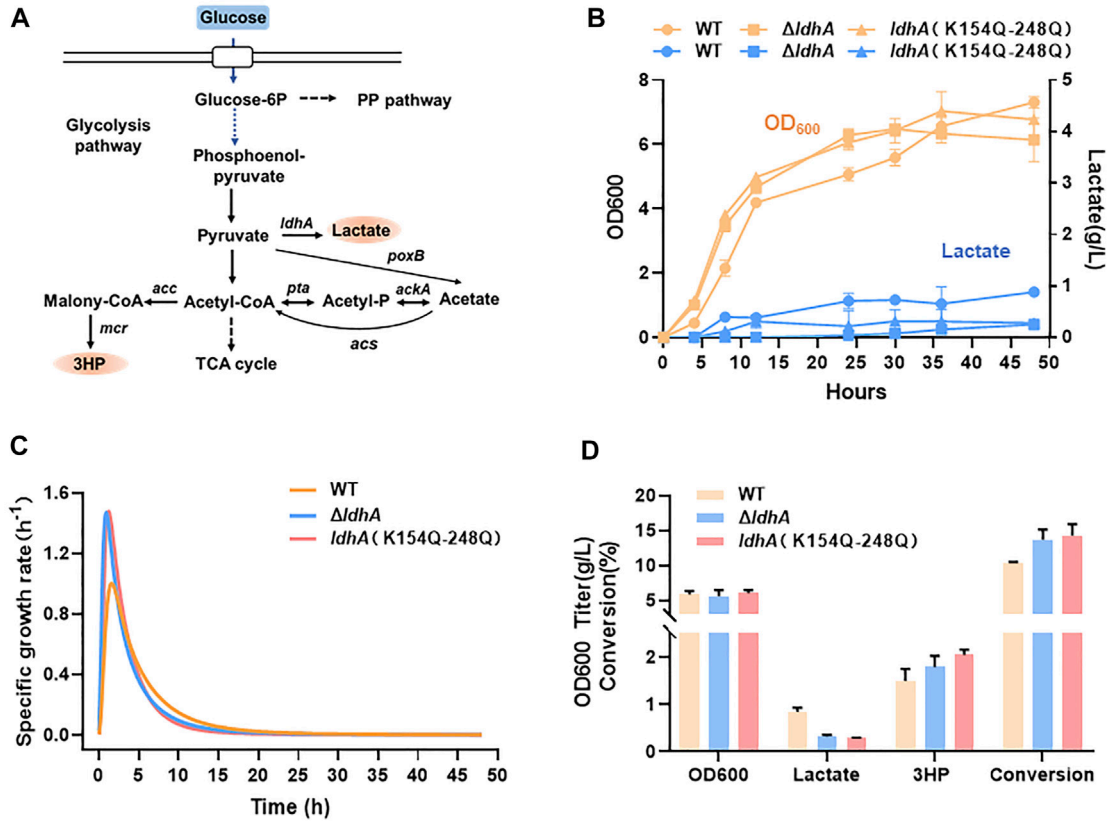

FIGURE 7
K154Q-K248Q mutant inhibits lactate accumulation and improves 3HP production. **(A)** The synthetic pathway of lactate and 3HP from glucose. **(B)** The cell growth and lactate accumulation of *E. coli* strains carrying wild-type LdhA and LdhA double mutant, and the *ldhA* deleted *E. coli* strain. The yellow line represents the cell growth, the blue line represents the lactate production. **(C)** The specific growth rate of these strains. **(D)** The biomass and metabolic profiles of these strains in 3HP fermentation.

cognate tRNA pyl (Fan et al., 2015) to read through the TAG stop codon in the gene introduced by site-directed mutagenesis and incorporate the acetyllysine from medium to the selected sites. Venkat et al. (2017) studied the effects of lysine acetylation on enzyme activity of isocitrate dehydrogenase and malate dehydrogenase using this genetic code expansion approach (Venkat et al., 2018). This approach enables rational design of lysine acetylated sites and promotes the potential applications of lysine acetylation in microbial synthesis. Furthermore, as lactate has been proved to play an important role in pathogenesis of cancer and diabetes (Feng et al., 2018; Lin et al., 2022), our results may provide some important references for the treatment of these diseases.

Conclusion

Protein lysine acetylation plays an important role in enzyme activity, metabolic flux distribution and other cellular physiology and metabolism processes, and its complex physiology effects and regulatory mechanism still remain unclear. This study systematically characterized the effects of lysine acetylated sites on *E. coli* LdhA and uncovered this regulatory mechanism. Lysine acetylation was also successfully used for regulating the lactate synthesis. Thus, our study established a paradigm for lysine acetylation to regulate lactate synthesis and proved that lysine acetylation can be a promising tool to improve the target production and conversion efficiency in metabolic engineering. Lysine acetylation is an evolutionarily conserved PTM from bacteria to higher animals and humans, and our results here may provide some important references for relevant research in other species.

Data availability statement

The original contributions presented in the study are included in the article/Supplementary Material, further inquiries can be directed to the corresponding authors.

Author contributions

ML and MH performed the experiments and numerical analysis; ML, GZ, and MX conceived the study, analyzed the data, wrote the manuscript and provided the funding; CL and QM performed structure analysis. LG, YD, and QQ performed some numerical analysis.

Funding

This work was supported by the National Key Research and Development Program of China (2021YFC2100503), National Natural Science Foundation of China (32170085, 31961133014), Young Scholars Program of Shandong University (ML), Distinguished Scholars Program of Shandong University (GZ), Foundation for Innovative Research Groups of State Key Laboratory of Microbial Technology, and Fundamental Research Funds for the Central Universities.

Acknowledgments

We thank Jing Zhu, Jingyao Qu, Zhifeng Li, Guangnan Lin from Analysis and Testing Center of SKLMT (State Key laboratory of Microbial Technology, Shandong University) for assistance in Liquid Chromatography-mass spectrometry of EASY-nLC and Nano-Tribrid MS Orbitrap Lumos and data processing.

Conflict of interest

This work has been included in patent applications by Shandong University.

Publisher's note

All claims expressed in this article are solely those of the authors and do not necessarily represent those of their affiliated organizations, or those of the publisher, the editors and the reviewers. Any product that may be evaluated in this article, or claim that may be made by its manufacturer, is not guaranteed or endorsed by the publisher.

Supplementary material

The Supplementary Material for this article can be found online at: https://www.frontiersin.org/articles/10.3389/fbioe.2022.966062/full#supplementary-material

References

Abdel-Rahman, M. A., Tashiro, Y., and Sonomoto, K. (2013). Recent advances in lactic acid production by microbial fermentation processes. *Biotechnol. Adv.* 31 (6), 877–902. doi:10.1016/j.biotechadv.2013.04.002

Baba, T., Ara, T., Hasegawa, M., Takai, Y., Okumura, Y., Baba, M., et al. (2006). Construction of *Escherichia coli* K-12 in-frame, single-gene knockout mutants: the Keio collection. *Mol. Syst. Biol.* 2, 2006.0008. doi:10.1038/msb4100050

Bernal, V., Castaño-Cerezo, S., and Cánovas, M. (2016). Acetate metabolism regulation in *Escherichia coli*: carbon overflow, pathogenicity, and beyond. *Appl. Microbiol. Biotechnol.* 100 (21), 8985–9001. doi:10.1007/s00253-016-7832-x

Bryson, D. I., Fan, C., Guo, L. T., Miller, C., Söll, D., and Liu, D. R. (2017). Continuous directed evolution of aminoacyl-tRNA synthetases. *Nat. Chem. Biol.* 13 (12), 1253–1260. doi:10.1038/nchembio.2474

Choi, S. Y., Cho, I. J., Lee, Y., Park, S., and Lee, S. Y. (2019). Biocatalytic synthesis of polylactate and its copolymers by engineered microorganisms. *Methods Enzym.* 627, 125–162. doi:10.1016/bs.mie.2019.04.032

Edwards, R. A., Keller, L. H., and Schifferli, D. M. (1998). Improved allelic exchange vectors and their use to analyze 987P fimbria gene expression. *Gene* 207 (2), 149–157. doi:10.1016/s0378-1119(97)00619-7

Eiteman, M. A., and Altman, E. (2006). Overcoming acetate in *Escherichia coli* recombinant protein fermentations. *Trends Biotechnol.* 24 (11), 530–536. doi:10.1016/j.tibtech.2006.09.001

Fan, C., Xiong, H., Reynolds, N. M., and Söll, D. (2015). Rationally evolving tRNAPyl for efficient incorporation of noncanonical amino acids. *Nucleic Acids Res.* 43 (22), e156. doi:10.1093/nar/gkv800

Feng, X., Ding, Y., Xian, M., Xu, X., Zhang, R., and Zhao, G. (2014). Production of optically pure d-lactate from glycerol by engineered *Klebsiella pneumoniae* strain. *Bioresour. Technol.* 172, 269–275. doi:10.1016/j.biortech.2014.09.074

Feng, X., Jiang, L., Han, X., Liu, X., Zhao, Z., Liu, H., et al. (2017). Production of D-lactate from glucose using *Klebsiella pneumoniae* mutants. *Microb. Cell Fact.* 16 (1), 209. doi:10.1186/s12934-017-0822-6

Feng, Y., Xiong, Y., Qiao, T., Li, X., Jia, L., and Han, Y. (2018). Lactate dehydrogenase A: a key player in carcinogenesis and potential target in cancer therapy. *Cancer Med.* 7 (12), 6124–6136. doi:10.1002/cam4.1820

Furukawa, N., Miyanaga, A., Togawa, M., Nakajima, M., and Taguchi, H. (2014). Diverse allosteric and catalytic functions of tetrameric d-lactate dehydrogenases from three Gram-negative bacteria. *Amb. Express* 4 (1), 76. doi:10.1186/s13568-014-0076-1

Furukawa, N., Miyanaga, A., Nakajima, M., and Taguchi, H. (2018). Structural basis of sequential allosteric transitions in tetrameric d-lactate dehydrogenases from three Gram-negative bacteria. *Biochemistry* 57 (37), 5388–5406. doi:10.1021/acs.biochem.8b00557

Hentchel, K. L., and Escalante-Semerena, J. C. (2015). Acylation of biomolecules in prokaryotes: a widespread strategy for the control of biological function and metabolic stress. *Microbiol. Mol. Biol. Rev.* 79 (3), 321–346. doi:10.1128/mmbr.00020-15

Juturu, V., and Wu, J. C. (2016). Microbial production of lactic acid: the latest development. *Crit. Rev. Biotechnol.* 36 (6), 967–977. doi:10.3109/07388551.2015.1066305

Kuhn, M. L., Zemaitaitis, B., Hu, L. I., Sahu, A., Sorensen, D., Minasov, G., et al. (2014). Structural, kinetic and proteomic characterization of acetyl phosphate-dependent bacterial protein acetylation. *PLoS ONE* 9 (4), e94816. doi:10.1371/journal.pone.0094816

Kumar, V., Sankaranarayanan, M., Durgapal, M., Zhou, S., Ko, Y., Ashok, S., et al. (2013). Simultaneous production of 3-hydroxypropionic acid and 1, 3-propanediol from glycerol using resting cells of the lactate dehydrogenase-deficient recombinant *Klebsiella pneumoniae* overexpressing an aldehyde dehydrogenase. *Bioresour. Technol.* 135, 555–563. doi:10.1016/j.biortech.2012.11.018

Lange, J., Müller, F., Bernecker, K., Dahmen, N., Takors, R., and Blombach, B. (2017). Valorization of pyrolysis water: a biorefinery side stream, for 1, 2-propanediol production with engineered corynebacterium glutamicum. *Biotechnol. Biofuels* 10 (1), 277. doi:10.1186/s13068-017-0969-8

Lin, Y., Bai, M., Wang, S., Chen, L., Li, Z., Li, C., et al. (2022). Lactate is a key mediator that links obesity to insulin resistance via modulating cytokine production from adipose tissue. *Diabetes* 71, 637–652. doi:10.2337/db21-0535

Liu, C., Wang, Q., Xian, M., Ding, Y., and Zhao, G. (2013). Dissection of malonyl-coenzyme A reductase of *Chloroflexus aurantiacus* results in enzyme activity improvement. *PLoS ONE* 8 (9), e75554. doi:10.1371/journal.pone.0075554

Liu, C., Ding, Y., Zhang, R., Liu, H., Xian, M., and Zhao, G. (2016). Dissection of malonyl-coenzyme A reductase of *Chloroflexus aurantiacus* results in enzyme activity improvement. *PLoS ONE* 8 (9), e75554. doi:10.1371/journal.pone.0075554

Liu, M., Guo, L., Fu, Y., Huo, M., Qi, Q., and Zhao, G. (2021). Bacterial protein acetylation and its role in cellular physiology and metabolic regulation. *Biotechnol. Adv.* 53, 107842. doi:10.1016/j.biotechadv.2021.107842

Moore, S. D. (2011). Assembling new *Escherichia coli* strains by transduction using phage P1. *Methods Mol. Biol.* 765, 155–169. doi:10.1007/978-1-61779-197-0_10

Rathnasingh, C., Raj, S. M., Jo, J. E., and Park, S. (2009). Development and evaluation of efficient recombinant *Escherichia coli* strains for the production of 3-hydroxypropionic acid from glycerol. *Biotechnol. Bioeng.* 104 (4), 729–739. doi:10.1002/bit.22429

Razeto, A., Kochhar, S., Hottinger, H., Dauter, M., Wilson, K. S., and Lamzin, V. S. (2002). Domain closure, substrate specificity and catalysis of D-lactate dehydrogenase from *Lactobacillus bulgaricus*. *J. Mol. Biol.* 318 (1), 109–119. doi:10.1016/s0022-2836(02)00086-4

Schilling, B., Basisty, N., Christensen, D. G., Sorensen, D., Orr, J. S., Wolfe, A. J., et al. (2019). Global lysine acetylation in *Escherichia coli* results from growth conditions that favor acetate fermentation. *J. Bacteriol.* 201 (9), e00768. doi:10.1128/jb.00768-18

Taguchi, H., and Ohta, T. (1991). D-lactate dehydrogenase is a member of the D-isomer-specific 2-hydroxyacid dehydrogenase family. Cloning, sequencing, and expression in *Escherichia coli* of the D-lactate dehydrogenase gene of *Lactobacillus plantarum*. *J. Biol. Chem.* 266 (19), 12588–12594. doi:10.1016/s0021-9258(18)98939-8

Tarmy, E., and Kaplan, N. O. (1968a). Chemical characterization of D-lactate dehydrogenase from *Escherichia coli* B. *J. Biol. Chem.* 243 (10), 2579–2586. doi:10.1016/s0021-9258(18)93413-7

Tarmy, E., and Kaplan, N. O. (1968b). Kinetics of *Escherichia coli* B D-lactate dehydrogenase and evidence for pyruvate-controlled change in conformation. *J. Biol. Chem.* 243 (10), 2587–2596. doi:10.1016/s0021-9258(18)93414-9

VanDrisse, C. M., and Escalante-Semerena, J. C. (2019). Protein acetylation in bacteria. *Annu. Rev. Microbiol.* 73, 111–132. doi:10.1146/annurev-micro-020518-115526

Venkat, S., Gregory, C., Sturges, J., Gan, Q. L., and Fan, C. G. (2017). Studying the lysine acetylation of malate dehydrogenase. *J. Mol. Biol.* 429 (9), 1396–1405. doi:10.1016/j.jmb.2017.03.027

Venkat, S., Chen, H., Stahman, A., Hudson, D., McGuire, P., Gan, Q. L., et al. (2018). Characterizing lysine acetylation of isocitrate dehydrogenase in *Escherichia coli*. *J. Mol. Biol.* 430 (13), 1901–1911. doi:10.1016/j.jmb.2018.04.031

Verdin, E., and Ott, M. (2015). 50 years of protein acetylation: from gene regulation to epigenetics, metabolism and beyond. *Nat. Rev. Mol. Cell Biol.* 16 (4), 258–264. doi:10.1038/nrm3931

Wang, Q., Zhang, Y., Yang, C., Xiong, H., Lin, Y., Yao, J., et al. (2010). Acetylation of metabolic enzymes coordinates carbon source utilization and metabolic flux. *Science* 327 (5968), 1004–1007. doi:10.1126/science.1179687

Wang, Q., Liu, C., Xian, M., Zhang, Y., and Zhao, G. (2012). Biosynthetic pathway for poly(3-hydroxypropionate) in recombinant *Escherichia coli*. *J. Microbiol.* 50 (4), 693–697. doi:10.1007/s12275-012-2234-y

Wang, Q., Zhang, Y., Yang, C., Xiong, H., Lin, Y., Yao, J., et al. (2010). Acetylation of metabolic enzymes coordinates carbon source utilization and metabolic flux. *Science* 327 (5968), 1004–1007. doi:10.1126/science.1179687

Waterhouse, A., Bertoni, M., Bienert, S., Studer, G., Tauriello, G., Gumienny, R., et al. (2018). SWISS-MODEL: homology modelling of protein structures and complexes. *Nucleic Acids Res.* 46 (W1), W296–W303. doi:10.1093/nar/gky427

Wu, H., Li, Z., and Ye, Q. J. (2009). Succinic acid production and CO_2 consumption in fed-batch culture of a *pflB ldhA* deficient *Escherichia coli* strain NZN111. *N. Biotechnol.* 25, S230. doi:10.1016/j.nbt.2009.06.206

Yu, B. J., Kim, J. A., Moon, J. H., Ryu, S. E., and Pan, J. G. (2008). The diversity of lysine-acetylated proteins in *Escherichia coli*. *J. Microbiol. Biotechnol.* 18 (9), 1529–1536.

Zhang, J., Sprung, R., Pei, J., Tan, X., Kim, S., Zhu, H., et al. (2009). Lysine acetylation is a highly abundant and evolutionarily conserved modification in *Escherichia coli*. *Mol. Cell. Proteomics* 8 (2), 215–225. doi:10.1074/mcp.m800187-mcp200

Zhang, K., Zheng, S., Yang, J. S., Chen, Y., and Cheng, Z. (2013). Comprehensive profiling of protein lysine acetylation in *Escherichia coli*. *J. Proteome Res.* 12 (2), 844–851. doi:10.1021/pr300912q

Zhao, D., Zou, S.-W., Liu, Y., Zhou, X., Mo, Y., Wang, P., et al. (2013). Lysine-5 acetylation negatively regulates lactate dehydrogenase A and is decreased in pancreatic cancer. *Cancer Cell* 23 (4), 464–476. doi:10.1016/j.ccr.2013.02.005

frontiers | Frontiers in Bioengineering and Biotechnology

TYPE Original Research
PUBLISHED 17 August 2022
DOI 10.3389/fbioe.2022.969012

OPEN ACCESS

EDITED BY
Xinglin Jiang,
Technical University of Denmark, Denmark

REVIEWED BY
Aitao Li,
Hubei University, China
Yi Gan,
Zhejiang Agriculture and Forestry University, China

*CORRESPONDENCE
Mo Xian,
xianmo@qibebt.ac.cn
Wei Liu,
liuwei@qibebt.ac.cn

SPECIALTY SECTION
This article was submitted to Industrial Biotechnology, a section of the journal Frontiers in Bioengineering and Biotechnology

RECEIVED 14 June 2022
ACCEPTED 13 July 2022
PUBLISHED 17 August 2022

CITATION
Liu W, Yuan S, Jin M and Xian M (2022), Biocatalytic synthesis of 2-fluoro-3-hydroxypropionic acid.
Front. Bioeng. Biotechnol. 10:969012.
doi: 10.3389/fbioe.2022.969012

Biocatalytic synthesis of 2-fluoro-3-hydroxypropionic acid

Wei Liu[1]*, Shan Yuan[1,2], Miaomiao Jin[1] and Mo Xian[1]*

[1]CAS Key Laboratory of Biobased Materials, Qingdao Institute of Bioenergy and Bioprocess Technology, Chinese Academy of Sciences, Shandong, China, [2]University of Chinese Academy of Sciences, Beijing, China

Fluorine has become an important element for the design of synthetic molecules for use in medicine, agriculture, and materials. The introduction of fluorine atoms into organic compound molecules can often give these compounds new functions and make them have better performance. Despite the many advantages provided by fluorine for tuning key molecular properties, it is rarely found in natural metabolism. We seek to expand the molecular space available for discovery through the development of new biosynthetic strategies that cross synthetic with natural compounds. Towards this goal, 2-fluoro-3-hydroxypropionic acid (2-F-3-HP) was first synthesized using *E. coli* coexpressing methylmalonyl CoA synthase (MatBrp), methylmalonyl CoA reductase (MCR) and malonate transmembrane protein (MadLM). The concentration of 2-F-3-HP reached 50.0 mg/L by whole-cell transformation after 24 h. 2-F-3-HP can be used as the substrate to synthesize other fluorides, such as poly (2-fluoro-3-hydroxypropionic acid) (FP3HP). Being entirely biocatalytic, our procedure provides considerable advantages in terms of environmental and safety impacts over reported chemical methods.

KEYWORDS

2-fluoro-3-hydroxypropionic acid, fluoride, one-pot synthesis, whole-cell transformation, biopolymer

Abbreviations: 2-F-3-HP, 2-fluoro-3-hydroxypropionic acid; 2-FMA, 2-fluoromalonic acid; MatBrp, methylmalonyl CoA synthase; MCR, methylmalonyl CoA reductase; MadLM, malonate transmembrane protein; PHA, poly(hydroxyalkanoate); SAM, S-adenosyl methionine; 3-HP, 3-hydroxypropionic acid; 3-HB, 3-hydroxybutyric acid; 2-F-3-HB, 2-fluoro-3-hydroxybutyric acid; IPTG, isopropyl beta-D-1-thiogalactopyranoside; P3HP, poly (3-hydroxypropionic acid); P3HB, poly (3-hydroxybutyric acid); FP3HP, poly (2-fluoro-3-hydroxypropionic acid); FP3HB, poly (2-fluoro-3-hydroxybutyric acid); Amp, ampicillin; Cm, chloromycetin.

Introduction

Organic fluorides are important compounds that are widely used in the fields of pharmaceuticals, molecular imaging, and materials (Klopries et al., 2014; Wu et al., 2020a; Cheng and Ma, 2021). Fluorinated natural products are extremely rare in nature (Cheng and Ma, 2021). However, the introduction of fluorine atoms into organic compound molecules can often give these compounds new functions and make them have better performance (Klopries et al., 2014; Ningning et al., 2020; Tu et al., 2020). The target compounds doped with fluorine are endowed with stronger stability and activity (Tu et al., 2020), longer half-life, and better bioabsorbability (Ningning et al., 2020), especially in the fields of pharmaceutical intermediates, cancer treatment (Lowe et al., 2019), antiviral agents, photovoltaics, diagnostic probes (Onega et al., 2010) and bioinspired materials (Ningning et al., 2020). For example, Benjamin W. Thuronyi et al. reported the introduction of fluorine into poly (3-hydroxybutyric acid) (P3HB) to obtain poly (2-fluoro-3-hydroxybutyric acid-co-3-hydroxybutyric acid) (poly (FHB-co-HB)), and the results show that the glass transition temperature of poly (FHB-co-HB) is much lower than that of P3HB (Thuronyi et al., 2017).

Despite the many advantages provided by fluorine for tuning key molecular properties, it is rarely found in natural metabolism, which limits the application of fluorine-containing compounds (Thuronyi and Chang, 2015; Cheng and Ma, 2021). Accordingly, the artificial synthesis of fluorinated compounds has become an important alternative in modern society. Nonetheless, these conventional chemical synthesis methods required precious metals, toxic and contaminating chemical reagents, high temperature and pressure and extreme conditions (Berger et al., 2020; Rodrigo et al., 2020). This is not conducive to the sustainable development of green chemicals and the global economy.

In contrast, the biosynthesis methods are good supplements in the field of chemical synthesis, especially for fluorinated compounds (Wu et al., 2020a). At present, of all enzyme-catalyzed synthesis methods, the direct formation of the C-F bond by fluorinase is the most effective and promising method (Cheng and Ma, 2021). Fluorinase can participate in biological metabolic pathways and synthesize valuable organic fluorides, such as fluoroacetic acid (Li et al., 2010; Stephanie et al., 2019) and 4-fluorothreonine (Wu et al., 2020b). However, the biosynthesis of organic fluorides by fluorinase is limited. On the one hand, fluoride ions have an inhibitory effect on the growth of *E. coli* (Last et al., 2016). On the other hand, fluorinase requires the expensive co-substrate S-adenosyl methionine (SAM) (Li et al., 2010; Feng et al., 2021; Kittila et al., 2022), and transmembrane transport of SAM requires the assistance of transporters (Schaffitzel et al., 1998). These all limit the catalytic efficiency of fluorinase. Therefore, there are few studies on the biosynthesis of organic fluorides.

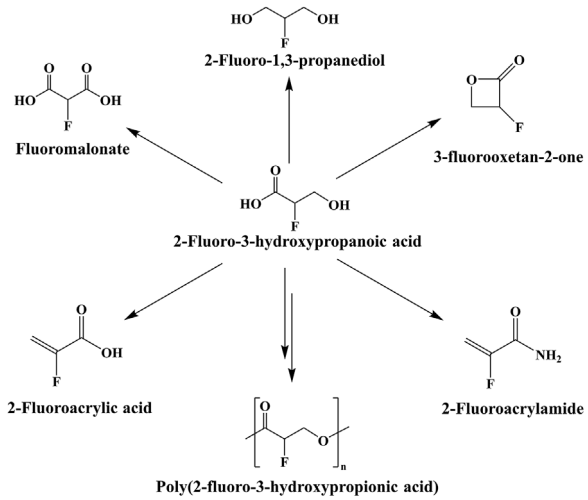

FIGURE 1
Potential products of 2-F-3-HP.

3-Hydroxypropionic acid (3-HP) is an important platform compound with a wide range of applications (Liu et al., 2016). It is easy to synthesize a variety of chemical products through different chemical reactions. For example, poly (3-hydroxypropionic acid) (P3HP) can be synthesized by 3-HP (Wang et al., 2013a; YongChang et al., 2014). Furthermore, malonate, 1,3-propanediol, acrylic acid, propiolactone and other products can be obtained through oxidation, reduction, dehydration, cyclization and other reactions, and the obtained products can be further used to synthesize products with higher added value (Valdehuesa et al., 2013). In theory, 2-fluoro-3-hydroxypropionic acid (2-F-3-HP) also produces many corresponding substances to expand the types of fluorine-containing organics, such as 2-fluoroacrylic acid (Figure 1). However, there is no biosynthetic pathway for 2-F-3-HP.

In this study, we constructed a four-gene, two-plasmid system for the biosynthesis of 2-F-3-HP using 2-fluoromalonic acid (2-FMA) as the initial fluorine source. 2-FMA is both relatively inexpensive and capable of being produced through enzymatic pathways while avoiding the acute organofluorine poisoning arising from the direct application of fluoroacetate to cells (Thuronyi et al., 2017). After whole-cell transformation, 2-F-3-HP (50.0 mg/L) was first synthesized by the engineered *E. coli* coexpressing methylmalonyl CoA synthase (MatBrp) from *Rhodopseudomonas palustris*, methylmalonyl CoA reductase (MCR) from *Thermophilic Filiculture* and malonate transmembrane protein (MadLM) from *Pseudomonas pf5* with 2-FMA as substrate (Scheme 1). The advantages of this method over chemical methods mainly included the use of green and cheap substrates, solvents and catalysts in mild and safe reaction conditions, and no toxic waste was generated. This method may be applicable to analogue of 2-F-3-HP, such as 2-fluoro-3-

hydroxybutyric acid. Furthermore, according to the previous research in our lab, manipulating the expression levels of 3-hydroxybutyric acid (3-HB) and 3-HP pathways resulted in biosynthesis of block copolymers P3HB-b-P3HP with varied compositions, which improved properties of copolymers (Wang et al., 2013b). Theoretically, 2-F-3-HP and 2-fluoro-3-hydroxybutyric acid (2-F-3-HB), which has already been biosynthesized (Thuronyi et al., 2017), could also achieve similar results and possibly have better properties. In a word, the 2-F-3-HP synthesized in this study has broad application prospects.

Materials and methods

Materials

2-FMA and other chemicals were obtained from Aladdin (Shanghai, China). A DNA gel extraction kit, plasmid purification kit, Primer STAR Max and DNA marker were obtained from TAKARA (Japan). Protein markers and T4 DNA ligase were obtained from Thermo Fisher Scientific (United States). M9 Minimal Salts (M9 buffer) were obtained from Sangon Biotech (Shanghai, China). *E. coli* BL21 (DE3) competent cells were purchased from Vazyme (Nanjing, China).

Construction of plasmids and strains

The *MatBrp* (WP_011155789.1), *Mcr* (AAS20429.1), *MadL* (AAY95003.2), *MadM* gene (WP_011063986.1) were synthesized by Beijing Genomics Institute (Beijing, China). The synthesized *MatBrp* was digested with *Bgl*II, and the synthesized Mcr was digested with *Bgl*II and *BamH*I. The digested *MatBrp* and *Mcr* were ligated into the pET28a vector, which was digested with *Nco*I, *Eco*RV and *Kpn*I. The MadLM gene was digested with *Bgl*II *and Xba*I, and the digested fragment was ligated into the pBAD, which was digested with the *Eco*RI, *Xba*I and *Hind*III. The constructed vector was transformed into *E. coli* BL21 (DE3).

Enzyme activity analysis

E. coli cells BL21 (DE3) harboring recombinant plasmids were incubated at 37 °C for 12 h in 5 ml of LB medium (containing 100 μg/ml Amp and 34 μg/ml Cm, pH7.0). The grown cells (5 ml) were then transferred into 50 ml of LB medium (containing 100 μg/ml Amp and 34 μg/ml Cm, pH7.0) and cultivated at 37 °C in the thermostatic incubator (ZHICHENG ZWYR-D2403, China). When $OD_{600\ nm}$ reached 0.6, 0.5 mM isopropyl beta-D-1-thiogalactopyranoside (IPTG) and 0.02% arabinose were added. The cells were harvested by centrifugation (Himac CR21N, Japan) at 6,000 rpm for 5 min and washed with 100 mM Tris-HCl (containing 10 mM $MgCl_2$, pH 7.8). After the cells (10 g of wet weight) were disrupted by a high-pressure cell cracker (Constant systems One shot 40KPSI, England), the cell debris was discarded, the supernatant (crude enzyme solution) was obtained by centrifugation (10000 rpm, 30 min, 4 °C). The standard assay was as followed: 1 mg/ml crude enzyme, 20 mM 2-FMA, 2 mM NADPH, 2 mM ATP, 1 mM CoA, 100 mM Tris-HCl buffer (10 mM $MgCl_2$), pH 7.8, 30 °C, 200 rpm, 12 h. The reaction solution was detected by LC-MS.

Whole-cell transformation

E. coli cells BL21 (DE3) harboring recombinant plasmids were incubated at 37 °C for 12 h in 5 ml of LB medium containing appropriate antibiotics. The grown cells (5 ml) were then transferred into 50 ml of LB medium containing appropriate antibiotics and cultivated at 37 °C in the thermostatic incubator. When $OD_{600\ nm}$ reached 0.6, 0.5 mM IPTG and 0.02% arabinose were added.

The cells were washed with M9 buffer (15.12 g/L $Na_2HPO_4{\cdot}12\ H_2O$, 3 g/L KH_2PO_4, 0.5 g/L NaCl and 1 g/L NH_4Cl, pH 7.0) to remove residual culture media and further resuspended in M9 buffer. The typical assay to directly measure reaction products was performed as follows: wet whole cells ($OD_{600\ nm}$ = 30), 4 mM 2-FMA, 8% glucose and 10 mM $MgSO_4$. Reactions were performed in M9 buffer (pH 7.0) at 30°C with persistent stirring at 200 rpm. After centrifugation, the supernatants were analyzed by HPLC.

Analytical methods

LC-MS conditions: ultra-high pressure liquid chromatography-triple quadrupole mass spectrometer (Agilent 1290–6430, United States); Mobile phase: A: H_2O (0.01% formic acid); B: acetonitrile; Column: Acclaim Organic Acid (Thermo 2.1 × 150, United States); column temperature: 25°C; velocity of flow: 0.2 ml/min; linear gradient: 0% B, 0–4 min; 0%–30% B, 4–20 min; 30%-80%B, 20–22 min; 80% B, 22–26 min; 80%–0% B, 26–27 min; 0%, 27–32 min. Injection volume: 1 μL. MS conditions: Source: ESI; Scan type: negative, full scan; Scan range (m/z): 15–300; Fragmentor (V): 50; Cell Accelerator Valtage: 3; Capillary: 4.0 KV; Gas Temp: 350°C; Gas Flow: 9 L/min; Nebulizar: 35 psi; 0–2 min, LC to waste; 2–32 min, LC to MS.

HPLC conditions: High-performance liquid chromatography (Shimadzu, Japan); Mobile phase: 5 mM H_2SO_4; Column: HPX-87H (Bio-RAD, United States); column temperature: 50°C; velocity of flow: 0.5 ml/min; Injection volume: 5 μL.

TABLE 1 Strains and plasmids used in this study.

No.	Strains and plasmids	Description	Source
Strain 0	*E.coli* BL21 (DE3)	F-, ompT, hsdS (rBB-mB-), gal, dcm (DE3)	Addgene
Strain 1	BL21 (DE3)/pACYCDuet1/pBAD	BL21 (DE3) carrying pACYCDuet1 and pBAD	This study
Strain 2	BL21 (DE3)/pACYCDuet1-*MatBrp-Mcr*/pBAD-*madLM*	BL21 (DE3) carrying pACYCDuet1-*MatBrp-Mcr* and pBAD-*madLM*	This study
P001	pACYCDuet1	T7 promoter, lacIq, pBR322 ori, Cmr	Addgene
P002	pBAD	araBAD promoter, araCq, pBR322 ori, Ampr	Addgene
P003	pACYCDuet1-*MatBrp-Mcr*	T7 promoter, *MatBrp* and *Mcr*, lacIq, pBR322 ori, Cmr	This study
P004	pBAD-*madLM*	araBAD promoter, *madL* and *malM*, araCq, pBR322 ori, Ampr	This study

TABLE 2 The titer of 2-F-3-HP by whole-cell transformation.

Strain	Concentration (mg/L)
Strain 1	0
Strain 2	50.0

Reactions were performed in M9 buffer (pH 7.0) containing 4 mM 2-FMA, 8% glucose, 10 mM $MgSO_4$, wet cells, $OD_{600\ nm}$ = 30 at 30°C with 200 rpm shaking for 24 h. Strain 1: BL21 (DE3)/pACYCDuet1/pBAD; Strain 2: BL21 (DE3)/pACYCDuet1-*MatBrp-Mcr*/pBAD-*madLM*.

NMR identification

The fermentation broth is centrifuged for 5 min, the supernatant is collected, and the spin distillation concentrates to 1 ml. Take 500 μL of concentrate, add 10 μL of trifluoroacetic acid as the internal standard, add 100 μL D_2O, transfer to a nuclear magnet tube to determine the chemical structure of 2-F-3 HP by fluorine spectrometry (^{19}F-NMR).

Results and discussions

Design of synthetic pathway for 2-F-3-HP

In this study, 2-FMA was used as a substrate to biosynthesize 2-F-3-HP by the catalysis of MatBrp and MCR. The synthetic process of the 2-FMA was simple and mild. On the one hand, 2-FMA can be synthesized by microorganisms (Thuronyi et al., 2017). On the other hand, diethyl 2-FMA and lithium hydroxide monohydrate are used as raw materials to synthesize 2-FMA by chemical method, which is simple to operate and stable in process conditions (Darren et al., 2021). Furthermore, 2-FMA can be catalyzed by MatBrp to generate fluoromalonyl-CoA, therefore, theoretically, the conversion of 2-FMA to 2-F-HP could be achieved by co-expressing MatBrp and MCR.

The malonate transporter MadLM from *Pseudomonas* can transport 2-FMA into cells and improve the yield of fluoromalonyl-CoA (Schaffitzel et al., 1998; Thuronyi et al., 2017). Therefore, MadLM was co-expressed with MatBrp and MCR to verify the effect of MadLM on the yield of 2-F-3-HP. All strains and plasmids used in this study listed in Table 1.

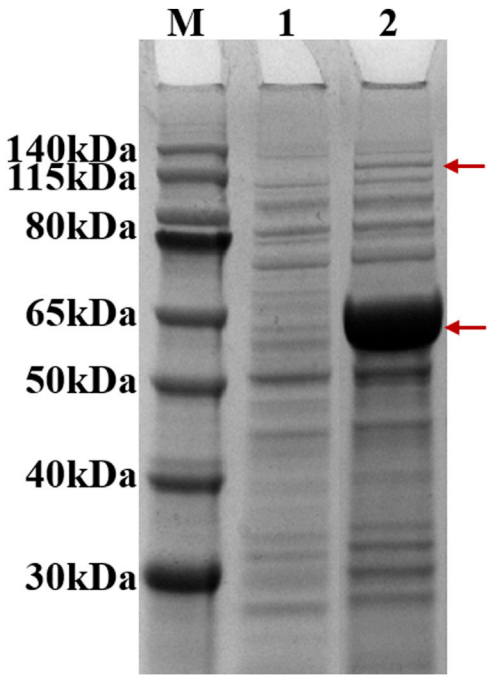

FIGURE 2
SDS-PAGE of crude enzymes. M: Marker; 1: strain 1 (BL21 (DE3)/pACYCDute1/pBAD); 2: strain 2 (BL21 (DE3)/pACYC-*matBrp-Mcr*/pBAD-*MadLM*).

Expression levels of MatBrp and MCR

After induction, recombinant strain 2 (Bl21 (DE3)/pACYCDuet1-*MatBrp-Mcr*/pBAD-*madLM*) was collected, and soluble expression levels of MatBrp and MCR were detected by SDS-PAGE. Compared with the control strain 1 (BL21 (DE3)/

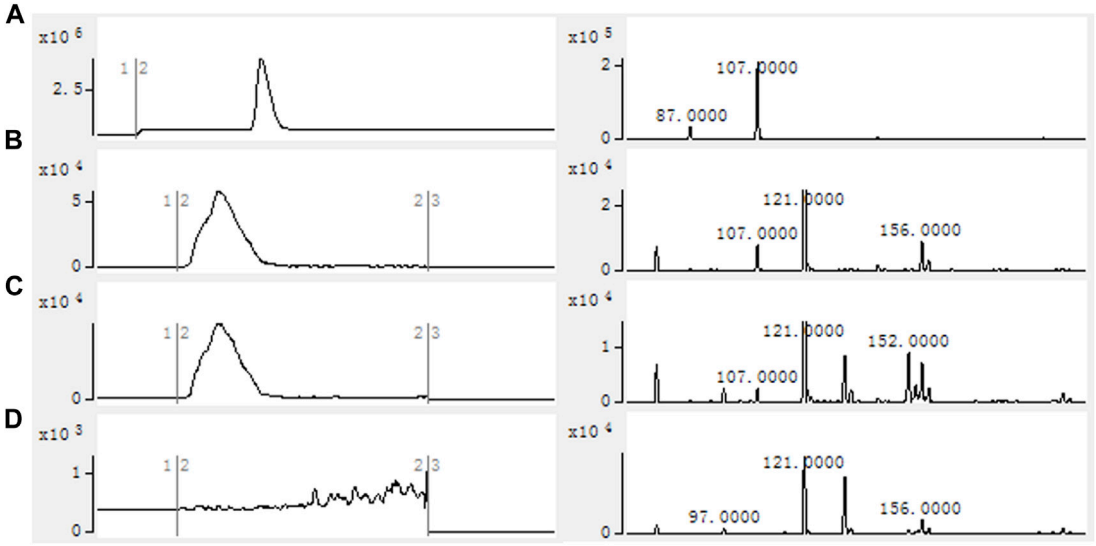

FIGURE 3
HPLC-MS results of *in vitro* catalytic reaction of crude enzyme. **(A)** 2-F-3-HP standard; **(B)** Strain 1 containing 2-F-3-HP standard; **(C)** Strain 2; **(D)** Strain 1. Reactions were performed in 100 mM Tris-HCl buffer (pH 7.8) containing 1 mg/ml crude enzyme, 20 mM 2-FMA, 2 mM NADPH, 2 mM ATP, 1 mM CoA, 10 mM $MgCl_2$ at 30°C with 200 rpm shaking for 12 h. Strain 1: BL21 (DE3)/pACYCDuet1/pBAD; Strain 2: BL21 (DE3)/pACYCDuet1-*MatBrp-Mcr*/pBAD-*madLM*.

pACYCDute1/pBAD), MatBrp (55 kDa) and MCR (135 kDa) were expressed in the recombinant strain 2 (Figure 2). The soluble expression of MatBrp is significantly higher than that of MCR, which may be that MatBrp has a small protein molecular weight and is easier to fold correctly.

Enzyme activity analysis

Using the crude enzyme of the recombinant strain as the catalyst, and NADPH, ATP and coenzyme A as the donors, the purpose was to verify that 2-FMA could be catalyzed by MatBrp and MCR to generate 2-F-3-HP. The formation of 2-F-3-HP was analyzed by HPLC-MS and the results are shown in Figure 3. Compared with strain 1, the reaction solution of strain 2 has a peak in about 2.50 min. In the strain 1 reaction solution containing 2-F-3-HP standard, the retention time of 2-F-3-HP was 2.5 min. Compared with strain 1, the reaction solution of strain 2 contains the characteristic peak EIC m/z = 107.0000. The results showed that MCR and MatBrp had the activity of catalyzing the formation of 2-F-3-HP. The retention time of the 2-F-3-HP standard is 3.0 min, which may be the complex environment of the crude enzyme system affecting the retention time of 2-F-3-HP, resulting in that the retention time of 2-F-3-HP in the sample was 2.5 min.

The concentrated reaction mixture was analyzed by ^{19}F-NMR, and all fluorometabolites present in the samples were scanned. The same peak (similar chemical shift) as that of the standard was detected in the sample, which indicated that 2-F-3-HP was generated in the sample (Figure 4).

Whole-cell biocatalytic synthesis of 2-F-3-HP

To assess the ability of strain 2 to produce the product, the titer of 2-F-3-HP was detected after whole-cell biocatalytic synthesis. Compared with strain 1, the concentration of 2-F-3-HP in strain 2 was 50.0 mg/L by HPLC detection (Table 2).

The concentration of the product is very low, which may be the low activity of the MatBrp and MCR for non-natural substrate, or the toxicity of the 2-FMA to the cells. In the future, two key enzymes can be rationally designed to improve the enzymatic activity for the corresponding substrate.

Conclusion

In this study, 2-F-3-HP was first synthesized by the engineered *E. coli* coexpressing MatBrp, MCR and MadLM

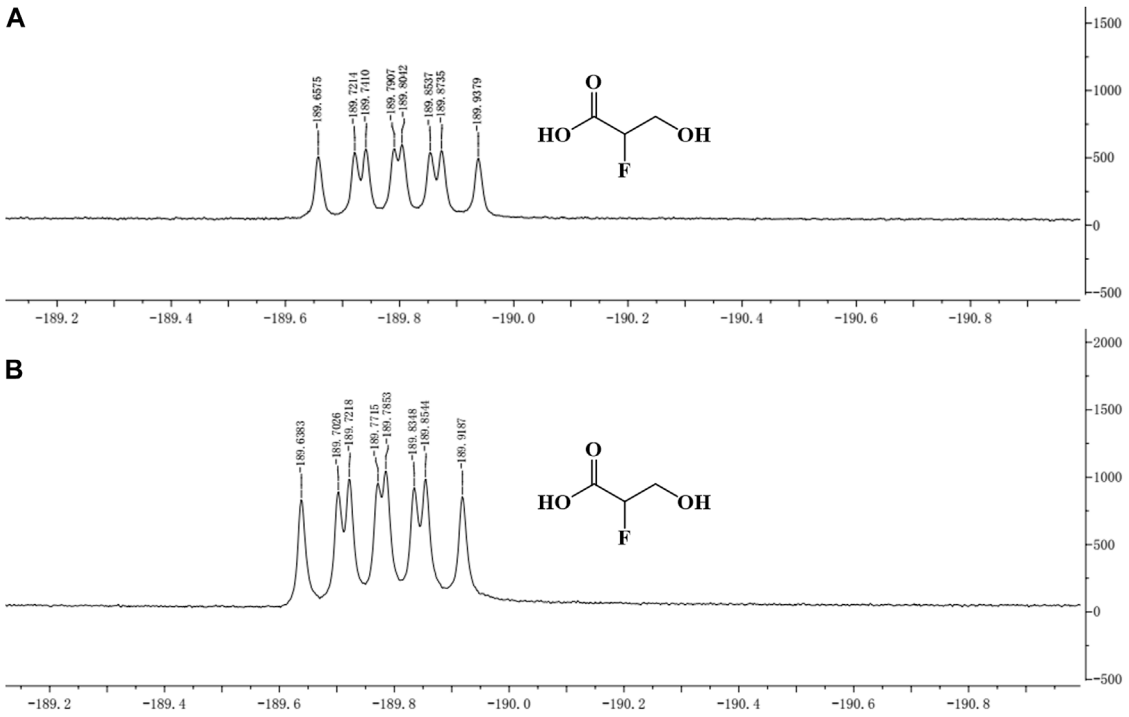

FIGURE 4
^{19}F-NMR of 2-F-3-HP standard and sample. **(A)** ^{19}F-NMR of the 2-F-3-HP standard; **(B)** ^{19}F-NMR of the sample.

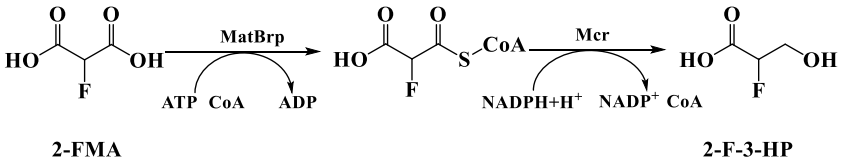

SCHEME 1
Synthesis of 2-F-3-HP designed in this study.

with 2-FMA as substate. After whole-cell transformation, the 50.0 mg/L 2-F-3-HP was produced. 2-F-3-HP can be used as the substrate to synthesize other fluorides, such as poly (2-fluoro-3-hydroxypropionic acid) (FP3HP) or poly (2-fluoro-3-hydroxypropionic acid)-block-poly (2-fluoro-3-hydroxybutyric acid) (FP3HB-b-FP3HP), which is expected to obtain fluorine-containing materials with better properties.

Data Availability Statement

The original contributions presented in the study are included in the article/Supplementary Material, further inquiries can be directed to the corresponding author.

Author contributions

WL: investigation, formal analysis, data curation, writing-original draft, performing experiment content. MX: investigation, writing-review and editing, supervision, project administration. SY: performing partial experiment content. MJ: investigation and date analysis. All authors read and approved the final manuscript.

Funding

This study was supported by the Taishan Scholars Project of Shandong (No. ts 201712076).

Conflict of Interest

The authors declare that the research was conducted in the absence of any commercial or financial relationships that could be construed as a potential conflict of interest.

The handling editor XJ declared a past co-authorship with the author(s) MX.

Publisher's Note

References

Berger, M., Herszman, J. D., Kurimoto, Y., Kruijff, G. H. M. d., Sch¨ull, A., Rufc, S., et al. (2020). Metal-free electrochemical fluorodecarboxylation of aryloxyacetic acids to fluoromethyl aryl ethers. *Chem. Sci.* 11, 6053–6057. doi:10.1039/d0sc02417a

Cheng, X., and Ma, L. (2021). Enzymatic synthesis of fluorinated compounds. *Appl. Microbiol. Biotechnol.* 105, 8033–8058. doi:10.1007/s00253-021-11608-0

Darren, H., Ben, J. M., Sili, Q., Sophie, J., Robert, M. S., Doods, K., et al. (2021). Synthesis of polyfunctional fluoro-quinoline and fluoro-pyridopyrimidinone derivatives. *J. Fluor. Chem.* 249, 109830. doi:10.1016/j.jfluchem.2021.109830

Feng, X., Jin, M., Huang, W., Liu, W., and Xian, M. (2021). Whole-cell catalysis by surface display of fluorinase on *Escherichia coli* using N-terminal domain of ice nucleation protein. *Microb. Cell Fact.* 20, 206. doi:10.1186/s12934-021-01697-x

Kittila, T., Calero, P., Fredslund, F., Lowe, P. T., Teze, D., Nieto-Domınguez, M., et al. (2022). Oligomerization engineering of the fluorinase enzyme leads to an active trimer that supports synthesis of fluorometabolites *in vitro*. *Microb. Biotechnol.* 15, 1622–1632. doi:10.1111/1751-7915.14009

Klopries, S., Koopmans, K. R. M., Sanchez-Garcia, E., and Schulz, F. (2014). Biosynthesis with fluorine. *Chembiochem* 15, 495–497. doi:10.1002/cbic.201300750

Last, N. B., Kolmakova-Partensky, L., Shane, T., and Miller, C. (2016). Mechanistic signs of double-barreled structure in a fluoride ion channel. *Elife* 5, e18767. doi:10.7554/eLife.18767

Li, X.-G., Domarkasc, J., and O'Hagan, D. (2010). Fluorinase mediated chemoenzymatic synthesis of [(18)F]-fluoroacetate. *Chem. Commun.* 46, 7819. doi:10.1039/c0cc02264k

Liu, C., Ding, Y., Zhang, R., Liu, H., Xian, M., Zhao, G., et al. (2016). Functional balance between enzymes in malonyl-CoA pathway for 3-hydroxypropionate biosynthesis. *Metab. Eng.* 34, 104–111. doi:10.1016/j.ymben.2016.01.001

Lowe, P. T., Dall'Angelo, S., Fleming, I. N., Zanda, M., O'Hagan, D., and O'Hagan, D. (2019). Enzymatic radiosynthesis of a (18)F-Glu-Ureido-Lys ligand for the prostate-specific membrane antigen (PSMA). *Org. Biomol. Chem.* 17, 1480–1486. doi:10.1039/c8ob03150a

Ningning, L., Bingjing, H., Anming, W., Huimin, L., Youcheng, Y., Tianyu, M., et al. (2020). Facile bioinspired preparation of Fluorinase@Fluoridated hydroxyapatite nanoflowers for the biosynthesis of 5′-fluorodeoxy adenosine. *Sustainability* 12, 431. doi:10.3390/su12010431

Onega, M., Domarkas, J., Deng, H., Schweiger, L. F., Smith, T. A. D., Welch, A. E., et al. (2010). An enzymatic route to 5-deoxy-5-[18F]fluoro-D-ribose, a [18F]-fluorinated sugar for PET imaging. *Chem. Commun.* 46, 139–141. doi:10.1039/b919364b

Rodrigo, S., Um, C., Mixdorf, J. C., Gunasekera, D., Nguyen, H. M., Luo, L., et al. (2020). Alternating current electrolysis for organic electrosynthesis: trifluoromethylation of (Hetero)arenes. *Org. Lett.* 22, 6719–6723. doi:10.1021/acs.orglett.0c01906

Schaffitzel, C., Berg, M., Dimroth, P., and Pos, K. M. (1998). Identification of an Na+-Dependent malonate transporter of malonomonas rubra and its dependence on two separate genes. *J. Bacteriol.* 180, 2689–2693. doi:10.1128/jb.180.10.2689-2693.1998

Stephanie, M., Frank, W., and Ralf, S. (2019). Synthesis of 2-fluoroacetoacetic acid and 4-Fluoro-3-hydroxybutyric acid. *Synthesis* 51, 2351–2358. doi:10.1055/s-0037-1610695

Thuronyi, B. W., and Chang, M. C. Y. (2015). Synthetic biology approaches to fluorinated polyketides. *Acc. Chem. Res.* 48, 584–592. doi:10.1021/ar500415c

Thuronyi, B. W., Privalsky, T. M., and Chang, M. C. Y. (2017). Engineered fluorine metabolism and fluoropolymer production in living cells. *Angew. Chem. Int. Ed.* 56, 13637–13640. doi:10.1002/anie.201706696

Tu, C., Zhou, J., Peng, L., Man, S., and Ma, L. (2020). Self-assembled nano-aggregates of fluorinases demonstrate enhanced enzymatic activity, thermostability and reusability. *Biomater. Sci.* 8, 648–656. doi:10.1039/c9bm00402e

Valdehuesa, K. N. G., Liu, H., Nisola, G. M., Chung, W.-J., Lee, S. H., Park, S. J., et al. (2013). Recent advances in the metabolic engineering of microorganisms for the production of 3-hydroxypropionic acid as C3 platform chemical. *Appl. Microbiol. Biotechnol.* 97, 3309–3321. doi:10.1007/s00253-013-4802-4

Wang, Q., Yang, P., Liu, C., Xue, Y., Xian, M., Zhao, G., et al. (2013a). Biosynthesis of poly(3-hydroxypropionate) from glycerol by recombinant *Escherichia coli*. *Bioresour. Technol.* 131, 548–551. doi:10.1016/j.biortech.2013.01.096

Wang, Q., Yang, P., Xian, M., Liu, H., Cao, Y., Yang, Y., et al. (2013b). Production of block copolymer poly(3-hydroxybutyrate)-block-poly(3-hydroxypropionate) with adjustable structure from an inexpensive carbon source. *ACS Macro Lett.* 2, 996–1000. doi:10.1021/mz400446g

Wu, L., Maglangit, F., and Deng, H. (2020a). Fluorine biocatalysis. *Curr. Opin. Chem. Biol.* 55, 119–126. doi:10.1016/j.cbpa.2020.01.004

Wu, L., Tong, M. H., Raab, A., Fang, Q., Wang, S., Kyeremeh, K., et al. (2020b). An unusual metal-bound 4-fluorothreonine transaldolase from Streptomyces sp. MA37 catalyses promiscuous transaldol reactions. *Appl. Microbiol. Biotechnol.* 104, 3885–3896. doi:10.1007/s00253-020-10497-z

YongChang, X., Peng, Y., Mo, X., Qi, W., and Guang, Z. (2014). Biosynthesis of poly(3-hydroxypropionate) and its copolymers. *Chin. Sci. Bull.* 59, 2137–2144. doi:10.1360/n972014-00010

frontiers | Frontiers in Bioengineering and Biotechnology

TYPE Original Research
PUBLISHED 02 September 2022
DOI 10.3389/fbioe.2022.987796

OPEN ACCESS

EDITED BY
Guang Zhao,
Shandong University, China

REVIEWED BY
Bo-Bo Zhang,
Shantou University, China
Xia Ke,
Zhejiang University of Technology, China

*CORRESPONDENCE
Jingwen Zhou,
zhoujw1982@jiangnan.edu.cn

SPECIALTY SECTION
This article was submitted to Industrial Biotechnology, a section of the journal Frontiers in Bioengineering and Biotechnology

RECEIVED 06 July 2022
ACCEPTED 08 August 2022
PUBLISHED 02 September 2022

CITATION
Xu S, Xu J, Zeng W, Shan X and Zhou J (2022), Efficient biosynthesis of exopolysaccharide in Candida glabrata by a fed-batch culture.
Front. Bioeng. Biotechnol. 10:987796.
doi: 10.3389/fbioe.2022.987796

Efficient biosynthesis of exopolysaccharide in *Candida glabrata* by a fed-batch culture

Sha Xu[1,2,3], Jinke Xu[2,4], Weizhu Zeng[2,3,4], Xiaoyu Shan[1,4] and Jingwen Zhou[1,2,3,4]*

[1]National Engineering Research Center for Cereal Fermentation and Food Biomanufacturing, Jiangnan University, Wuxi, China, [2]School of Biotechnology and Key Laboratory of Industrial Biotechnology, Ministry of Education, Jiangnan University, Wuxi, China, [3]Jiangsu Provisional Research Center for Bioactive Product Processing Technology, Jiangnan University, Wuxi, China, [4]Science Center for Future Foods, Jiangnan University, Wuxi, China

Polysaccharides are important natural biomacromolecules. In particular, microbial exopolysaccharides have received much attention. They are produced by a variety of microorganisms, and they are widely used in the food, pharmaceutical, and chemical industries. The *Candida glabrata* mutant 4-C10, which has the capacity to produce exopolysaccharide, was previously obtained by random mutagenesis. In this study we aimed to further enhance exopolysaccharide production by systemic fermentation optimization. By single factor optimization and orthogonal design optimization in shaking flasks, an optimal fermentation medium composition was obtained. By optimizing agitation speed, aeration rate, and fed-batch fermentation mode, 118.6 g L^{-1} of exopolysaccharide was obtained by a constant rate feeding fermentation mode, with a glucose yield of 0.62 g g^{-1} and a productivity of 1.24 g L^{-1} h^{-1}. Scaling up the established fermentation mode to a 15-L fermenter led to an exopolysaccharide yield of 113.8 g L^{-1}, with a glucose yield of 0.60 g g^{-1} and a productivity of 1.29 g L^{-1} h^{-1}.

KEYWORDS

***Candida glabrata*, exopolysaccharide, medium composition, fed-batch fermentation, overproduction**

Introduction

Polysaccharides are important natural biomacromolecules. They are widely present in microorganisms, plants, and animals (Liao et al., 2022; Rajoka et al., 2022). Because of the unique physical and chemical characteristics, such as degradability, bioactivity, nontoxicity, and biocompatibility, polysaccharides are widely applied in the food, pharmaceutical, and chemical industries, where they serve as texture enhancers, stabilizers, gelatinizing agents, emulsifiers, drug carriers, etc. (Kokoulin et al., 2021; Yang et al., 2021; Zhang et al., 2022). Recently, microbial polysaccharides have attracted extensive attention from researchers for their anti-tumor, anti-oxidation, hypoglycemic, and immune-enhancing activities (Saadat et al., 2019; Zeng Y. J. et al., 2019). Microbial polysaccharides are traditionally divided into three types: intracellular polysaccharides,

cell wall polysaccharides, and secreted exopolysaccharide (Nachtigall et al., 2020; Tian et al., 2021). In particular, exopolysaccharides have broad application prospects and have attracted increasing attention because of advantages such as relatively high titer, simple separation, and easy large-scale production (Zeng Y. J. et al., 2019).

Exopolysaccharide could be synthesized by various microorganisms, including bacteria, archaea, yeast, fungi, and microalgae (Nambiar et al., 2018; Schmid, 2018). Generally, exopolysaccharides with various structures and high molecular weights are produced and released into the external environment during the process of cell growth or in response to changes in the surrounding environments, such as pH, temperature, ionic strength, and nutritional content (Ayyash et al., 2020; Gan et al., 2020). With the increasing demand for natural biopolymers for diverse industrial applications, various types of exopolysaccharides from different microbial species were investigated and applied (Becker, 2015; Schmid, 2018); for example, hyaluronic acid produced by *Streptococcus zooepidemicus* (Mohan et al., 2022), xanthan gum produced by *Xanthomonas campestris* (Wang Z. C. et al., 2016), and scleroglucan produced by *Sclerotium rolfsii* (Tan et al., 2019). Some kinds of exopolysaccharides have also been isolated from different yeast species, such as *Rhodotorula mucilaginosa* (Ma et al., 2018) and *Zygosaccharomyces rouxii* (Zhang et al., 2022).

Candida glabrata is a classical nonconventional yeast and also a multi-vitamin auxotrophic yeast (Raschmanova et al., 2018). Due to the easy cultivation process, the simple culture medium, and the possibility to use renewable resources, *C. glabrata* has become the dominant producer for the important chemical compound pyruvic acid with the microbiological fermentation route (Luo et al., 2019; Guo et al., 2020a). To enhance the production of pyruvic acid, several strategies have been tried, including selecting high-producing strains combined with high-throughput screening and mutagenesis approaches, metabolic engineering to strengthen the synthesis pathway and extracellular transport, and systematic optimization of the fermentation process (Luo et al., 2018; Guo et al., 2020a; Luo et al., 2020). Interestingly, the *C. glabrata* mutant strain 4-C10, which has the capacity to accumulate exopolysaccharide, was obtained by screening for high pyruvic acid production with random mutagenesis in our previous work. The monosaccharide components and formation mechanism of the exopolysaccharide were also analyzed. By knocking out the genes involved in exopolysaccharide synthesis, the pyruvic acid production was enhanced, while the exopolysaccharide accumulation was decreased (Luo et al., 2017a; Luo et al., 2017b).

To further enhance the production of exopolysaccharide with the obtained mutant, *C. glabrata* 4-C10, a systematic optimization of the fermentation process should be conducted. In the present study, based on the employed fermentation medium compositions for pyruvic acid production, suitable fermentation medium compositions for exopolysaccharide production were first obtained with single factor optimization and orthogonal design optimization at the shaking flask level. Then, the effects of agitation speed and aeration rate on exopolysaccharide accumulation were investigated in a 1-L fermenter, and a constant rate feeding fermentation mode was established. The production of exopolysaccharide reached 118.6 g L^{-1}. Finally, the established constant rate feeding fermentation mode was scaled up to a 15-L fermenter. The exopolysaccharide production and the product yield were basically stable, laying a foundation for industrial production.

Materials and methods

Microorganisms

The producer, *C. glabrata* 4-C10 (CCTCC M2017047), used in this research is a four-vitamin auxotrophic strain (thiamine, biotin, niacin, and pyridoxine), which was previously obtained by random mutagenesis in *C. glabrata* (CCTCC M202019) (Luo et al., 2017a; Luo et al., 2017b).

Medium

The medium for slant and seeds were consisted of (gL^{-1}): glucose 30, plant protein extract 10, KH_2PO_4 1.0 and $MgSO_4{\cdot}7H_2O$ 0.5. Additionally, 20 g L^{-1} of agar was needed to add in the slant medium. The initial fermentation medium consisted of (gL^{-1}): glucose 120, urea 3.84, KH_2PO_4 2.0, $MgSO_4{\cdot}7H_2O$ 0.8, CH_3COONa 3, $CaCO_3$ 40. The trace element mixture (10 ml L^{-1}) and vitamin mixture (6 ml L^{-1}) were added separately. The optimized fermentation medium contained (gL^{-1}): glucose 150, urea 5.0, KH_2PO_4 3.0, $MgSO_4{\cdot}7H_2O$ 0.9, CH_3COONa 3, $CaCO_3$ 40. The trace element mixture (10 ml L^{-1}) and vitamin mixture (6 ml L^{-1}) were also added separately. The trace element mixture was dissolved with 2 M of HCl, consisting of (gL^{-1}): $MnCl_2{\cdot}4H_2O$ 12, $FeSO_4{\cdot}7H_2O$ 2, $CaCl_2{\cdot}2H_2O$ 2, $CuSO_4{\cdot}5H_2O$ 0.05, $ZnCl_2$ 0.5. The vitamin mixture was dissolved with 2 M of HCl, consisting of (gL^{-1}): biotin 0.004, thiamine 0.00075, pyridoxine 0.04, niacin 0.8 (Luo et al., 2017a).

Culture condition

C. glabrata 4-C10 was incubated in seed culture medium at 30°C for 16 h. The seed cultures and fermentation cultivation were implemented in 500 ml shaking flasks consisting of 50 ml of culture medium at 30°C on a reciprocal shaker at 220 $rmin^{-1}$ (Zhichu, Shanghai, China). Batch fermentation and fed-batch fermentation were performed in a 1-L parallel bioreactor (T&J Bio-engineering, Shanghai, China) with a 0.6-L working volume. The agitation speed, aeration rate, and fed-batch mode were

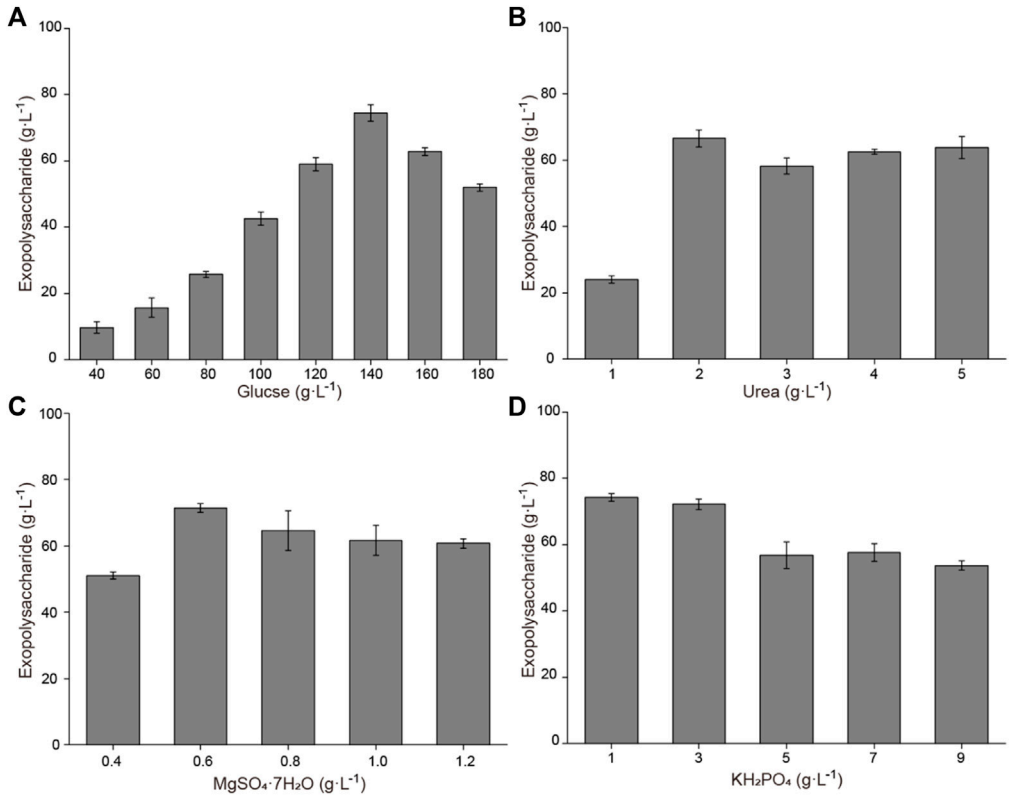

FIGURE 1
Effects of medium components on exopolysaccharide accumulation in flasks. **(A)** Effects of glucose concentration on exopolysaccharide accumulation. **(B)** Effects of urea concentration on exopolysaccharide accumulation. **(C)** Effects of $MgSO_4{\cdot}7H_2O$ concentration on exopolysaccharide accumulation. **(D)** Effects of KH_2PO_4 concentration on exopolysaccharide accumulation.

adjusted (see Results and discussion section). Fermentation was conducted in a 15-L bioreactor (T&J Bio-engineering, Shanghai, China) containing a 12-L working volume with an agitation speed of 500 $rmin^{-1}$, 1.0 vvm, and a pressure of 0.035 MPa. The pH was automatically kept at 5.5 by adding 8 M of NaOH. The inoculation size was 10% (v/v) and all cultivations were carried out at 30°C (Luo et al., 2017a; Guo et al., 2020b).

Analytical method

Determination of biomass: The different samples taken in the fermentation process were all diluted to a certain concentration with 2 M HCl. The optical density (OD) of the diluted fermentation broth was detected using a Biospe-1601 spectrophotometer (Shimadzu Co., Kyoto, Japan) at 660 nm. The dry cell weight (DCW) was calculated with the relationship $DCW = 0.23{\times}OD_{660}$. (Luo et al., 2020).

Determination of glucose and pyruvic acid: The glucose was detected with a glucose-lactate biosensor (Sieman Technology, Shenzhen, China), and the pyruvic acid were detected by high-performance liquid chromatography (HPLC, Agilent 1260, CA, United States) with a UV detector at 210 nm with an Aminex HPX-87H column (Bio-Rad, CA, United States). The specific detection conditions were as follows: an injection volume of 10 μl, a mobile phase of 5 mM H_2SO_4, a flow rate of 0.5 ml min^{-1}, and a column temperature of 40°C (Zhou et al., 2009).

Determination of the concentration of exopolysaccharide: The different samples of fermentation broths were centrifuged at 5000 × *g* for 15 min. Then, two volumes of precooled ethanol (4°C) were added to the obtained supernatant. After 1 h, the precipitate was centrifuged at 5000 × *g* for 15 min. The exopolysaccharide concentration was determined after the precipitate was freeze-dried to a constant weight (Luo et al., 2017a).

Statistical analysis

All fermentation processes were carried out in triplicate and the results were presented as mean values. The orthogonal experiment was designed by Design Expert and the experimental data were analyzed by Origin 2019b.

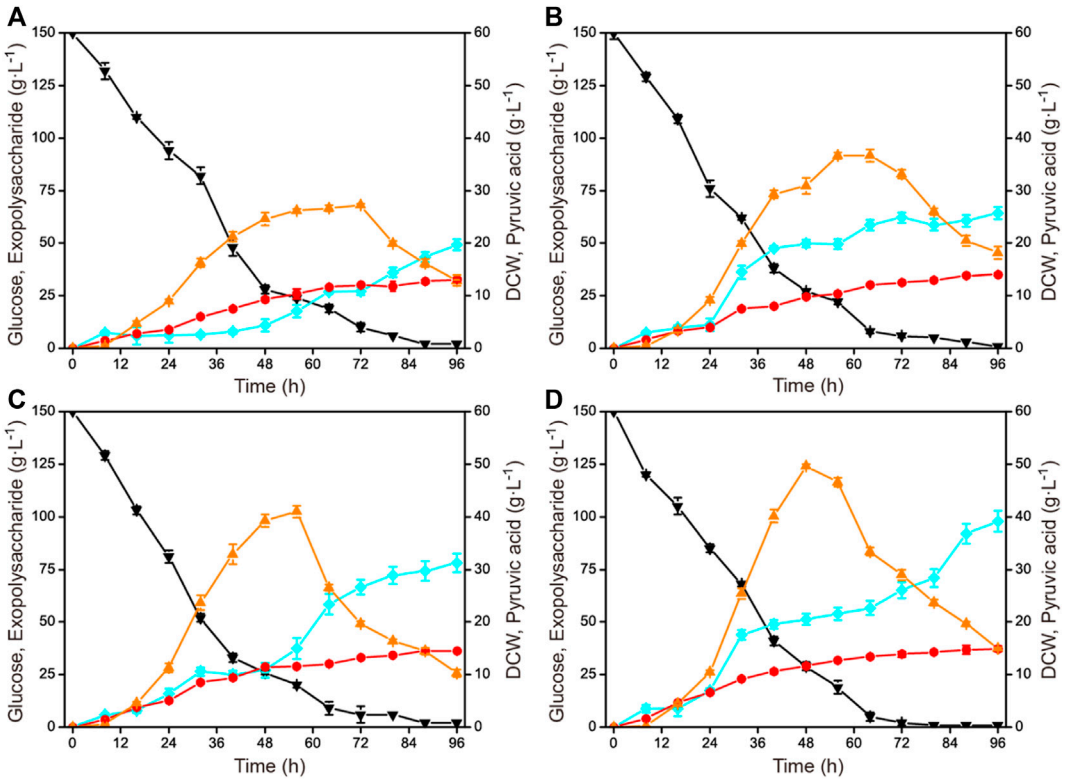

FIGURE 2
Time courses of exopolysaccharide production at different agitation speeds in a 1-L fermenter. **(A)** 1.0 vvm and 300 rmin^{-1}. **(B)** 1.0 vvm and 400 rmin^{-1}. **(C)** 1.0 vvm and 500 rmin^{-1}. **(D)** 1.0 vvm and 600 rmin^{-1}. Black down triangles, glucose; orange up triangles, pyruvic acid; red circles, DCW; blue squares, exopolysaccharide.

Results and discussion

Effects of medium components on exopolysaccharide accumulation

For the biosynthesis of specific target metabolites by microbial fermentation, the composition of fermentation medium is usually the preferred optimization factor to enhance the production during the fermentation process (Xin et al., 2017; Wagh et al., 2022). For pyruvic acid production, the optimization of fermentation medium composition and process control was systematically conducted, and significant enhancements in titer and productivity was obtained (Xu et al., 2009; Guo et al., 2020b). For exopolysaccharide production, the optimal addition of vitamin mixture has also been determined (Luo et al., 2017a). To further enhance the exopolysaccharide accumulation, the concentrations of some important components of the medium could be investigated.

Based on the previously obtained initial fermentation medium, the influence of different medium components (glucose, urea, $MgSO_4{\cdot}7H_2O$, and KH_2PO_4) on exopolysaccharide accumulation is shown in Figure 1. Increasing glucose concentrations result in enhanced exopolysaccharide production. When the concentration was 140 g L^{-1}, the exopolysaccharide production was highest, reaching 74.4 g L^{-1}. The effect of urea addition on exopolysaccharide production was not significant; the production was highest when the concentration was 2 g L^{-1}. A relatively high exopolysaccharide production was obtained when the $MgSO_4{\cdot}7H_2O$ concentration was 0.6 g L^{-1}. A high exopolysaccharide production could be obtained when the KH_2PO_4 concentration was 1 g L^{-1} or 3 g L^{-1}, while the exopolysaccharide production decreased when the KH_2PO_4 concentration was further increased. To obtain the optimal combination, an orthogonal experiment for addition of glucose, urea, $MgSO_4{\cdot}7H_2O$, and KH_2PO_4 was designed. Results showed that 89.7 g L^{-1} of exopolysaccharide was harvested with a composition of 150 g L^{-1} of glucose, 5 g L^{-1} of urea, 0.9 g L^{-1} of $MgSO_4{\cdot}7H_2O$, and 3 g L^{-1} of KH_2PO_4 (Table S1). Statistical analysis showed that the effect of the initial glucose concentration on exopolysaccharide accumulation is extremely significant (Table S2).

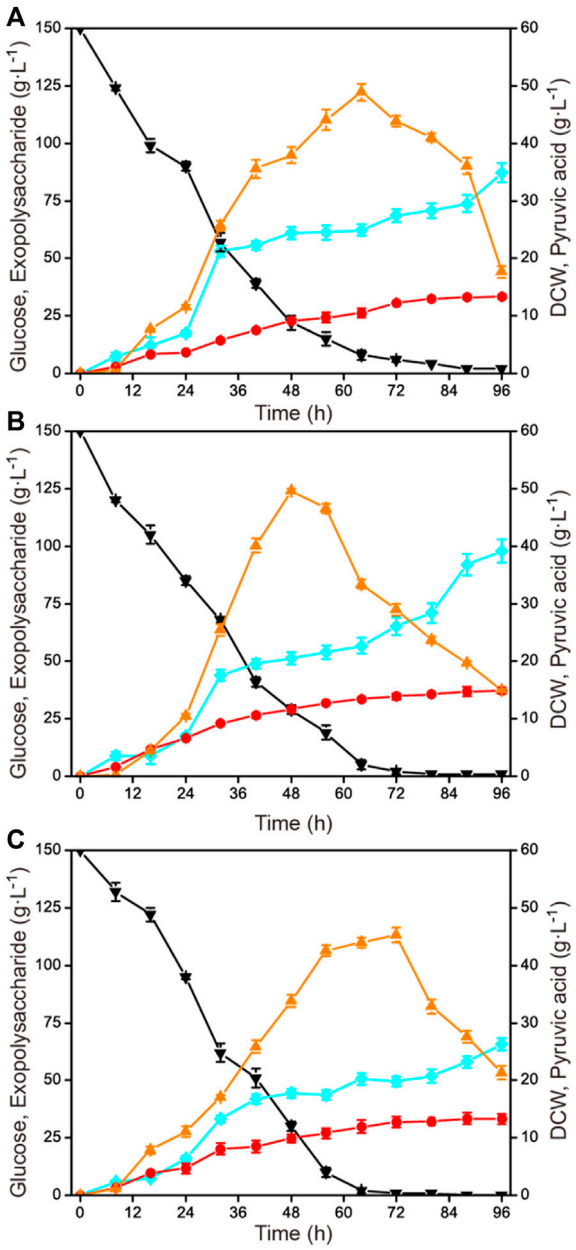

FIGURE 3
Time courses of exopolysaccharide production at different aeration rates in a 1-L fermenter. **(A)** 600 rmin^{-1} and 0.5 vvm. **(B)** 600 min^{-1} and 1.0 vvm. **(C)** 600 rmin^{-1} and 1.5 vvm. Black down triangles, glucose; orange up triangles, pyruvic acid; red circles, DCW; blue squares, exopolysaccharide.

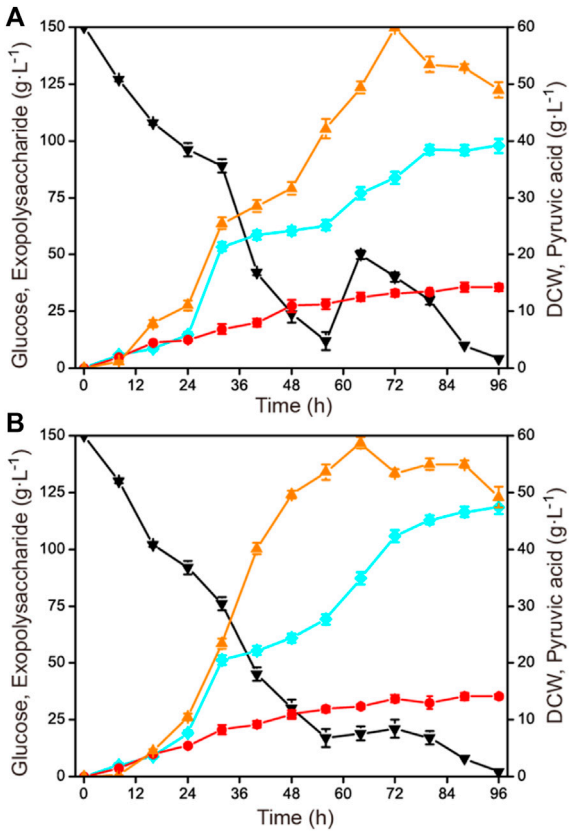

FIGURE 4
Effects of different feeding strategies on exopolysaccharide production in a 1-L fermenter. The initial concentration of glucose was 150 g L^{-1}, and then 40 g L^{-1} of glucose was fed with different feeding strategies. **(A)** One-dose feeding fermentation mode of 40 g L^{-1} glucose at 56 h. **(B)** Constant rate feeding fermentation mode of 40 g L^{-1} glucose during 56–84 h. Black down triangles, glucose; orange up triangles, pyruvic acid; red circles, DCW; blue squares, exopolysaccharide.

Effects of agitation speed on exopolysaccharide accumulation

To enhance the exopolysaccharide production, the cultivation condition was further optimized based on obtaining the optimal fermentation medium compositions. The influences of different agitation speeds (300 rmin^{-1}, 400 rmin^{-1}, 500 rmin^{-1}, and 600 rmin^{-1}) on exopolysaccharide production in a 1-L fermenter are shown in Figure 2. With the increase of agitation speed, the biomass and the exopolysaccharide production improved. The highest exopolysaccharide production was obtained when the agitation speed was 600 rmin^{-1}, reaching 97.9 g L^{-1} with a glucose yield of 0.65 g g^{-1}. In addition, the time profiles of the by-product pyruvic acid accumulation showed the same trend under different agitation speeds. The accumulation gradually increased and then decreased, but the fermentation time for pyruvic acid to peak value gradually shortened.

Agitation speed is an important parameter affecting the dissolved oxygen level during the fermentation process (Huang et al., 2020; Fang et al., 2021). Considering the cultivation mode without pressure on the glass fermenter,

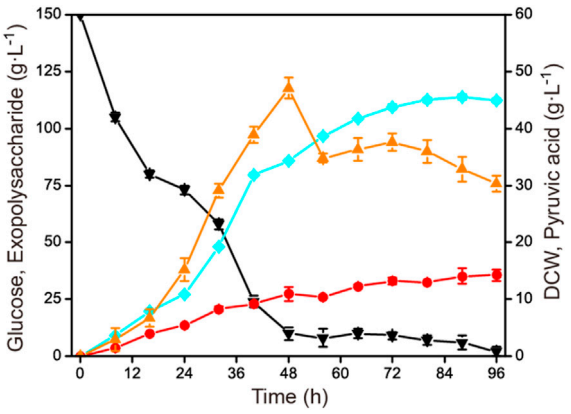

FIGURE 5
Time course of exopolysaccharide accumulation in a 15-L fermenter. The initial concentration of glucose was 150 g L^{-1}, and then 40 g L^{-1} glucose was fed constantly during 56–84 h. Fermentation was conducted at 30°C, 500 $rmin^{-1}$, and 1.0 vvm for 96 h. Black down triangles, glucose; orange up triangles, pyruvic acid; red circles, DCW; blue squares, exopolysaccharide.

it is generally preferred to optimize the agitation speed. There have been many examples of improving the accumulation of specific target products by systematically optimizing the agitation speed. By establishing a two-stage agitation speed controlling strategy, the production and molecular weight of pullulan with *Aureobasidium pullulans* were simultaneously enhanced (Wang D. H. et al., 2016). By studying the influence of the agitation speed, an optimal agitation speed was obtained for 1,3-propanediol production with *Shimwellia blattae* (Rodriguez et al., 2016). *C. glabrata* has been proved to require a relatively high agitation speed for pyruvic acid production (Luo et al., 2018; Guo et al., 2020b). The results obtained in this study indicated that a higher stirring speed was also beneficial to the accumulation of polysaccharides.

Effects of aeration rate on exopolysaccharide accumulation

To investigate the influence of aeration rate on exopolysaccharide accumulation, three different aeration rates (0.5 vvm, 1.0 vvm, and 1.5 vvm) were selected. The results are shown in Figure 3. When the aeration rate was controlled at a relatively low value (0.5 vvm), the growth rate and the glucose consumption rate were obviously lower than under the other two conditions (1.0 vvm and 1.5 vvm). When the aeration rate was 1.5 vvm, the highest exopolysaccharide production was just 65.8 g L^{-1}, which was significantly lower than at 0.5 vvm and 1.0 vvm. Exopolysaccharide yields of 87.2 g L^{-1} and 97.9 g L^{-1} were obtained under 0.5 vvm and 1.0 vvm, respectively.

Aeration rate is another important parameter affecting the dissolved oxygen level during the fermentation process. In many fermentation processes, the supply of oxygen plays a crucial role in the growth of cells and the synthesis of specific target compounds (Alonso et al., 2012; Fang et al., 2021). Generally, the optimization of aeration rate is combined with the agitation speed for co-regulating dissolved oxygen levels. A series of combinatorial optimization strategies have been applied for the synthesis of some important products (Wang et al., 2010; Song et al., 2018). A high dissolved oxygen level could promote cell growth and pyruvic acid production at the expense of glucose consumption in *C. glabrata*, and a strategy has been used to reduce the dependence of cells on oxygen (Luo et al., 2019; Luo et al., 2020). Notably, a high aeration rate was detrimental to exopolysaccharide production, as shown in Figure 3.

Enhancement of exopolysaccharide production by fed-batch strategy

After the optimization of agitation speed and aeration rate in the 1-L fermenter, feeding strategies were tried to further improve the accumulation of exopolysaccharide, such as single-dose fed-batch mode and constant rate feeding mode. The initial concentration of glucose was 150 g L^{-1} and the total concentration was 190 g L^{-1}. When the residual glucose concentration was reduced to 15–20 g L^{-1}, an additional 40 g L^{-1} of glucose was fed by a single dose at 56 h and by a constant rate of 1.43 g L^{-1} h^{-1} during 56–84 h, respectively (Figure 4). It was shown that the constant rate feeding mode yielded a better result, with a highest exopolysaccharide production of 118.6 g L^{-1}, a glucose yield of 0.62 g g^{-1}, and a productivity of 1.24 g L^{-1} h^{-1}, which were all higher than those of by the single-dose fed-batch mode (with a highest exopolysaccharide production of 97.7 g L^{-1}, a glucose yield of 0.51 g g^{-1}, and a productivity of 1.02 g L^{-1} h^{-1}).

The fed-batch fermentation mode is a common fermentation strategy in the field of microbial industrial fermentation. It can be divided into a variety of feeding modes, including single-dose fed-batch mode, intermittent fed-batch mode, constant rate feeding mode, exponential feeding mode, etc. (Zeng W. Z. et al., 2019; Wang et al., 2020; de Oliveira et al., 2021). These established feeding modes have been widely applied to improve the production, yield, and productivity of some specific target products, such as 2-phenylethanol, scleroglucan, and keto acids (Zeng et al., 2017; Tan et al., 2019; Tian et al., 2020). However, it should be noted that the optimal feeding mode for industrial microorganisms to produce diverse metabolites is different. In this study, the constant rate feeding mode was proved more suitable for exopolysaccharide production in *C. glabrata*, but the

TABLE 1 Fermentation characteristics in 1-L and 15-L fermenters.

Fermentation characteristics	Bach fermentation (1 L)	Constant speed feeding fermentation (1 L)	Constant speed feeding fermentation (15 L)
Time (h)	96	96	88
Glucose consumption ($g{\cdot}L^{-1}$)	150	190	190
DCW ($g{\cdot}L^{-1}$)	14.9	14.1	14.0
Exopolysaccharide ($g{\cdot}L^{-1}$)	97.9	118.6	113.8
Yield of exopolysaccharide ($g{\cdot}g^{-1}$)	0.65	0.62	0.60
Productivity of exopolysaccharide ($g{\cdot}L^{-1}\ h^{-1}$)	1.02	1.24	1.29
Pyruvic acid ($g{\cdot}L^{-1}$)	14.4	49.3	32.8

fed-batch strategy could be optimized more detailedly in the future, for example by comparing other feeding modes or combining with other strategies in the fed-batch process.

Scaling up of exopolysaccharide production in a 15-L fermenter

In order to verify the constant rate feeding mode under the conditions that were closest to industrial production, the established process was further scaled up to a 15-L fermenter. As in the 1-L fermenter, the aeration rate was controlled at 1.0 vvm and 40 g L^{-1} was fed with a constant rate of 1.43 g L^{-1} h^{-1} during 56–84 h. The agitation speed was maintained at 500 $rmin^{-1}$ under a fermenter pressure of 0.035 MPa. The result is shown in Figure 5. The highest exopolysaccharide titer was obtained at 88 h, reaching 113.8 g L^{-1} with a glucose yield of 0.60 g g^{-1} and a productivity of 1.29 g L^{-1} h^{-1}. Compared with the constant rate feeding mode in the 1-L fermenter, the exopolysaccharide production was slightly decreased. Additionally, during the fermentation process in the 15-L fermenter, the highest and the final accumulation of by-product pyruvic acid were also obviously less than in the 1-L fermenter. The specific fermentation characteristics in 1-L and 15-L fermenters are presented in Table 1.

The development of commercial production methods of a specific product with microorganism fermentation is a long amplification process, from microtiter plates, to shaking flasks, to bench-scale fermenters, to pilot-scale fermenters, and ultimately to commercial fermenters (Wehrs et al., 2019; Ganeshan et al., 2021). The scaling up of the fermentation process for a target product is a systematic project, but not simply a matter of increasing cultivation and vessel volume (Hewitt & Nienow, 2007; Krajang et al., 2021). A reliable scaling up process at the lab scale should reasonably solve the problem from shaking flasks to bench-scale fermenters, particularly the fermenters equipped with pressure control. A series of scaling up processes has been published for some exopolysaccharides, such as glucan, xanthan gum, levan, and pullulan (Freitas et al., 2017; Bzducha-Wrobel et al., 2018; Vaishnav et al., 2022). In this study, the exopolysaccharide production after scaling up to a 15-L fermenter was slightly decreased. But the time to reach the maximum was shortened, thereby achieved a relatively higher space time yield. To further enhance the production, the feeding rate and the glucose concentration could be appropriately increased in the fed-batch process.

Conclusion

In this study, the fermentation medium components were optimized in shaking flasks to enhance exopolysaccharide production with *C. glabrata* strain 4-C10, which was obtained by random mutagenesis. By optimizing the agitation speed and aeration rate and establishing a constant rate feeding fermentation mode in a 1-L fermenter, the exopolysaccharide titer was enhanced to 118.6 g L^{-1}, with a glucose yield of 0.62 g g^{-1} and a productivity of 1.24 g L^{-1} h^{-1}. After scaling up to a 15-L fermenter, the production was slightly decreased, reaching 113.8 g L^{-1}. The obtained results could provide references for industrial exopolysaccharide production.

Data availability statement

The original contributions presented in the study are included in the article/Supplementary Material, further inquiries can be directed to the corresponding author.

Author contributions

SX: methodology, investigation, formal analysis, writing—original draft. JX: investigation. WZ: supervision, writing—review and editing, validation. XS: methodology, investigation. JZ: supervision, funding acquisition, writing—review and editing.

Funding

This work was supported by the National Key Research and Development Program of China (2021YFC2101400), and the Foundation for Innovative Research Groups of the National Natural Science Foundation of China (32021005).

Conflict of interest

The authors declare that the research was conducted in the absence of any commercial or financial relationships that could be construed as a potential conflict of interest.

Publisher's note

Supplementary material

The Supplementary Material for this article can be found online at: https://www.frontiersin.org/articles/10.3389/fbioe.2022.987796/full#supplementary-material

References

Alonso, S., Rendueles, M., and Diaz, M. (2012). Role of dissolved oxygen availability on lactobionic acid production from whey by *Pseudomonas taetrolens*. *Bioresour. Technol.* 109, 140–147. doi:10.1016/j.biortech.2012.01.045

Ayyash, M., Abu-Jdayil, B., Itsaranuwat, P., Almazrouei, N., Galiwango, E., Esposito, G., et al. (2020). Exopolysaccharide produced by the potential probiotic *Lactococcus garvieae* C47: Structural characteristics, rheological properties, bioactivities and impact on fermented camel milk. *Food Chem. x.* 333, 127418. doi:10.1016/j.foodchem.2020.127418

Becker, A. (2015). Challenges and perspectives in combinatorial assembly of novel exopolysaccharide biosynthesis pathways. *Front. Microbiol.* 6, 687. doi:10.3389/fmicb.2015.00687

Bzducha-Wrobel, A., Pobiega, K., Blazejak, S., and Kieliszek, M. (2018). The scale-up cultivation of *Candida utilis* in waste potato juice water with glycerol affects biomass and beta(1, 3)/(1, 6)-glucan characteristic and yield. *Appl. Microbiol. Biotechnol.* 102 (21), 9131–9145. doi:10.1007/s00253-018-9357-y

de Oliveira, P. M., Santos, L. P., Coelho, L. F., Neto, P. M. A., Sass, D. C., and Contiero, J. (2021). Production of L (+) lactic acid by *Lactobacillus casei* Ke11: Fed batch fermentation strategies. *Ferment. (Basel).* 7 (3), 151. doi:10.3390/fermentation7030151

Fang, J., Zeng, W. Z., and Zhou, J. W. (2021). Breeding and process optimization of *Yarrowia lipolytica* for high-yield α-ketoglutaric acid production. *Food Fermen Ind.* 47 (2), 137–144. doi:10.13995/j.cnki.11-1802/ts.024665

Freitas, F., Torres, C. A. V., and Reis, M. A. M. (2017). Engineering aspects of microbial exopolysaccharide production. *Bioresour. Technol.* 245, 1674–1683. doi:10.1016/j.biortech.2017.05.092

Gan, L. Z., Li, X. G., Wang, H. B., Peng, B. Y., and Tian, Y. Q. (2020). Structural characterization and functional evaluation of a novel exopolysaccharide from the moderate halophile *Gracilibacillus* sp. SCU50. *Int. J. Biol. Macromol.* 154, 1140–1148. doi:10.1016/j.ijbiomac.2019.11.143

Ganeshan, S., Kim, S. H., and Vujanovic, V. (2021). Scaling-up production of plant endophytes in bioreactors: Concepts, challenges and perspectives. *Bioresour. Bioprocess.* 8 (1), 63. doi:10.1186/s40643-021-00417-y

Guo, L. K., Zeng, W. Z., Xu, S., and Zhou, J. W. (2020a). Fluorescence-activated droplet sorting for enhanced pyruvic acid accumulation by *Candida glabrata*. *Bioresour. Technol.* 318, 124258. doi:10.1016/j.biortech.2020.124258

Guo, L. K., Zeng, W. Z., and Zhou, J. W. (2020b). Process optimization of fed-batch fermentation for pyruvic acid production with *Candida glabrata*. *Food Fermen Ind.* 46 (7), 10–16. doi:10.13995/j.cnki.11-1802/ts.022872

Hewitt, C. J., and Nienow, A. W. (2007). The scale-up of microbial batch and fed-batch fermentation processes. *Adv. Appl. Microbiol.* 62, 105–135. doi:10.1016/S0065-2164(07)62005-X

Huang, M. W., Chen, H. Q., Tang, X., Lu, H. Q., Zhao, J. X., Zhang, H., et al. (2020). Two-stage pH control combined with oxygen-enriched air strategies for the highly efficient production of EPA by *Mortierella alpina* CCFM698 with fed-batch fermentation. *Bioprocess Biosyst. Eng.* 43 (9), 1725–1733. doi:10.1007/s00449-020-02367-9

Kokoulin, M. S., Kuzmich, A. S., Romanenko, L. A., and Chikalovets, I. V. (2021). Structure and *in vitro* antiproliferative activity of the acidic capsular polysaccharide from the deep-sea bacterium *Psychrobacter submarinus* KMM 225^T. *Carbohydr. Polym.* 262, 117941. doi:10.1016/j.carbpol.2021.117941

Krajang, M., Malairuang, K., Sukna, J., Rattanapradit, K., and Chamsart, S. (2021). Single-step ethanol production from raw cassava starch using a combination of raw starch hydrolysis and fermentation, scale-up from 5-L laboratory and 200-L pilot plant to 3000-L industrial fermenters. *Biotechnol. Biofuels* 14 (1), 68. doi:10.1186/s13068-021-01903-3

Liao, Y. T., Gao, M., Wang, Y. T., Liu, X. Z., Zhong, C., and Jia, S. R. (2022). Structural characterization and immunomodulatory activity of exopolysaccharide from *Aureobasidium pullulans* CGMCC 23063. *Carbohydr. Polym.* 288, 119366. doi:10.1016/j.carbpol.2022.119366

Luo, Z. S., Liu, S., Du, G. C., Xu, S., Zhou, J. W., and Chen, J. (2018). Enhanced pyruvate production in *Candida glabrata* by carrier engineering. *Biotechnol. Bioeng.* 115 (2), 473–482. doi:10.1002/bit.26477

Luo, Z. S., Liu, S., Du, G. C., Zhou, J. W., and Chen, J. (2017a). Identification of a polysaccharide produced by the pyruvate overproducer *Candida glabrata* CCTCC M202019. *Appl. Microbiol. Biotechnol.* 101 (11), 4447–4458. doi:10.1007/s00253-017-8245-1

Luo, Z. S., Zeng, W. Z., Du, G. C., Chen, J., and Zhou, J. (2019). Enhanced pyruvate production in *Candida glabrata* by engineering ATP futile cycle system. *ACS Synth. Biol.* 8 (4), 787–795. doi:10.1021/acssynbio.8b00479

Luo, Z. S., Zeng, W. Z., Du, G. C., Chen, J., and Zhou, J. W. (2020). Enhancement of pyruvic acid production in *Candida glabrata* by engineering hypoxia-inducible factor 1. *Bioresour. Technol.* 295, 122248. doi:10.1016/j.biortech.2019.122248

Luo, Z. S., Zeng, W. Z., Du, G. C., Liu, S., Fang, F., Zhou, J. W., et al. (2017b). A high-throughput screening procedure for enhancing pyruvate production in *Candida glabrata* by random mutagenesis. *Bioprocess Biosyst. Eng.* 40 (5), 693–701. doi:10.1007/s00449-017-1734-x

Ma, W. J., Chen, X. F., Wang, B., Lou, W. J., Chen, X., Hua, J. L., et al. (2018). Characterization, antioxidativity, and anti-carcinoma activity of exopolysaccharide extract from *Rhodotorula mucilaginosa* CICC 33013. *Carbohydr. Polym.* 181, 768–777. doi:10.1016/j.carbpol.2017.11.080

Mohan, N., Pavan, S. S., Jayakumar, A., Rathinavelu, S., and Sivaprakasam, S. (2022). Real-time metabolic heat-based specific growth rate soft sensor for monitoring and control of high molecular weight hyaluronic acid production by *Streptococcus zooepidemicus*. *Appl. Microbiol. Biotechnol.* 106 (3), 1079–1095. doi:10.1007/s00253-022-11760-1

Nachtigall, C., Surber, G., Herbi, F., Wefers, D., Jaros, D., and Rohm, H. (2020). Production and molecular structure of heteropolysaccharides from two lactic acid bacteria. *Carbohydr. Polym.* 236, 116019. doi:10.1016/j.carbpol.2020.116019

Nambiar, R. B., Sellamuthu, P. S., Perumal, A. B., Sadiku, E. R., Phiri, G., and Jayaramudu, J. (2018). Characterization of an exopolysaccharide produced by *Lactobacillus plantarum* HM47 isolated from human breast milk. *Process Biochem.* 73, 15–22. doi:10.1016/j.procbio.2018.07.018

Rajoka, M. S. R., Mehwish, H. M., Kitazawa, H., Barba, F. J., Berthelot, L., Umair, M., et al. (2022). Techno-functional properties and immunomodulatory potential of exopolysaccharide from *Lactiplantibacillus plantarum* MM89 isolated from human breast milk. *Food Chem. x.* 377, 131954. doi:10.1016/j.foodchem.2021.131954

Raschmanova, H., Weninger, A., Glieder, A., Kovar, K., and Vogl, T. (2018). Implementing CRISPR-Cas technologies in conventional and non-conventional yeasts: Current state and future prospects. *Biotechnol. Adv.* 36 (3), 641–665. doi:10.1016/j.biotechadv.2018.01.006

Rodriguez, A., Wojtusik, M., Ripoll, V., Santos, V. E., and Garcia-Ochoa, F. (2016). 1, 3-Propanediol production from glycerol with a novel biocatalyst *Shimwellia blattae* ATCC 33430: Operational conditions and kinetics in batch cultivations. *Bioresour. Technol.* 200, 830–837. doi:10.1016/j.biortech.2015.10.061

Saadat, Y. R., Khosroushahi, A. Y., and Gargari, B. P. (2019). A comprehensive review of anticancer, immunomodulatory and health beneficial effects of the lactic acid bacteria exopolysaccharides. *Carbohydr. Polym.* 217, 79–89. doi:10.1016/j.carbpol.2019.04.025

Schmid, J. (2018). Recent insights in microbial exopolysaccharide biosynthesis and engineering strategies. *Curr. Opin. Biotechnol.* 53, 130–136. doi:10.1016/j.copbio.2018.01.005

Song, X. Q., Zhang, Y., Xue, J. Y., Li, C., Wang, Z. J., and Wang, Y. H. (2018). Enhancing nemadectin production by *Streptomyces cyaneogriseus* ssp *noncyanogenus* through quantitative evaluation and optimization of dissolved oxygen and shear force. *Bioresour. Technol.* 255, 180–188. doi:10.1016/j.biortech.2017.09.033

Tan, R. Q., Lyu, Y. B., Zeng, W. Z., and Zhou, J. W. (2019). Enhancing scleroglucan production by *Sclerotium rolfsii* WSH-G01 through a pH-shift strategy based on kinetic analysis. *Bioresour. Technol.* 293, 122098. doi:10.1016/j.biortech.2019.122098

Tian, J. J., Zhang, C. P., Wang, X. M., Rui, X., Zhang, Q. Q., Chen, X. H., et al. (2021). Structural characterization and immunomodulatory activity of intracellular polysaccharide from the mycelium of *Paecilomyces cicadae* TJJ1213. *Food Res. Int.* 147, 110515. doi:10.1016/j.foodres.2021.110515

Tian, S. F., Liang, X. L., Chen, J., Zeng, W. Z., Zhou, J. W., and Du, G. C. (2020). Enhancement of 2-phenylethanol production by a wild-type *Wickerhamomyces anomalus* strain isolated from rice wine. *Bioresour. Technol.* 318, 124257. doi:10.1016/j.biortech.2020.124257

Vaishnav, A., Upadhyay, K., Koradiya, M., Tipre, D., and Dave, S. (2022). Valorisation of fruit waste for enhanced exopolysaccharide production by *Xanthomonas campestries* using statistical optimisation of medium and process. *Food Biosci.* 46, 101608. doi:10.1016/j.fbio.2022.101608

Wagh, V. S., Said, M. S., Bennale, J. S., and Dastager, S. G. (2022). Isolation and structural characterization of exopolysaccharide from marine *Bacillus* sp. and its optimization by Microbioreactor. *Carbohydr. Polym.* 285, 119241. doi:10.1016/j.carbpol.2022.119241

Wang, D. H., Bian, J. J., Wei, G. Y., Jiang, M., and Dong, M. S. (2016). Simultaneously enhanced production and molecular weight of pullulan using a two-stage agitation speed control strategy. *J. Chem. Technol. Biotechnol.* 91 (2), 467–475. doi:10.1002/jctb.4600

Wang, X. L., Zhou, J. J., Shen, J. T., Zheng, Y. F., Sun, Y. Q., and Xiu, Z. L. (2020). Sequential fed-batch fermentation of 1, 3-propanediol from glycerol by *Clostridium butyricum* DL07. *Appl. Microbiol. Biotechnol.* 104 (21), 9179–9191. doi:10.1007/s00253-020-10931-2

Wang, Y. H., Fang, X. L., Li, Y. P., and Zhang, X. (2010). Effects of constant and shifting dissolved oxygen concentration on the growth and antibiotic activity of *Xenorhabdus nematophila*. *Bioresour. Technol.* 101 (19), 7529–7536. doi:10.1016/j.biortech.2010.04.070

Wang, Z. C., Wu, J. R., Zhu, L., and Zhan, X. B. (2016). Activation of glycerol metabolism in *Xanthomonas campestris* by adaptive evolution to produce a high-transparency and low-viscosity xanthan gum from glycerol. *Bioresour. Technol.* 211, 390–397. doi:10.1016/j.biortech.2016.03.096

Wehrs, M., Tanjore, D., Eng, T., Lievense, J., Pray, T. R., and Mukhopadhyay, A. (2019). Engineering robust production microbes for large-scale cultivation. *Trends Microbiol.* 27 (6), 524–537. doi:10.1016/j.tim.2019.01.006

Xin, F. X., Chen, T. P., Jiang, Y. J., Lu, J. S., Dong, W. L., Zhang, W. M., et al. (2017). Enhanced biobutanol production with high yield from crude glycerol by acetone uncoupled *Clostridium* sp strain CT7. *Bioresour. Technol.* 244, 575–581. doi:10.1016/j.biortech.2017.08.002

Xu, Q. L., Xu, X. P., Liu, L. M., Shi, Z. P., Du, G. C., and Chen, J. (2009). Effects of environmental conditions on pyruvate production. *Chin. J. Bioproc Eng.* 7 (1), 13–18.

Yang, X. L., Wei, S. Q., Lu, X. M., Qiao, X. G., Simal-Gandara, J., Capanoglu, E., et al. (2021). A neutral polysaccharide with a triple helix structure from ginger: Characterization and immunomodulatory activity. *Food Chem. x.* 350, 129261. doi:10.1016/j.foodchem.2021.129261

Zeng, W. Z., Cai, W., Liu, L., Du, G. C., Chen, J., and Zhou, J. W. (2019). Efficient biosynthesis of 2-keto-D-gluconic acid by fed-batch culture of metabolically engineered *Gluconobacter japonicus*. *Synth. Syst. Biotechnol.* 4 (3), 134–141. doi:10.1016/j.synbio.2019.07.001

Zeng, W., Zhang, H., Xu, S., Fang, F., and Zhou, J. (2017). Biosynthesis of keto acids by fed-batch culture of *Yarrowia lipolytica* WSH-Z06. *Bioresour. Technol.* 243, 1037–1043. doi:10.1016/j.biortech.2017.07.063

Zeng, Y. J., Yang, H. R., Zong, M. H., Yang, J. G., and Lou, W. Y. (2019). Novel antibacterial polysaccharides produced by endophyte *Fusarium solani* DO7. *Bioresour. Technol.* 288, 121596. doi:10.1016/j.biortech.2019.121596

Zhang, M., Che, Y. L., and Wu, C. D. (2022). A novel exopolysaccharide produced by *Zygosaccharomyces rouxii* with cryoprotective and freeze-drying protective activities. *Food Chem. x.* 392, 133304. doi:10.1016/j.foodchem.2022.133304

Zhou, J. W., Huang, L. X., Liu, L. M., and Chen, J. (2009). Enhancement of pyruvate productivity by inducible expression of a F0F1-ATPase inhibitor INH1 in *Torulopsis glabrata* CCTCC M202019. *J. Biotechnol.* 144 (2), 120–126. doi:10.1016/j.jbiotec.2009.09.005

Advantages of publishing in Frontiers

OPEN ACCESS
Articles are free to read for greatest visibility and readership

FAST PUBLICATION
Around 90 days from submission to decision

HIGH QUALITY PEER-REVIEW
Rigorous, collaborative, and constructive peer-review

TRANSPARENT PEER-REVIEW
Editors and reviewers acknowledged by name on published articles

Frontiers
Avenue du Tribunal-Fédéral 34
1005 Lausanne | Switzerland

Visit us: www.frontiersin.org
Contact us: frontiersin.org/about/contact

REPRODUCIBILITY OF RESEARCH
Support open data and methods to enhance research reproducibility

DIGITAL PUBLISHING
Articles designed for optimal readership across devices

FOLLOW US
@frontiersin

IMPACT METRICS
Advanced article metrics track visibility across digital media

EXTENSIVE PROMOTION
Marketing and promotion of impactful research

LOOP RESEARCH NETWORK
Our network increases your article's readership